On the transcriptome of ovarian carcinoma and immune cells found in ascites

Dissertation

aus dem Institut für Molekularbiologie und Tumorforschung
Geschäftsführender Direktor: Prof. Dr. Rolf Müller

zur Erlangung des Doktorgrades
der Naturwissenschaften
(Dr. rer. nat.)

dem Fachbereich Medizin
der Philipps-Universität Marburg
vorgelegt

von
Dipl. biol. **Florian Finkernagel**

geboren in Gießen

Marburg/Lahn, 2017

Angenommen vom
Fachbereich Medizin der Philipps-Universität Marburg (Hochschulkennziffer 1180)
am: 13. November 2017

Gedruckt mit Genehmigung des Fachbereichs.

Dekan: Prof. Dr. Helmut Schäfer
Referent: Prof. Dr. Rolf Müller
1. Korreferent: Prof. Dr. Bernd Schmeck

CONTENTS

CHAPTER 1

ABSTRACT

1.1 English abstract

Ovarian carcinoma kills hundreds of thousands of women annually. High grade serous carcinoma is the most common subtype. Like other tumors, high grade serous ovarian carcinoma successfully evades elemination by the immune system - for example, a pro-inflammatory activation state of macrophages is suppresed. Unlike other cancer types, it spreads not only via blood and the lymphatic system, but via peritoneal fluid and growth along the omentum. It is often acompanied by a malignant accumulation of peritoneal fluid, called ascites in which tumor cells and host (immune) cells, such as macrophages, float and interact.

Prior to the publications summarized in this cumulative dissertation, no detailed map of these interactions had been published. We compiled a detailed picture of mediators and receptors based on gene expression data from macrophages and tumor cells harvested from the ascites of patients undergoing primary surgery. Though the map is of limited accuracy due to the additional layers of regulation between gene expression and actual effector molecule release, it revealed candidates which were tested for their association with relapse free survival. Among the strongly (negatively) associated mediators were arachidonic acid and its derivatives as well as cytokines such as IL-6 and IL-10.

To discern the tumor influence on macrophages, tumor associated macrophages and monocyte derived (i.e. cultured) macrophages were compared. They showed large differences in their gene expression patterns and activation state. The experiment however could not distinguish between tumor and cell culture induced effects. Therefore a more appropriate control, peritoneal macrophages from non-malignant diseases, was sought. These peritoneal macrophages turned out to be very similar to tumor associated macrophages in both gene expression and activation state, suggesting that the tumor ascites environment does not induce, but rather suppresses, a change in activation state. The only discernible difference was a cluster of co-regulated genes related to extra cellular matrix reorganization, which hints that macrophages might play a role in establishing metastases within the coelom.

A second focus of this thesis is the role of the nuclear receptor PPARβ/δ in tumor associated macrophages. We found PPARβ/δ to be induced during the differentiation of monocytes into macrophages and ascites to contain PPARβ/δ ligands, e.g. arachidonic acid. PPARβ/δ signaling was accordingly activated and rendered tumor associated macrophages unresponsive to further stimulation by (synthetic) PPARβ/δ agonists but susceptible to inverse agonists. Using *in vitro* differentiated macrophages and *ex vivo* tumor associated macrophages we could show that PPARβ/δ induces a distinct activation state in macrophages and were able to characterize its target gene network in great detail.

1.2 Deutsche Zusammenfassung / German abstract

Eierstockkarzinom tötet jährlich hundertausende Frauen. Dabei ist hochgradiges seröses Karzinom der am häufigsten vorkommende Subtyp. Wie andere Tumoren entzieht sich das hochgradige seröse Ovarialkarzinom erfolgreich der Elimination durch das Immunsystem - zum Beispiel wird ein entzündungsfördernder Aktivierungszustand von Makrophagen unterdrückt. Im Gegensatz zu anderen Krebsarten verbreitet es sich nicht nur über Blut und das lymphatische System, sondern auch über Peritonealflüssigkeit und Wachstum entlang des Omentums. Es wird oft von einer bösartigen Ansammlung von Peritonealflüssigkeit begleitet, welche Aszites genannt wird, und in der Tumorzellen und Wirtszellen, beispielsweise Makrophagen und andere Immunzellen, schwimmen und interagieren.

Vor den in dieser kumulativen Dissertation zusammengefassten Publikationen gab es keine detaillierte Charakterisierung dieser Interaktionen. Auf der Grundlage von Genexpressionsdaten aus Makrophagen und Tumorzellen, die aus dem Aszites von ersmals operierten Patienteninnen gewonnen wurden, haben. haben eine Karte von Mediatoren und Rezeptoren auf erstellt. Obwohl zusätzliche Regulierungsschichten zwischen Genexpression und tatsächliche Effektormolekülfreisetzung die Genauigkeit begrenzen konnten wir Kandidaten identifizieren und auf ihre Assoziation mit krankheitsfreiem Überleben testen. Unter den stark (negativ) assoziierten Mediatoren waren Arachidonsäure und deren Derivate sowie Zytokine wie IL-6 und IL-10.

Um den Einfluss des Tumors auf Makrophagen zu untersuchen wurden tumor-assoziierte Makrophagen und monozyten-abgeleitete (kultivierte) Makrophagen verglichen. Sie zeigten große Unterschiede in ihren Genexpressionsmustern und ihrem Aktivierungszustand. Das Experiment ist jedoch nicht geeignet um zwischen zwischen Tumor und Zellkultur induzierten Veränderungen zu unterscheiden. In Folge wurden daher peritoneale Makrophagen aus benignen Krankheiten untersucht. Diese peritonealen Makrophagen erwiesen sich als sehr ähnlich zu tumor-assoziierten Makrophagen in Genexpression und Aktivierungszustand, was darauf hindeutet, dass Aszites keine Veränderungen des Aktivierungszustands auslösst, sondern eine solche eher unter-

drückt. Der einzige erkennbare Unterschied war ein Cluster von co-regulierten Genen deren Produkte die extrazelluläre Matrix beeinflussen können, was suggeriert, dass Makrophagen bei der Etablierung von Metastasen im Zölom eine Rolle spielen könnten.

Ein zweiter Schwerpunkt dieser Arbeit ist die Rolle des Kernrezeptors PPARβ/δ in tumor-assoziierten Makrophagen. Wir haben festgestellt, dass PPARβ/δ während der Differenzierung von Monozyten zu Makrophagen induziert wird und dass Aszites PPARβ/δ-Liganden, wie z.B. Arachidonsäure enthält. Entsprechend waren PPARβ/δ Zielgene in tumor-assozierte Makrophagen exprimiert und unempfänglich für weitere Stimulation durch (synthetische) PPARβ/δ -Agonisten, aber responsiv für inverse Agonisten. Unter Verwendung *in vitro* differenzierter Makrophagen und *ex vivo* tumor-assozierter Makrophagen konnten wir die Zielgene von PPARβ/δ charakterisieren und zeigen, dass PPARβ/δ einen bislang unbeschriebenen Aktivierungszustand in Makrophagen induziert.

CHAPTER 2

INTRODUCTION

2.1 Ovarian carcinoma

Ovarian carcinoma (OvCa) killed 42,704 women in the European Union in 2012 [52]. With more than 65,000 new cases annually, the estimate lifetime risk in the same region is 1.8%. Compared to other cancers, the patients prognosis is bleak, with survival rates at two, five and ten years of 65%, 44% and 36%, respectively [6].

OvCa may be divided into two groups, designated type I and type II carcinoma. Type I is generally low-grade and slow growing, while type II includes aggressive high grade carcinomas. Type I has well-established precursor lesions, while no precursor for type II has been discovered on the ovary itself [53] (see below).

High grade serous ovarian carcinoma (HGSOC), the focus of this work, is the most common among the eight major classifications of ovarian tumors [52]. Among the gynecological malignancies, HGSOC is the one with the highest mortality rate. Diagnosis often occurs at advanced stages of the disease, when other regions of the abdomen (FIGO [78] stage III) or those outside the peritoneal cavity (stage IV) have been invaded [77].

The cellular origin of HGSOC has long been unclear [53]. Recent research points to a fallopian origin, where lesions in the fimbriae develop into serous

tubal intraepithelial carcinoma (STIC) which acts as a precursor to HGSOC. This would imply that the HGSOC themselves are already metastases [52, 102].

HGSOC typically metastasizes early, spreading via blood, the lymphatic system, lateral growth and peritoneal fluid within the abdominal cavity [53]. An accumulation of such fluid, called ascites, is a functionally pro-tumorigenic environment containing cancer cells [53], tumor-promoting growth factors [48], extracellular vesicles [74] and immune cells [82, 96].

2.2 Tumor associated macrophages

Among the hallmarks of cancer are the successful evasion of the innate and adaptive immune system and the establishment of a tumor-promoting inflammatory environment [38]. Tumors influence their infiltrating macrophage population ("tumor associated macrophages" or TAMs) by altering macrophage activation.

Historically, pro-inflammatory and anti-inflammatory activated macrophages have been labeled as M1 and M2, respectively. This classification, originally proposed by Mills et al. [62] (in *Mus musculus*), was based on the production of either nitric oxide, a cytotoxic compound, or trophic polyamines. Later works have led to a more nuanced view, placing differently *in vitro* stimulated macrophages on a continuum between M1 and M2 (M2a, M2b and M2c) [57].

The *in vivo* situation however is more complex - macrophages are exposed to a combination of M1- and M2-inducing signals (see [59] for a recent review). A recent high-throughput transcriptional *in vitro* study [110] showed that macrophage activation is not a spectrum with two distinct end points. To accurately characterize macrophage populations, it is thus necessary to describe them in more detail, for example by their input signals (as suggested for *in vitro* experiments by Murray et al. [65]) or by the measurement of a large number of markers.

TAMs accordingly show a mixed transcriptional and phenotypical activation (see page 28). They serve a pro-tumorigenic role, enhancing tumor growth and progression by aiding in proliferation, invasion, angiogenesis, immune suppression and intravasation [16, 28, 79]. There is a clear correlation between

the presence of CD163[1]$_{high}$ TAMs in ascites and early relapse [82], consistent with the inverse correlation between macrophage density within tumors and clinical outcome in other cancers [16].

In mice it has been proposed that there are two sources of macrophages; (I) tissue resident macrophages derived from the yolk sac and (II) infiltrating macrophages derived from peripheral blood monocytes, which derive from hematopoietic stem cells in the bone marrow [30]. More recent data suggests that there is an additional macrophage source: embryonal hematopoietic stem cells, and that the source of macrophages is tissue specific [92]. Most of our knowledge of macrophage origin is derived from mouse models, but monocytopenia[2] patients still harbor tissue-resident macrophages [104], suggesting that the dichotomy (or trichotomy) of macrophage sources is conserved in mammals.

TAMs, peritoneal and monocyte-derived macrophages are the subject of all publications in this cumulative dissertation.

2.3 Peroxisome proliferator-activated receptor β/δ

PPARβ/δ[3] is a member of the nuclear hormone receptor superfamily of transcription factors [46].

Human *PPARD* is expressed in virtually all tissues[4] [101], and has been associated with modulating a wide range of functions, such as metabolism (especially fatty acid oxidation and glucose homeostasis), wound healing, cell proliferation and immune regulation [22]. PPARβ/δ also plays a role in a number of illnesses such as psoriasis [86], Huntington's disease [19], bipolar disorders [114], and possibly in cardiovascular diseases [22]. Its role in cancer is unclear - conflicting reports in the literature suggest two hypothesis: on the one hand an overexpression in tumors promoting anti-apoptotic activities and cell pro-

[1] Cluster of Differentiation family member
[2] A deficiency of monocytes.
[3] Peroxisome proliferator-activated receptor family member
[4] see `http://www.proteinatlas.org/ENSG00000112033-PPARD/tissue`

liferation; and on the other hand a promotion of terminal differentiation and inhibition of pro-inflammatory signaling which abates tumorigenesis [75].

Chemically induced skin carcinogenis is enhanced in PPARβ/δ-null mice but not in mice lacking PPARβ/δ only in basal keratinocytes [63], suggesting a function in other cell types within the skin cancer tumor stroma. Targeted disruption of the *PPARD* gene in colon endothelial cells greatly reduced the incidence of chemically induced colon tumors in another mouse model [117], possibly via reduced expression of VEGF.

All endogenous PPARβ/δ ligands so far identified, such as arachidonic acid (AA), linoleic acid (LA) [103] and 15-Hydroxyeicosatetraenoic acid (15-HETE) [67] are lipids and have an agonistic effect - they induce target gene expression[1]. PPARs bind to PPAR response elements (PPREs) together with its heterodimeric partner RXR[2] [7]. The agonist induced increase in target gene transcription is mediated by the recruitment of co-activators [105].

Synthetic - non fatty-acid - ligands developed in recent years can elicit agonistic, antagonistic and inverse agonistic effects. The agonists (e.g. GW501516 [71] or L165,041 [42] induce transcription beyond the effect of endogenous ligands; antagonists (e.g. GSK0660 [35]) compete with endogenous ligands and thereby reduce target gene transcription and inverse agonists (e.g. ST247 [68]) recruit co-repressors co-factors leading to a strong transcriptional repression.

PPARβ/δ's role in disease and its druggability make it an interesting potential target. A large number of potential ligands has been tested in sufficient detail to build predictive binding models [44]. The agonistic ligand GW501516 has been evaluated in two clinical phase II studies for the treatment of dyslipidemia, but the work has been abandoned because GW501516 appears to induce cancer in several organs of mice and rats [89]. MBX-8025 has been evaluated for the treatment of dyslipidemia in 166 patients and was able to affect presumably beneficial changes in lipoprotein particle concentration when co-administrated with atorvastatin [14].

[1] There is some evidence that Prostaglandin I_2 (PGI2) can act as a PPARβ/δ agonist [33], but a massive induction in PGI2 synthesis did not lead to an activation of PPARβ/δ in 3T3-derived cells, and the original experimental setup could not be reproduced in another lab [24].

[2] Retinoid-X-receptor

PPARβ/δ is necessary for in the anti-inflammatory activation of macrophages in adipose tissue and liver [12] and we could characterize an effect of PPARβ/δ ligands on macrophage activation (see chapter 3.2). Ascites contains fatty acids [11], some of which we found to be PPARβ/δ ligands (see chapter 3.3).

2.4 Issues with primary cell transcriptome analysis and sample isolation

When isolating primary cells from complex, multi-cellular eukaryotes one usually procures a mixture of cell types. For solid tissues, laser dissection provides a low through-put method to select and extract (dead) cells by morphology or stained surface markers. For cells in fluids such as blood or ascites, fluorescence activated cell sorting (FACS) or magnetic activated cell sorting (MACS) allow antibody based selection of living cells in great numbers. Solid tissues can be separated by the same methods after dissolution of cell-cell contacts and the extra cellular matrix. Macrophages adhere to standard cell culture dishes much more quickly than other cells, allowing for adherence selection [1].

The methods differ in applicability, cost, processing time and output purity, leaving no clear winner. All methods trigger signal cascades and subsequent transcriptomic and surface marker changes, the magnitude of which increases with processing time. FACS allows the user to trade of specificity for sensitivity, but is the most expensive and time consuming of the three methods. Adherence selection is only available for macrophages. MACS can be applied to a larger number of cells than FACS, but it is in essence an enrichment, not a selection, method and as such leaves a (variable) number of other cells in the resulting suspension.

The lack of cellular purity leads to obvious problems when trying to discern differences between cell types. Many algorithmic methods to quantify cell mixture contents from transcriptome data ('deconvolution') have been established

[1] For completeness, it should be mentioned that macrophages can also be derived from peripheral blood monocytes by simple adhesion. Monocyte derived macrophages are different from primary tissue macrophages, as we show in section 3.4, page 26.

for micro arrays (see [111] for a review), but fewer methods were available for RNAseq data sets. I have developed such a method for the work described in this dissertation.

2.5 Aims of this dissertation

This dissertation

- characterizes and compares the transcriptomes of high grade serous ovarian carcinoma ascites tumor and macrophage cells (see pages 8 and 26)
- studies the effect of artificial PPARβ/δ ligands on the activation state of monocyte-derived macrophages (see page 16)
- describes the effect of endogenous PPARβ/δ ligands on tumor associated macrophages (see page 22).
- includes a novel method for the deconvolution of RNAseq data from populations of mixed primary cells (see page 74).

CHAPTER 3

PUBLICATION SUMMARIES

3.1 A transcriptome based global map of signaling pathways in the ovarian cancer micro-environment associated with clinical outcome[1]

3.1.1 Results

3.1.1.1 Correction of RNAseq data for contaminating cells

In this work [81], tumor cell (TU), tumor associtated macrophage (TAM) and tumor associtated T cell (TAT) were isolated from 28 patients with HGSOC. RNA sequencing (RNAseq) was performed on 21 TU, 18 TAM and 5 TAT samples and aligned to the human genome using STAR [20]. To correct TU and TAM samples for contaminating cells of the other kinds ten previously published algorithms for transcriptome deconvolution were evaluated. Most were found out to have restrictions making them unsuitable for our setting. DeMix [4], Dsection [111] and PSEA [47] had only been established on microarray data. ContamDE [91] required at least two clean samples of each kind. ESTIMATE [113] does not estimate a percentage but an "ImmunoScore" unsuitable to correction. UNDO [107] requires no clean samples, but requires two samples generated from the same mixtures (i.e., two mixed samples per patient, at differing mixture percentages). TEMT [54] works on transcript level - an analysis unsuitable to both our single ended 50 bp dataset and the cell-cell network investigated in this study. IsoPure [80] assumes that the two cell types being deconvoluted are closely related which cannot be assumed for TUs and TAMs.

Two algorithms, CIBERSORT [70] and DeconRNASeq [31] appeared to be suitable and were tested alongside a custom deconvolution and correction algorithm we developed.

In brief, our algorithm first selects cell type specific genes from (externally defined) clean reference samples, uses their apparent expression to estimate a

[1] Published in S. Reinartz et al. "A transcriptome-based global map of signaling pathways in the ovarian cancer microenvironment associated with clinical outcome." In: *Genome biology* (2016). DOI: 10.1186/s13059-016-0956-6, see page 51 for full text.

contamination percentage and subtracts the linearly scaled reference sample. See Additional File 1, "Description of algorithm", page 74 for details.

Only our algorithm offers an automated method to select marker genes (or "cell type signatures" in CIBERSORT parlance). Running all three in a simulation setting approximating our conditions[1], using the exact same mixtures and the same number of ad-hoc selected marker genes for each algorithm showed that only our algorithm was able to exploit the information inherent in the *in silico* mixtures (Additional File 1 Figure 2, page 79). This was independent of the dataset used for simulation (Additional File 1, Figure 3, page 80). We could also show that our algorithm is of use across both mixtures of closely related cell types (such as $CD4^+$ and $CD8^+$ T-cells from the GSE60424 dataset, Figure 1A, page 55, Additional File 1, Table 1, page 75) and of very different cell types (Datasets GTex and E-MTAB-2836, Additional File 1, Table 2 and 3, page 77, Figure 2, page 79 and Figure 3, page 80).

We applied our algorithm to our actual samples and discovered less than 2% contamination (per contaminating cell type) in most of the $CD45^+$-MACS purified TU samples (Figure 1B, page 55), but higher contamination in the $CD14^+$-MACS purified TAM samples (10 samples with more than 2% contamination, Figure 1C, page 55). Three samples showed contamination of more than >25% and were excluded from further analysis. Since even a single-digit contamination can add hundreds of Transcripts per Million (TPM) units for specific genes, we applied a correction to the remaining samples. The correction did succeed in removing macrophage markers from tumor samples, as can be seen in Figure 1D, page 55 (note that CD163 is not among the markers used to determine contamination percentage). It did not affect tumor markers such as *PAX8*[2] (Figure 1D, page 55) or unrelated genes, except in fairly contaminated samples (>10%) where it lead to a slight increase in TPM due to the renormalization to one million. The correction of TAMs was similarly successful (not shown).

In summary, we were able to establish a method to correct our dataset for contamination with other cell types *in silico*.

[1] Which were arguably unfavourable with only one sample of each class available to learn from.

[2] Paired box gene/protein 8

3.1.1.2 Protein mediators and their receptors

We were interested in cell-cell signaling between TUs and TAMs.

A major class of signaling molecules are cytokines and growth factors - which we define broadly to be protein mediators. Using the gene ontology (GO) annotation, the Ensembl [26] human genome annotation, and a literature search, we assembled a dataset of 502 cytokine and 289 cytokine receptors genes, of which 159 and 173, respectively, were expressed in at least 65% of our TU and/or TAM samples. We estimated confidence intervals on the ratio of TU vs. TAM expression based on a bootstrapping method[1] (Figure 2A and 2B respectively, page 56).

Selected genes were analyzed by reverse transcription quantitative polymerase chain reaction (RT-qPCR) in a larger number of patients[2] (Figure 3A, page 57), which generally confirmed the RNAseq data. Expression of IL-8[3] and S100A8/A9[4] as well as cell surface expression of LIFR[5] and TGFBR3[6] confirmed the RNAseq results (Figure 3C, page 57). No significant expression difference was found for S100A14, although the ribonucleic acid (RNA) levels differed 100-fold (Figure 3C, page 57). No signal for IL-4, IL-12-p70[7], IL-13 or GM-CSF[8] was detected in ascites by ELISA (Figure 3D, page 57), as predicted by low messenger RNA (mRNA) levels (not shown). IL-6 and VEGFC[9] were present in higher amounts than expected from mRNA levels. We found that attachment of tumor cells *in vitro* leads to an induction of the transcription of both *IL6* and *VEGFC*, suggesting that high levels of the corresponding proteins were derived from solid tumor tissue rather than from cells floating in ascites (Figure 3E, page 57).

[1] Bootstrapping estimates the accuracy of sample estimates using random subsampling (with replacement).
[2] Not all patients provide enough RNA for sequencing, but RT-qPCR requires less material.
[3] Interleukin family member
[4] S100 calcium binding protein family member
[5] Leukmia inhibitory factor receptor
[6] TGFβ receptor 3
[7] Interleukin 12; active heterodimer (p70)
[8] Granulocyte macrophage colony-stimulating factor
[9] Vascular endothelial growth factor C

Among the signaling networks identified by this approach (Figure 4, page 58) were STAT3[1] and TGFβ[2] centered networks, WNT[3] signalling, pathways driven by S100 proteins, semaphorin and ephrin signaling as well as chemokine mediated pathways.

3.1.1.3 Lipid-mediators, their producing enzymes and receptors

Another major class of signaling molecules are lipids. Using the same methods as above, a set of genes coding for lipid mediator producing enzyme and the corresponding receptors was build and applied to our dataset (Figure 5A, 5B, page 61). RT-qPCR results generally supported the RNAseq data, both on unmatched and matched samples (Figure 5C, 5D, page 61). Ascites concentrations of AA and lysophosphatidic acids (LPA) were in the micromolar range, while prostaglandin E_2, 6-keto-prostaglandin F1A, leukotrine B4 (LTB_4), 5-Hydroxy-eicosatetraenoic acid (5-HETE) and 15-HETE were present in nanomolar concentrations (Figure 5E, page 61). All measured lipids varied by at least one order of magnitude between patients.

3.1.1.4 Lipid-mediator concentrations and gene expression associated with differences in clinical outcome

To establish a biological role of the identified signaling pathways, we tested cytokine and lipid mediator concentrations in ascites for their association with relapse-free-survival (RFS) using Kaplan-Meier plots [45] and the log-rank tests [56]. We found IL10, IL-6, PLA_2G7[4], AA and LTB_4 to be inversely associated with RFS (i.e. patients with low ascites levels of these substances had a prolonged survival time, Figure 7A-G, page 64). No positive association was observed for any of the investigated molecules (Figure 7A, page 64).

Using a published dataset associating microarray expression data with OvCa RFS [34] (n=1018), we tested genes predominantly expressed in tumor cells by Kaplan-Meier and log-rank tests. We focused on tumor specific genes since no

[1] Signal transducer and activator of transcription family member
[2] Tumor growth factor β family family member
[3] Wnt signaling pathway
[4] Lipoprotein-associated phospholipase A2

information about the presence of other cell populations in the tumor samples was available. The two most prominent results were a favorable association of WNT receptor frizzled 4 (*FZD4*[1]) and *NDP*[2] expression; and an adverse association of *PTGIS*[3] and *TGFβ3* with clinical outcome (both $p < 0.001$, Figure 9A, 9B, 9D, 9F, 9G, page 66).

3.1.2 Discussion

Using transcriptional data from 20 HGSOC TU and 16 TAM samples, we identified and characterized several cell-cell signaling networks mediating communication between these cell types (Figure 4, page 58 and Figure 6, page 62). In the following sections the pathways showing the strongest link to clinical outcome will be discussed.

3.1.2.1 STAT3 inducing signaling

The activation of the transcription factor STAT3 has a detrimental function in OvCa [87]. STAT3 inducing cytokines were made both by TUs (e.g. LIF[4]) and TAMs (e.g. IL10, IL-6). Both cell types could receive IL-6 signaling, though TAMs had a stronger expression of the receptor genes (Figure 4A, page 58). The expression of LIF receptor in tumor cells points to a role beyond macrophage activation [21] of this pathway. IL-6 protein concentration in ascites (Figure 3D, page 57) was higher than one would expect from the gene expression level in TAMs, suggesting a different cell population as the major IL-6 source. *In vitro* experiments comparing floating and attached OvCa tumor cells showed an increase of *IL6* expression (Figure 3E, page 57). It is therefore possible that the solid tumor cells - as opposed to the floating population analyzed in this work - are the major source for IL-6. Consistent with previous studies [82, 100, 17], low levels of IL-6 and IL10 in ascites were associated with a longer RFS interval (Figure 7B, C, page 64).

[1] Frizzled family member
[2] Norrie disease protein
[3] Prostaglandin-I2 synthase
[4] Leukemia inhibitory factor

3.1.2.2 TGFβ

The TGFβ family members TGFβ1, 2 and 3 were associated with earlier relapse (Figure 7G, page 64, Figure 9A, D, page 66). TGFβ1 was mainly produced by TAMs, while the TGFβ2 and TGFβ3 were produced by TUs (Figure 4B, page 58). Multiple studies have associated TGFβ family members with OvCa progression [23, 58, 83], and our results are in agreement with known functions of TGFβ ligands [72, 108]. The TGFβ super family members BMP2[1] and BMP4 have been previously described in the context of OvCa [61]. They were described as being produced by mesenchymal stem cells which fits with the extremely low expression levels we observed in both TAMs and TUs.

3.1.2.3 Frizzled

We found evidence that both the canonical and the non-canonical WNT signaling pathways were operational in both TAMs and TUs (Fig 4C, page 58). Canonical WNT signaling depends on FZ and LRP[2] protein family members and stimulates β-catenin[3] signaling. Non-canonical WNT signaling occurs without the involvement of LRP coreceptors and triggers a calcineurin dependent pathway. Both cell types expressed overlapping sets of *FZ* and *LRP* family members. Five of the seven WNT ligand encoding genes observed were expressed predominantly by tumor cells, including *WNT7A*[4] and *WNT11*, which were both associated with a more rapid relapse (Fig 9A).

For optimal canonical WNT signaling RSPO[5] family members and their receptor LGR5[6] are necessary [50], but neither were expressed in our samples.

We found evidence of autocrine norrin (an alternative FZD4 ligand [43]) signaling. NDP, its receptor FZD4 and a signal amplifying component of the receptor complex (TSPAN12[7] [43]) were found to be expressed in TU (though

[1] Bone morphogenetic protein family member
[2] lipoprotein receptor-related proteins
[3] Subunit of the cadherin complex
[4] Wnt signaling pathway family member
[5] R-spondin
[6] Leucine-rich repeat-containing G-protein coupled receptor 5
[7] Tetraspanin 12

NDP was only expressed in a subset of samples). All three were associated with a delayed relapse, which is surprising since norrin also has the ability to induce β-catenin, which is generally thought to be pro-tumorigenic; and because they were recently linked to colon cancer angiogenesis [76]. This suggests a previously unknown function of NDP signaling.

3.1.2.4 Semaphorins and ephrins

Autocrine and paracrine signaling via semaphorins and ephrins was evident in our RNAseq data. At least 13 semaphorins, six of their receptors, six ephrin members and seven of their receptors were expressed in tumor cells and TAMs (Fig 4E, page 58). In different cancers, both pro- and anti-tumorigenic roles have been described for the semaphorin receptor PLXNB1[1] [94], which here was expressed exclusively in tumor cells. In the context of OvCa, we found five semaphorins and four ephrin receptors to be associated with early relapse (none were associated with a protective status).

3.1.2.5 Arachidonic acid and its metabolites

We found high concentrations of AA in ascites to be associated with early relapse (Figure 7F, page 64). This association was increased in combination with high IL10, IL-6 or TGFβ levels (Figure 8, page 65), all of which were also linked to earlier relapse by themselves (Figure 7, page 64). Since the level of AA and the above cytokines were independent (Figure 8D, page 65), it can be presumed that their synthesis is as well.

As for AA derivatives, we observed an adverse link between LTB_4 ascites levels and RFS (Figure 6A, page 62, 7A and 7G, page 64) as well as for the genes *PTGIS* and *PTGER3*[2], which encode for PGI_2 synthase and PGE_2 receptor (Figure 6A, page 62). The receptors for PGI_2, PGE_2 and 15-HETE were predominantly expressed on TAMs, unlike the LTB_4 receptor, which was expressed on both TAMs and TUs. It is tempting to speculate that these AA derivatives also mediate the AA-RFS association described above, but it currently cannot be

[1] Plexin B1

[2] Prostaglandin EP3 receptor

excluded that non-metabolized AA was a contributor. Though PPARβ/δ is agonized by AA and AA-derivates [90] (see section 3.3, page 22), the most abundant agonistic polyunsaturated fatty acid (PUFA) linoleic acid was not linked to survival at all (Figure 7A, page 64), making it unlikely that AA is acting via PPARβ/δ.

3.1.2.6 Conclusion

In this study, we have developed a deconvolution (or mixture correction) algorithm that allowed successful correction of our datasets. We constructed a signaling map between OvCa ascites tumor cells and tumor associated macrophages, based on RNAseq data and the maxim that gene expression is related to protein expression.

We identified and characterized, with respect to the cellular origin of their components, several known (STAT3, TGFβ, WNT) and previously undescribed (NDP, AA) signaling pathways associated with relapse free survival, as well as pathways that do not appear to affect cancer recurrence.

3.1.3 My contribution

My contribution was the analysis and visualization of all RNAseq and RT-qPCR data (Figures 1B, 1C, 1D, 1E, 2A, 2B, 3A, 3E, 5A, 5B, 5C, 5D, Tables 1 and S1, Supplemental Datasets[1] S1, S2, S3, S4, S5, S6, S7, S8, S9), the drafting of the inspected gene sets (cytokines and their receptors (Datasets S2, S4), lipid signaling associated enzymes, accessory proteins (Dataset S6) and receptors (Dataset S9) (Additional File 3 - Description of the creation of the gene sets used), and the development, implementation and evaluation of the deconvolution algorithm (Figure 1A, Additional File 1 description and evaluation of the algorithm, Additional File 6 - source code). I also participated in the conception and writing of the manuscript. I share first authorship in this work with one other author.

[1] Supplemental Figures, datasets, supplemental Datasets and Additional files (except for Additional File 1) are not included in this dissertation, but available from the journal's website at https://genomebiology.biomedcentral.com/articles/10.1186/s13059-016-0956-6

3.2 The transcriptional PPARβ/δ network in human macrophages defines a unique agonist-induced activation state[1]

3.2.1 Results

3.2.1.1 PPARβ/δ is present and functional in monocyte-derived macrophages

PPAR ligands have long been associated with an anti-inflammatory role in various disease models [95]. Until our work published in Adhikary et al. [2], the PPARβ/δ dependent signaling network in primary macrophages had been uncharacterized on both a transcriptional and cistronic level.

To establish an *in vitro* model we verified an intact PPARβ/δ signaling network in monocyte-derived macrophages (MDMs) as follows: During the adhesion induced maturation of blood monocytes into MDMs, *PPARD* mRNA and PPARβ/δ protein levels rose for 5 to 6 days before gradually declining again, with the mRNA preceding the protein (Figure 1A, 1B, page 89). PPARβ/δ target gene induction via synthetic agonists (and repression via synthetic inverse agonists) followed the same pattern (Figure 1C, page 89). Using ChIP followed by quantitative polymerase chain reaction (ChIP-qPCR) both PPARβ/δ and its obligatory desoxyribonucleic acid (DNA)-binding partner RXR could be shown to be present in the regulatory region of the PPARβ/δ target gene *PDK4*[2] even before differentiation (Figure 1D, page 89). Taken together, these facts indicate that MDMs are a suitable model to study macrophage PPARβ/δ signaling.

3.2.1.2 Canonical and inverse PPARβ/δ target genes

ChIP followed by sequencing (ChIPseq) analysed using Bowtie 2 [49] and MACS [116] identified 1,175 PPARβ/δ and 27,255 RXR binding sites[3] after false positive

[1] Published in T. Adhikary et al. "The transcriptional PPARβ/δ network in human macrophages defines a unique agonist-induced activation state." In: *Nucleic acids research* (2015). DOI: 10.1093/nar/gkv331, see page 84 for full text.

[2] Pyruvate dehydrogenase kinease 4

[3] The large discrepancy in the number of binding sites may be explained by a higher affinity antibody and the fact that RXR forms alternative DNA binding complexes with other nuclear

filtering. The changes in transcription effected by agonist and inverse agonist treatment were profiled by RNAseq and analysed with STAR [20] (Figure 2A, 2B, page 90).

Agonist regulated genes were associated with immune related functions such as "adhesion of immune cells" and "inflammation" (Figures 2C, 2D, page 90). Upstream regulator analysis (Figure 2E, page 90) showed clear differences between agonist induced (i.e. canonical) genes, which correspond to known PPARα and PPARγ ligands (high activation z-score), and inverse target genes (low activation z-score), which are targets of common pro-inflammatory regulators such as lipopolysaccharide (LPS), TNFα[1], IFNγ[2], IL-1β, STAT3 and TLR4[3].

Association of binding sites with genes within 50 kbp and an overlap analysis with genes induced in MDMs by agonist L165,041 showed that about half (46.3%, or 132 genes) of the latter had a PPARβ/δ binding site. Almost all (98.5%) of these sites also showed RXR occupancy (Figure 3A, page 91). Nine out of ten upstream regulators of these 132 genes were either PPAR ligands or the PPAR co-activator PPARGC1A[4] (Figure 3D, page 91). In contrast, among the agonist repressed genes only a small subset (9%) showed a PPARβ/δ or RXR binding site (Figure 4A, page 93). Cytokine signaling pathways such as e.g. STAT1, STAT3, IL10, IL-4 and IL-1β were identified as upstream regulators for the agonist repressed genes (Figure 4C, page 93). Comparison to published ChIPseq sites (in other cell types) revealed a significant overlap with NF-κB-p65[5], BCL6[6] and LPS-induced EP300[7] bound sites. NF-κB-p65, EP300 and STAT3 have been described as involved in cross talking pathways [40]. This suggests a model were agonist induced genes are direct (cis-) PPARβ/δ target genes and (largely) the same among cell types[8] while agonist repressed target genes are indirect (trans-) and cell type specific.

receptors [29].

[1] Tumor necrosis factor α

[2] Interferon γ

[3] Toll-like receptor 4

[4] PPARγ coactivator 1 alpha

[5] NF-κB subunit p65

[6] B-cell lymphoma 6

[7] E1A binding protein p300

[8] since they appear in target lists of PPARβ/δ ligands which were compiled in other cell types

3.2.1.3 Morphologically and functional consequences of PPARβ/δ activation

Morphologically, MDMs treated with agonist during differentiation resemble IL-4 treated cells ("M2"-phenotype), while inverse agonist ones appear more similar to LPS treated ("M1"-phenotype) cells (Figure 6, page 95).

Functional networks built from expression data (Figure 5, page 94) using IPA (Ingenuity® Systems, www.ingenuity.com) predicted an increased T-cell activation by agonist treated MDMs. This hypothesis was tested in co-culture experiments. Results were supportive, with L165,041 pretreatment of MDMs leading to more IFNγ^{+}CD8^{+} cells in five out of six donors (Figure 7A, page 96). This effect might be mediated by *IDO1*[1], an inverse PPARβ/δ target gene whose RNA and protein levels were decreased under agonist treatment (Figure 7B, 7C, page 96). IDO1 produces kynurenine, a suppressor of T-cell activation [64]. Kynurenine levels dropped upon agonist treatment (Figure 7D, page 96), providing a possible explanation.

3.2.1.4 Comparison with other macrophage states

To better characterize the PPARβ/δ-agonist induced macrophage phenotype, we compared the transcriptional ligand response to 49 signatures derived by stimulating MDMs with 28 stimuli (plus baseline) [110] (Figure 8A, page 98). Five of the 49 signatures were enriched in our PPARβ/δ-MDM target gene set based on a hypergeometrical overlap test. For these five modules, the agreement between direction of stimuli response (respective to baseline) and L165,041 response was discretized and ploted as a heat map (Figure 8B, page 98). This clearly shows that the agonist response was outside of the classical M1/M2 classification, since module 15 and 43 were regulated in the same direction by L165,041 and the M2-polarizing stimulus IL-4, but module 16 was regulated discrepantly. The same argument can be made for IL-13, another M2-stimulus.

[1] Indoleamine-pyrrole 2,3-dioxygenase 1

3.2.1.5 Cell type dependent regulation of PPARβ/δ target genes

Intrigued by the apparent distinction of direct and indirect target genes suggested by ChIPseq and upstream regulator analysis (see page 17) we compared the actual binding site locations with previously published data from a human myofibroblasts cell line [1] (WPMY-1 cells) and a breast cancer cell line [3] (MDA-MB-231).

This showed a clear overlap of PPARβ/δ binding site associated target genes[1] (n=129) (Figure 9A, page 99). These cell type independent target genes were highly enriched for the annotations "energy production" and "lipid metabolism". In contrast, inverse target genes - i.e. those responding to agonist treatment with a repression of their transcriptional activity independent of the presence of a PPARβ/δ binding site in their vicinity - showed no (n=0) overlap between the three cell types (Figure 9B, page 99).

This together with the large number of inverse target genes (n=292-447, Figure 9B, page 99) suggests that the cell type specific response to PPARβ/δ agonists is mediated by other transcription factors downstream of PPARβ/δ.

3.2.2 Discussion

Our study was aimed to identify the mechanisms behind the anti-inflammatory effects of PPARβ/δ agonists. To this end we established MDMs as a model system and characterized them by ChIPseq and RNAseq.

Besides a set of fatty acid oxidation and lipid metabolism target genes representing the canonical, cell type independent function of PPARβ/δ, we have identified two classes of immunoregulation associated genes: (i) direct and induced targets and (ii) indirect and repressed targets.

Both groups were only responsive in MDMs (and (murine) bone marrow-derived macrophages (BMDMs)), thus cell type specific, and most likely PPARβ/δ specific as well – tested genes that were responsive in wild type BMDMs were not responsive in cells from PPARβ/δ-null mice (Figure 2F, page 90).

[1] i.e. those having a ChIPseq identified PPARβ/δ binding site in their promotor region

The mechanism of the transregulation of a large part of group (ii) indirect target genes is likely via NF-κB[1] and STAT1, since the group showed large overlaps with genes controlled by these pathways.

In agreement with this hypothesis, NF-κB activation inhibitor MG132[2] diminished PPARβ/δ agonist effects on several NF-κB target genes (from group (ii)) (Figure 4E, page 93).

The set of immune-regulatory target genes suggested a primarily anti-inflammatory effect (e.g. via *IL8*, *IFNγ*, *CCL3*[3] with some immuno-stimulatory secondary effects (e.g. via *IL-10*, *IL13*). In accordance with this, bioinformatic analysis revealed a distinct activation state for PPARβ/δ agonists which combines anti-inflammatory, immune stimulatory, and lipid-triggered activation states outside of the M1-M2 axis.

Several key components of the NALP inflammosome [60] were identified as PPARβ/δ target genes, establishing a second PPARβ/δ-dependent immunoregulatory axis.

A third axis is the repression of *CD300E*, a pro-inflammatory subtype by PPARβ/δ agonist together with an induction of *CD300A*, which suggests an immuno-suppressive activity via CD300 members [9].

In summary, we have characterized the PPARβ/δ signaling network in a macrophage model with special regard to potential mediators of (anti-) inflammatory effects. While this produced a useful map for further experiments, finding an appropriate setting mimicking the physiological environment remains an open (and major) challenge.

3.2.3 My contribution

My contributions included the analysis of ChIPseq and RNAseq data, the comparison with published ChIPseq datasets of non-PPARβ/δ factors, the comparison to published stimulus-specific MDM transcriptomes and the comparison with published PPARβ/δ binding sites. This led to figures 2B, 2C, 2D, 3A, 3C,

[1] Nuclear factor κ-light-chain-enhancer of activated B cells
[2] which also functions as a proteasome inhibitor
[3] Chemokine (c-C motif) ligand 3, also known as macrophage inflammatory protein 1-alpha

3B, 4A, 4B, 4D, 8, 9A and 9B. I assisted in all statistical analyses and share first author-ship with two other authors.

3.3 Deregulation of PPARβ/δ target genes in tumor-associated macrophages by fatty acid ligands in the ovarian cancer micro-environment[1]

3.3.1 Results

Having established the PPARβ/δ immuno-regulatory response in an *in vitro* system (MDMs, see section 3.2), we focused our investigation onto its effects in the (ascites) tumor environment and tumor derived *in vitro* systems.

Initially, we compared the (global) transcriptional and phenotypic responses of TAMs (cultivated in ascites) and MDMs (cultivated in RPMI-1640 + 10% fetal calf serum (FCS)) to the PPARβ/δ agonist L165,041. MDMs were chosen as a reference because TAMs were believed to derive from invading blood monocytes (See section 3.4.2.2). Transcriptionally, TAMs were refractory to PPARβ/δ agonists across many genes (Figure 2B, 2C, page 106), but showed an increased (and dosage dependent) response to inverse agonist treatment when compared with MDMs (Figure 2B, page 106, Figure 6E, page 112). There was no difference in PPARβ/δ chromatin immunoprecipitation (ChIP) enrichment (Figure 2A, page 106), leading to the hypothesis that there was a significant amount of PPARβ/δ agonist(s) in ascites which causes the refractory phenotype.

The refractory effect on PPARβ/δ target genes in TAMs initially persisted when TAMs were kept in RPMI-1640 + 10% FCS for 24 h (Figure 2D, page 106), but was attenuated after 4 d (Figure 7C, page 113). Macrophages can accumulate lipid droplets [106], and the attenuation co-occurred with a decrease of lipid droplets in TAMs (Figure 7A, 7C, page 113). Lipid droplet accumulation in MDMs was inducible by exposing the cells to LA at a level comparable to that in ascites. The droplets persisted for at least 4 d in RPMI-1640 after removal of the LA stimulus (Figure 7D, 7E, page 113) and interfered with inducibility by synthetic ligands (compare Figure 7F with the induction in MDMs in Figure 7C, page 113).

[1] Published in T. Schumann et al. "Deregulation of PPARβ/δ target genes in tumor-associated macrophages by fatty acid ligands in the ovarian cancer microenvironment". In: *Oncotarget* (2015). DOI: 10.18632/oncotarget.3826, see page 103 for full text.

3.3 Deregulation of PPARβ/δ target genes in tumor-associated macrophages by fatty acid ligands in the ovarian cancer microenviroment

We defined a set of PPARβ/δ target genes in MDMs by comparing agonist and inverse agonist treated cells from five healthy donors via RNAseq. Of these 195 genes, 54 showed increased expression in freshly isolated (*ex vivo*) TAMs compared to MDMs (Figure 3A, page 109), with a large overlap (n=21) to an TAM vs. MDM comparison (Figure 3B, page 109). Also, a majority of them (32 of 54) were refractory to L165,041 treatment (Figure 3C, page 109). This was confirmed for selected genes in RT-qPCR and Western blot experiments using samples from additional donors (Figure 3D, 3E, page 109). It should be noted that another large fraction of the MDM-PPARβ/δ-target genes (n=49) was expressed at lower levels in freshly isolated TAMs (cyan dots in Figure 3A, page 109), possibly because they were repressed by other signaling pathways triggered by the tumor environment. One of the most induced genes in TAMs is *ANGPTL4*[1], which encodes for a secreted protein that has previously been associated with cancer cell invasion and metastasis in breast cancer [3]. ANGPTL4 could be detected in the ascites at nanogram/ml concentrations (Figure 3F, page 109) and high ANGPTL4 expression showed a weak association with shortened RFS in a HGSOC microarray dataset from The Cancer Gene Atlas (TCGA) [69] (Figure 3G, page 109).

To test wether a soluble mediator was responsible for the increased PPARβ/δ target gene expression in TAMs, MDMs were cultured in cell free ascites samples. Expression of all five measured target genes was indeed induced by ascites (Figure 5A, page 111) and could not be further induced by co-treatment with L165,041 (Figure 5B, page 111). Induction of a luciferase reporter by ascites was dependant on the presence of a PPRE (Figure 5C, page 111), strongly hinting at a PPAR-family member being involved. Cell free ascites induced the target genes *PDK4* and *ANGPTL4* in murine bone marrow-derived macrophages of wild type mice, but not in cells from a *PPARD* deletion mutant (Figure 5D, page 111).

Since all known endogenous PPARβ/δ agonists are fatty acids, an analysis of 97 fatty acid molecules in 38 different ascites samples was performed by liquid chromatography mass spectometry mass spectometry (LC-MS/MS). Several known PPARβ/δ agonists were present in concentrations that exceed

[1] Angiopoietin-like 4

their half maximal effective concentration (EC_{50}) by three orders of magnitude (Figure 6A, page 112). A selection of the polyunsaturated fatty acids present in ascites (LA, AA, docosahexaenoic acid (DHA), eicosapentaenoic acid and α-linolenic acid (ALA)) were added to MDM cultures (at a concentration of 20 µM, which is comparable to that found in ascites (Figure 6A, page 112)). LA, AA and DHA led to an induction (>10x) of the PPARβ/δ target gene *PDK4* after 24 h (Figure 6B, page 112). Induction by LA (or a number of its derivatives) was rapid (3 h), dosage dependent (Figure 6C, page 112) and not restricted to *PDK4*: *ANGPTL4*, *CD300A*, *CPT1A*[1], *LRP5*[2], *PLIN2*[3], and *SLC25A20*[4] were also induced (Figure 6D, page 112). The previously described PPARβ/δ agonists 15-HETE [66] and prostacyclin[5] were present at concentrations two orders of magnitude below their respective EC_{50} (Figure 6F, page 112).

3.3.2 Discussion

We have, for the first time, characterized the previously described high fatty acid content in ascites [11, 112] via lipidomic analysis. The level of known PPARβ/δ agonistic PUFAs exceeded their respective EC_{50} by orders of magnitude. The observed PPARβ/δ target gene expression in TAMs, the lack of response to synthetic PPARβ/δ agonist and the strong response to PPARβ/δ inverse agonist are in agreement with these PUFAs acting as bona-fide PPARβ/δ agonists in ascites. While blood plasma also contains large concentrations of PUFAs [27], PPARβ/δ itself was expressed in blood monocytes at a very low level (Figure 2A, page 106, and [2] Figures 1A, 1B, page 88), precluding target gene induction. The PUFA effect on PPARβ/δ target genes was sustained for several days when the PUFAs were no longer present in the surrounding medium, possibly due to their storage in lipid droplets (Figure 7, page 113)[6].

[1] Carnitine palmitoyltransferase I

[2] lipoprotein receptor-related proteins family member

[3] Perilipin 2

[4] solute carrier family 25 member 20 (carnitine/acylcarnitine translocase)

[5] Prostacyclin levels were measured by its stable degradation product 6-keto-prostaglandin $F_{1\alpha}$

[6] MDM were kept in serum-free medium for 7 days during differentiation and presumably consumed all blood PUFAs that monocytes might have accumulated during this time.

Among the deregulated PPARβ/δ target genes are *ANGPTL4*, which is a known tumor metastasis and invasion promoter [3, 73]; *CD300A* and *FOS*[1], which act in macrophage polarization [98, 39]; and *LRP5*, an activator of WNT signaling [97]. The massive induction of *PDK4* suggests that the TAMs might be shifted to a more glycolytic metabolism [115], improving survival in hypoxic conditions.

Inverse PPARβ/δ agonists are capable of repressing target gene expression even in the presence of endogenous agonists at ascites levels, suggesting that they could potentially be used to interfere with the tumor promoting effects of ascites via PPARβ/δ target genes.

3.3.3 My contribution

My contributions were the analysis of ChIPseq (Figure 2E, 2F) and RNAseq (Figure 2B, 2C, 3A, 3B, 3C, Table 1) data. I am a co-author of this manuscript.

[1] Fos proto-oncogene, AP-1 transcription factor subunit

3.4 The transcriptional signature of human ovarian carcinoma macrophages is associated with extracellular matrix reorganization[1]

3.4.1 Results

Schumann et al [90] established that cultured, monocyte-derived macrophages had a quite different morphological and transcriptional phenotype from *ex vivo* tumor associtated macrophages (see section: 3.3). In our quest to understand the role of tumor associated macrophages in ascites, we therefore looked for a less artificial non-cancer reference and found it in peritoneal macrophages (pMPHs) from patients with non-malignant afflictions, such as uterine myomatosis, ovarian cysts or endometriosis. Using only primary cells *ex vivo* allowed us to avoid cell culture artefacts.

3.4.1.1 TAMs and pMPHs appear as one phenotype, distinct from MDMs

There was little difference in the percentage of positive cells for various macrophage and M2 markers between the TAM and pMPH populations (Figure 1A, page 123).

Only $\%CD163_{positive}$ and $\%CD206_{positive}$ reached basic statistical significance, but the distributions were overlapping. On the level of mean fluorescence intensity (MFI), no significant difference was observed except for CD206 and HLA-DR[2] which were increased 2-3 fold on pMPHs (Figure 1B, page 123). In summary there were detectable differences between the two cell types that very weakly (and unexpectedly) suggest a more immuno-suppressive state in pMPHs.

Next, we compared pMPHs with TAMs and with MDMs (which were *in vitro* differentiated and unactivated) on a transcriptional level (4, 17 and 3 samples, respectively). pMPHs were much more similar to TAMs than to MDMs

[1] Published in F. Finkernagel et al. "The transcriptional signature of human ovarian carcinoma macrophages is associated with extracellular matrix reorganization." In: *Oncotarget* (2016). DOI: 10.18632/oncotarget.12180, see page 121 for full text.

[2] Human Leukocyte Antigen - antigen D Related

on both a global (Figure 2A, 2B, 2C, page 124) and single gene level (Figure 3A, page 125) as evidenced by RNAseq and quantitative polymerase chain reaction (qPCR) respectively. TAMs and pMPHs had very similar macrophage activation marker expression, the pattern of which did not fit into the classical M1-M2 polarization scheme (or to the unactivated MDMs, Figure 3A, page 125).

The expression of a set of pro-tumorigenic cytokine and signaling molecule genes, previously identified to be primarily expressed by TAMs (but not by tumor cells) in ascites ([81], see page 10) was analyzed by RNAseq. pMPHs (but not MDMs) expressed these at TAM-like levels (Figure 3B, page 125). We therefore concluded that pMPHs and TAMs have a common activation phenotype.

In mice, residential macrophages can be discriminated from blood derived macrophages by the expression of residential marker genes. *ADGRE1*[1] [30], *GATA6*[2] [18] and *TIMD4*[3] [99] expression marks residential macrophages, while *CD52* is a marker for monocyte-derived cells [10]. The human homologues of the residential markers (and their proteins) are expressed in TAMs and pMPHs, but not in MDMs, and the inverse holds true for *CD52* (Figure 3A, page 125, Figure 1D, page 123). This is evidence of a residential origin of TAMs and pMPHs.

3.4.1.2 Activation state of TAMs

The similarity in global expression profiles between TAMs and pMPHs suggested that TAMs retain some macrophage-mediated immune functions. Indeed, TAMs were capable of phagocytosis at the same level as MDMs (as a positive control) (Figure 4A, 4B, page 126). TAMs also showed no difference in antigen-specific $CD8^+$T-cell activation (Figure 4C, page 126). In contrast, the transcriptional activation of *IL12B* by LPS is abrogated in TAMs (Figure 4D, page 126). The same is true for the secretion of p40[4], the product of *IL12B* (Figure 4E, page 126). p40 is a subunit of IL-12 which enhances the cytotoxic activity of $CD8^+$T-cells [55].

[1] EGF-like module-containing mucin-like hormone receptor-like 1 - also known as F4/80
[2] GATA-binding factor 6
[3] T-cell immunoglobulin and mucin domain containing 4
[4] Interleukin 12 subunit beta protein; product of gene *IL12B*

3.4.1.3 Gene expression differences between TAMs and pMPHs reveal an extracellular matrix related gene cluster

Though the two peritoneal macrophages groups appeared largely similar, differential gene expression analysis using edgeR [84] revealed 30 genes that have increased expression in TAMs compared to pMPHs (Figure 5B, page 127). Only five genes were regulated in an opposite manner. In contrast, the number of differentially induced genes between TAMs and MDMs was much higher: 497 genes. The induced gene sets were overlapping with 20 of the genes found to be differentially regulated when comparing TAM vs. pMPH also showing significant induction when comparing TAMs and MDMs (Figure 5B, page 127). None of the 5 repressed genes were seen in both comparisons. We therefore focused on the 20 genes with the stronger evidence of TAM specificity.

Functional annotation indicated that the set of induced genes was enriched for extracellular matrix (ECM) organization (Figure 5C, page 127). Based on Pearson-correlation-based clustering across the patients, the ECM genes are not only induced in TAMs, but also appeared to be co-regulated (Figure 5E, page 127, "ECM Cluster"). Figure 6A, page 127, shows that all but three of these genes were induced not only when comparing TAMs vs. pMPHs, but also when comparing TAMs to MDMs.

While these genes are TAM specific in the sense that they're induced when compared to pMPHs, TAMs are not the only cells expressing them in the ascites environment: tumor cells express them at TAM-like levels (Figure 6B, page 127).

3.4.2 Discussion

3.4.2.1 TAMs are pMPH derived cells

Our data showed surprisingly little difference between TAMs and tissue resident macrophages from patients with non-cancerous afflictions (pMPHs). The activation state of TAMs appears identical to that of pMPHs (Figures 1A-C, page 123). In agreement with their expression of the M2 markers CD163 [51] and CD206 [5], TAMs were capable of efficient phagocytosis. Antigen-specific

T cell response in TAMs was at levels similar to pMPHs [109]. (Figures 2 A-C, page 124).

TAMs express pro-tumorigenic proteins [81] (see Reinartz *et al.* Figure 4, page 58), but their gene expression did not differ between TAMs and pMPHs (Figure 3B, page 125). In agreement with the literature [8, 32, 36, 37, 88, 93]), we found TAMs to be refractory to inflammatory stimuli such as LPS (Figure 2D, page 124), which appears to be ascites-mediated[1]. This finding suggests that the tumor environment does not induce anti-inflammatory polarization in macrophages nor does it inhibit pro-inflammatory polarization any more than the benign peritoneal environment.

3.4.2.2 Human TAMs resemble residential macrophages

In mice, macrophages derive from at least two sources with distinct functional properties [30]. Residential cells, which are of fetal origin, differ from infiltrating monocytes by specific expression markers, such as TIMD4, GATA6 and ADGRE1. TAMs and pMPHs also show higher expression levels for these genes than the *in vitro* monocyte-derived macrophages. This finding suggests that, if such a dichotomy is also present in *Homo sapiens*, residential macrophages are a likely source of TAMs.

3.4.2.3 The extracellular-matrix cluster

Our analysis of RNAseq data identified a cluster of 19 closely co-regulated genes that are expressed more strongly in TAMs than in pMPHs or MDMs (Figure 5E, page 127). All of these genes - which we denote as ECM cluster - are involved in extracellular-matrix related processes such as collagen deposition, fibrillogenesis and ECM remodeling.

Our data is compatible with a model in which macrophages aid in tumor progression by secreting ECM remodeling factors. Macrophages clearly increase peritoneal colonization as shown in macrophage depletion experiments

[1] It would have been of interest to perform this experiment in pMPHs, but no appropriate culture model was available

in mice [85]. In another study, MMP9[1] deletion resulted in reduced tumor incidence, growth and decreased macrophage infiltration when injected with human ovarian cancer cell [41]. Injecting wild type spleen cells rescued the effect.

A link between ECM remodeling genes and a poor clinical outcome in ovarian cancer has been noted previously (e.g. [13]). Together with our data this suggests that macrophage triggered ECM remodelling is at least one of the mechanisms by which TAMs promote ovarian cancer progression [15].

3.4.3 My contribution

My contribution was the extensive analysis of RNAseq data.

[1] matrix metalloprotease 9

CHAPTER 4

REFERENCES

[1] T. Adhikary et al. "Genomewide analyses define different modes of transcriptional regulation by peroxisome proliferator-activated receptor-β/δ (PPARβ/δ)". In: *PLoS ONE* (2011). DOI: 10.1371/journal.pone.0016344.

[2] T. Adhikary et al. "The transcriptional PPARβ/δ network in human macrophages defines a unique agonist-induced activation state." In: *Nucleic acids research* (2015). DOI: 10.1093/nar/gkv331.

[3] T. Adhikary et al. "Inverse PPARβ/δ agonists suppress oncogenic signaling to the ANGPTL4 gene and inhibit cancer cell invasion". In: *Oncogene* (2013). DOI: 10.1038/onc.2012.549.

[4] J. Ahn et al. "DeMix: Deconvolution for mixed cancer transcriptomes using raw measured data". In: *Bioinformatics* (2013). DOI: 10.1093/bioinformatics/btt301.

[5] R. Alan, B. Ezekowitz, and S. Gordon. "Alterations of Surface Properties by Macrophage Activation: Expression of Receptors for Fc and Mannose-Terminal Glycoproteins and Differentiation Antigens". In: 1984. DOI: 10.1007/978-1-4757-1445-6_2.

[6] L. A. Baldwin et al. "Ten-year relative survival for epithelial ovarian cancer." In: *Obstetrics and gynecology* (2012). DOI: 10.1097/AOG.0b013e318264f794.

[7] O. Bardot et al. "PPAR-RXR Heterodimer Activates a Peroxisome Proliferator Response Element Upstream of the Bifunctional Enzyme Gene". In: *Biochemical and Biophysical Research Communications* (1993). DOI: 10.1006/bbrc.1993.1378.

[8] S. K. Biswas et al. "A distinct and unique transcriptional program expressed by tumor-associated macrophages (defective NF-κB and enhanced IRF-3/STAT1 activation)". In: *Blood* (2006). DOI: 10.1182/blood-2005-01-0428.

[9] F. Borrego. "The CD300 molecules: an emerging family of regulators of the immune system." In: *Blood* (2013). DOI: 10.1182/blood-2012-09-435057.

[10] A. G. S. Buggins et al. "Peripheral blood but not tissue dendritic cells express CD52 and are depleted by treatment with alemtuzumab." In: *Blood* (2002). Pubmed ID: 12176892.

[11] W. H. Caselmann and D. Jüngst. "Isolation and characterization of a cellular protein-lipid complex from ascites fluid caused by various neoplasms." In: *Cancer research* (1986). Pubmed ID: 3080244.

[12] A. Chawla. "Control of macrophage activation and function by PPARs." In: *Circulation research* (2010). DOI: 10.1161/CIRCRESAHA.110.216523.

[13] D.-J. J. Cheon et al. "A collagen-remodeling gene signature regulated by TGF-β signaling is associated with metastasis and poor survival in serous ovarian cancer." In: *Clinical cancer research : an official journal of the American Association for Cancer Research* (2014). DOI: 10.1158/1078-0432.CCR-13-1256.

[14] Y. J. Choi et al. "Effects of the PPAR-δ agonist MBX-8025 on atherogenic dyslipidemia". In: *Atherosclerosis* (2012). DOI: 10.1016/j.atherosclerosis.2011.10.029.

[15] E. K. Colvin. "Tumor-associated macrophages contribute to tumor progression in ovarian cancer." In: *Frontiers in oncology* (2014). DOI: 10.3389/fonc.2014.00137.

[16] J. Condeelis and J. W. Pollard. "Macrophages: obligate partners for tumor cell migration, invasion, and metastasis." In: *Cell* (2006). DOI: 10.1016/j.cell.2006.01.007.

[17] J. Coward et al. "Interleukin-6 as a therapeutic target in human ovarian cancer." In: *Clinical cancer research : an official journal of the American Association for Cancer Research* (2011). DOI: 10.1158/1078-0432.CCR-11-0945.

[18] L. C. Davies and P. R. Taylor. "Tissue-resident macrophages: then and now". In: *Immunology* (2015). DOI: 10.1111/imm.12451.

[19] A. S. Dickey et al. "PPAR-δ is repressed in Huntington's disease, is required for normal neuronal function and can be targeted therapeutically". In: *Nature Medicine* (2015). DOI: 10.1038/nm.4003.

[20] A. Dobin et al. "STAR: ultrafast universal RNA-seq aligner." In: *Bioinformatics (Oxford, England)* (2013). DOI: 10.1093/bioinformatics/bts635.

[21] D. Duluc et al. "Tumor-associated leukemia inhibitory factor and IL-6 skew monocyte differentiation into tumor-associated macrophage-like cells." In: *Blood* (2007). DOI: 10.1182/blood-2007-02-072587.

[22] E. Ehrenborg and J. Skogsberg. "Peroxisome proliferator-activated receptor delta and cardiovascular disease". In: *Atherosclerosis* (2013). DOI: 10.1016/j.atherosclerosis.2013.08.027.

[23] K. H. Eng and C. Ruggeri. "Connecting prognostic ligand receptor signaling loops in advanced ovarian cancer". In: *PLoS One.* (2014). DOI: 10.1371/journal.pone.0107193.

[24] T. Fauti et al. "Induction of PPARβ and prostacyclin (PGI2) synthesis by Raf signaling: Failure of PGI2 to activate PPARβ". In: *FEBS Journal* (2006). DOI: 10.1111/j.1742-4658.2005.05055.x.

[25] F. Finkernagel et al. "The transcriptional signature of human ovarian carcinoma macrophages is associated with extracellular matrix reorganization." In: *Oncotarget* (2016). DOI: 10.18632/oncotarget.12180.

[26] P. Flicek et al. "Ensembl 2014." In: *Nucleic acids research* (2014). DOI: 10.1093/nar/gkt1196.

[27] D. A. Fraser et al. "Changes in plasma free fatty acid concentrations in rheumatoid arthritis patients during fasting and their effects upon T-lymphocyte proliferation." In: *Rheumatology (Oxford, England)* (1999). DOI: 10.1093/rheumatology/38.10.948.

[28] D. I. Gabrilovich, S. Ostrand-Rosenberg, and V. Bronte. "Coordinated regulation of myeloid cells by tumours". In: *Nature Reviews Immunology* (2012). DOI: 10.1038/nri3175.

[29] P. Germain et al. "International Union of Pharmacology. LXIII. Retinoid X receptors." In: *Pharmacological reviews* (2006). DOI: 10.1124/pr.58.4.7.

[30] E. Gomez Perdiguero et al. "Tissue-resident macrophages originate from yolk-sac-derived erythro-myeloid progenitors". In: *Nature* (2014). DOI: 10.1038/nature13989.

[31] T. Gong and J. D. Szustakowski. "DeconRNASeq: A statistical framework for deconvolution of heterogeneous tissue samples based on mRNA-Seq data". In: *Bioinformatics* (2013). DOI: 10.1093/bioinformatics/btt090.

[32] I. O. Gordon and R. S. Freedman. "Defective antitumor function of monocyte-derived macrophages from epithelial ovarian cancer patients". In: *Clinical Cancer Research* (2006). DOI: 10.1158/1078-0432.CCR-05-2254.

[33] R. A. Gupta et al. "Prostacyclin-mediated activation of peroxisome proliferator-activated receptor delta in colorectal cancer." In: *Proceedings of the National Academy of Sciences of the United States of America* (2000). DOI: 10.1073/pnas.97.24.13275.

[34] B. B. Gyorffy et al. "Implementing an online tool for genome-wide validation of survival-associated biomarkers in ovarian-cancer using microarray data from 1287 patients." In: *Endocrine-related cancer* (2012). DOI: 10.1530/ERC-11-0329.

[35] K. Hack et al. "Skin-targeted inhibition of PPAR ??/?? by selective antagonists to treat PPAR ??/?? - mediated psoriasis-like skin disease in vivo". In: *PLoS ONE* (2012). DOI: 10.1371/journal.pone.0037097.

[36] T. Hagemann et al. ""Re-educating" tumor-associated macrophages by targeting NF-kappaB". In: *The Journal of experimental medicine* (2008). DOI: 10.1084/jem.20080108.

[37] T. Hagemann et al. "Regulation of macrophage function in tumors: the multifaceted role of NF-kappaB." In: *Blood* (2009). DOI: 10.1182/blood-2008-12-172825.

[38] D. Hanahan and R. A. Weinberg. "Hallmarks of cancer: the next generation." In: *Cell* (2011). DOI: 10.1016/j.cell.2011.02.013.

[39] Y. Higuchi et al. "Enhancement of c-fos expression is associated with activated macrophages". In: *Oncogene* (1988). Pubmed ID: 3131720.

[40] B. Hoesel and J. A. Schmid. "The complexity of NF-κB signaling in inflammation and cancer". In: *Molecular Cancer* (2013). DOI: 10.1186/1476-4598-12-86.

[41] S. Huang et al. "Contributions of stromal metalloproteinase-9 to angiogenesis and growth of human ovarian carcinoma in mice." In: *Journal of the National Cancer Institute* (2002). DOI: 10.1093/jnci/94.15.1134.

[42] A. Iwashita et al. "Neuroprotective efficacy of the peroxisome proliferator-activated receptor delta-selective agonists in vitro and in vivo." In: *The Journal of pharmacology and experimental therapeutics* (2007). DOI: 10.1124/jpet.106.115758.

[43] H. J. Junge et al. "TSPAN12 Regulates Retinal Vascular Development by Promoting Norrin- but Not Wnt-Induced FZD4/β-Catenin Signaling". In: *Cell* (2009). DOI: 10.1016/j.cell.2009.07.048.

[44] S. Kahremany et al. "Activation of PPARδ: from computer modelling to biological effects." In: *British journal of pharmacology* (2015). DOI: 10.1111/bph.12950.

[45] E. L. Kaplan and P. Meier. "Nonparametric Estimation from Incomplete Observations". In: *Journal of the American Statistical Association* (1958). DOI: 10.2307/2281868.

[46] G. Krey et al. "Xenopus peroxisome proliferator activated receptors: genomic organization, response element recognition, heterodimer formation with retinoid X receptor and activation by fatty acids." In: *The Journal of steroid biochemistry and molecular biology* (1993). DOI: 10.1016/0960-0760(93)90058-5.

[47] A. Kuhn et al. "Population-specific expression analysis (PSEA) reveals molecular changes in diseased brain". In: *Nature Methods* (2011). DOI: 10.1038/nmeth.1710.

[48] H. Kulbe et al. "A Dynamic Inflammatory Cytokine Network in the Human Ovarian Cancer Microenvironment". In: *Cancer Research* (2012). DOI: 10.1158/0008-5472.CAN-11-2178.

[49] B. Langmead and S. L. Salzberg. "Fast gapped-read alignment with Bowtie 2". In: *Nature Methods* (2012). DOI: 10.1038/nmeth.1923.

[50] W. Lau et al. "The R-spondin/Lgr5/Rnf43 module: regulator of Wnt signal strength". In: *Genes & Development* (2014). DOI: 10.1101/gad.235473.113.

[51] S. K. Law et al. "A new macrophage differentiation antigen which is a member of the scavenger receptor superfamily." In: *European journal of immunology* (1993). DOI: 10.1002/eji.1830230940.

[52] J. A. Ledermann et al. "Newly diagnosed and relapsed epithelial ovarian carcinoma: ESMO Clinical Practice Guidelines for diagnosis, treatment and follow-up". In: *Annals of Oncology* (2013). DOI: 10.1093/annonc/mdt333.

[53] E. Lengyel. "Ovarian Cancer Development and Metastasis". In: *The American Journal of Pathology* (2010). DOI: 10.2353/ajpath.2010.100105.

[54] Y. Li and X. Xie. "A mixture model for expression deconvolution from RNA-seq in heterogeneous tissues." In: *BMC bioinformatics* (2013). DOI: 10.1186/1471-2105-14-S5-S11.

[55] J. N. Macgregor et al. "Ex vivo culture with interleukin (IL)-12 improves CD8(+) T-cell adoptive immunotherapy for murine leukemia independent of IL-18 or IFN-gamma but requires perforin." In: *Cancer research* (2006). DOI: 10.1158/0008-5472.CAN-05-3507.

[56] N. Mantel. "Evaluation of survival data and two new rank order statistics arising in its consideration." In: *Cancer chemotherapy reports. Part 1* (1966). Pubmed ID: 5910392.

[57] A. Mantovani et al. "The chemokine system in diverse forms of macrophage activation and polarization." In: *Trends in immunology* (2004). DOI: 10.1016/j.it.2004.09.015.

[58] S. Marchini et al. "Resistance to platinum-based chemotherapy is associated with epithelial to mesenchymal transition in epithelial ovarian cancer." In: *European journal of cancer (Oxford, England : 1990)* (2013). DOI: 10.1016/j.ejca.2012.06.026.

[59] F. O. Martinez and S. Gordon. "The M1 and M2 paradigm of macrophage activation: time for reassessment". In: *F1000Prime Reports* (2014). DOI: 10.12703/P6-13.

[60] F. Martinon et al. "NALP inflammasomes: a central role in innate immunity." In: *Seminars in immunopathology* (2007). DOI: 10.1007/s00281-007-0079-y.

[61] K. McLean et al. "Human ovarian carcinoma–associated mesenchymal stem cells regulate cancer stem cells and tumorigenesis via altered BMP production." In: *The Journal of clinical investigation* (2011). DOI: 10.1172/JCI45273.

[62] C. D. Mills et al. "M-1/M-2 macrophages and the Th1/Th2 paradigm." In: *Journal of immunology (Baltimore, Md. : 1950)* (2000). DOI: 10.4049/jimmunol.164.12.6166.

[63] R. Müller et al. "A Role for PPARbeta/delta in Tumor Stroma and Tumorigenesis". In: *PPAR Research* (2008). DOI: 10.1155/2008/534294.

[64] D. H. Munn and A. L. Mellor. "Indoleamine 2,3 dioxygenase and metabolic control of immune responses". In: *Trends in Immunology* (2013). DOI: 10.1016/j.it.2012.10.001.

[65] P. J. Murray et al. “Macrophage Activation and Polarization: Nomenclature and Experimental Guidelines”. In: *Immunity* (2014). DOI: 10.1016/j.immuni.2014.06.008.

[66] S. Naruhn, W. Meissner, and T. Adhikary. “15-Hydroxyeicosatetraenoic Acid Is a Preferential Peroxisome Proliferator-Activated Receptor B/Δ Agonist”. In: *Molecular Pharmacology* (2010). DOI: 10.1124/mol.109.060541.pressors.

[67] S. Naruhn et al. “15-hydroxyeicosatetraenoic acid is a preferential peroxisome proliferator-activated receptor beta/delta agonist.” In: *Molecular pharmacology* (2010). DOI: 10.1124/mol.109.060541.

[68] S. Naruhn et al. “High-Affinity Peroxisome Proliferator-Activated Receptor / -Specific Ligands with Pure Antagonistic or Inverse Agonistic Properties”. In: *Molecular Pharmacology* (2011). DOI: 10.1124/mol.111.074039.

[69] T. Network et al. “Integrated genomic analyses of ovarian carcinoma”. In: *Nature* (2011). DOI: 10.1038/nature10166.

[70] A. M. Newman et al. “Robust enumeration of cell subsets from tissue expression profiles.” In: *Nature methods* (2015). DOI: 10.1038/nmeth.3337.

[71] W. R. Oliver et al. “A selective peroxisome proliferator-activated receptor delta agonist promotes reverse cholesterol transport.” In: *Proceedings of the National Academy of Sciences* (2001). DOI: 10.1073/pnas.091021198.

[72] D. Padua and J. Massague. “Roles of TGFbeta in metastasis”. In: *Cell Res.* (2009). DOI: 10.1038/cr.2008.316.

[73] D. Padua et al. “TGFbeta primes breast tumors for lung metastasis seeding through angiopoietin-like 4.” In: *Cell* (2008). DOI: 10.1016/j.cell.2008.01.046.

[74] P. Peng, Y. Yan, and S. Keng. “Exosomes in the ascites of ovarian cancer patients: origin and effects on anti-tumor immunity.” In: *Oncology reports* (2011). DOI: 10.3892/or.2010.1119.

[75] J. M. Peters, Y. M. Shah, and F. J. Gonzalez. "The role of peroxisome proliferator-activated receptors in carcinogenesis and chemoprevention". In: *Nature Reviews Cancer* (2012). DOI: 10.1038/nrc3214.

[76] K. Planutis, M. Planutiene, and R. F. Holcombe. "A novel signaling pathway regulates colon cancer angiogenesis through Norrin". In: *Sci Rep.* (2014). DOI: 10.1038/srep05630.

[77] C. Præstegaard et al. "The association between socioeconomic status and tumour stage at diagnosis of ovarian cancer: A pooled analysis of 18 case-control studies". In: *Cancer Epidemiology* (2016). DOI: 10.1016/j.canep.2016.01.012.

[78] J. Prat. "FIGO's staging classification for cancer of the ovary, fallopian tube, and peritoneum: abridged republication". In: *Journal of Gynecologic Oncology* (2015). DOI: 10.3802/jgo.2015.26.2.87.

[79] B.-Z. Qian and J. W. Pollard. "Macrophage Diversity Enhances Tumor Progression and Metastasis". In: *Cell* (2010). DOI: 10.1016/j.cell.2010.03.014.

[80] G. Quon et al. "Computational purification of individual tumor gene expression profiles leads to significant improvements in prognostic prediction". In: *Genome Med.* (2013). DOI: 10.1186/gm433.

[81] S. Reinartz et al. "A transcriptome-based global map of signaling pathways in the ovarian cancer microenvironment associated with clinical outcome." In: *Genome biology* (2016). DOI: 10.1186/s13059-016-0956-6.

[82] S. Reinartz et al. "Mixed-polarization phenotype of ascites-associated macrophages in human ovarian carcinoma: Correlation of CD163 expression, cytokine levels and early relapse". In: *International Journal of Cancer* (2014). DOI: 10.1002/ijc.28335.

[83] M. Riester et al. "Risk prediction for late-stage ovarian cancer by meta-analysis of 1525 patient samples". In: *Journal of the National Cancer Institute* (2014). DOI: 10.1093/jnci/dju048.

[84] M. D. Robinson, D. J. McCarthy, and G. K. Smyth. "edgeR: A Bioconductor package for differential expression analysis of digital gene expression data". In: *Bioinformatics* (2009). DOI: 10.1093/bioinformatics/btp616.

[85] T. M. Robinson-Smith et al. "Macrophages mediate inflammation-enhanced metastasis of ovarian tumors in mice." In: *Cancer research* (2007). DOI: 10.1158/0008-5472.CAN-06-4375.

[86] M. Romanowska et al. "Activation of PPARβ/δ Causes a Psoriasis-Like Skin Disease In Vivo". In: *PLoS ONE* (2010). DOI: 10.1371/journal.pone.0009701.

[87] D. G. Rosen et al. "The role of constitutively active signal transducer and activator of transcription 3 in ovarian tumorigenesis and prognosis." In: *Cancer* (2006). DOI: 10.1002/cncr.22293.

[88] A. Saccani et al. "p50 nuclear factor-kappaB overexpression in tumor-associated macrophages inhibits M1 inflammatory responses and antitumor resistance." In: *Cancer research* (2006). DOI: 10.1158/0008-5472.CAN-06-1867.

[89] A. Sahebkar, G. T. Chew, and G. F. Watts. "New peroxisome proliferator-activated receptor agonists: potential treatments for atherogenic dyslipidemia and non-alcoholic fatty liver disease." In: *Expert opinion on pharmacotherapy* (2014). DOI: 10.1517/14656566.2014.876992.

[90] T. Schumann et al. "Deregulation of PPARβ/δ target genes in tumor-associated macrophages by fatty acid ligands in the ovarian cancer microenvironment". In: *Oncotarget* (2015). DOI: 10.18632/oncotarget.3826.

[91] Q. Shen et al. "contamDE : Differential expression analysis of RNA-seq data for contaminated tumor samples". In: *Bioinformatics* (2015). DOI: 10.1093/bioinformatics/btv657.

[92] J. Sheng, C. Ruedl, and K. Karjalainen. "Most Tissue-Resident Macrophages Except Microglia Are Derived from Fetal Hematopoietic Stem Cells". In: *Immunity* (2015). DOI: 10.1016/j.immuni.2015.07.016.

[93] A. Sica and A. Mantovani. "Macrophage plasticity and polarization: in vivo veritas". In: *J Clin Invest.* (2012). DOI: 10.1172/JCI59643.

[94] L. Stevens et al. "Plexin B1 Suppresses c-Met in Melanoma: A Role for Plexin B1 as a Tumor-Suppressor Protein through Regulation of c-Met". In: *Journal of Investigative Dermatology* (2010). DOI: 10.1038/jid.2010.13.

[95] D. S. Straus and C. K. Glass. "Anti-inflammatory actions of PPAR ligands: new insights on cellular and molecular mechanisms". In: *Trends in Immunology* (2007). DOI: 10.1016/j.it.2007.09.003.

[96] K. Takaishi et al. "Involvement of M2-polarized macrophages in the ascites from advanced epithelial ovarian carcinoma in tumor progression via Stat3 activation." In: *Cancer science* (2010). DOI: 10.1111/j.1349-7006.2010.01652.x.

[97] K. Tamai et al. "LDL-receptor-related proteins in Wnt signal transduction". In: *Nature* (2000). DOI: 10.1038/35035117.

[98] T. Tanaka et al. "PPARβ/δ activation of CD300a controls intestinal immunity." In: *Scientific reports* (2014). DOI: 10.1038/srep05412.

[99] T. B. Thornley et al. "Fragile TIM-4-expressing tissue resident macrophages are migratory and immunoregulatory." In: *The Journal of clinical investigation* (2014). DOI: 10.1172/JCI73527.

[100] S. Uddin et al. "Overexpression of leptin receptor predicts an unfavorable outcome in Middle Eastern ovarian cancer." In: *Molecular cancer* (2009). DOI: 10.1186/1476-4598-8-74.

[101] M. Uhlen et al. "Tissue-based map of the human proteome". In: *Science* (2015). DOI: 10.1126/science.1260419.

[102] R. Vang, I.-M. Shih, and R. J. Kurman. "Fallopian tube precursors of ovarian low- and high-grade serous neoplasms". In: *Histopathology* (2013). DOI: 10.1111/his.12046.

[103] T. Varga, Z. Czimmerer, and L. Nagy. "PPARs are a unique set of fatty acid regulated transcription factors controlling both lipid metabolism and inflammation". In: *Biochimica et Biophysica Acta (BBA) - Molecular Basis of Disease* (2011). DOI: 10.1016/j.bbadis.2011.02.014.

[104] C. Varol, A. Mildner, and S. Jung. "Macrophages: Development and Tissue Specialization". In: *Annual Review of Immunology* (2015). DOI: 10.1146/annurev-immunol-032414-112220.

[105] N. Viswakarma et al. "Coactivators in PPAR-Regulated Gene Expression." In: *PPAR research* (2010). DOI: 10.1155/2010/250126.

[106] H. Vosper et al. "The Peroxisome Proliferator-activated Receptor d Promotes Lipid Accumulation in Human Macrophages". In: *J. Biol. Chem.* (2001). DOI: 10.1074/jbc.M108482200.

[107] N. Wang et al. "UNDO: a Bioconductor R package for unsupervised deconvolution of mixed gene expressions in tumor samples". In: *Bioinformatics* (2015). DOI: 10.1093/bioinformatics/btu607.

[108] S. H. Wrzesinski, Y. Y. Wan, and R. A. Flavell. "Transforming Growth Factor- and the Immune Response: Implications for Anticancer Therapy". In: *Clinical Cancer Research* (2007). DOI: 10.1158/1078-0432.CCR-07-1157.

[109] W. Xu et al. "Human peritoneal macrophages show functional characteristics of M-CSF-driven anti-inflammatory type 2 macrophages." In: *European journal of immunology* (2007). DOI: 10.1002/eji.200737042.

[110] J. Xue et al. "Transcriptome-Based Network Analysis Reveals a Spectrum Model of Human Macrophage Activation". In: *Immunity* (2014). DOI: 10.1016/j.immuni.2014.01.006.

[111] V. K. Yadav and S. De. "An assessment of computational methods for estimating purity and clonality using genomic data derived from heterogeneous tumor tissue samples". In: *Briefings in Bioinformatics* (2015). DOI: 10.1093/bib/bbu002.

[112] D. Yam et al. "Subcutaneous, omentum and tumor fatty acid composition, and serum insulin status in patients with benign or cancerous ovarian or endometrial tumors. Do tumors preferentially utilize polyunsaturated fatty acids?" In: *Cancer Letters* (1997). DOI: 10.1016/S0304-3835(96)04530-2.

[113] K. Yoshihara et al. "Inferring tumour purity and stromal and immune cell admixture from expression data". In: *Nature Communications* (2013). DOI: 10.1038/ncomms3612.

[114] P. P. Zandi et al. "Association study of wnt signaling pathway genes in bipolar disorder". In: *Archives of General Psychiatry* (2008). DOI: 10.1001/archpsyc.65.7.785.

[115] S. Zhang et al. "The pivotal role of pyruvate dehydrogenase kinases in metabolic flexibility". In: *Nutrition & Metabolism* (2014). DOI: 10.1186/1743-7075-11-10.

[116] Y. Zhang et al. "Model-based Analysis of ChIP-Seq (MACS)". In: *Genome Biology* (2008). DOI: 10.1186/gb-2008-9-9-r137.

[117] X. Zuo et al. "Targeted Genetic Disruption of Peroxisome Proliferator-Activated Receptor- and Colonic Tumorigenesis". In: *JNCI Journal of the National Cancer Institute* (2009). DOI: 10.1093/jnci/djp078.

CHAPTER 5

GLOSSARIES

5.1 Abbreviations

5-HETE 5-Hydroxyeicosatetraenoic acid 11

15-HETE 15-Hydroxyeicosatetraenoic acid 4, 11, 24

AA arachidonic acid 4, 11, 14, 15, 24

ALA α-linolenic acid 24

BMDM (murine) bone marrow-derived macrophage 19

ChIP chromatin immunoprecipitation 22

ChIP-qPCR ChIP followed by quantitative polymerase chain reaction 16

ChIPseq ChIP followed by sequencing 16, 17, 19, 20, 25

DHA docosahexaenoic acid 24

DNA desoxyribonucleic acid 16

EC_{50} half maximal effective concentration 24

ECM extracellular matrix 28, 29

FACS fluorescence activated cell sorting 5

FCS fetal calf serum 22

GO gene ontology 10

HGSOC high grade serous ovarian carcinoma 1, 2, 8, 12, 23

L165,041 [4-[3-(4-acetyl-3-hydroxy-2-propylphenoxy)propoxy]phenoxy]acetic acid, a PPARβ/δ agonist 4, 17, 18, 22, 23

LA linoleic acid 4, 15, 22, 24

LC-MS/MS liquid chromatography mass spectometry mass spectometry . 23

LPA lysophosphatidic acids 11

LPS lipopolysaccharide 17, 18, 27, 29

LTB_4 leukotrine B4 ..... 11, 14

MACS magnetic activated cell sorting 5, 9

MDM monocyte-derived macrophage ..... iv, 16–20, 22–24, 26–29

MFI mean fluorescence intensity 26

mRNA messenger RNA 10, 16

OvCa Ovarian carcinoma 1, 11–15

PGI2 Prostaglandin I_2 4

pMPH peritoneal macrophage ..... iv, 26–29

PPRE PPAR response element 4, 23

PUFA polyunsaturated fatty acid 15, 24

qPCR quantitative polymerase chain reaction 27

RFS relapse-free-survival 11, 12, 14, 23

RNA ribonucleic acid 10

RNAseq RNA sequencing 8, 10, 11, 14, 15, 17, 19, 20, 23, 25, 27, 29, 30

RPMI-1640 Roswell Park Memorial Institute cell culture medium 1640 22

RT-qPCR reverse transcription quantitative polymerase chain reaction 10, 11, 15, 23

STIC serous tubal intraepithelial carcinoma 1

TAM tumor associtated macrophage ..... iv, 2, 3, 8–10, 12–14, 22–30

TAT tumor associtated T cell 8

TCGA The Cancer Gene Atlas 23

TPM Transcripts per Million 9

TU tumor cell 8–10, 12–14

5.2 Protein and gene names

ADGRE1 EGF-like module-containing mucin-like hormone receptor-like 1 - also known as F4/80 ..... 27, 29

ANGPTL4 Angiopoietin-like 4 23–25

β-catenin Subunit of the cadherin complex 13, 14

BCL6 B-cell lymphoma 6 17

BMP2 Bone morphogenetic protein 2 13

BMP4 Bone morphogenetic protein 4 13

CCL3 Chemokine (c-C motif) ligand 3, also known as macrophage inflammatory protein 1-alpha 20

CD8 Cluster of Differentiation 8 18

CHAPTER 6

PUBLICATIONS

Reinartz et al. Genome Biology (2016) 17:108
DOI 10.1186/s13059-016-0956-6

Genome Biology

RESEARCH Open Access

A transcriptome-based global map of signaling pathways in the ovarian cancer microenvironment associated with clinical outcome

Silke Reinartz[1†], Florian Finkernagel[2†], Till Adhikary[2], Verena Rohnalter[2], Tim Schumann[2], Yvonne Schober[3], W. Andreas Nockher[3], Andrea Nist[4], Thorsten Stiewe[4], Julia M. Jansen[1], Uwe Wagner[1], Sabine Müller-Brüsselbach[2] and Rolf Müller[2*]

Abstract

Background: Soluble protein and lipid mediators play essential roles in the tumor environment, but their cellular origins, targets, and clinical relevance are only partially known. We have addressed this question for the most abundant cell types in human ovarian carcinoma ascites, namely tumor cells and tumor-associated macrophages.

Results: Transcriptome-derived datasets were adjusted for errors caused by contaminating cell types by an algorithm using expression data derived from pure cell types as references. These data were utilized to construct a network of autocrine and paracrine signaling pathways comprising 358 common and 58 patient-specific signaling mediators and their receptors. RNA sequencing based predictions were confirmed for several proteins and lipid mediators. Published expression microarray results for 1018 patients were used to establish clinical correlations for a number of components with distinct cellular origins and target cells. Clear associations with early relapse were found for STAT3-inducing cytokines, specific components of WNT and fibroblast growth factor signaling, ephrin and semaphorin axon guidance molecules, and TGFβ/BMP-triggered pathways. An association with early relapse was also observed for secretory macrophage-derived phospholipase PLA_2G_7, its product arachidonic acid (AA) and signaling pathways controlled by the AA metabolites PGE_2, PGI_2, and LTB_4. By contrast, the genes encoding norrin and its receptor frizzled 4, both selectively expressed by cancer cells and previously not linked to tumor suppression, show a striking association with a favorable clinical course.

Conclusions: We have established a signaling network operating in the ovarian cancer microenvironment with previously unidentified pathways and have defined clinically relevant components within this network.

Keywords: Ovarian carcinoma, Tumor-associated macrophages, Tumor microenvironment, Malignancy-associated ascites, Signaling network, Arachidonic acid, IL-10, TGFβ

* Correspondence: rmueller@imt.uni-marburg.de
Silke Reinartz and Florian Finkernagel are Joint first authors
†Equal contributors
[2]Institute of Molecular Biology and Tumor Research (IMT), Center for Tumor Biology and Immunology (ZTI), Philipps University, Hans-Meerwein-Str. 3, Marburg 35043, Germany
Full list of author information is available at the end of the article

Background

Ovarian carcinoma ranks fifth as the cause of death from cancer in women with >40,000 new cases annually in the European Union [1]. Ovarian cancer has a dire prognosis with an overall five-year survival rate of <25 %. The World Health Organization classification distinguishes six major entities of ovarian tumor [1]. Of these, high grade serous ovarian carcinoma is not only the most common ovarian cancer, but also the deadliest of all gynecological malignancies. Up to 95 % of these patients with advanced stage disease present with tumor masses in the abdomen beyond the pelvis and/or lymph node metastases (FIGO stage III) or organs outside the peritoneal cavity (stage IV). These facts clearly attest to the malicious nature of this disease and identify serous ovarian cancer as a major health issue world-wide.

Several features contribute to the fatal nature of serous ovarian carcinoma, some of which make this cancer unique among all human tumors [2]. Tumor cells are often shed at a very early stage of the disease. Even at a stage when primary tumors are still confined to one or both of the ovaries, cancer cells can be detected in peritoneal lavage fluid (stage IC). While blood and the lymphatic system are major routes of dissemenation in other cancers, the spread of ovarian tumor cells is driven by the peritoneal fluid. Ovarian cancer cells then adhere to and superficially invade the omentum and the serous membranes lining other peritoneal organs, giving rise to tumor foci growing into the open space of the peritoneal cavity [2]. The peritoneal microenvironment, which is formed by the ascites building up in the peritoneal cavity, is an essential determinant of metastatic disease progression due to its tumor-promoting soluble factors [3], exosomes [4], highly tumorigenic cancer cells [5], and different types of immune cells, including pro-tumorigenic tumor-associated macrophages (TAMs) [6, 7].

TAMs are blood monocyte-derived cells polarized by factors of the tumor microenvironment to adopt phenotypes that clearly deviate from classically or alternatively activated macrophages [8–10]. This also applies to TAMs isolated from ovarian cancer ascites [7]. TAMs are pro-tumorigenic and promote all aspects of cancer growth and progression, including tumor cell proliferation, invasion, angiogenesis, formation of metastasis, and immune suppression [8, 9, 11, 12]. The critical role of TAMs has been demonstrated in numerous mouse models and is strongly supported by the correlation of clinical outcome with intratumoral macrophage density in different types of cancer [11], including ovarian carcinoma [13]. Consistent with these observations, the presence of $CD163^{high}$ TAMs in the malignancy-associated ascites showed a strong correlation with early relapse of serous ovarian carcinoma after first-line therapy [7].

Cytokines and growth factors released into the tumor microenvironment are pivotal to all aspects of tumor progression. Tumor growth, cancer dissemination, and immune escape are promoted by a plethora of growth factors and cytokines that are also found in ovarian cancer ascites [7, 14–16]. These factors (1) induce cell proliferation, such as epidermal growth factor (EGF) family members and interleukin (IL)-6, (2) trigger angiogenesis, e.g. vascular EGF (VEGF), basic FGF, and IL-8, (3) attract immune cells to the tumor, in particular chemokines of the CCL and CXCL families [17], and (4) polarize these to pro-tumorigenic and immune suppressive cells, for example VEGF, IL-6, IL-10, and LIF [18]. One of the central factors promoting tumor progression is transforming growth factor (TGF) β [19], which triggers epithelial-mesenchymal transition (EMT), cancer cell invasion, metastasis, and immune suppression. Soluble factors may also play a role in promoting stemness properties, for example, KIT ligand and R-spondins as ligands for CD117 [20] and LGR5 [21, 22], respectively. Several growth factors and cytokines also inhibit apoptosis and the efficacy of chemotherapeutic drugs, such as IL-6, IL-10, and TGFβ [23]. Finally, ascites fluid promotes its own accumulation, mainly though the action of VEGF as a vascular permeability factor [24].

A recent study evaluating publicly available genomic data has identified a number of clinical associations of signaling loops established by polypeptide ligands and their receptors in advanced ovarian cancer, including TGFβ, PDGF, VEGF, ephrin, CXCL12, and CCL chemokines [25]. However, since all expression data were derived from solid tumor tissue, tumor and host cell-specific contributions could not be analyzed, which also suggests that pathways involving host cells as major constituent were missed.

Molecules generated by the cleavage of phospholipids and present in malignant effusions represent another important class of soluble cancer-promoting mediators, in particular lysophosphatitic acid (LPA) [26–31] and arachidonic acid (AA)-derived eicosanoids [32–34]. The latter include prostanoids, hydroxyeicosatetraenoic acids (HETEs), and leukotrienes that are produced from AA by enzymatic cascades initiated either by cyclooxygenases or lipoxygenases. The importance of lipid mediators for tumorigenesis is exemplified by LPA as a mediator of cancer cell invasion and chemoresistance [28, 31, 35] and prostaglandin E_2 as an immune suppressor and trigger of angiogenesis [36].

To be able to understand the biological role of the large number of soluble mediators in the tumor microenvironment, a global picture of their cellular origins and targets is indispensible, but currently not available. One possibility is to address this question by a genomic approach. However, although transcriptomic data for a large number of solid tumor samples from ovarian

cancer patients have been published [37–39], these are not suitable to determine expression levels in tumor cells and specific tumor-associated host cells. We have addressed this issue by determining the transcriptomes for the major cell types of serous ovarian carcinoma, i.e. tumor cells and TAMs, purified from the ascites of patients. Ascites-associated cancer cells occur as single cells or multicellular spheroids and are likely to be responsible for peritoneal dissemination and to contribute to relapse of the disease [2]. In spite of their clinical relevance, genome-wide studies have not been performed with ascites-associated cells from ovarian cancer.

In the present study, we determined the transcriptome for tumor cells and TAMs from ovarian cancer ascites and used these data to construct a network comprising cytokines, growth factors, lipid mediators, and their receptors, which we confirmed for several components at the level of the respective proteins or lipids. These data defined a multitude of specific signaling pathways between tumor cells and TAMs as well as cell-type restricted, autocrine mechanisms. Furthermore, by establishing correlations with disease progression, we provide clear evidence for the biological relevance of soluble mediators in the ovarian cancer microenvironment. Thus, our data identified a highly significant link to disease recurrence not only for several cytokines and AA, but also a striking synergistic association between these proteins and AA. These findings underscore the biological relevance of functional interactions in the ovarian cancer microenvironment.

Results

Characterization of patient samples

Tumor cells and/or TAMs were isolated from the ascites of 28 patients with high grade serous ovarian carcinoma and one patient with serous borderline tumor (low grade carcinoma) (Additional file 4: Table S1). If feasible, tumor cell spheroids from the same patients were fractionated according to size (single cells: "sc"; small: <30 μm, "s"; medium: 30–40 μm, "m"; large: >40 μm, "L"). Surprisingly, small and large spheroids from the same patients frequently showed clear genetic and biological differences (Additional file 4: Table S2). For instance, small spheroids usually comprised pseudo-diploid cells, rapidly adhered to culture dishes in the presence of autologous ascites and were chemosensitive, whereas large spheroids were largely aneuploid, persisted as floating spheres in culture and were completely chemoresistant. Therefore, both small and large spheroids were included in all subsequent studies and analyzed separately.

Adjustment of RNA sequencing data for contaminating cell types

A central goal of the present study was an RNA sequencing (RNA-Seq) based comparison of the expression of signaling components of tumor cells and TAMs. We focused our study on primary, non-cultured cells in order to obtain a faithful picture of the signaling network operating in vivo. However, the presence of variable amounts (0–50 %) of TAMs in isolated tumor cell fractions and vice versa may lead to incorrect conclusions in particular for genes that show a differential, cell type-specific expression. The impact of such "contaminations" on gene expression profiles is a well-known problem and has consequently been addressed by numerous published algorithms [40–50]. However, none of these fulfills all the criteria required by our specific conditions, as explained in detail in Additional file 1.

A particularly relevant aspect in this context is the mixed-polarization phenotype of ovarian cancer ascites-associated TAMs, which share only small subsets of upregulated genes with M1 and M2 macrophages (Additional file 2: Figure S1). This precludes the use of literature data obtained with canonically activated macrophages as, for example, in CIBERSORT [48]. Likewise, the transcriptome of tumor cells from ovarian cancer ascites has not been determined yet. Therefore, appropriate reference data for ascites-derived tumor cells and TAMs were not available prior the present study. Finally, most published algorithms generate estimates of the fraction of contaminating cell types, but do not adjust the TPM values in RNA-Seq datasets.

To establish a bioinformatic tool to adjust our datasets, we used a simple but highly effective approach. First, pure reference samples representing the cell type of interest ("target") and the contaminating cell type are selected, the purity of which was confirmed by flow cytometry or other methods. RNA-Seq data for these references samples are then used to select a set of contamination marker genes, suitable for estimating the extent of contamination. Finally, the target dataset is adjusted by a linear model. A detailed description of our algorithms is found in Additional file 1. For testing our method we simulated mixtures from published RNA-Seq datasets, which showed a clear improvement, as exemplified in Fig. 1a for mixtures of purified immune cells (RNA-Seq data from GSE60424 [51]) or different tissues (Additional file 1). Furthermore, none of the previously described algorithms matched this performance (Additional file 1).

The algorithm was then applied to our set of RNA-Seq samples of tumor cells (n = 21), TAMs (n = 18), and tumor-associated T cells (TATs; n = 5). The detected contamination of tumor cell or TAM samples ranged from 0 % to 17 % (Fig. 1b, c) and was in agreement with prior analyses (as in Additional file 4: Table S2). To test the power of the algorithm, we also included RNA-Seq data from a heavily contaminated tumor sample (OC65s: 25.7 % TAMs; striped bars in Fig. 1b) and two heavily

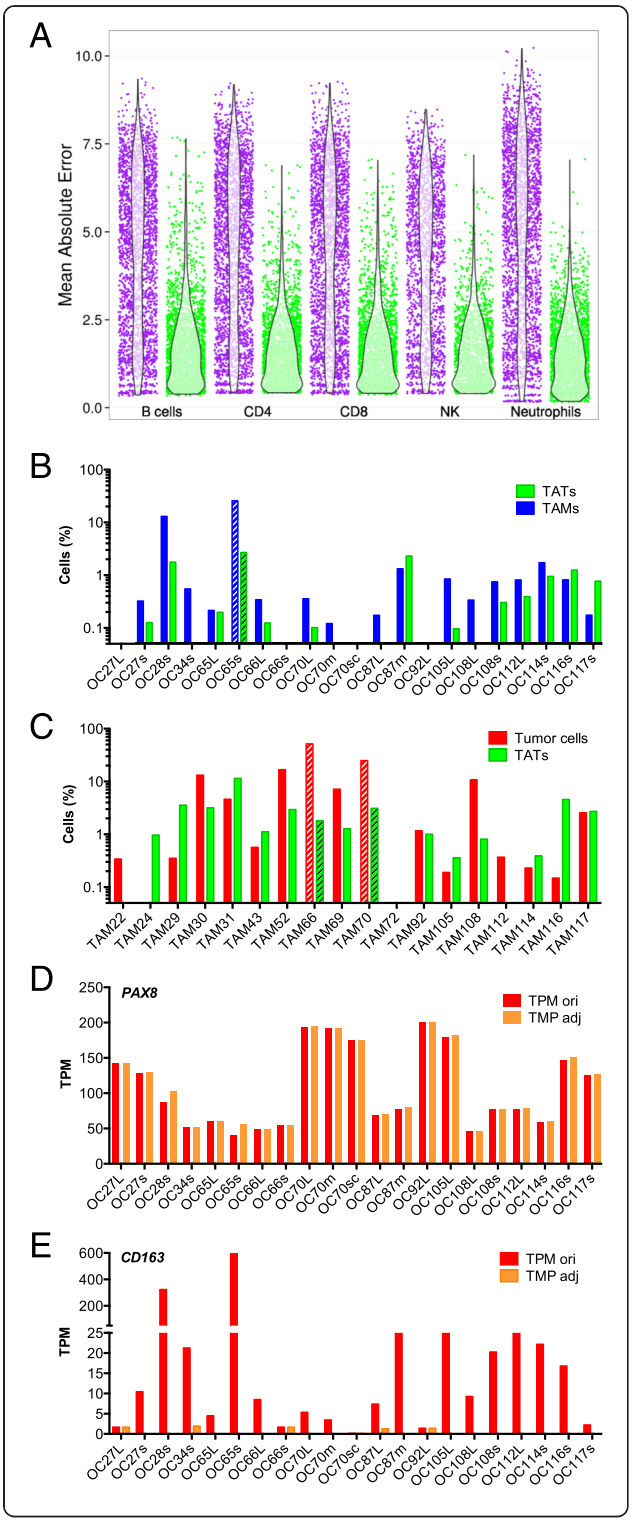

Fig. 1 Adjustment RNA-Seq data based on RNA-Seq mixture modeling. **a** Simulation results from *in-silico* mixture of different purified immune cells with purified monocytes from dataset GSE60424 [51]. Deviation of TPM values from ground truth (unmixed sample) was quantified as the mean absolute error (MAE). *Purple*: uncorrected samples; *green*: corrected samples. Each *dot* represents one simulation with a random mixture percentage between 0 % and 50 %. *Violin plots* show the distribution of MAE values. See "Results" for description of dataset used. The algorithm was applied for estimation of contamination and data adjustment as described in Additional file 1. **b** Estimated TAM contamination of tumor samples used in the present study, based on RNA-Seq mixture modeling. **c** Estimated tumor cell contamination of TAM samples. *Striped bars* in (**b**) and (**c**) denote samples excluded from further analysis. **d**, **e** Effect of adjustment by RNA-Seq mixture modeling on marker gene expression (*PAX8*, *CD163*) in tumor cell samples. ori, original TPM values; adj, adjusted TPM

contaminated TAM samples (TAM66s: 49.4 % tumor cells and TAM70: 24.9 %; striped bars in Fig. 1c). These three samples were excluded from all subsequent experiments.

These data were used to adjust the RNA-Seq data for cross-contaminating tumor cells, TAMs, and TATs. Adjustment was successful, as exemplified in Fig. 1d and e for tumor cells. While the macrophage marker gene *CD163* was reduced, the epithelial cell marker gene *PAX8* was not. The observed increase in *PAX8* is due to the fact that TPM values represent a relative measure, thus resulting in a redistribution from reduced to non-reduced genes.

These adjusted RNA-Seq data for 20 tumor cell and 16 TAM samples (Additional file 3: Dataset S1) were analyzed for expression of two classes of mediators and their receptors: (1) cytokines and polypeptide growth factors, collectively referred to as protein mediators in the following; and (2) phospholipid breakdown products and eicosanoids functioning as lipid mediators, as described in detail below.

Common expression of protein mediators and their receptors by tumor cells and TAMs

We first established datasets of 791 genes encoding protein mediators and their receptors based on literature and database-derived data, in total 502 cytokine and growth factor genes (Additional file 3: Dataset S2) and 289 receptor genes (Additional file 3: Dataset S4). Genes with TPM values ≥3 in at least 65 % of all tumor cell or TAM samples were considered expressed and part of a common signaling network. Using these criteria, we identified 159 cytokine and 173 receptor genes to be expressed in tumor cells and/or TAMs (Fig. 2a, b; Additional file 3: Dataset S4 and S5). Genes were defined as cell type-selective if expression levels between tumor cells and TAMs differed at least threefold (thresholds indicated by the shaded areas in Fig. 2) and the individual TPM values determined for one cell type were either larger or smaller than the values for the other cell type, allowing maximum

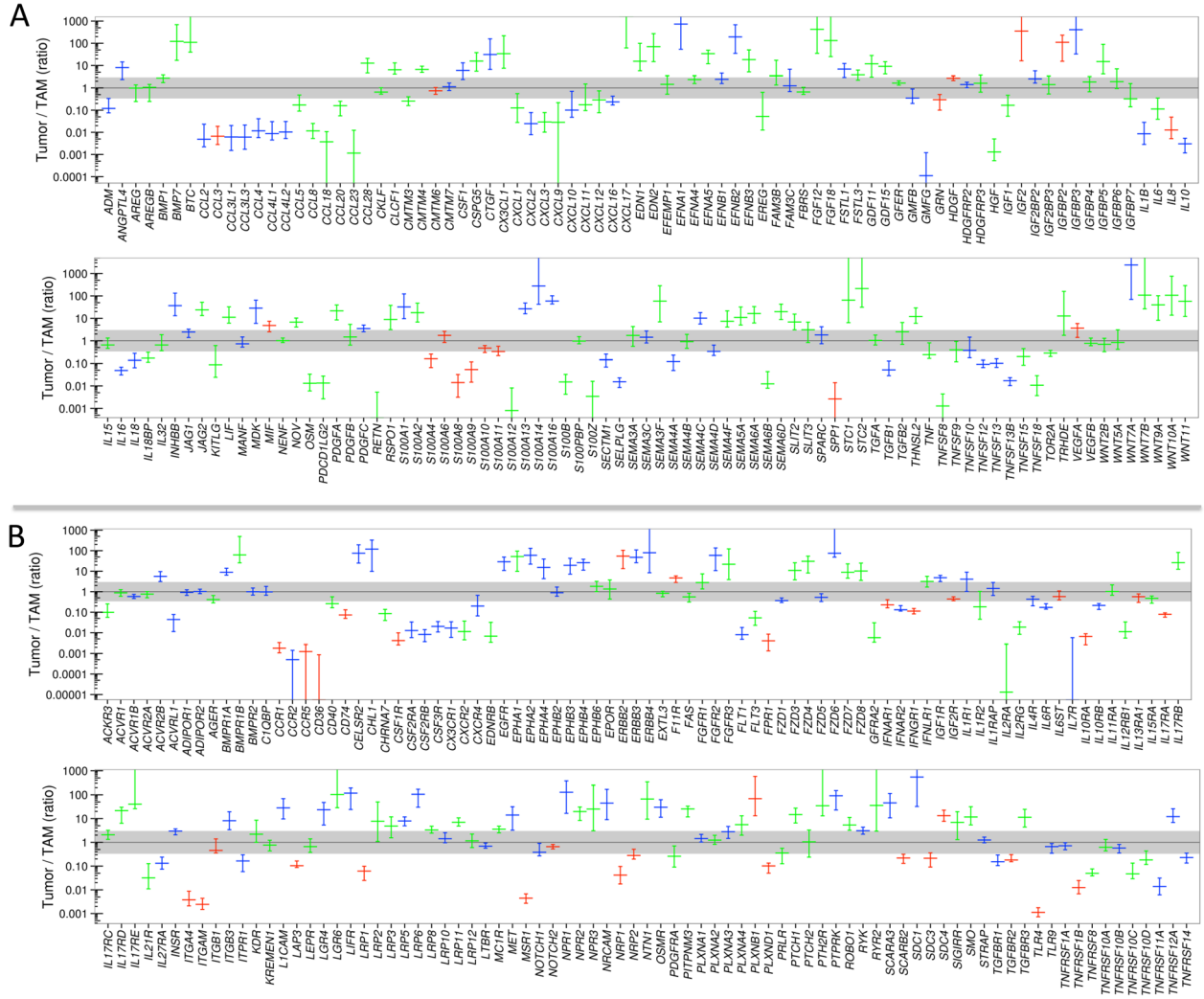

Fig. 2 Genes coding for components of cytokine and growth factor signaling expressed in ovarian cancer cells and/or TAMs (RNA-Seq). **a** Genes coding for cytokines and growth factors. Values represent the ratio of expression in tumor cells versus TAMs (median and 95 % CI). The color code indicates the level of expression: *green*, low expression (TPM 3–20); *blue*, moderate expression (TPM 20–100); *red*, high expression (TPM >100). **b** Genes coding for cytokine/growth factor receptors. For further details see Additional file 3: Datasets S2–S5

one outlier (Additional file 3: Datasets S4, S5: column "no overlap"). These datasets were further split into groups showing low (green bars in Fig. 2a, b), median (blue), or high (red) expression levels according to the observed TPM values.

Differences of more than 1000-fold were observed with respect to the expression levels of different genes as well as the cell type selectivity of individual genes. These results were confirmed by RT-qPCR using a larger number of patient-derived samples for all instances tested, including a statistically highly significant preferential expression of *IL10*, *TGFB1*, *S100A8*, *S100A9*, and *IL10RA* by TAMs and *LIFR* by tumor cells (Fig. 3a). The analysis of matched tumor cell and TAM samples from the same patients are in agreement with these conclusions with the exception of *TGFB1* (Fig. 3b).

We next determined the levels of protein expression for several examples by flow cytometry of non-separated ascites samples and confirmed the preferential expression of S100A8/A9 and IL-8 in TAMs, and of LIFR and TGFBR3 in tumor cells (Fig. 3c and Additional file 2: Figure S2). Finally, we measured the levels of a number of protein mediators in the ascites of up to 40 serous ovarian cancer patients (Additional file 4: Table S3) and found readily detectable levels for all mediators shown in Fig. 3d, whereas IL4, IL12, IL13, and GM-CSF were not detectable, consistent with the RNA-Seq and RT-qPCR data (Fig. 2a and 3a). However, in a few cases, ascites levels were unexpectedly high in view of the low expression of the corresponding mRNAs in tumor cells and TAMs, e.g. IL-6 and VEGF-C (Fig. 2; Additional file 3: Datasets S3 and S5). We therefore investigated

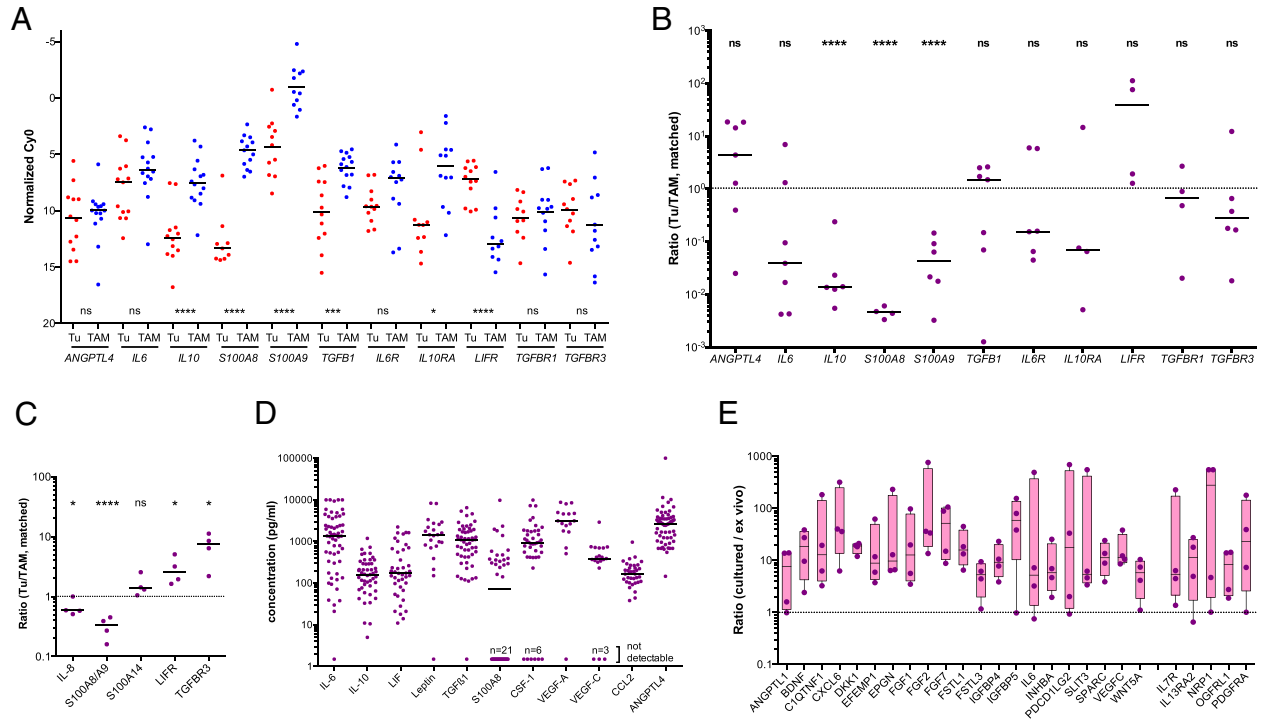

Fig. 3 Expression of cytokines, growth factors, and their receptors in ovarian cancer ascites. **a** Validation of RNA-Seq data by RT-qPCR of tumor cell and TAM samples (each *dot* represents a different sample). **b** RT-qPCR analysis of matched tumor cell and TAM samples from the same patients (each *dot* represents a matched pair). Data are represented as the ratio of expression in tumor cells and TAMs. The *dotted line* indicates a ratio of 1. **c** FACS analysis of cytokine (intracellular IL-8, S100A8/A9, and S100A14) and receptor (LIFR and TGFBR3) expression by tumor cells and TAMs. Data in (**a**)–(**c**) were statistically analyzed by Student's *t*-test (two-sided, unequal variance). *Horizontal bars* indicate the median. Gene names are explained in Additional file 3: Datasets S4 and S5. **d** Concentrations of cytokines and growth factors in the ascites fluid from ovarian cancer patients. Each *dot* represent a different patient, *horizontal lines* indicate the median. **e** RNA-Seq analysis of tumor cell spheroids before and after a 6-day culture in serum-free medium supplemented with 10 % autologous ascites (n = 4). The *figure* shows the ratio of matched pairs for all protein mediator-encoding genes induced under these conditions at least tenfold (each *dot* represents a matched pair; median: *horizontal bar*; 95 % CI: *box*; min–max: *whiskers*)

whether this apparent discrepancy could be due to differences in expression levels in unattached tumor cells in suspension, as in spheroids, and in attached tumor cells. To address this question, we performed RNA-Seq analyses for four matched pairs of uncultured and cultured spheroids. The latter were kept in serum-free medium supplemented with autologous ascites for 6 days, under which conditions the cells partly adhere to the plastic surface. The results clearly show that a small number of cytokine genes were indeed induced under these conditions, including *IL6* and *VEGFC* (Fig. 3e), while other ones, such as *IL10* and *LIF* were not. It is therefore possible that adherent tumor cells and solid tumor masses rather than floating cells are the major source of some of the ascites-associated protein mediators.

Delineation of a common signaling network of protein mediators established by tumor cells and TAMs

Based on these data, we derived a model of a signaling network involving ovarian cancer cells and TAMs (Fig. 4). The predicted cellular origins and targets of cytokines and growth factors are also summarized in Additional file 2: Figure S3. In the following sections, we will describe the most prominent signaling pathways identified by our analyses.

(i) The STAT3-inducing cytokines IL-10, IL-6, and LIF were identified as part of the signaling network established in the present study (Fig. 4a). *IL10* and the gene encoding its receptor *IL10R* were expressed mainly by TAMs, *LIF* and *LIFR* by tumor cells, *IL6* and the genes for IL6 receptor subunits *IL6R* and *IL6ST* by both cell types.

(ii) *TGFB1*, mainly expressed by TAMs, codes for the major ligands of the TGFβ network, which also comprises tumor cell-derived *TGFB2* and *BMP7* (encoding bone morphogenetic protein 7) as well as *BMP1* expressed by both cell types (Fig. 4b). These ligands target both cell types, as suggested by the expression patterns of the *TGFBR* and *BMPR2* genes.

(iii) *WNT7A* is the most strongly expressed WNT gene preferentially expressed by tumor cells (Fig. 4c).

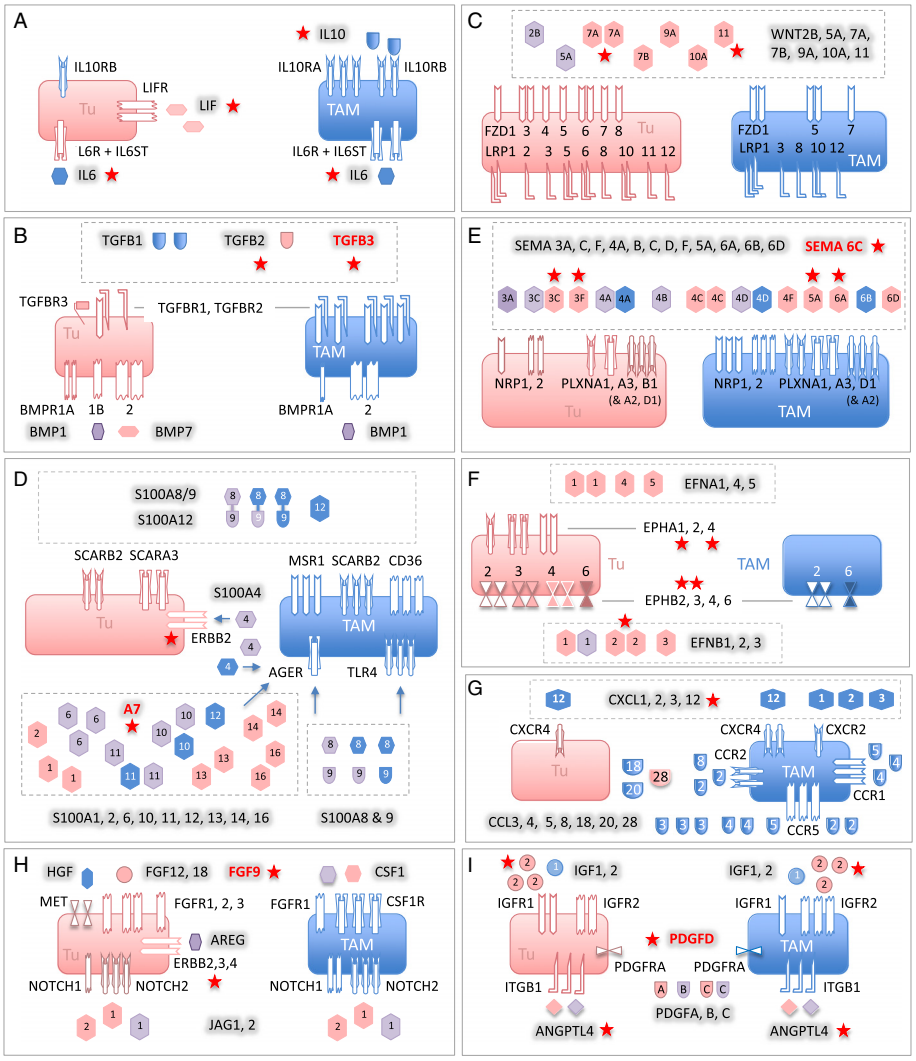

Fig. 4 A common cytokine signaling network of ovarian cancer cells and TAMs. Ligands are represented as "free floating" symbols, receptors as membrane-associated symbols. Ligands derived from tumor cells are shown in *red*, ligands originating from TAMs in *blue*, ligands expressed by both cell types at similar levels (less than tenfold difference in TPM) in *purple*. Each ligand or receptor is represented by one or more identical symbols according to their expression levels (1, 2, and 3 symbols corresponding to *green*, *blue*, and *red*, respectively in Fig. 2). The model is based on the data in Figs. 2, 9c and Table 1 and assumes that protein levels follow gene expression. Gene names are explained in Additional file 3: Datasets S4 and S5. *Red asterisks* denote components associated with a poor clinical outcome (based on Figs. 7–9). Ligands shown in *red letters* are expressed only in a subset of patients (Table 1) and associated with a short relapse-free survival (RFS) (Fig. 9c)

Other ligands of the network include *WNT2B*, *WNT5A*, and *WNT9A*, differentially expressed by tumor cells and TAMs. These ligands include inducers of both canonical and non-canonical WNT signaling [52]. The canonical pathway depends on both frizzled receptors (*FZD*) and LRP coreceptors, whereas non-canonical signaling does not require LRPs. As multiple LRP genes are expressed by tumor cells and TAMs (Fig. 4c), canonical WNT signaling would be functional in both cell types.

(iv) Multiple *S100* genes are highly expressed in tumor cells and/or TAMs, including *S100A8* and *S100A9* (Fig. 4d). S100A8 and S100A9 proteins interact with surface receptors either as monomers with advanced glycation end products receptor RAGE (*AGER*) and TLR4 or bind as heterodimers to different scavenger receptors [53], all of which are expressed by TAMs (*MSR1*, *SCARA/B*, *CD36*). Taken together with the particular high expression of both genes in TAMs, these findings point to a pivotal role for TAMs in generating and processing S100A8/A9-associated signals, which also applies to S100A12. Tumor cells express scavenger receptor genes, but not *AGER* and *TLR4* at significant levels, suggesting that these cells are primarily targeted by S100A8/A9 heterodimers. On the other hand, tumor cells but not TAMs

express *ERB2*, encoding a receptor for S100A4, suggesting a tumor-selective effect. In contrast, multiple S100 members of varying cellular origins seem to target preferentially TAMs, as suggested by the lack of RAGE expression by tumor cells.

(v) Both tumor cells and TAMs express multiple semaphorins and their receptors (plexins and neuropilins), thereby establishing autocrine as well as paracrine signaling mechanisms (Fig. 4e). While *SEMA3F*, *5A*, *6A*, and *6D* expression is clearly higher in tumor cells, the opposite is true for *SEMA 4A* and *6B*. The semaphorin receptor genes *PLXNA1*, *PLXNA3*, *NRP1*, and *NRP2* are expressed by both cell types, whereas *PLXNB1* and *PLXND1* expression is selective for tumor cells and TAMs, respectively.

(vi) Ephrins are also part of the signaling network, with tumor cells playing a major role (Fig. 4f). Thus, tumor cells are the main origin of six different ephrin family members, compared to one subtype expressed by TAMs. Likewise, A-type receptor expression is
restricted to tumor cells and B-type receptor expression is considerably higher in, or selective for, tumor cells, the latter exemplified by *EPHB3* and *EPHB4*.

(vii) TAMs play a major role both as producers and targets of multiple chemokines of the *CCL* family (Figs. 2a and 4g). Thus, TAMs preferentially express multiple *CCL* genes, with *CCL2*, *CCL3*, and *CCL4* being the most strongly expressed ones. Moreover, significant expression of receptor genes for these cytokines (*CCR1*, *CCR2*, *CCR5*) was detected only in TAMs. In contrast, several *CXCL* type chemokine genes are expressed by both cell types, however, significant expression of genes coding for their cognate receptor genes was only detectable for *CXCR4* in both cell types, consistent with its description as an independent predictor of a poor clinical outcome of ovarian cancer [54].

(viii) Our study also predict a number of other pathways known to play important roles in tumor progression (Figs. 2 and 4h, i). These include: (1) stimulation of the MET receptor on tumor cells by TAM-produced HGF; (2) the interaction of amphiregulin (*AREG*) produced by both cell types with ERB2, 3, and 4 receptors on tumor cells; (3) the activation of NOTCH receptors on both cell types by JAG1/2
ligands, mainly produced by tumor cells; (4) PDGF signaling by all different family members via PDGFR-A on both cell types; (5) IGF1/2 signaling particularly through IGFR2; and (6) the interaction of angiopoietin-like 4 (*ANGPTL4*) with integrin β1 (*ITGB1*).

Expression of signaling components in tumor cells from subsets of patients

A number of genes encoding protein mediators were uniformly expressed by tumor cells and/or TAMs (e.g. *IL8*, *KITLG*, *LEP*), but median expression of the corresponding receptor genes was extremely low in both cell types (Figs. 2 and 4; Additional file 3: Datasets S2–S5). Likewise, several receptor genes (e.g. *IL4R*, *INFAR/INFGR*, *PTCH/SMO*) were consistently expressed by tumor cells and/or TAMs, but ligand expression was not detectable. This may be due to the expression of the "missing" ligands and receptors by other host-derived cells or by tumor cell subsets not present in ascites. On the other hand, some of these genes may not be part of the common network due to a restricted expression in smaller subsets of patients. Such genes may be of particular interest, since their expression could be related to the aggressiveness of the disease and thus to its clinical outcome.

We therefore searched for genes not found in the common network but potentially complementing this in a small subfraction of patients. These genes had to fulfill two conditions: (1) TPM >3 in n ≥2 tumor cell or TAM samples (but below the 65 % quantile used in Fig. 2); and (2) coding for proteins representing ligands or receptors for the pathways constructed in Fig. 4. Genes identified by this approach in tumor cells (n = 35; Table 1) and TAMs (n = 14; Additional file 4: Table S4) may indeed be of high relevance, as they code for components of chemokine, TGFβ/BMP, FGF, ephrin, semaphoring, and WNT pathways. We also found the gene coding for norrin (*NDP*), a frizzled 4 ligand unrelated to the WNT family [55], to be expressed in tumor cells from a subset of patients (Table 1).

Identification of a common transcriptome-based signaling network of lipid mediators between tumor cells and TAMs

Lipids derived from phospholipids represent another major group of soluble mediators in ovarian cancer ascites. These comprise mainly breakdown products of phospholipids and metabolites of polyunsaturated fatty acids (PUFAs), in particular AA-derived [30] products of the cyclooxygenase and lipooxygenase pathways [33]. While the first group of mediators, including lysophosphatidic acid (LPA) and PUFAs, is mostly generated by secreted phospholipases, eicosanoid metabolites of the second group are produced exclusively intracellularly. We therefore focused our attention on proteins generating signaling compounds of either group and their receptors and performed an analogous study as described above using datasets of 93 genes encoding enzymes, accessory proteins (Additional file 3: Dataset S6; n = 69), or lipid receptors (Additional file 3: Dataset S8; n = 24).

Table 1 Patient-specific expression of cytokine and receptor genes by tumor cells complementing the signaling networks constructed in Figs. 4 and 6

Gene	Description	Min. TPM	Max. TPM
Cytokines			
BMP8B	Bone morphogenetic protein 8b	0.32	32.17
CXCL6	Chemokine (C-X-C motif) ligand 6	0.00	7.74
CXCL14	Chemokine (C-X-C motif) ligand 14	0.00	5.74
DKK1	Dickkopf WNT signaling pathway inhibitor 1	0.00	7.49
EFNA3	Ephrin-A3	0.95	16.74
EGF	Epidermal growth factor	0.09	10.16
FGF2	Fibroblast growth factor 2 (basic)	0.02	29.35
FGF9	Fibroblast growth factor 9	0.08	15.31
FGF11	Fibroblast growth factor 11	0.48	6.17
FGF13	Fibroblast growth factor 13	0.08	9.04
FGFBP1	Fibroblast growth factor binding protein 1	0.00	28.97
KITLG	KIT ligand	0.04	7.48
NDP	Norrin (Norrie disease pseudoglioma)	0.00	5.44
NRG1	Neuregulin 1	0.02	5.23
NRG2	Neuregulin 2	0.04	4.59
NRG3	Neuregulin 3	0.00	13.39
PDGFD	Platelet derived growth factor D	0.29	6.58
RSPO3	R-spondin 3	0.02	8.90
S100A7	S100 calcium binding protein A7	0.00	4.03
S100P	S100 calcium binding protein P	0.00	12.00
SEMA3D	Semaphorin 3D	0.00	6.07
SEMA3E	Semaphorin 3E	0.13	93.32
SEMA4G	Semaphorin 4G	0.16	6.74
SEMA5B	Semaphorin 5B	0.03	19.94
SEMA6C	Semaphorin 6C	0.68	4.76
SEMA7A	Semaphorin 7A	0.26	9.55
SFRP1	Secreted frizzled-related protein 1	0.00	527.58
TGFB3	Transforming growth factor, beta 3	0.07	4.51
Cytokine receptors			
AGER	Advanced glycosylation end product receptor	0.30	5.01
EPHA6	EPH receptor A6	0.13	25.52
FGFR4	Fibroblast growth factor receptor 4	0.33	3.76
FZD2	Frizzled family receptor 2	0.22	6.18
FZD10	Frizzled family receptor 10	0.00	7.95
IL10RA	Interleukin 10 receptor, alpha	0.00	5.91
Lipid mediators			
ALOX15B	Arachidonate 15-lipoxygenase, type B	0.06	8.03
Lipid receptors			
LTB4R2	Leukotriene B4 receptor 2	1.11	3.78
PTGER3	Prostaglandin E receptor 3 (subtype EP3)	0.10	11.87

The RNA-Seq data summarized in Fig. 5a and Additional file 3: Datasets S7 and S9 identified 31 genes involved in the enzymatic generation of lipid mediators and expressed in ovarian cancer cells and/or TAMs. Figure 5b shows the data for expression of the corresponding receptor genes (n = 17). A number of key observations were confirmed by RT-qPCR analysis of a larger number of clinical samples (Fig. 5c, d).

We also investigated whether genes expressed at higher levels in tumor cells or TAMs only from a small subfraction (n ≥2) of patients participate might also participate in lipid-mediated signaling pathways. This analysis identified three genes expressed in tumor cells, i.e. *ALOX15B*, the leukotriene B_4 receptor gene *LTB4R2* and the PGE_2 receptor gene *PTGER3* (Table 1).

These findings point to a network of lipid mediators established by both tumor cells and TAMs, involving several distinct groups of signaling molecules, as described below.

(i) The first network is based on products of phospholipid hydrolysis that are generated by

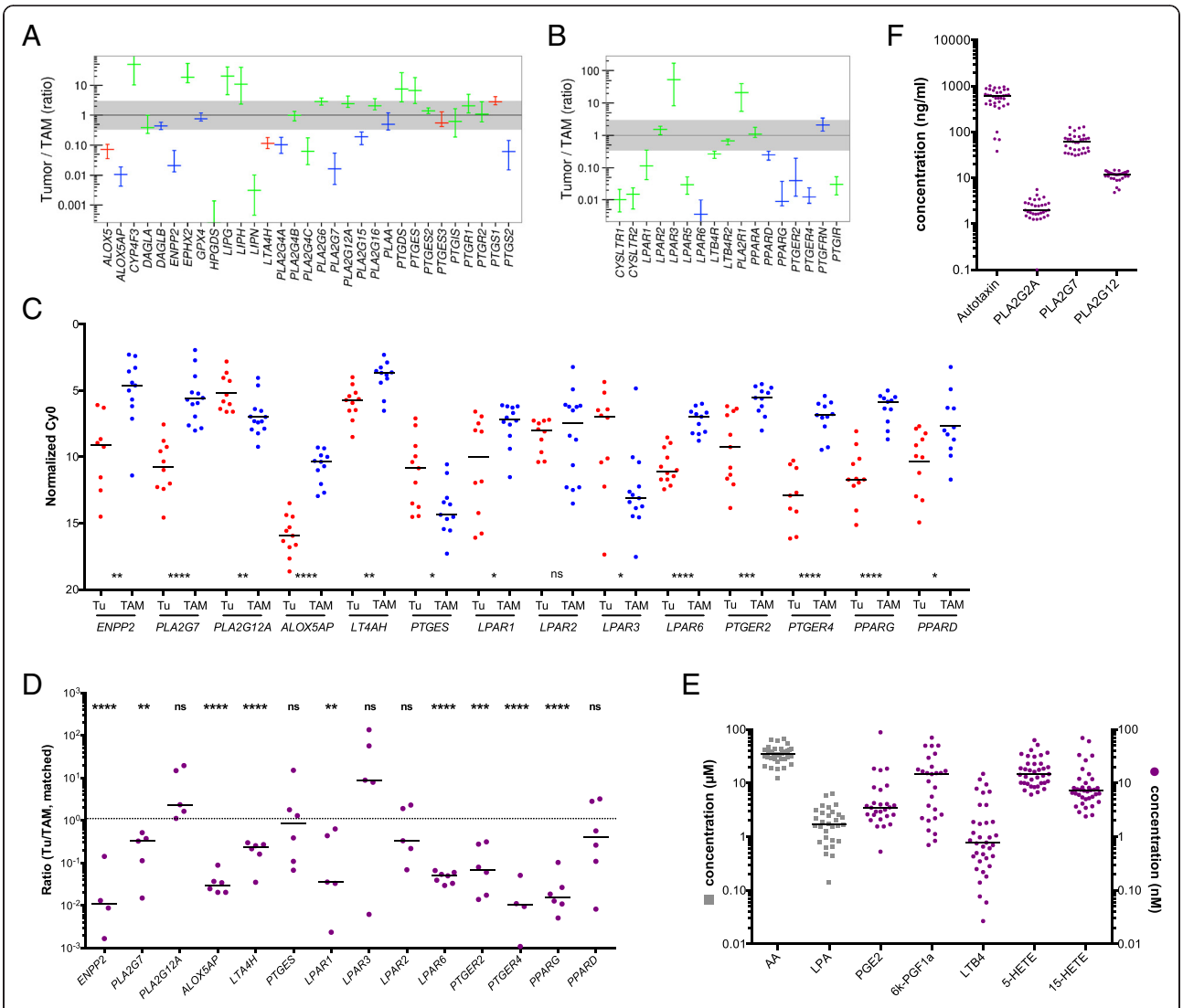

Fig. 5 Genes coding for components of lipid signaling expressed in ovarian cancer cells and/or TAMs (RNA-Seq). **a**, **b** Genes coding for enzymes involved in the generation lipid mediators and their receptors. Values represent the ratio of expression in tumor cells versus TAMs (median and 95 % CI). Color code as in Fig. 2. Detailed results are summarized in Additional file 3: Datasets S6-S9. **c** Validation of RNA-Seq data by RT-qPCR of tumor cell samples (each *dot* represents a different sample). **d** RT-qPCR analysis of matched tumor cell and TAM samples from the same patients (each *dot* represents a matched pair). Data are represented as the ratio of expression in tumor cells and TAMs. The *dotted line* indicates a ratio of 1. Data in (**c**) and (**d**) were statistically analyzed by Student's *t*-test (two-sided, unequal variance). **e** Concentrations of lipid mediators in the ascites fluid from ovarian cancer patients determined by LC-MS/MS. Each *dot* represents a different patient, *horizontal lines* indicate the median. **f** Concentrations of autotaxin (*ENPP2*) and PLA_2 isoforms in ascites quantified by ELISA

specific phospholipases (Figs. 5 and 6a). This conclusion is consistent with the presence of high levels of LPA, AA, specific A2-type phospholipases (in particular PLA_2G7), and autotaxin in ascites (Fig. 5f). TAMs seem to play an essential role in this context, since they express *PLA2G7* and *ENPP2* at higher levels than tumor cells (Fig. 5a, c). Importantly, the protein levels of 3 phospolipases (PLA_2G2, PLA_2G7, and PLA_2G12A) measured in ascites fluid (Fig. 5f) are consistent with mRNA expression levels in tumor cells and TAMs (Fig. 5a; Additional file 3: Dataset S6). LPA in ascites apparently targets tumor cells and TAMs via specific receptors, since *LPAR1* and *LPAR2* are expressed at similar levels by both cell types, *LPAR3* is selective for tumor cells, *LPAR5* and *LPAR6* for TAMs (Fig. 5b–d). AA is taken up by tumor and host cells [56], where it can regulate signaling pathways, either directly or after metabolic conversion.

(ii) The second network is established by prostanoids (Fig. 6b), in particular prostanglandin E_2 (PGE_2) and PGI_2 (prostacyclin), both found at substantial levels in ascites (Fig. 5e; 6k-PGF1a is the stable degradation product of PGI_2), as previously described [56]. Most genes encoding the enzymes required for their synthesis (cyclooxygenases and prostaglandin synthases) are expressed at similar levels by both cells types (*PTGS1*, *PTGES2/3*, *PTGIS*; Fig. 5a, c, d), whereas *PTGS2* is selective for TAMs. A major target of their products seem to be TAMs, which express considerable higher levels of the PGE_2 and PGI_2 receptor genes *PTGER2*, *PTGER4*, and *PTGIR* (Fig. 5b, c) with the exception of *PTGER3* expressed only by a small subset of tumor cells (Table 1). In

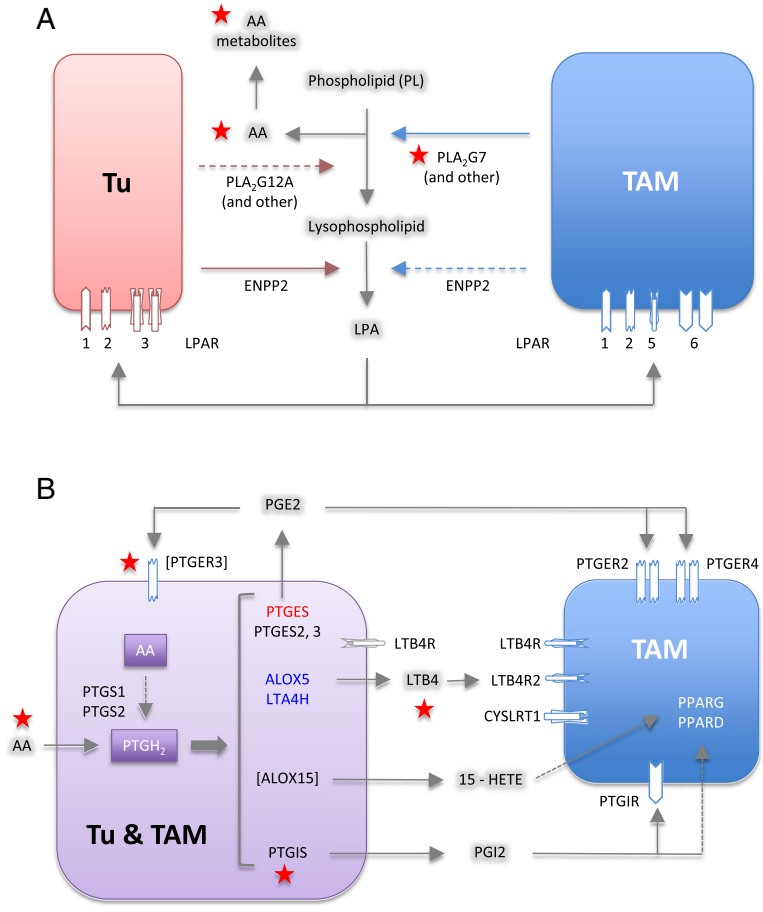

Fig. 6 Common lipid signaling in the ovarian cancer microenvironment. **a** A *transcriptome-derived model* depicting the cellular origins and targets (tumor cells, TAMs) of phospholipid degrading enzymes, AA and LPA. **b** An *analogous model* for AA-derived eicosanoid mediators and the sources of enzymes involved in their synthesis. The models are based on the data in Fig. 5a and b. Genes in *square brackets* are expressed in tumor cells in small subset of patients (Table 1). The source of ligands is indicated as follows: *red* for tumor cells, *blue* for TAMs, and *purple* for both. Colored gene names indicate higher expression tumor cells (*red*) or TAMs (*blue*). Each receptor is represented by one or more identical symbols according to their expression levels (as in Fig. 4). [ ]: expressed in subset of patients. *Red asterisks* denote components associated with a poor clinical outcome (based on the data in Figs. 7–9). Gene names are explained in Additional file 3: Datasets S8 and S9

addition, TAMs also show a higher expression of *PPARD* (Fig. 5b–d), encoding the nuclear receptor PPARβ/δ, a possible target for PGI_2 [57]. Figure 6b shows a schematic representation of these results.

(iii) Products of the lipoxygenase pathway, i.e. 5-HETE, 15-HETE and leukotriene A_4 (LTA_4) represent the third network (Fig. 6b). These AA metabolites are present in ascites at readily detectable concentrations (Fig. 5e; LTB_4 is a stable metabolite of the unstable LTA_4). This is consistent with the expression of the corresponding lipoxygenase (*ALOX5*), 5-lipoxygenase activating protein (*ALOX5AP*), and leukotriene synthase (*LTA4H*) genes (Fig. 5a, c) in TAMs. In contrast, TAMs also preferentially express the LTB_4 surface receptor genes *LTB4R*, *LTB4R2*, and *CYSLRT1*/2. 15-HETE has been described as a ligand for the nuclear receptors PPARγ [58] and PPARβ/δ [59], which are both expressed at higher levels in TAMs (Fig. 5b–d). The gene coding for the presumptive 5-HETE receptor *OXER1* [60] is expressed at very low levels in both cell types, if at all (Additional file 3: Dataset S8), suggesting that 5-HETE is more likely to act as a precursor of LTA_4 in these cells.

Association of mediator concentrations with clinical outcome

We next asked whether mediators in the tumor microenvironment are associated with the clinical outcome of high-grade serous ovarian carcinoma. We therefore assessed potential associations of the ascites levels of cytokines and lipids prior to first-line therapy with RFS by Kaplan–Meier analysis (see Additional file 4: Table S3 for patient-specific clinical features). The logrank *p* values depicted in Fig. 7a demonstrate a clear association of the STAT3-inducing cytokines IL-10, IL-6, and LIF with early relapse (Fig. 7a–c), with IL-10 being the strongest indicator of a poor outcome ($p < 0.0001$; logrank hazard ratio [HR] = 4.54; 95 % confidence interval [CI] = 4.56–40.5; median survival 12.0 versus 26.0 months), which is in agreement with a previous study of a smaller cohort of patients [7]. The present study identified inverse associations with RFS for four additional mediators, i.e. TGFβ1, PLA_2G7, AA, and its metabolite LTB_4 (Fig. 7a, d–g). In contrast, PLA_2G12A, autotaxin, and the PLA_2/autotaxin product LPA did not show any correlation (Fig. 7a). Likewise, the AA metabolites PGE_2, PGI_2, 5-HETE, and 15-HETE, also components of the lipid signaling network identified above, were not linked to RFS.

The relevance of these cytokines and AA as indicators of an adverse clinical outcome became particularly evident when we determined the RFS for combinations of these mediators. Thus, patients with a high level of either IL-10 and AA, IL-6 and AA, or TGFβ and AA showed a clearly worse outcome compared to those with a high concentration for only one mediator (red versus gray curves in Fig. 8a–c; $p = 0.016$ for IL-10; $p < 0.0001$ for IL-6; $p = 0.0002$ for TGFβ). For IL-10, a similar difference was observed between patients showing a high concentration for either IL-10 or AA versus those with low levels of both mediators (Fig. 8a; $p = 0.0045$). A similar analysis for the other two cytokines was not possible due to an insufficient number of cases in the "both low" group. A striking association was observed when patients were compared with high IL-10 and high AA levels to those with low concentrations of both mediators (Fig. 8a; $p < 0.0001$; logrank HR = 9.50; 95 % CI = 4.38–47.3; median survival 12.0 versus >34 months).

Pearson analysis revealed low correlation coefficients (r) when cytokine levels were compared to lipid concentrations (Fig. 8d), indicating that the observed clinical associations are not simply a consequence of their co-synthesis. Likewise, the concentrations of AA did not correlate with any of the AA metabolites tested. In contrast, IL-6 and LIF levels were highly correlated (R = 0.87), pointing to common regulatory pathways.

Association of gene expression levels with clinical outcome

Finally, we sought to establish clinical correlations with components of the common signaling network established above (Fig. 4). Toward this end, we made use of published microarray results for 1018 high-grade serous ovarian cancer patients with documented RFS [38]. The samples used for these analyses were derived from solid tumor masses and therefore contained variable amounts of host-derived cells, including TAMs, as confirmed by the large range of expression values observed for macrophage marker genes across this cohort. Kaplan–Meier analysis for these genes actually showed a clear association of RFS with the expression of these genes (Additional file 2: Figure S4), presumably reflecting the known adverse effect of TAM infiltration on the clinical outcome. In addition, this scenario means that genes not primarily expressed in tumor cells cannot be faithfully analyzed, since it is not possible to separate effects of gene expression from host cell "contamination" in the sample and the algorithm developed in the present study for RNA-Seq cannot be applied to microarrays.

We therefore decided to focus our survival analysis on genes expressed at a higher level in tumor cells relative to TAMs (i.e. more than twofold in Fig. 2). We identified multiple mediator and receptor genes that are clearly ($p < 0.01$) associated with a shorter RFS (red in Fig. 9a, b), consistent with their established or suspected functions in tumor progression. These include the cytokine genes *CCL28*, *IGF2*, *SEMA5A*, and *WNT11*, and the receptor genes *EPHB2*, *ERBB2* and *3*, *FGFR2*, *ITGB1*, *LRP12* as

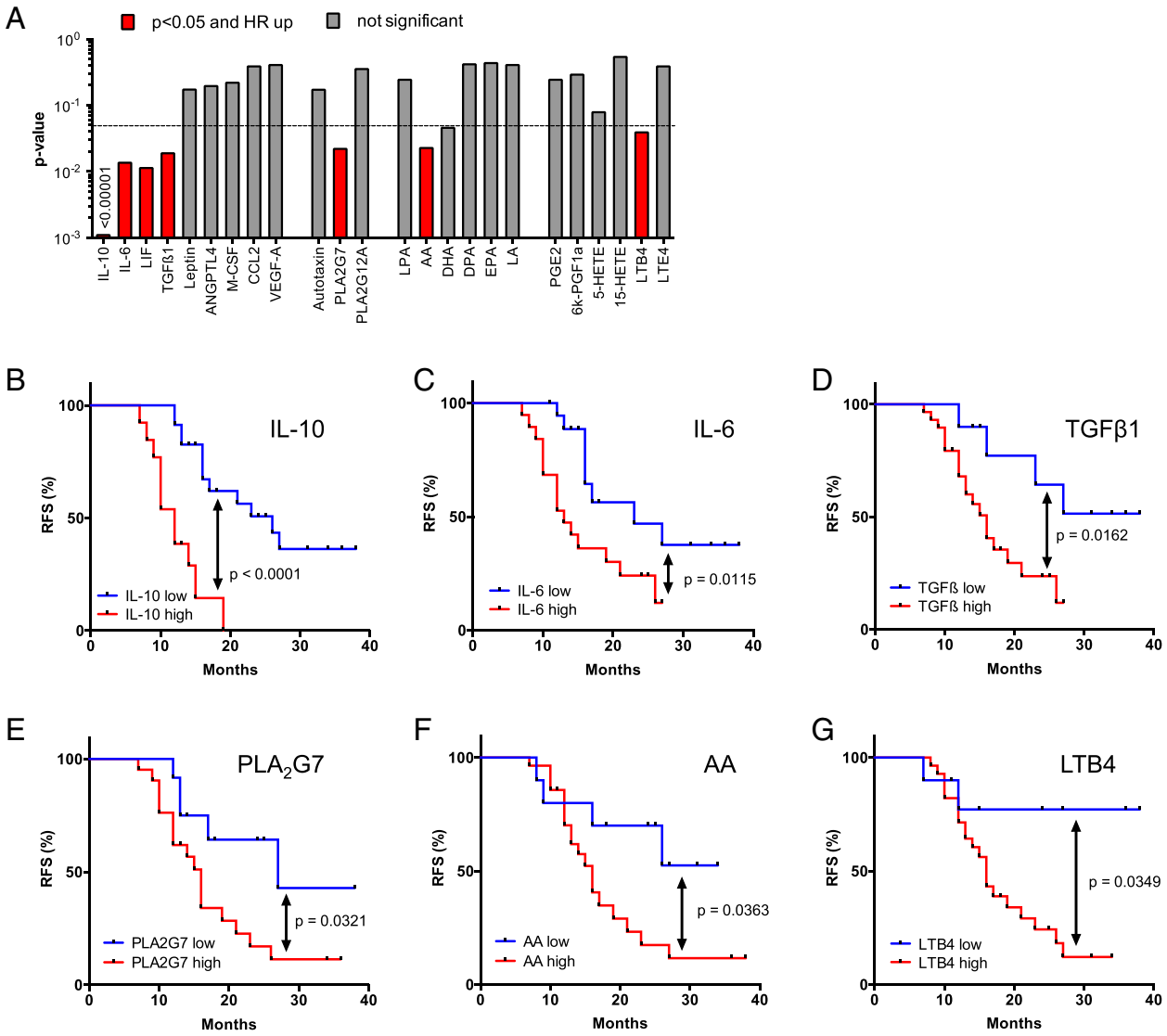

Fig. 7 Association of RFS with the levels of cytokines and lipid mediators in ovarian carcinoma ascites. **a** Summary of RFS analyses showing the *p* values determined by Mantel-Cox log rank test. Patients were dichotomized into high and low expressing groups according to the following quantiles (best-fit) and number or patients: IL-10, Q = 0.66 (n = 36); IL-6, Q = 0.5 (n = 39); TGFβ1, Q = 0.25 (n = 39); AA, Q = 0.25 (n = 38); LTB_4, Q = 0.25 (n = 38); PLA_2G7, Q = 0.33 (n = 33). Significant instances with a HR >1 are shown in *red*; *grey bars* indicate lack of significant associations. Significance was defined as logrank $p < 0.05$ and $p <$ Benjamini-Hochberg critical value for false discovery rate (FDR) = 0.10. **b**–**g** Kaplan–Meier plots showing the RFS of patients with high or low ascites levels (best-fit) of IL-10, IL-6, TGFβ1, PLA_2G7, AA, and LTB_4 (see "Methods" for details)

well as *NPR1* and *3* (Fig. 9a, b). We also found a surprising association of a favorable clinical outcome with WNT receptor frizzled 4 (*FZD4*) gene expression (Fig. 9a). We performed an analogous survival analysis for genes associated with lipid signaling and expressed at higher levels by tumor cells relative to TAMs (rightmost genes in Fig. 9a, b), based on the data in Fig. 5a and b. A particularly strong association with an adverse clinical outcome was observed for *PTGIS* ($p = 0.0005$), which codes for prostaglandin I_2 (prostacyclin) synthase (Fig. 6b).

Finally, we performed Kaplan–Meier analyses (Fig. 9d–g) of genes expressed only in small subgroups of our patients (Table 1). A very strong adverse effect on RFS ($p = 0.0001$) was seen with *TGFB3* (Fig. 9c, d), in line with the central role of the associated signaling pathways in cancer, and with *PTGER3* (Fig. 9c, e; $p < 0.0001$), encoding a prostaglandin E_2 receptor (Fig. 6b). Strong associations with poor RFS ($p < 0.001$) were also seen with *PDGFD* and *SEMA6C*. However, the most intriguing finding was the identification of *NDP* as a powerful indicator of a favorable clinical course ($p < 0.0001$; Fig. 9c, f). *NDP*

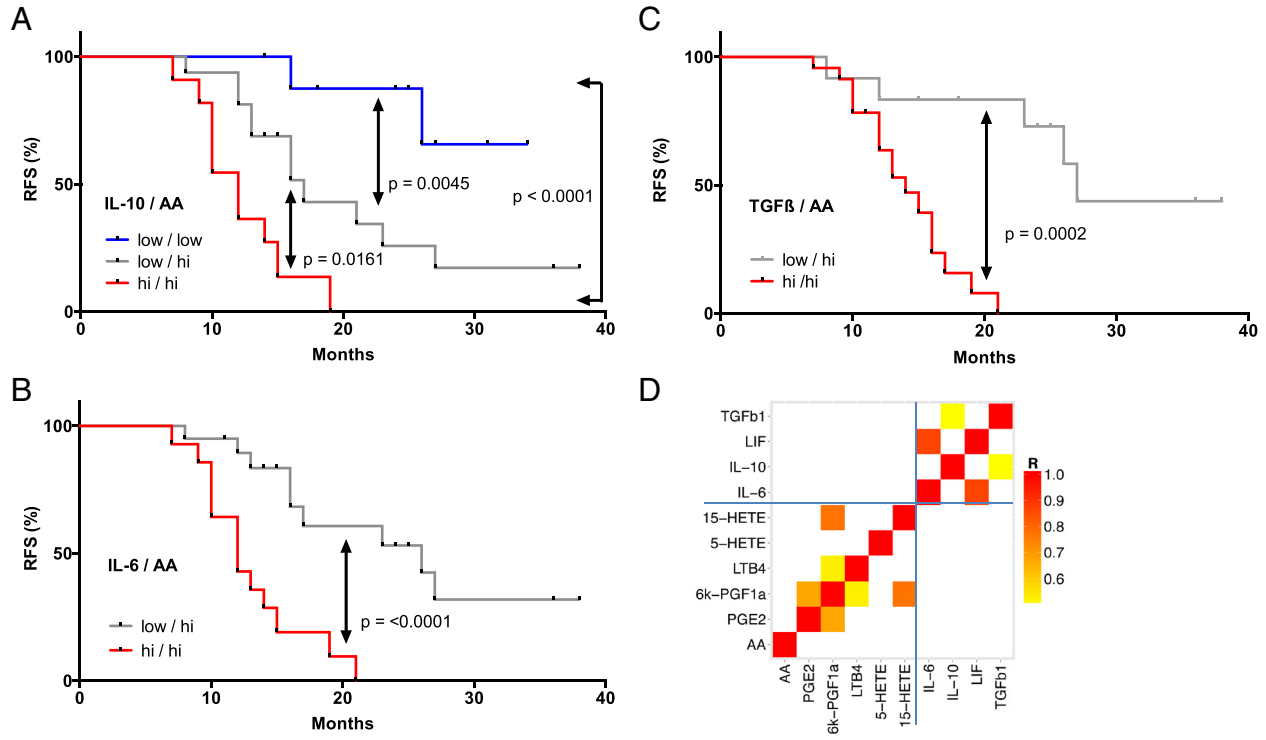

Fig. 8 Synergistic association of RFS with the levels of AA and cytokines in ovarian carcinoma ascites. **a**–**c** Patients were trichotomized for RFS analysis, using the best fit thresholds determined in Fig. 7: group 1, cytokine and AA high; group 2, one high/one low; group 3, both low. See "Methods" for details. **d** Pearson correlation matrix for soluble mediators in ovarian cancer ascites shown to be of particular relevance in the present study. The *heatmap* depicts different levels of positive correlation (*red*: high, *yellow*: low, corresponding to a range of R = 0.5–1.0)

codes for norrin, which interacts with the receptor frizzled 4 [55, 61] and TSPAN12, a signal-amplifying component of the norrin–frizzled 4 complex [55]. This presumably explains the strong association of *FZD4* with RFS ($p = 0.0004$; Fig. 9g) described above. Furthermore, *TSPAN12* was also inversely associated with RFS ($p = 0.0343$; Fig. 9h). Taken together, these findings provide strong evidence for novel tumor suppressor function of norrin–frizzled 4–TSPAN12 signaling in ovarian cancer.

Discussion

We have defined a tumor cell and macrophage-driven signaling network operating within the environment of ovarian cancer-associated carcinomatosis involving interleukins, chemokines, members of the TGFβ, WNT, S100, semaphorin and ephrin families, the phospholipid breakdown products LPA, and AA as well as AA metabolites. This network is composed of mostly common, but also patient-specific mediators and receptors and includes pathways previously not identified in the context of ovarian cancer or intercellular signaling in the tumor microenvironment (Figs. 4 and 6). We will discuss these pathways in the following sections, in particular with respect to their association with disease progression after first-line therapy.

STAT3-inducing cytokines

In agreement with the established function of deregulated STAT3 in ovarian cancer [62], IL-10, IL-6, and LIF were confirmed as components of the signaling network established by tumor cells and TAMs (Figs. 3–5). Their cellular origins and target cells clearly support a pivotal role for TAMs within this network, since these cells are the main producers of IL-10, a major source of IL-6 and the predominant target of IL-10, which presumably plays an important role in their protumorigenic conversion. Expression of LIF and its receptor are higher in tumor cells, pointing to a function for this cytokine beyond its proposed function in TAM polarization [18]. The pathways triggered by these cytokines are also directly relevant to progression of the disease as shown by the inverse association of their ascites levels (Fig. 7) with RFS, consistent with previous studies [7, 63, 64]. Taken together, these data clearly confirm a critical role for cytokine-mediated STAT3 deregulation in ovarian cancer by exerting pro-tumorigenic effects on both tumor cells and macrophages and its potential as a drug target [65].

TGFβ family

Multiple TGFβ family members have previously been associated with ovarian cancer [19, 25, 66]. In agreement

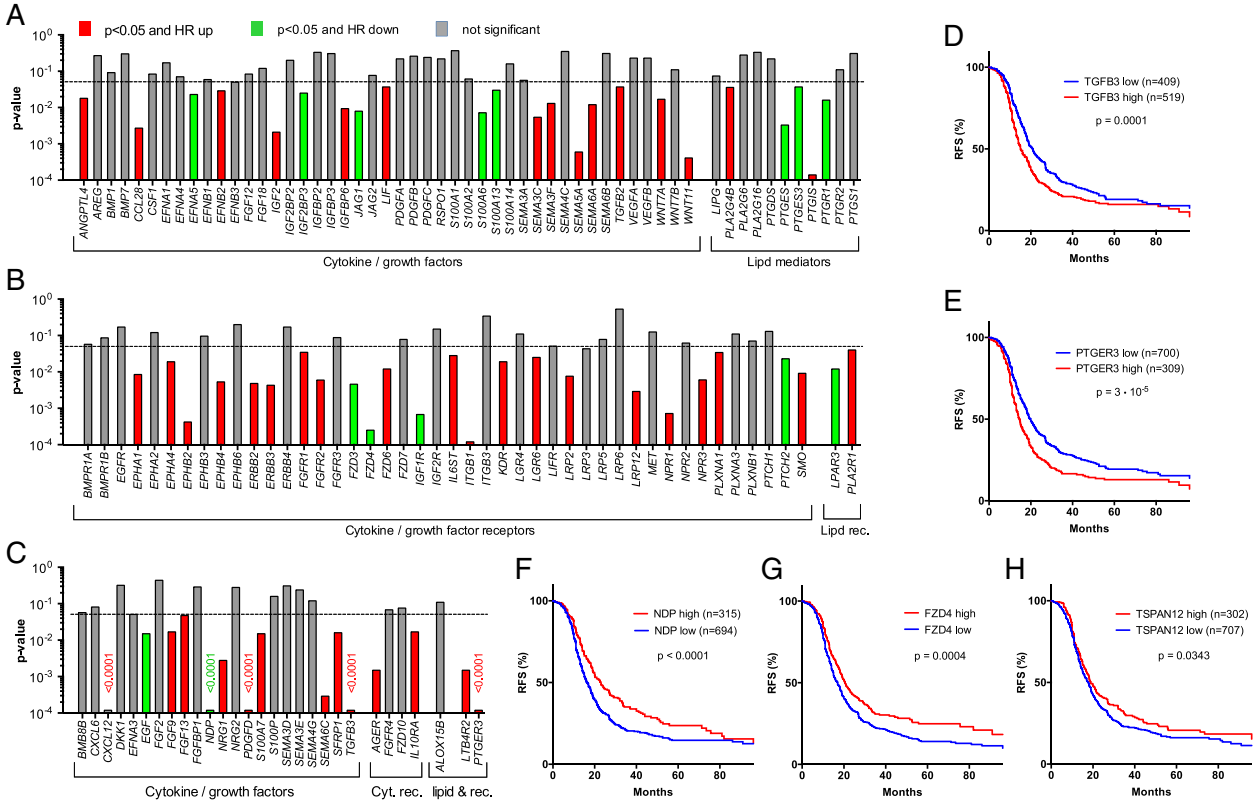

Fig. 9 Association of RFS with the expression of genes coding cytokines, growth factors, and lipid mediators or their receptors. Panels (**a**)–(**c**) represent summaries of RFS analyses for 1018 serous ovarian carcinoma patients depicting the results of logrank P tests and the directions of the respective hazard ratio (HR), using the KM plotter database [38]. **a**, **b** Survival analysis for genes in Fig. 2 with an expression ratio (tumor cell/TAM) >0.3. Genes missing from the microarray datasets used by KM Plotter were not included in panels (**a**)–(**c**). Significant instances (for "JetSet best probe") are shown in *red* (HR >1) or *green* (HR <1); *gray bars* indicate lack of significant associations ($p \geq 0.5$) or $p >$ Benjamini-Hochberg critical value for FDR = 0.10. Significance was determines as in Fig. 8. **c** Survival analysis as before, but for genes expressed only in small subgroups of patients (see Table 1 and Additional file 3: Dataset S1). **d**–**h** Kaplan–Meier plots analyzing the RFS of patients with high or low levels of *TGFB3*, *PTGER3*, *NDP*, or *TSPAN12A* expression. See "Methods" for details

with this established knowledge, we identified several components of this signaling system as important constituents of the ovarian cancer microenvironment, with both tumor cells and TAMs as essential contributors (Fig. 4b). This conclusion is strongly supported by the observed clinical correlations. Thus, the ascites concentration of TGFβ1, mainly produced by TAMs, was associated with early relapse (Fig. 7). A similar adverse link was observed between RFS and the expression of *TGFB2* and *TGFB3* genes by tumor cells, with the latter representing one of the strongest indicators of a poor clinical outcome (Fig. 9c, d). These observations are fully compatible with the known functions of TGFβ ligands in tumor progression [67] and immune suppression [68], as well as the adverse effect of *TGFBR2* and phosphorylated SMAD2/3 on survival [66]. Previous studies have also associated BMP2 and BMP4 with ovarian cancer, both of which are expressed at extremely low levels in tumor cells and TAMs (Additional file 3: Dataset S2), which may be explained by the previous identification of ovarian cancer-associated mesenchymal stem cells as a major source of these cytokines [69].

Frizzled-mediated signaling

WNT signaling is another major signaling mechanism identified in the present study (Fig. 4c). Seven genes encoding inducers of canonical and/or non-canonical WNT signaling [52], most of which were found to be preferentially expressed by tumor cells. Non-canonical WNT signaling is induced by WNT interaction with FZD without involvement of LRP coreceptors and triggers a calcineurin-NFAT pathway. The expression of at least seven *FZD* genes strongly suggests that the non-canonical pathway is operational. The canonical pathway depends on both FZD and LRP proteins and stimulates β-catenin signaling. Nine *LRP* genes are expressed by tumor cells and/or TAMs (Fig. 4c), suggesting that the canonical pathway is functional in both cell types and utilizes cell type-specific receptors. Importantly, we found a strong inverse association of *WNT11* expression

with RFS (Fig. 9a), and also confirmed the previously described [70] correlation of *WNT7A* expression with a poor clinical outcome (Fig. 9a).

R-spondins (*RSPO*) and their receptor LGR5 are required for optimal canonical WNT signaling [22], but expression was insignificant in all samples (*LGR5*; Additional file 3: Dataset S3) or was found in tumor cells from a subset of patients only (*RSPO* genes; Table 1). Since *LGR5* has been identified as a stem-cell specific gene in ovarian epithelial cells in mice [21], this pathway may be restricted to tumor cells with stem-like properties, although the role of LGR5 in human ovarian epithelial cells is unclear.

We also found tumor cell selective expression of the *NDP*, *FZD4*, and *TSPAN12* genes (Fig. 4c, f, g), encoding norrin, its receptor frizzled 4, and a norrin signal-amplifying component of the receptor complex, respectively [55], which were linked to colon cancer angiogenesis in a recent study [61]. Intriguingly, we identified *NDP*, *FZD4*, and *TSPAN12* to be associated with a delayed tumor progression, thus pointing to a novel tumor suppressor function of this signaling pathway in ovarian cancer. This finding is puzzling, since norrin shares with canonical WNT ligands the ability to induce β-catenin, generally considered a pro-tumorigenic pathway. In view of the currently very limited knowledge on norrin-mediated signaling, the mechanism underlying a putative function in tumor suppression remains elusive and may involve hitherto unidentified signal transduction events.

S100 family

S100 proteins play essential roles in tumor growth and progression, chemoresistance, and immune modulation [53]. Several S100 members are secreted or otherwise released in the extracellular space and interact with surface receptors, including the advanced glycation end products receptor RAGE (*AGER*), scavenger receptors (*MSR1*, *SCARA/B* gene products, *CD36*), EGF family receptors and toll-like receptor 4 (*TLR4*), and stimulate multiple signaling transduction pathways, including NFκB and MAP kinases [53]. Our data show that several *S100* genes, i.e. *S100A4*, *S100A6*, *S100A10*, *S100A8*, and *S100A9*, are expressed at very high levels in both tumor cells and TAMs (Fig. 4d). Furthermore, multiple receptors interacting with different S100 proteins or S100A8/A9 heterodimers are expressed by both tumor cells and TAMs (*SCARA/B*, *CD36*), preferentially by TAMs (*AGER*, *MSR1*, *TLR4*) or by tumor cells (*ERBB2*), pointing to extensive functional interactions between both cell types. Surprisingly, none of the *S100* genes showed an association with early relapse (Fig. 9b), which is in line with the lack of literature data supporting a role for S100 proteins in the clinical progression of ovarian cancer.

Semaphorins and ephrins

Semaphorins and ephrins, originally identified as axon guidance molecules, also have essential physiological functions during organ development, angiogenesis, and immune regulation [71–73]. More recently, their involvement in cancer cell migration, invasion, and metastasis has been uncovered, but is currently only partially understood. Activation of plexins by semaphorins results in the transactivation of oncogenic receptor tyrosine kinases, including MET, ERBB2, and KDR [73, 74]. Individual family members can be associated with either stimulatory or inhibitory effects on tumorigenesis and angiogenesis. For instance, a potential role in suppression of malignant melanoma has been described for *PLXNB1* [75], while cooperation with ERBB2 and a pro-metastatic role was reported for breast cancer cells [76]. We have identified multiple genes encoding components of both semaphorin and ephrin signaling in both tumor cells and TAMs, i.e. 13 semaphorins and at least six cognate receptors, as well as six ephrin members and seven receptors. These findings point to a complex signaling network established by tumor cells and TAMs (Fig. 4e), involving both autocrine and paracrine signaling mechanisms, as well as cell type-selective expression of ligands and receptors. Five of these genes, *SEMA3C*, *3 F*, *5A*, *6A* and in particular *6C*, are associated with early relapse (Fig. 9a and c). Likewise, four ephrin receptor genes (*EPHA1*, *EPHA4*, *EPHB2*, *EPHB4*) showed an adverse clinical association (Fig. 9b). Our findings therefore strongly support a tumor-promoting role for axon guidance ligands and their receptor in ovarian cancer. As these are expressed by tumor cells as well as TAMs, it is likely that both cell types play a role in this context.

Chemokines

Chemokines are produced by and target tumor and tumor-associated host cells through a large number of ligand-selective surface receptors, thereby establishing a large intercellular signaling network. These include TAMs [77], but their precise integration into the microenvironment of a human cancer has not been established. Our data support an essential role of TAMs within the chemokine network, since they express 11 *CCL* members (Fig. 2a) and three CCR receptors (Fig. 2b), of which two (*CCL2* and *CCL5*) are also expressed by tumor cells. TAMs also play an important role as producers of ten different chemokines of the CXCL family (Fig. 2a), but express only two *CXCR* receptor genes. One of these is CXCR4, thus confirming the prosed role of the CXCL12–CXCR4 axis in the progression of many tumor types [78], including ovarian cancer [54]. Since chemokines mainly address other cell types, in particular T-cells, the lack of expression of other *CXCR* genes in tumor cells and TAMs is conceivable.

Phospholipid breakdown products

Tumor cell and TAMs express multiple genes for secreted phospholipases, with *PLA2G7*, preferentially expressed by TAMs, as the major subtype (Fig. 5a). Intriguingly, PLA2G7 ascites levels are associated with a short RFS (Fig. 7a, e), indicating a clinical relevance for the phospholipid breakdown products. These include LPA, generated from lysophospholipids by autotaxin, and PUFAs. Our survival analyses did not show any significant correlation of LPA or autotaxin levels in ascites with the clinical outcome (Fig. 7a). However, the former result must be considered with some caution, since LPA represents a mixture of several compounds with different fatty acids in the sn1 position. It has been shown that different LPA species can exert different biological effects, which may be obscured when these are collectively quantified. Furthermore, according to the manufacturer, the antibody used for this analysis (ELISA) recognizes the minor forms (e.g. linolenic 18:3 LPA) with a higher affinity compared to the more common LPA species (e.g. oleic 18:1 LPA). The relevance of LPA as a potential indicator of early ovarian cancer relapse has therefore to be re-evaluated in future studies using methods that are able to discriminate different LPA species.

On the other hand, a clear inverse association with RFS was observed for AA (Figs. 4, 7a, f). The clinical relevance of AA is strongly supported by our finding that the adverse effect of cytokines, like IL-6, IL-10, and TGFβ were enhanced by the simultaneous presence of high AA levels, pointing to a hitherto unknown cooperation in causing therapy failure and disease progression. Importantly, AA concentrations did not show any significant correlation with IL-6, IL-10, or TGFβ (Fig. 8d), excluding the possibility that the observed clinical correlations are due to a common mechanism regulating the synthesis of these mediators.

Arachidonic acid metabolites

AA is metabolized to a number of highly bioactive eicosanoid derivatives, in particular cyclooxygenase-derived prostanoids and lipoxygenase-derived HETEs and leukotrienes. In ovarian cancer, several components of these pathways are present in ascites, and the required enzymes are expressed by both tumor cells and TAMs (Fig. 6b). These mediators seem to act primarily on TAMs, including PGE2, PGI2, and 15-HETE, as judged by the expression of their cognate receptors. An exception was LTB_4 with receptors on both cell types. A clinical relevance of these mediators is suggested by the observed inverse associations of RFS with the ascites levels of LTB_4 (Figs. 4, 7a, g) and the expression of the *PTGIS* and *PTGER3* genes (Figs. 4, 9b, e), encoding PGI_2 synthase and a PGE_2 receptor, respectively (Fig. 6b). These findings could, at least in part, explain the adverse effect of AA on survival, i.e. by serving as a precursor of pro-tumorigenic metabolites.

It can, however, not be excluded that non-metabolized AA contributes to this effect. We have recently shown that PPARβ/δ, which is expressed preferentially in TAMs (Fig. 2b), is deregulated by PUFA ligands in ovarian cancer ascites [56]. It is, however, very unlikely that PPARβ/δ mediates the adverse effect of AA on RFS, because the major ascites-associated PUFA with strong agonistic effect on PPARβ/δ is linoleic acid [56], which, in turn, is not linked to survival at all (Fig. 7a). Even though other targets for non-metabolized AA have been identified [79–82], AA-triggered signaling is poorly understood, making it difficult to speculate on the molecular mechanism underlying the clinical effect discovered in the present study.

Conclusions

In spite of the clearly documented pivotal role of the tumor microenvironment in tumor growth, progression, and immune escape, the reciprocal interactions of tumor and host cells through soluble mediators are only partially understood. In the present study we have established a global RNA-Seq based strategy to address this problem using tumor cells and TAMs from ovarian carcinoma ascites. As a first step, we developed an algorithm to adjust sequencing data for the presence of contaminating cells in the samples analyzed, i.e. macrophages in tumor cell fractions or vice versa. After optimization on training datasets the algorithm was successfully applied to the ovarian cancer samples used in the present study, indicating that the method should be generally applicable to tackle the problem of contaminating cells in RNA-Seq samples.

Taken together, our observations suggest that the strategy used in the present work is a generally applicable approach to address complex interactions in the tumor microenvironment. These include several important questions not addressed by the current study. First, it is possible that we missed clinically relevant genes, because of the necessity to exclude genes expressed at high levels in TAMs from our survival analysis. Thus, survival-associated receptor genes expressed primarily in TAMs would not have been found. Future sufficiently large RNA-Seq studies of pure cell types or single cells in conjunction with survival analyses will have to answer this question. Second, host cells other than TAMs are clearly important constituents of the tumor microenvironment, but their role within a signaling network are even less understood. In ascites these are primarily other immune cells and mesothelial cells, while fibroblasts and endothelial cells are rare or absent. Thus, the integration of T cells into the signaling network operating among the ascites-associated cells will be an important next step.

Third, it is unknown how ascites-associated tumor and host cells differ from their counterparts in solid tumor masses. Purification of cells from metastases of the same patients could be used to address this question, and also to analyze the contribution of host-derived cell types restricted to solid tumor tissue.

Methods

Patient samples

Ascites was collected from patients with high grade serous ovarian carcinoma undergoing primary surgery at the University Hospital in Marburg. Written informed consent for the use of ascites for research purposes and publication of the results obtained from this research was obtained from all patients prior to surgery according to the protocols approved by the ethics committee of Marburg University (Az 205/10). Patient characteristics are presented in Additional file 4: Tables S1 and S3. Clinical courses were evaluated by RECIST criteria [83] in patients with measurable disease or profiles of serum CA125 levels [84], according to the recommendations by the Gynecologic Cancer InterGroup (GCIG). Only patients with observations periods ≥12 months after first-line surgery were included in the survival analysis. All experimental methods comply with the Helsinki Declaration.

Isolation of TAMs from ovarian cancer ascites

Mononuclear cells were isolated from ascites by Lymphocyte Separation Medium 1077 (PromoCell) density gradient centrifugation and further purified by magnetic cell sorting (MACS) using CD14 microbeads (Miltenyi Biotech). TAMs were directly analyzed by FACS as described below or lysed in PeqGold (Peqlab) for RNA preparation.

Tumor cell/spheroid isolation from ascites

Mononuclear cells were isolated from ascites by Lymphocyte Separation Medium 1077 (PromoCell) density gradient centrifugation. Tumor spheroids were separated by filtration using 30 μm and 40 μm cell strainer (Miltenyi Biotech) resulting in either spheroids of medium size (30–40 μm = "m") or large size (>40 μm = "L"). Small tumor spheroids (<30 μm = "s") and tumor single cells (sc) were further purified by depletion of peritoneal leucocytes using CD45 microbeads and magnetic cell sorting (MACS) (Miltenyi Biotech). Purified tumor cells were lysed in PeqGold (Peqlab) for RNA preparation, analyzed by flow cytometry, or cultured for testing of chemoresistance. The purity of tumor spheroids/cells was >90 % EpCAM+ cells, except for sample OC84s (>85 %, Additional file 4: Table S2).

Characterization of tumor cells/spheroids by flow cytometry

Prior to FACS staining, tumor spheroids were dissociated into single cells by trypsination for 10 min at 37 °C, followed by vortexing for 10 s. To analyze cell cycle distribution, tumor single cells were fixed in 70 % ice-cold ethanol, washed with PBS + 2 % FCS, and treated with 100 μL RNAse (1 mg/mL) at 37 °C for 20 min. Cells were stained with 10 μL propidium iodide (1 mg/mL) for 30 min. FACS analysis was performed on a FACS Canto II instrument using Diva Software (BD Biosciences). Proliferation was analyzed by FACS after staining tumor single cells with anti-Ki67 PEVio770, anti-CD45 FITC, and anti-EpCAM PE antibodies (all Miltenyi Biotech).

Flow cytometry analysis of ascites-associated cells

Gene expression profiles generated from RNA-Seq datasets were verified in TAMs and tumor cells by FACS analysis. Mononuclear cells from patients' ascites were simultaneously stained with Vioblue-labeled anti-human EpCAM (Miltenyi Biotech) as tumor marker and FITC-labeled anti-CD14 (Miltenyi Biotech), PE-labeled anti-CD163 (eBioscience), or APC-labeled anti-CD206 (Biozol) as TAM marker. In addition, FITC-labeled anti-TGFbeta RIII and PE-labeled anti-LIF-R (all R&D Systems) were used for surface staining. Intracellular staining of permeabilized cells was performed with APC-labeled anti-IL-8 (eBioscience), FITC-labeled anti-S100A8/A9 (Life Technologies) and FITC-labeled anti-S100A14 (antibodies-online) as described previously [7]. Isotype control antibodies were purchased from BD Biosciences, Miltenyi Biotech, and eBioscience. Cells were analyzed by flow cytometry and results were calculated as percentage of positive cells and mean fluorescence intensities (MFI).

In vitro testing of chemoresistance

Tumor spheroids or single cells from patients were cultured in M199 media (Life Technologies) plus 10 % autologous, cell-free ascites with or without 10 μM carboplatin (Sigma Aldrich) and 10 nM paclitaxel (AdipoGen) at 37 °C, 5 % CO_2 (approximately $2.5–5 \times 10^5$ cells/mL). After 6 days, the 3-[4,5-dimethylthiazol-2-yl]-2,5-diphenyl tetrazoliumbromid (MTT) assay was performed to assess cell viability as described previously [85]. The percentage of chemoresistant tumor cells in the carboplatin/paclitaxel treated culture was calculated relative to cells treated with solvent control (DMSO).

Analysis of soluble mediators in cell-free ascites

Soluble mediators in ascites of ovarian cancer patients were quantified using commercial ELISA Kits according to the instructions of the manufacturers. Human IL-6, IL-10, LIF, VEGF-A, CCL-2, and TGFβ1 levels in ascites were analyzed by ELISA kits purchased from eBioscience. ANGPTL4 levels were determined using ELISA kit from Aviscera Bioscience, leptin by ELISA Kit

from RayBiotech and LPA by ELISA kit from Echelon. The phospholipase A2, Group XIIA (PLA2G12A) ELISA Kit was from antibodies-online, the PLA2G2A ELISA kit from Biozol, and the ENPP-2/Autotaxin, CSF-1, S100A8, and PLA2G7 ELISAs from R&D Systems.

Quantification of lipids by liquid chromatography - tandem mass spectrometry (LC-MS/MS)

Ascites samples (1 mL) were spiked with 100 μL deuterated internal standard and extracted using solid reverse phase extraction columns (Strata-X 33, Phenomenex). Fatty acids derivatives were eluted into 1.0 mL of methanol, lyophilized, and resuspended in 100 mL of water/acetonitrile/formic acid (70:30:0.02, v/v/v; solvent A) and analyzed by LC-MS/MS on an Agilent 1290 separation system. Samples were separated on a Synergi reverse-phase C18 column (2.1 × 250 mm; Phenomenex) using a gradient as follows: flow rate = 0.3 μL/min, 1 min (acetonitrile/isopropyl alcohol, 50:50, v/v; solvent B), 3 min (25 % solvent B), 11 min (45 % solvent B), 13 min (60 % solvent B), 18 min (75 % solvent B), 18.5 min (90 % solvent B), 20 min (90 % solvent B), 21 min (0 % solvent). The separation system was coupled to an electrospray interface of a QTrap 5500 mass spectrometer (AB Sciex). Compounds were detected in scheduled multiple reaction monitoring mode. For quantification a 12-point calibration curve for each analyte was used. Data analysis was performed using Analyst (v1.6.1) and MultiQuant (v2.1.1) (AB Sciex).

RT-qPCR and RNA-Seq

cDNA isolation and qPCR analyses were performed as described [86], using *L27* for normalization and evaluated by the Cy0 method [87]. Primer sequences are listed in Additional file 4: Table S5. RNA-Seq was carried out on an Illumina HiSeq 1500 as described [85]. Summarized read counts are shown in Additional file 3: Dataset S1. Genome assembly and gene model data were retrieved from Ensembl revision 74.

Sequencing data availability

Sequencing data were deposited at EBI ArrayExpress (accession numbers E-MTAB-3167 and E-MTAB-4162).

Bioinformatic analysis of RNA-Seq data

RNA-Seq data were aligned to Ensembl v74 using STAR (version STAR_2.4.1a) [88]. Gene read counts were established as read count within merged exons of protein coding transcripts (for genes with a protein gene product) or within merged exons of all transcripts (for non-coding genes). TPM (transcripts per million) were calculated based on the total gene read counts and length of merged exons. Genes were considered expressed if they had a minimum TPM of 3. All genomic sequence and gene annotation data were retrieved from Ensembl release 74, genome assembly hg19. Our full analysis scripts and computational pipeline are available upon request.

Adjustment of RNA-Seq data for contaminating cells

The development and testing of our algorithm, including benchmarking against other published algorithms, are described in detail in Additional files 1 and 5.

Simulations for Fig. 1a were performed 12,000 times on data retrieved from GSE60424 [51]. The dataset consists of highly purified immune cells from patients with various autoimmune diseases. Samples annotated "whole blood" and sample lib264 were excluded, as the latter showed monocyte contamination. Mixtures were calculated by resampling the larger sample to the size of the smaller one and mixing at a chosen percentage. Reference expressions were calculated from all non-mixed samples of the respective tissues. Contamination estimation and correction was performed as described in detail in Additional file 1.

OC66s, TAM72, and TAT31 were used as reference samples for pure tumor cell, TAM, and TAT populations, respectively (see Fig. 1b, c). The automated procedure selected the following marker genes for adjusting tumor cell datasets:

TAM marker genes: *AIF1*, *C1QB*, *C1QC*, *CCR1*, *CD36*, *CMKLR1*, *CR1*, *FCGR2A*, *FCGR3B*, *FPR3*, *ITGAM*, *MARCO*, *MPEG1*, *MRC1L1*, *STAB1*, *TLR4*, *VCAN*.
TAT marker genes: *ATP2A3*, *C16orf54*, *CCR4*, *CCR7*, *CD2*, *CD247*, *CD3E*, *CD96*, *GZMK*, *IL2RB*, *IL2RG*, *KCNA3*, *LEF1*, *NKG7*, *PRF1*, *RHOH*, *ZNF831*.

For adjusting TAM datasets the following marker genes were selected:

Tumor cell marker genes: *ASS1*, *CDH1*, *CLDN4*, *CT45A1*, *CT45A3*, *CT45A4*, *CT45A5*, *DSP*, *EPCAM*, *ESRP1*, *IGFBP3*, *KRT7*, *LRP6*, *MEIS1*, *PRAME*, *SLPI*, *VTCN1*.
TAT marker genes: *ATP2A3*, *CAMK4*, *CCR4*, *CD8A*, *CD8B*, *CST7*, *KCNA3*, *KLF12*, *LCK*, *LIME1*, *MT1X*, *NKG7*, *PRF1*, *RHOH*, *RLTPR*, *TCF7*, *TGFBR3*.

The source code for implementing our algorithm and the simulations described in the present study are included as Additional file 6 and deposited at GitHib (https://github.com/IMTMarburg/rnaseqmixture) and Zonodo (doi:10.5281/zenodo.48872).

Statistical analysis of experimental data

Comparative data were statistically analyzed by Student's *t*-test (two-sided, unequal variance) using GraphPad

Prism 6.0. Results were expressed as follows: *p <0.05; **p <0.01; ***p <0.001; ****p <0.0001. CIs were calculated using the bootstrap method.

Survival-associated gene expression analysis

Associations between gene expression and relapse-free survival of ovarian cancer patients were analyzed using the web based tool "KM Plotter" [38] (http://kmplot.com) with the following settings: "auto select best cutoff," probe set option: "JetSet best probe," histology: serous, datasets: all; other settings: default). The 2015 version of KM Plotter used contains the following 13 datasets: GSE14764 (n = 80), GSE15622 (n = 36), GSE18520 (n = 63), GSE19829 (n = 28), GSE23554 (n = 28), GSE26193 (n = 107), GSE26712 (n = 195), GSE27651 (n = 49), GSE30161 (n = 58), GSE3149 (n = 116), GSE51373 (n = 28), GSE9891 (n = 285), TCGA (n = 565). The GraphPad Prism software was used to analyze associations of soluble mediator concentrations in ascites fluid with RFS (Kaplan-Meier plots, logrank p values, logrank HR, and median survival times). Multiple hypothesis testing was accounted for out by controlling the FDR using the Benjamini-Hochberg method.

Additional files

Additional file 1: Description and optimization of the algorithm and benchmarking against published methods. (PDF 5117 kb)

Additional file 2: Supplementary Figures S1–S4. (PDF 946 kb)

Additional file 3: Datasets S1–S7. (XLS 26437 kb)

Additional file 4: Supplementary Table S1–S5. (XLS 48 kb)

Additional file 5: Source code. (TXT 9 kb)

Additional file 6: Assembly of gene sets. (PDF 200 kb)

Abbreviations

AA: arachidonic acid; ChIP: chromatin immunoprecipitation; CI: confidence interval; ELISA: enzyme-linked immunosorbent assay; FDR: false discovery rate; HR: hazard ratio; LPA: lysophosphatitic acid; LC-MS/MS: liquid chromatography - tandem mass spectrometry; LT: leukotriene; MAE: mean absolute error; PG: prostaglandin; PUFA: polyunsaturated fatty acid; RNA-Seq: RNA sequencing; RFS: relapse-free survival; TAM: tumor-associated macrophage; TAT: tumor-associated lymphocyte; TPM: transcripts per million.

Acknowledgements

We are grateful to Dr. Marco Memberger for useful discussions of bioinformatic analyses, to N. Dinesh and R. Yerabolu for help with RT-qPCR experiments, and to T. Plaum, A. Allmeroth, and M. Alt for expert technical assistance. This work was supported by grants from the Wilhelm Sander-Stiftung (2011.082.2) to SM-B, SR, and UW and from UKGM to SR, TA, VR, and UW.

Authors' contributions

SR prepared and characterized all tumor cell and TAM samples and performed the FACS and ELISA-based analyses; FF performed bioinformatics analysis; VR and TSch carried out RNA isolation and RT-qPCR analyses; TA constructed RNA-Seq libraries and performed quality control experiments; YS and WAN carried out LC-MS/MS analyses; AN and TSt established NGS methodologies and acquired the RNA-Seq data; JMJ and UW provided clinical samples and analyzed clinical data; SR, SMB, and RM conceived the study, oversaw the project, and wrote the paper. All authors read and approved the final manuscript.

Competing interests

The authors declare that they have no competing interests.

Author details

[1]Clinic for Gynecology, Gynecological Oncology and Gynecological Endocrinology, Center for Tumor Biology and Immunology (ZTI), Philipps University, Marburg, Germany. [2]Institute of Molecular Biology and Tumor Research (IMT), Center for Tumor Biology and Immunology (ZTI), Philipps University, Hans-Meerwein-Str. 3, Marburg 35043, Germany. [3]Metabolomics Core Facility and Institute of Laboratory Medicine and Pathobiochemistry, Center for Tumor Biology and Immunology (ZTI), Philipps University, Marburg, Germany. [4]Genomics Core Facility, Center for Tumor Biology and Immunology (ZTI), Philipps University, Marburg, Germany.

Received: 17 December 2015 Accepted: 15 April 2016
Published online: 23 May 2016

References

1. Colombo N, Peiretti M, Parma G, Lapresa M, Mancari R, Carinelli S, Sessa C, Castiglione M, Group EGW. Newly diagnosed and relapsed epithelial ovarian carcinoma: ESMO Clinical Practice Guidelines for diagnosis, treatment and follow-up. Ann Oncol. 2010;21 Suppl 5:v23–30.
2. Lengyel E. Ovarian cancer development and metastasis. Am J Pathol. 2010;177:1053–64.
3. Kulbe H, Chakravarty P, Leinster DA, Charles KA, Kwong J, Thompson RG, Coward JI, Schioppa T, Robinson SC, Gallagher WM, et al. A dynamic inflammatory cytokine network in the human ovarian cancer microenvironment. Cancer Res. 2012;72:66–75.
4. Peng P, Yan Y, Keng S. Exosomes in the ascites of ovarian cancer patients: origin and effects on anti-tumor immunity. Oncol Rep. 2011;25:749–62.
5. Latifi A, Luwor RB, Bilandzic M, Nazaretian S, Stenvers K, Pyman J, Zhu H, Thompson EW, Quinn MA, Findlay JK, Ahmed N. Isolation and characterization of tumor cells from the ascites of ovarian cancer patients: molecular phenotype of chemoresistant ovarian tumors. PLoS One. 2012;7:e46858.
6. Takaishi K, Komohara Y, Tashiro H, Ohtake H, Nakagawa T, Katabuchi H, Takeya M. Involvement of M2-polarized macrophages in the ascites from advanced epithelial ovarian carcinoma in tumor progression via Stat3 activation. Cancer Sci. 2010;101:2128–36.
7. Reinartz S, Schumann T, Finkernagel F, Wortmann A, Jansen JM, Meissner W, Krause M, Schworer AM, Wagner U, Muller-Brusselbach S, Muller R. Mixed-polarization phenotype of ascites-associated macrophages in human ovarian carcinoma: Correlation of CD163 expression, cytokine levels and early relapse. Int J Cancer. 2014;134:32–42.
8. Qian BZ, Pollard JW. Macrophage diversity enhances tumor progression and metastasis. Cell. 2010;141:39–51.
9. Gabrilovich DI, Ostrand-Rosenberg S, Bronte V. Coordinated regulation of myeloid cells by tumours. Nat Rev Immunol. 2012;12:253–68.
10. Sica A, Mantovani A. Macrophage plasticity and polarization: in vivo veritas. J Clin Invest. 2012;122:787–95.
11. Condeelis J, Pollard JW. Macrophages: obligate partners for tumor cell migration, invasion, and metastasis. Cell. 2006;124:263–6.
12. Sica A, Bronte V. Altered macrophage differentiation and immune dysfunction in tumor development. J Clin Invest. 2007;117:1155–66.
13. Kawamura K, Komohara Y, Takaishi K, Katabuchi H, Takeya M. Detection of M2 macrophages and colony-stimulating factor 1 expression in serous and mucinous ovarian epithelial tumors. Pathol Int. 2009;59:300–5.
14. Mills GB, May C, Hill M, Campbell S, Shaw P, Marks A. Ascitic fluid from human ovarian cancer patients contains growth factors necessary for intraperitoneal growth of human ovarian adenocarcinoma cells. J Clin Invest. 1990;86:851–5.
15. Lane D, Matte I, Rancourt C, Piche A. Prognostic significance of IL-6 and IL-8 ascites levels in ovarian cancer patients. BMC Cancer. 2011;11:210.
16. Matte I, Lane D, Laplante C, Rancourt C, Piche A. Profiling of cytokines in human epithelial ovarian cancer ascites. Am J Cancer Res. 2012;2:566–80.
17. Mishra P, Banerjee D, Ben-Baruch A. Chemokines at the crossroads of tumor-fibroblast interactions that promote malignancy. J Leukoc Biol. 2011;89:31–9.
18. Duluc D, Delneste Y, Tan F, Moles MP, Grimaud L, Lenoir J, Preisser L, Anegon I, Catala L, Ifrah N, et al. Tumor-associated leukemia inhibitory factor and IL-6 skew monocyte differentiation into tumor-associated macrophage-like cells. Blood. 2007;110:4319–30.

19. Marchini S, Fruscio R, Clivio L, Beltrame L, Porcu L, Fuso Nerini I, Cavalieri D, Chiorino G, Cattoretti G, Mangioni C, et al. Resistance to platinum-based chemotherapy is associated with epithelial to mesenchymal transition in epithelial ovarian cancer. Eur J Cancer. 2013;49:520–30.
20. Zhang S, Balch C, Chan MW, Lai HC, Matei D, Schilder JM, Yan PS, Huang TH, Nephew KP. Identification and characterization of ovarian cancer-initiating cells from primary human tumors. Cancer Res. 2008;68:4311–20.
21. Flesken-Nikitin A, Hwang CI, Cheng CY, Michurina TV, Enikolopov G, Nikitin AY. Ovarian surface epithelium at the junction area contains a cancer-prone stem cell niche. Nature. 2013;495:241–5.
22. de Lau W, Peng WC, Gros P, Clevers H. The R-spondin/Lgr5/Rnf43 module: regulator of Wnt signal strength. Genes Dev. 2014;28:305–16.
23. Hodge DR, Hurt EM, Farrar WL. The role of IL-6 and STAT3 in inflammation and cancer. Eur J Cancer. 2005;41:2502–12.
24. Byrne AT, Ross L, Holash J, Nakanishi M, Hu L, Hofmann JI, Yancopoulos GD, Jaffe RB. Vascular endothelial growth factor-trap decreases tumor burden, inhibits ascites, and causes dramatic vascular remodeling in an ovarian cancer model. Clin Cancer Res. 2003;9:5721–8.
25. Eng KH, Ruggeri C. Connecting prognostic ligand receptor signaling loops in advanced ovarian cancer. PLoS One. 2014;9:e107193.
26. Xu Y, Gaudette DC, Boynton JD, Frankel A, Fang XJ, Sharma A, Hurteau J, Casey G, Goodbody A, Mellors A, et al. Characterization of an ovarian cancer activating factor in ascites from ovarian cancer patients. Clin Cancer Res. 1995;1:1223–32.
27. Westermann AM, Havik E, Postma FR, Beijnen JH, Dalesio O, Moolenaar WH, Rodenhuis S. Malignant effusions contain lysophosphatidic acid (LPA)-like activity. Ann Oncol. 1998;9:437–42.
28. Mills GB, Moolenaar WH. The emerging role of lysophosphatidic acid in cancer. Nat Rev Cancer. 2003;3:582–91.
29. Houben AJ, Moolenaar WH. Autotaxin and LPA receptor signaling in cancer. Cancer Metastasis Rev. 2011;30:557–65.
30. Chun J, Hla T, Spiegel S, Moolenaar W, editors. Lysophospholipid receptors: signaling and biochemistry. Hoboken, NJ: Wiley; 2013.
31. Tsujiuchi T, Araki M, Hirane M, Dong Y, Fukushima N. Lysophosphatidic acid receptors in cancer pathobiology. Histol Histopathol. 2014;29:313–21.
32. Punnonen R, Seppala E, Punnonen K, Heinonen PK. Fatty acid composition and arachidonic acid metabolites in ascitic fluid of patients with ovarian cancer. Prostaglandins Leukot Med. 1986;22:153–8.
33. Wymann MP, Schneiter R. Lipid signalling in disease. Nat Rev Mol Cell Biol. 2008;9:162–76.
34. Obermajer N, Muthuswamy R, Odunsi K, Edwards RP, Kalinski P. PGE(2)-induced CXCL12 production and CXCR4 expression controls the accumulation of human MDSCs in ovarian cancer environment. Cancer Res. 2011;71:7463–70.
35. Brindley DN, Lin FT, Tigyi GJ. Role of the autotaxin-lysophosphatidate axis in cancer resistance to chemotherapy and radiotherapy. Biochim Biophys Acta. 1831;2013:74–85.
36. Kalinski P. Regulation of immune responses by prostaglandin E2. J Immunol. 2012;188:21–8.
37. Network TCGAR. Integrated genomic analyses of ovarian carcinoma. Nature. 2011;474:609–15.
38. Gyorffy B, Lanczky A, Szallasi Z. Implementing an online tool for genome-wide validation of survival-associated biomarkers in ovarian-cancer using microarray data from 1287 patients. Endocr Relat Cancer. 2012;19:197–208.
39. Verhaak RG, Tamayo P, Yang JY, Hubbard D, Zhang H, Creighton CJ, Fereday S, Lawrence M, Carter SL, Mermel CH, et al. Prognostically relevant gene signatures of high-grade serous ovarian carcinoma. J Clin Invest. 2013;123:517–25.
40. Erkkila T, Lehmusvaara S, Ruusuvuori P, Visakorpi T, Shmulevich I, Lahdesmaki H. Probabilistic analysis of gene expression measurements from heterogeneous tissues. Bioinformatics. 2010;26:2571–7.
41. Kuhn A, Thu D, Waldvogel HJ, Faull RL, Luthi-Carter R. Population-specific expression analysis (PSEA) reveals molecular changes in diseased brain. Nat Methods. 2011;8:945–7.
42. Spite M, Hellmann J, Tang Y, Mathis SP, Kosuri M, Bhatnagar A, Jala VR, Haribabu B. Deficiency of the leukotriene B4 receptor, BLT-1, protects against systemic insulin resistance in diet-induced obesity. J Immunol. 2011;187:1942–9.
43. Ahn J, Yuan Y, Parmigiani G, Suraokar MB, Diao L, Wistuba II, Wang W. DeMix: deconvolution for mixed cancer transcriptomes using raw measured data. Bioinformatics. 2013;29:1865–71.
44. Gong T, Szustakowski JD. DeconRNASeq: a statistical framework for deconvolution of heterogeneous tissue samples based on mRNA-Seq data. Bioinformatics. 2013;29:1083–5.
45. Li Y, Xie X. A mixture model for expression deconvolution from RNA-seq in heterogeneous tissues. BMC Bioinformatics. 2013;14 Suppl 5:S11.
46. Quon G, Haider S, Deshwar AG, Cui A, Boutros PC, Morris Q. Computational purification of individual tumor gene expression profiles leads to significant improvements in prognostic prediction. Genome Med. 2013;5:29.
47. Yoshihara K, Shahmoradgoli M, Martinez E, Vegesna R, Kim H, Torres-Garcia W, Trevino V, Shen H, Laird PW, Levine DA, et al. Inferring tumour purity and stromal and immune cell admixture from expression data. Nat Commun. 2013;4:2612.
48. Newman AM, Liu CL, Green MR, Gentles AJ, Feng W, Xu Y, Hoang CD, Diehn M, Alizadeh AA. Robust enumeration of cell subsets from tissue expression profiles. Nat Methods. 2015;12:453–7.
49. Shen Q, Hu J, Jiang N, Hu X, Luo Z, Zhang H. contamDE: Differential expression analysis of RNA-seq data for contaminated tumor samples. Bioinformatics. 2016;32(5):705-12.
50. Wang N, Gong T, Clarke R, Chen L, Shih Ie M, Zhang Z, Levine DA, Xuan J, Wang Y. UNDO: a Bioconductor R package for unsupervised deconvolution of mixed gene expressions in tumor samples. Bioinformatics. 2015;31:137–9.
51. Linsley PS, Speake C, Whalen E, Chaussabel D. Copy number loss of the interferon gene cluster in melanomas is linked to reduced T cell infiltrate and poor patient prognosis. PLoS One. 2014;9:e109760.
52. Thrasivoulou C, Millar M, Ahmed A. Activation of intracellular calcium by multiple Wnt ligands and translocation of beta-catenin into the nucleus: a convergent model of Wnt/Ca2+ and Wnt/beta-catenin pathways. J Biol Chem. 2013;288:35651–9.
53. Donato R, Cannon BR, Sorci G, Riuzzi F, Hsu K, Weber DJ, Geczy CL. Functions of S100 proteins. Curr Mol Med. 2013;13:24–57.
54. Popple A, Durrant LG, Spendlove I, Rolland P, Scott IV, Deen S, Ramage JM. The chemokine, CXCL12, is an independent predictor of poor survival in ovarian cancer. Br J Cancer. 2012;106:1306–13.
55. Junge HJ, Yang S, Burton JB, Paes K, Shu X, French DM, Costa M, Rice DS, Ye W. TSPAN12 regulates retinal vascular development by promoting Norrin- but not Wnt-induced FZD4/beta-catenin signaling. Cell. 2009;139:299–311.
56. Schumann T, Adhikary T, Wortmann A, Finkernagel F, Lieber S, Schnitzer E, Legrand N, Schober Y, Nockher WA, Toth PM, et al. Deregulation of PPARβ/δ target genes in tumor-associated macrophages by fatty acid ligands in the ovarian cancer microenvironment. Oncotarget. 2015;6:13416–33.
57. Gupta RA, Tan J, Krause WF, Geraci MW, Willson TM, Dey SK, DuBois RN. Prostacyclin-mediated activation of peroxisome proliferator-activated receptor delta in colorectal cancer. Proc Natl Acad Sci U S A. 2000;97:13275–80.
58. Huang JT, Welch JS, Ricote M, Binder CJ, Willson TM, Kelly C, Witztum JL, Funk CD, Conrad D, Glass CK. Interleukin-4-dependent production of PPAR-gamma ligands in macrophages by 12/15-lipoxygenase. Nature. 1999;400:378–82.
59. Naruhn S, Meissner W, Adhikary T, Kaddatz K, Klein T, Watzer B, Müller-Brüsselbach S, Müller R. 15-hydroxyeicosatetraenoic acid is a preferential peroxisome proliferator-activated receptor β/δ agonist. Mol Pharmacol. 2010;77:171–84.
60. Bishayee K, Khuda-Bukhsh AR. 5-lipoxygenase antagonist therapy: a new approach towards targeted cancer chemotherapy. Acta Biochim Biophys Sin Shanghai. 2013;45:709–19.
61. Planutis K, Planutiene M, Holcombe RF. A novel signaling pathway regulates colon cancer angiogenesis through Norrin. Sci Rep. 2014;4:5630.
62. Rosen DG, Mercado-Uribe I, Yang G, Bast Jr RC, Amin HM, Lai R, Liu J. The role of constitutively active signal transducer and activator of transcription 3 in ovarian tumorigenesis and prognosis. Cancer. 2006;107:2730–40.
63. Uddin S, Bu R, Ahmed M, Abubaker J, Al-Dayel F, Bavi P, Al-Kuraya KS. Overexpression of leptin receptor predicts an unfavorable outcome in Middle Eastern ovarian cancer. Mol Cancer. 2009;8:74.
64. Coward J, Kulbe H, Chakravarty P, Leader D, Vassileva V, Leinster DA, Thompson R, Schioppa T, Nemeth J, Vermeulen J, et al. Interleukin-6 as a therapeutic target in human ovarian cancer. Clin Cancer Res. 2011;17:6083–96.
65. Wang X, Crowe PJ, Goldstein D, Yang JL. STAT3 inhibition, a novel approach to enhancing targeted therapy in human cancers (review). Int J Oncol. 2012;41:1181–91.
66. Riester M, Wei W, Waldron L, Culhane AC, Trippa L, Oliva E, Kim SH, Michor F, Huttenhower C, Parmigiani G, Birrer MJ. Risk prediction for late-stage ovarian cancer by meta-analysis of 1525 patient samples. J Natl Cancer Inst. 2014;106:pii:dju048.

67. Padua D, Massague J. Roles of TGFbeta in metastasis. Cell Res. 2009;19:89–102.
68. Wrzesinski SH, Wan YY, Flavell RA. Transforming growth factor-beta and the immune response: implications for anticancer therapy. Clin Cancer Res. 2007;13:5262–70.
69. McLean K, Gong Y, Choi Y, Deng N, Yang K, Bai S, Cabrera L, Keller E, McCauley L, Cho KR, Buckanovich RJ. Human ovarian carcinoma-associated mesenchymal stem cells regulate cancer stem cells and tumorigenesis via altered BMP production. J Clin Invest. 2011;121:3206–19.
70. Yoshioka S, King ML, Ran S, Okuda H, MacLean 2nd JA, McAsey ME, Sugino N, Brard L, Watabe K, Hayashi K. WNT7A regulates tumor growth and progression in ovarian cancer through the WNT/beta-catenin pathway. Mol Cancer Res. 2012;10:469–82.
71. Pasquale EB. Eph receptors and ephrins in cancer: bidirectional signalling and beyond. Nat Rev Cancer. 2010;10:165–80.
72. Rehman M, Tamagnone L. Semaphorins in cancer: biological mechanisms and therapeutic approaches. Semin Cell Dev Biol. 2013;24:179–89.
73. Worzfeld T, Offermanns S. Semaphorins and plexins as therapeutic targets. Nat Rev Drug Discov. 2014;13:603–21.
74. Tamagnone L. Emerging role of semaphorins as major regulatory signals and potential therapeutic targets in cancer. Cancer Cell. 2012;22:145–52.
75. Stevens L, McClelland L, Fricke A, Williamson M, Kuo I, Scott G. Plexin B1 suppresses c-Met in melanoma: a role for plexin B1 as a tumor-suppressor protein through regulation of c-Met. J Invest Dermatol. 2010;130:1636–45.
76. Worzfeld T, Swiercz JM, Looso M, Straub BK, Sivaraj KK, Offermanns S. ErbB-2 signals through Plexin-B1 to promote breast cancer metastasis. J Clin Invest. 2012;122:1296–305.
77. Mukaida N, Sasaki S, Baba T. Chemokines in cancer development and progression and their potential as targeting molecules for cancer treatment. Mediators Inflamm. 2014;2014:170381.
78. Sun X, Cheng G, Hao M, Zheng J, Zhou X, Zhang J, Taichman RS, Pienta KJ, Wang J. CXCL12/CXCR4/CXCR7 chemokine axis and cancer progression. Cancer Metastasis Rev. 2010;29:709–22.
79. Khan WA, Blobe GC, Hannun YA. Arachidonic acid and free fatty acids as second messengers and the role of protein kinase C. Cell Signal. 1995;7:171–84.
80. Rizzo MT, Carlo-Stella C. Arachidonic acid mediates interleukin-1 and tumor necrosis factor-alpha-induced activation of the c-jun amino-terminal kinases in stromal cells. Blood. 1996;88:3792–800.
81. Huang XP, Pi Y, Lokuta AJ, Greaser ML, Walker JW. Arachidonic acid stimulates protein kinase C-epsilon redistribution in heart cells. J Cell Sci. 1997;110(Pt 14):1625–34.
82. O'Flaherty JT, Chadwell BA, Kearns MW, Sergeant S, Daniel LW. Protein kinases C translocation responses to low concentrations of arachidonic acid. J Biol Chem. 2001;276:24743–50.
83. Therasse P, Arbuck SG, Eisenhauer EA, Wanders J, Kaplan RS, Rubinstein L, Verweij J, Van Glabbeke M, van Oosterom AT, Christian MC, Gwyther SG. New guidelines to evaluate the response to treatment in solid tumors. European Organization for Research and Treatment of Cancer, National Cancer Institute of the United States, National Cancer Institute of Canada. J Natl Cancer Inst. 2000;92:205–16.
84. Rustin GJ, Timmers P, Nelstrop A, Shreeves G, Bentzen SM, Baron B, Piccart MJ, Bertelsen K, Stuart G, Cassidy J, Eisenhauer E. Comparison of CA-125 and standard definitions of progression of ovarian cancer in the intergroup trial of cisplatin and paclitaxel versus cisplatin and cyclophosphamide. J Clin Oncol. 2006;24:45–51.
85. Adhikary T, Wortmann A, Schumann T, Finkernagel F, Lieber S, Roth K, Toth PM, Diederich WE, Nist A, Stiewe T, et al. The transcriptional PPARβ/δ network in human macrophages defines a unique agonist-induced activation state. Nucleic Acids Res. 2015;43:5033–51.
86. Naruhn S, Toth PM, Adhikary T, Kaddatz K, Pape V, Dörr S, Klebe G, Müller-Brüsselbach S, Diederich WE, Müller R. High-affinity peroxisome proliferator-activated receptor beta/delta-specific ligands with pure antagonistic or inverse agonistic properties. Mol Pharmacol. 2011;80:828–38.
87. Guescini M, Sisti D, Rocchi MB, Stocchi L, Stocchi V. A new real-time PCR method to overcome significant quantitative inaccuracy due to slight amplification inhibition. BMC Bioinformatics. 2008;9:326.
88. Dobin A, Davis CA, Schlesinger F, Drenkow J, Zaleski C, Jha S, Batut P, Chaisson M, Gingeras TR. STAR: ultrafast universal RNA-seq aligner. Bioinformatics. 2013;29:15–21.

Algorithms for deconvoluting different cell types from expression data sets: applicability to the adjustment of RNA-Seq data of ovarian cancer associated cells

Background

Enrichment of specific cell types from ovarian cancer associated ascites is often faced with the problem of other “contaminating” cell types. Determining such contaminations from gene expression profiles *in silico* is a well-established problem commonly referred to as "”deconvolution” (see a recent review of available algorithms [1]). Once the composition of a sample has been established, a correction against the contamination can be implemented.

We found that none of the available algorithms is suitable for our specific conditions:

(i) we are dealing with RNA-Seq data, while many older algorithms have been established on micro array data,

(ii) we have a relatively small number of samples to correct and learn from,

(iii) our datasets reflect two or three cell types involved, which are highly dissimilar,

(iv) there is no prior knowledge of appropriate marker genes (since TAMs are not canonically activated macrophages,

(v) the profile of tumor cells in ascites was undetermined prior to the present study, and

(vi) we require both an estimate of the contamination and a correction of expression gene profiles.

Description of algorithm

Our chosen approach is mathematically straightforward: Starting with two pure reference samples representing the cell type of interest ("target") and the contaminating cell type we select a set of suitable contamination marker genes, use these to estimate the extent of contamination and then adjust the target dataset by a linear model. The purity of reference samples must be determined by other methods, e.g. microscopy or flow cytometry.

Potential marker genes are defined as genes with (i) at least a three fold change between target and contaminating cell types and (ii) a maximum expression of 10 TPM in non-target cell types. These candidates are ranked by fold change, the top j are skipped (see below) and a fixed number is chosen.

Expression of marker genes is modeled as

$$y_{observed} = y_{contamination} * p + y_{target} * (1 - x)$$

with y_S being gene expression in TPM and x the contamination percentage of a single contamination. We replace $y_{target} * (1 - x)$ with the expression in our target cell type reference sample ($y_{reference}$), thereby introducing a slight bias to underestimate the contamination percentage. Note that for marker genes, y_{target} is less than 10 TPM, while $y_{contamination}$ is typically much larger. An underestimation of the contamination keeps our correction conservative, preventing too harsh a correction.

Our final estimation (P) is the median of

$$p = \frac{(y_{observed} - y_{reference})}{y_{contamination}}$$

x smaller than 0 is replaced by 0, P >1.0 is rejected.

To correct, for each gene we replace $y_{observed}$ with

$$\frac{y_{corrected} = (y_{observed} - P * y_{contamination})}{(1.0 - P)}$$

thereby rescaling to TPM.

To extend the approach to a three-cell line setting, we estimate contamination percentages for each cell type independently using disjunct mark sets and replace $y_{observed}$ with

$$y_{corrected} = \frac{y_{observed} - P_1 * y_{contamination1} - P_2 * y_{contamination2}}{1.0 - P_1 - P_2}$$

Implausible results ($P_1 + P_2 > 1.0$) are rejected.

Estimation of nuisance parameters

The algorithm has two nuisance parameters, the number of genes to choose (k), and the number of ranks to skip (j). Nuisance parameters were optimized in a simulation setting with 1,000 repetitions per parameter value. Monocyte samples (contamination) from GSE60424 (Table 1) were mixed with samples from other blood cells (target) at randomized percentages. One monocyte and one target sample (not part of the mixture) were chosen as reference. It was found that no straightforward correlation between the nuisance parameters and the accuracy of the algorithm exists (Figure 1).

Table 1: Samples in dataset GSE60424

Tissue	Sample count	**Comment**
B-Cells	20	
CD4	20	
CD8	19	Sample lib264 omitted due to monocyte signal
NK	14	
Monocytes	20	
Neutrophils	20	
Whole blood	20	

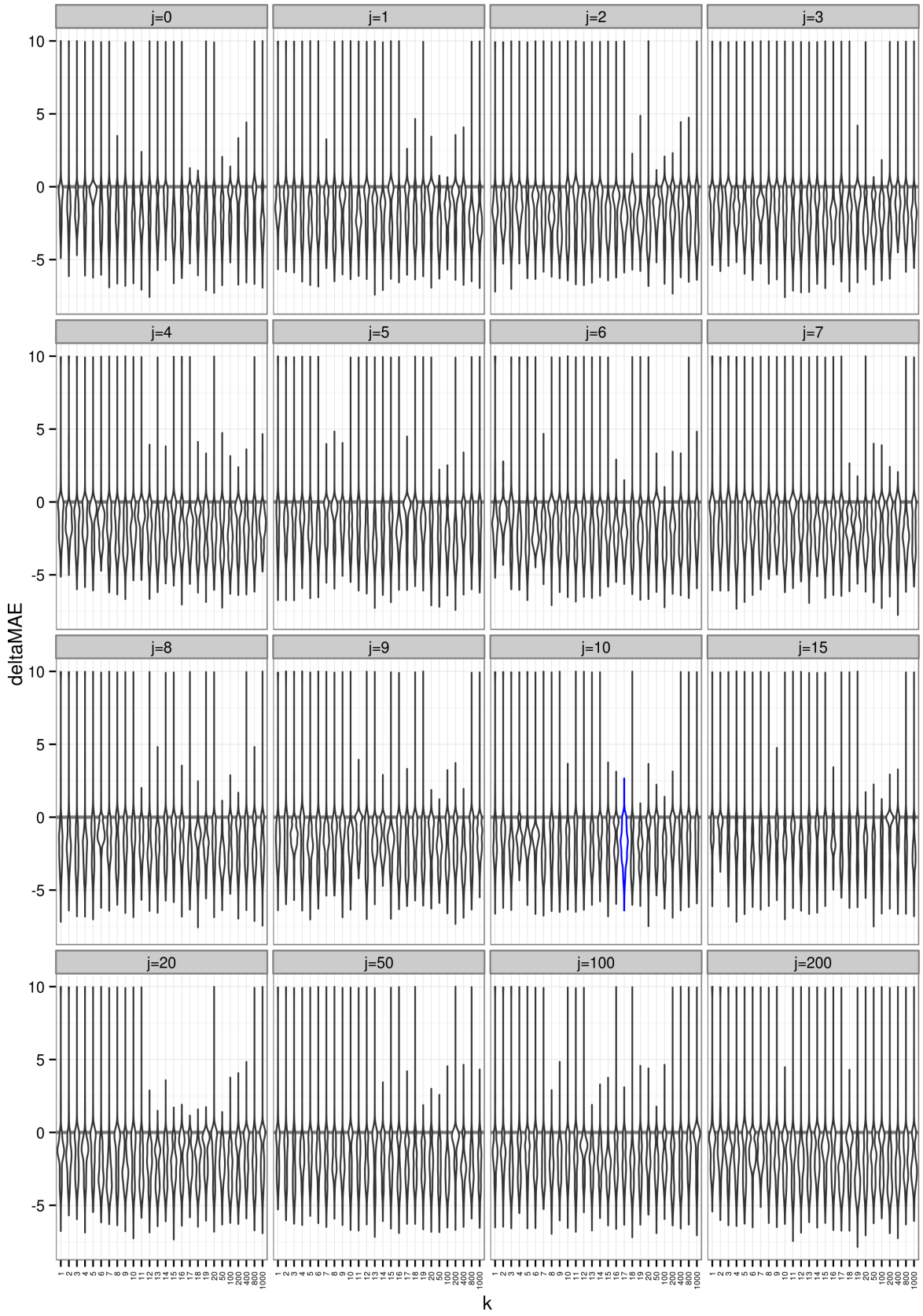

Figure 1: Parameter sweep. Shown is the change in mean absolute error between (corrected) mixture TPM and ground truth. We performed 500 simulations per data point. Blue: values chosen for correction in the main paper.

Evaluation of algorithms

We evaluated algorithms in a simulation setting, in which arbitrary percentages of randomly chosen samples of different tissues were mixed. Different samples from the same tissue were chosen as references. Two RNA-Seq data sets of different tissues were used: the large Gene Tissue-Expression (GTEx) dataset [2] (Table 2), and E-MTAB-2836 [3], a smaller dataset that includes immune related tissue (Table 3). Simulations were run 10,000 times.

Table 2: Tissues in GTExdataset
(retrieved on 2015-06-08, only the samples in the GTEx pilot study were used).

Tissue	Sample count
Adipose - Subcutaneous	128
Artery - Tibial	137
Heart - Left Ventricle	95
Lung	133
Muscle - Skeletal	157
Nerve - Tibial	114
Skin - Sun Exposed (Lower	126
Thyroid	120
Whole Blood	191

Table 3: Tissues in E-MTAB-2836 dataset

Tissue	Sample count
adipose tissue	7
bone marrow	8
colon	8
endometrium	9
gall bladder	7
heart	9
lung	8
lymph node	13
placenta	7
prostate	7
small intestine	8
testis	8
thyroid	9

The in-silico mixture allowed evaluation of algorithms on the difference between corrected and uncorrected Mean-Absolute-Error (MAE)

$$\text{deltaMAE} = \text{mean}(|y_{corrected} - y_{groundtruth}|) - mean(|y_{mixture} - y_{groundtruth})|).$$

Comparison with CIBERSORT and DeconRNASeq

We next compared our algorithm with two recently published methods, CIBERSORT and DeconRNASeq.

CIBERSORT [4] was established to distinguish 22 closely related immune cell types via support vector regression from microarray data, although the authors expect it to work with RNA-Seq data. Besides an estimation of the distribution of cell types, it provides a p-value "to test the null hypothesis that no cell types in the signature matrix […] are present in a given GEP [gene expression profile] mixture". The 22 immune cell type signature (LM22) provided with CIBERSORT is unable to estimate macrophage contents in our tumor cell samples according to its own p-value estimation (our most contaminated sample: $p = 0.02$; all other samples: $p > 0.1$).

To generate a custom signature matrix using CIBERSORT's automated procedure three pure samples of each cell type are required. In addition, the CIBERSORT FAQ states "Building the specific collection of genes in a signature matrix is a nuanced process, and is critical for its performance on complex tissues. Construction and validation of LM22 required more than a year of investigation". Consequently, we ran CIBERSORT with ad-hoc signature matrices composed of the 500 genes showing the highest extent of differential expression (250 up, 250 down, min. 10 TPM in the higher tissue).

DeconRNASeq [5] models RNA-Seq samples as linear mixtures estimated via quadratic programing using a signature matrix. The signature matrix captures the expression difference of hundreds of genes across pure samples. The implementation does not offer correction, nor an automated way to build the signature matrix. We build an ad-hoc signature matrix as above for CIBERSORT.

Our algorithm was run $k = 250$, $j = 0$ in order to keep comparable parameters. While our algorithm was able to predict the contamination in most cases ($r = 0.8$), both CIBERSORT and DeconRNAseq ($r < 0.3$) failed using these ad-hoc signature matrices (Figures 2 and 3).

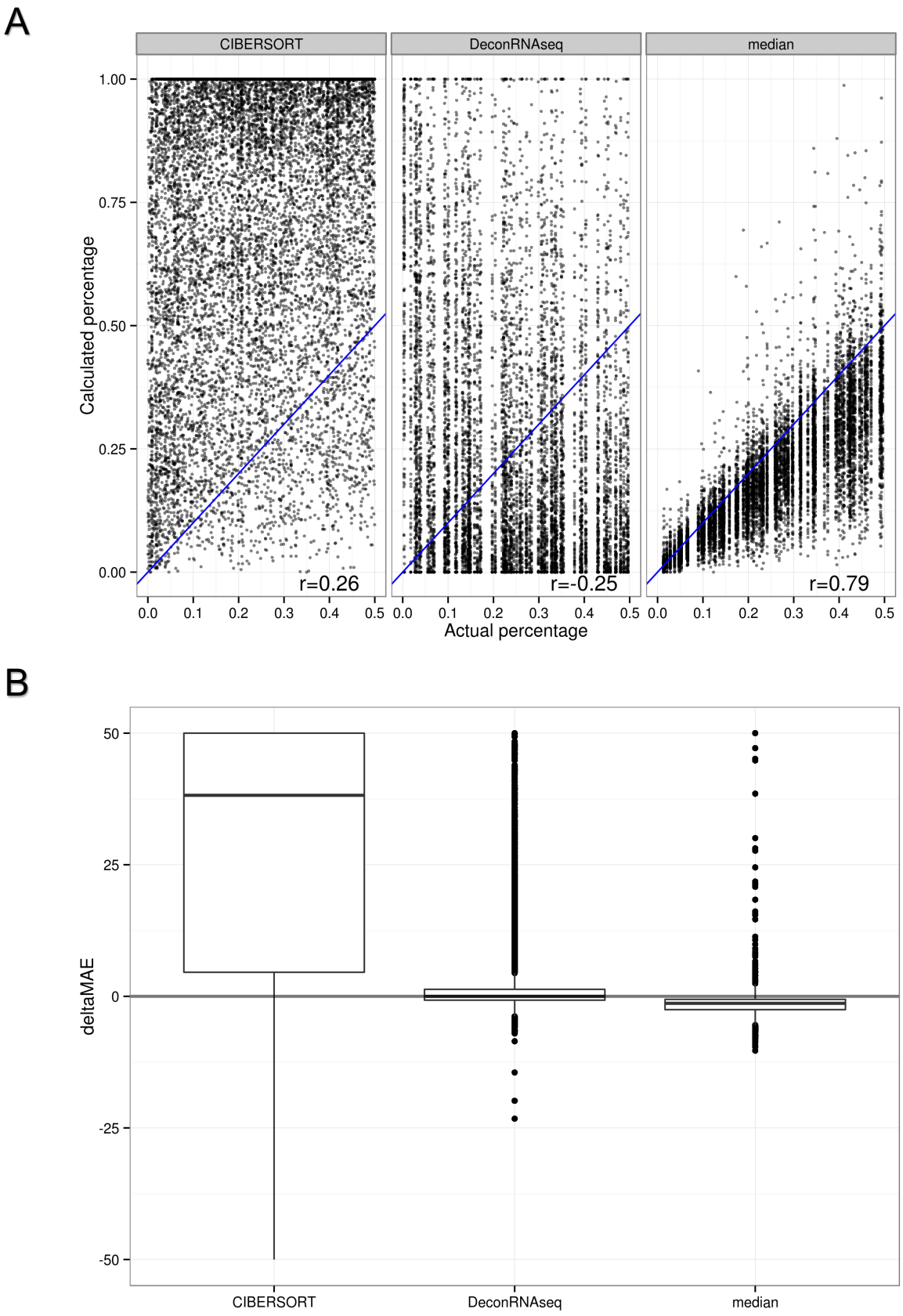

Figure 2: Algorithm comparison with CIBERSORT and DeconRNASeq on GTEx samples [2]. Conditions: 10,000 simulations per algorithm, random percentage between 0 and 50%, single randomly chosen reference per tissue and simulation. **(A)** Actual versus calculated percentage. Blue: diagonal. **(B)** Resulting deltaMAE between corrected and uncorrected mixtures in comparison to the ground truth.

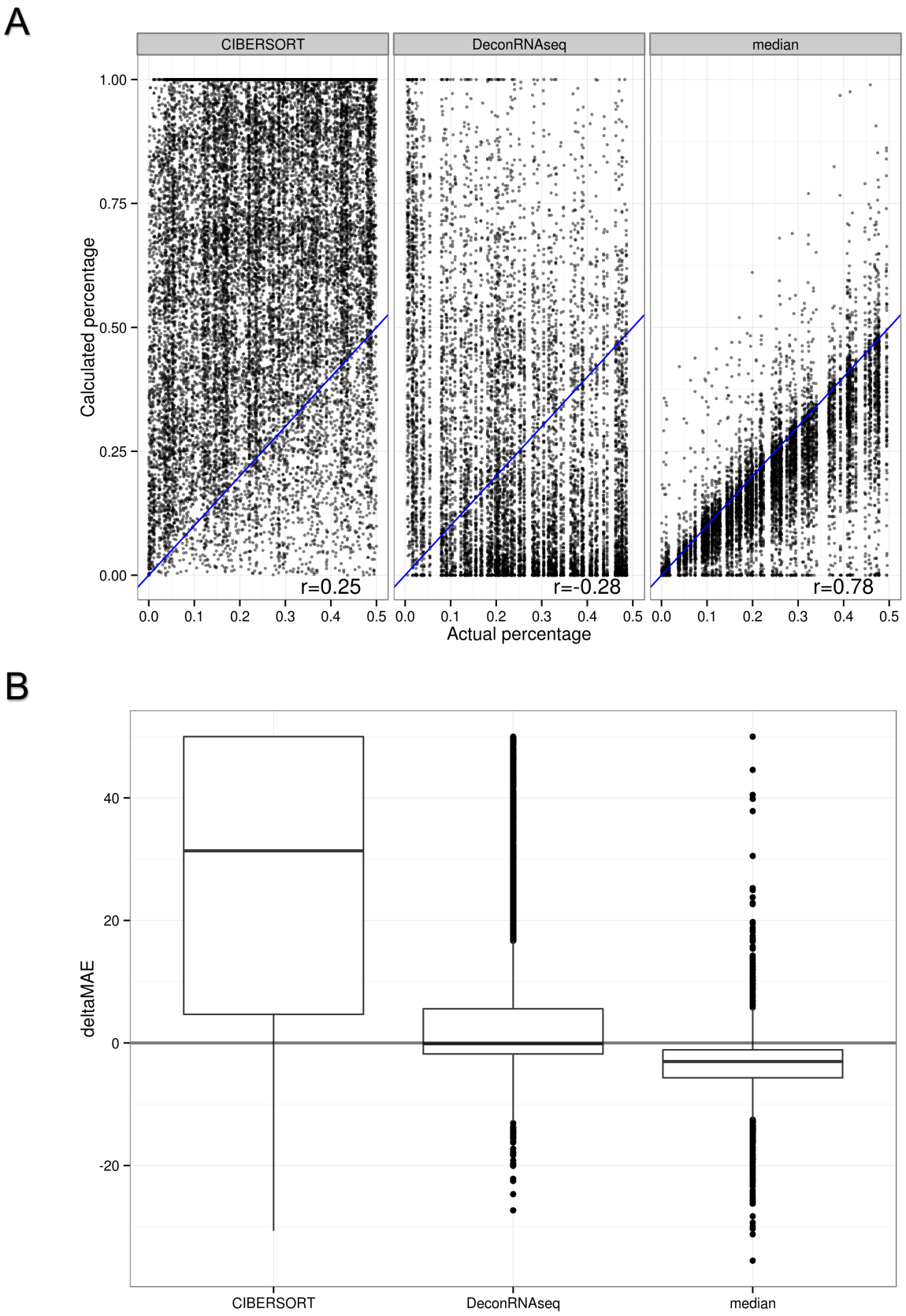

Figure 3: Algorithm comparison on E-MTAB-2836 dataset [3]. Conditions: 10,000 simulations per algorithm, random percentage between 0 and 50%, single randomly chosen reference per tissue and simulation. **(A)** Actual vs calculated percentage. Blue: diagonal. **(B)** Resulting deltaMAE between corrected and uncorrected mixtures in comparison to the ground truth.

Other algorithms

A number of other algorithms were considered, but their application was rejected for technical reasons.

ContamDE's [6] focus is on differential expression between tumor (mixture) and normal (pure) samples. It requires at least two of each and has a long runtime (on the order of minutes), complicating simulations.

UNDO [7] is a completely unsupervised algorithm that merely uses mixture samples to deconvolute tumor and normal tissue. It does not use pure references and determines suitable marker genes solely from the mixture data. Although it was established on microarray data, it has been used with some success on RNA-Seq data [6]. When adjusting our simulation to provide two mixture samples, we found that UNDO only works if both mixtures are mixtures of the same (sample, contamination) samples. This makes it unusable in our setting, where there is only one mixture per patient available.

TEMT [8] works on transcription level RNA-Seq alignments. Transcription level analysis is inappropriate for the cell-cell network investigated in this study.

ESTIMATE [9] produces an 'ImmunoScore' that is not usable for correction.

IsoPure [10] explicitly biases its results to the assumption that the two cell types being deconvoluted are closely related (tumor and normal tissue).

DeMix [11], **Dsection** [12] and **PSEA** [13] have only been established on microarrays.

Limitations of our algorithm

Finally, two important limitations of our approach need to be briefly addressed, although these are not relevant to the present study:

First, our algorithm is unable to distinguish closely related cell types, such as the CD4 and CD8 sample from GSE60424 (Figure 4).

Second, as shown in Figure 5, small numbers of reference sample combinations caused all instances in Figure 3 where the algorithm actually increased MAE. Therefore, the references must be well chosen to represent the contaminating cell types.

Availability

A python implementation of our algorithm is included as Additional File 6.

The code is also available, together with our simulation code, from
https://github.com/IMTMarburg/rnaseqmixture

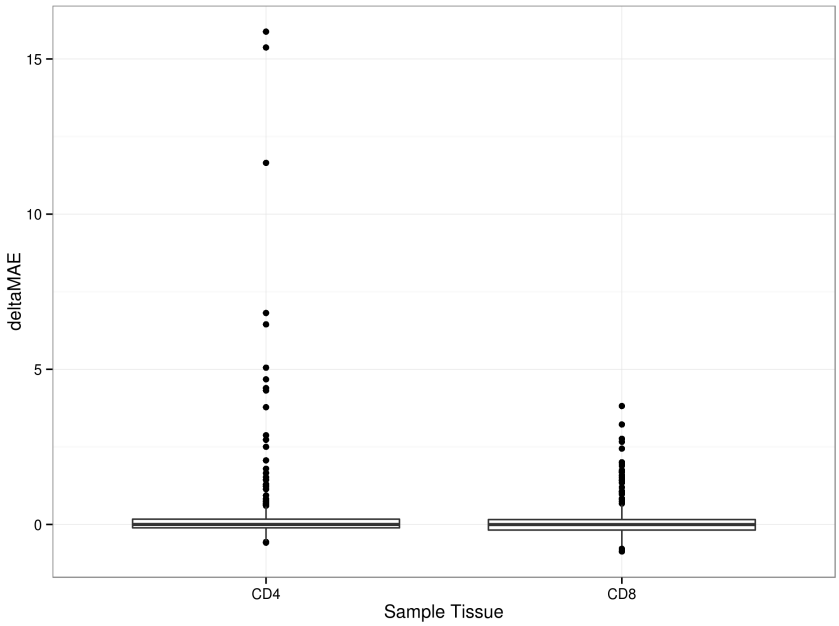

Figure 4: Failure of correction on closely related cell types from GSE604242. 10,0 simulations. CD4 samples were contaminated with CD8 and *vice versa.*

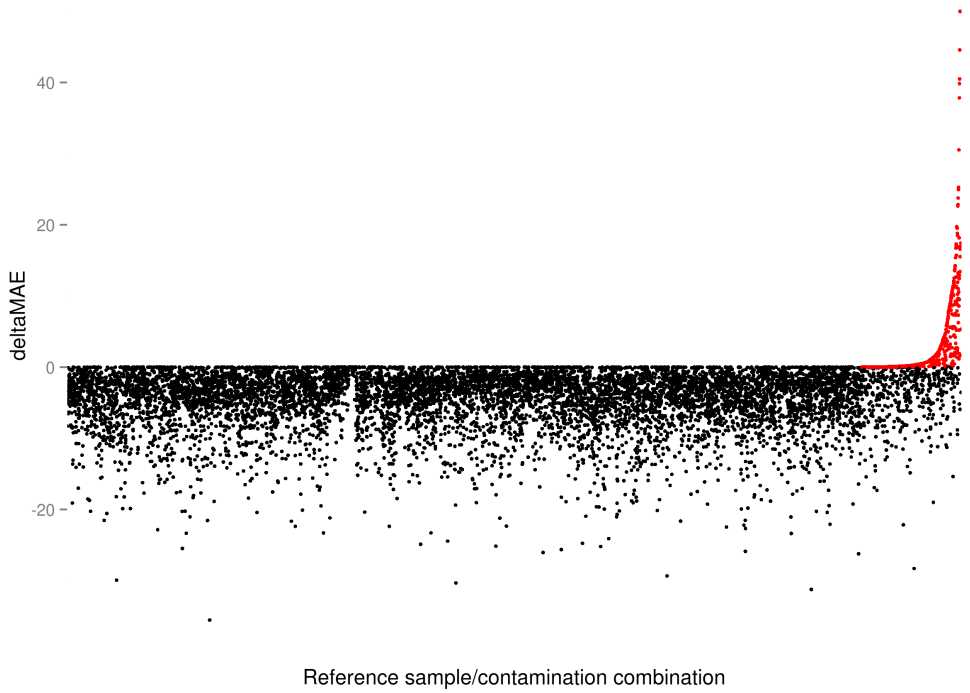

Figure 5: Reference sample dependency of the algorithm. Data from Figure 3, 'median' subset. Red: simulations with worse MAE after correction.

References

1. Yadav VK, De S: **An assessment of computational methods for estimating purity and clonality using genomic data derived from heterogeneous tumor tissue samples.** *Brief Bioinform* 2015, **16:**232-241.
2. GTEx Consortium: **Human genomics. The Genotype-Tissue Expression (GTEx) pilot analysis: multitissue gene regulation in humans.** *Science* 2015, **348:**648-660.
3. Uhlen M, Fagerberg L, Hallstrom BM, Lindskog C, Oksvold P, Mardinoglu A, Sivertsson A, Kampf C, Sjostedt E, Asplund A, et al: **Proteomics. Tissue-based map of the human proteome.** *Science* 2015, **347:**1260419.
4. Newman AM, Liu CL, Green MR, Gentles AJ, Feng W, Xu Y, Hoang CD, Diehn M, Alizadeh AA: **Robust enumeration of cell subsets from tissue expression profiles.** *Nat Methods* 2015, **12:**453-457.
5. Gong T, Szustakowski JD: **DeconRNASeq: a statistical framework for econvolution of heterogeneous tissue samples based on mRNA-Seq data.** *Bioinformatics* 2013, **29:**1083-1085.
6. Shen Q, Hu J, Jiang N, Hu X, Luo Z, Zhang H: **contamDE: Differential expression analysis of RNA-seq data for contaminated tumor samples.** *Bioinformatics* 2015.
7. Wang N, Gong T, Clarke R, Chen L, Shih Ie M, Zhang Z, Levine DA, Xuan J, Wang Y: **UNDO: a Bioconductor R package for unsupervised deconvolution of mixed gene expressions in tumor samples.** *Bioinformatics* 2015, **31:**137-139.
8. Li Y, Xie X: **A mixture model for expression deconvolution from RNA-seq in heterogeneous tissues.** *BMC Bioinformatics* 2013, **14 Suppl 5:**S11.
9. Yoshihara K, Shahmoradgoli M, Martinez E, Vegesna R, Kim H, Torres-Garcia W, Trevino V, Shen H, Laird PW, Levine DA, et al: **Inferring tumour purity and stromal and immune cell admixture from expression data.** *Nat Commun* 2013, **4:**2612.
10. Quon G, Haider S, Deshwar AG, Cui A, Boutros PC, Morris Q: **Computational purification of individual tumor gene expression profiles leads to significant improvements in prognostic prediction.** *Genome Med* 2013, **5:**29.
11. Ahn J, Yuan Y, Parmigiani G, Suraokar MB, Diao L, Wistuba, II, Wang W: **DeMix: deconvolution for mixed cancer transcriptomes using raw measured data.** *Bioinformatics* 2013, **29:**1865-1871.
12. Erkkila T, Lehmusvaara S, Ruusuvuori P, Visakorpi T, Shmulevich I, Lahdesmaki H: **Probabilistic analysis of gene expression measurements from heterogeneous tissues.** *Bioinformatics* 2010, **26:**2571-2577.
13. Kuhn A, Thu D, Waldvogel HJ, Faull RL, Luthi-Carter R: **Population-specific expression analysis (PSEA) reveals molecular changes in diseased brain.** *Nat Methods* 2011, **8:**945-947.

Published online 30 April 2015

Nucleic Acids Research, 2015, Vol. 43, No. 10 ***5033–5051***
doi: 10.1093/nar/gkv331

The transcriptional PPARβ/δ network in human macrophages defines a unique agonist-induced activation state

Till Adhikary[1,†], Annika Wortmann[1,†], Tim Schumann[1,†], Florian Finkernagel[1,†], Sonja Lieber[1], Katrin Roth[2], Philipp M. Toth[3], Wibke E. Diederich[3], Andrea Nist[4], Thorsten Stiewe[4], Lara Kleinesudeik[5], Silke Reinartz[5], Sabine Müller-Brüsselbach[1] and Rolf Müller[1,*]

[1]Institute of Molecular Biology and Tumor Research (IMT), Center for Tumor Biology and Immunology (ZTI), Philipps University, 35043 Marburg, Germany, [2]Cellular Imaging Core Facility, Philipps University, Center for Tumor Biology and Immunology (ZTI), 35043 Marburg, Germany, [3]Medicinal Chemistry Core Facility and Institute of Pharmaceutical Chemistry, Center for Tumor Biology and Immunology (ZTI), Philipps University, 35043 Marburg, Germany, [4]Genomics Core Facility, Center for Tumor Biology and Immunology (ZTI), Philipps University, 35043 Marburg, Germany and [5]Clinic for Gynecology, Gynecological Oncology and Gynecological Endocrinology, Center for Tumor Biology and Immunology (ZTI), Philipps University, 35043 Marburg, Germany

Received December 18, 2014; Revised March 28, 2015; Accepted April 01, 2015

ABSTRACT

Peroxisome proliferator-activated receptor β/δ (PPARβ/δ) is a lipid ligand-inducible transcription factor with established metabolic functions, whereas its anti-inflammatory function is poorly understood. To address this issue, we determined the global PPARβ/δ-regulated signaling network in human monocyte-derived macrophages. Besides cell type-independent, canonical target genes with metabolic and immune regulatory functions we identified a large number of inflammation-associated NFκB and STAT1 target genes that are repressed by agonists. Accordingly, PPARβ/δ agonists inhibited the expression of multiple pro-inflammatory mediators and induced an anti-inflammatory, IL-4-like morphological phenotype. Surprisingly, bioinformatic analyses also identified immune stimulatory effects. Consistent with this prediction, PPARβ/δ agonists enhanced macrophage survival under hypoxic stress and stimulated CD8$^+$ T cell activation, concomitantly with the repression of immune suppressive target genes and their encoded products CD274 (PD-1 ligand), CD32B (inhibitory Fcγ receptor IIB) and indoleamine 2,3-dioxygenase 1 (IDO-1), as well as a diminished release of the immune suppressive IDO-1 metabolite kynurenine. Comparison with published data revealed a significant overlap of the PPARβ/δ transcriptome with coexpression modules characteristic of both anti-inflammatory and pro-inflammatory cytokines. Our findings indicate that PPARβ/δ agonists induce a unique macrophage activation state with strong anti-inflammatory but also specific immune stimulatory components, pointing to a context-dependent function of PPARβ/δ in immune regulation.

INTRODUCTION

Macrophages display an enormous degree of plasticity and react to their microenvironment by profoundly different phenotypes, with classically activated, pro-inflammatory macrophages [e.g. by tumor necrosis factor-α (TNFα) or interleukin-1β (IL-1β)] and anti-inflammatory macrophages [e.g. by interleukin 4 or 10 (IL-4 or IL-10)] as the extremes, originally designated as M1 and M2 macrophages (1). However, the macrophage phenotype is highly dynamic, depending on the precise environmental cues (2). Consequently, a spectrum of defined activation/polarization states has recently been proposed (3). A protein involved in the regulation of macrophage activation and polarization is the nuclear receptor peroxisome proliferator-activated receptor β/δ (PPARβ/δ). PPARβ/δ is a ligand-inducible transcription factor with established functions in intermediary metabolism and a less well-defined anti-inflammatory role in immune regu-

*To whom correspondence should be addressed. Tel: +49 6421 2866236; Fax: +49 6421 2868923; Email: rmueller@imt.uni-marburg.de
†These authors contributed equally to the paper as first authors.

lation (4–7). Thus, PPARβ/δ deficiency exacerbated the inflammatory response to topical O-tetradecanoylphorbol-13-acetate in mice (8). Furthermore, PPARβ/δ dampened the inflammatory response in a human model of dermal wound healing by stimulating the secretion of IL-1 receptor antagonist in dermal fibroblasts (9). Anti-inflammatory effects of PPARβ/δ agonists have also been observed in mouse models of intestinal inflammation (10) and experimental allergic encephalomyelitis, the latter involving an inhibition of interferon γ (IFNγ) and IL-17 production by Th1 and Th17 cells (11). An anti-inflammatory function of PPARβ/δ in macrophages has been demonstrated in two studies reporting that M2 polarization of murine macrophages in adipose tissue and liver is dependent on the induction of PPARβ/δ expression by IL-4 or IL-13 (12,13). The precise mechanism of anti-inflammatory macrophage polarization by PPARβ/δ remains, however, unclear. Moreover, inconsistent with a purely anti-inflammatory function, PPARβ/δ is overexpressed in human psoriasis (14) and ligand activation induces a proinflammatory psoriasis-like response in a mouse model (15,16), even though the molecular mechanisms underlying the latter observation and its relevance for the human system remain unclear.

PPARβ/δ regulates its direct target genes through binding to PPAR response elements (PPREs) as a heterodimer with a retinoid X receptor (RXR) (17). Genome-wide analyses have identified PPRE-mediated repression as a major mechanism of transcriptional regulation in the absence of a PPARβ/δ agonist and showed that an agonist-mediated switch induces a subset of these genes (18). PPRE-mediated repression is enhanced by inverse agonists, which establish a repressor complex that apparently is different from the unliganded receptor complex (19). Besides this canonical mechanism, agonist-bound PPARβ/δ can also repress genes by interacting with specific transcription factors without establishing direct DNA contact. For example, PPARβ/δ interacts with the p65 subunit of the nuclear factor kappa B (NFκB) dimer in different cell types (14,20,21), PPARβ/δ ligands decrease NFκB activity via crosstalk with other signaling pathways, including ERK in adipocytes (22) and BCL-6 in macrophages (23). BCL-6 is a transcriptional repressor of inflammatory genes, many of which are targets of NFκB (24). Deletion of *Ppard* or application of a PPARβ/δ ligand abolishes the sequestration of BCL-6 by PPARβ/δ, resulting in the repression of BCL-6 target genes (23).

PPARβ/δ serves as a receptor for a broad range of natural agonists with function in inflammatory processes, including unsaturated fatty acids (25) and 15-hydroxyeicosatetraenoic acid (15-HETE) (26). The function of prostaglandin I_2 (prostacyclin) as a PPARβ/δ agonist is controversial (27,28), which might be due to its extreme instability at pH values below 7.8 (29), making the microenvironment an essential determinant in this context. Owing to the association of PPARβ/δ with major human diseases a number of PPARβ/δ-specific agonists have been developed, several of which are well characterized and have been used in numerous preclinical studies (30,31). Furthermore, several synthetic inhibitory ligands for PPARβ/δ have been described over the past years. These include the PPARβ/δ-specific GSK0660 (32) and its improved derivative ST247 (33,34). These ligands inhibit the basal expression of PPARβ/δ target genes by enhancing the recruitment of transcriptional corepressors, classifying them as inverse agonists (33).

To date, genome-wide studies addressing the transcriptional PPARβ/δ signaling network in primary macrophages have not been performed. Recently published transcriptome data for myeloid leukemia THP-1 cells, induced to differentiation toward macrophage-like cells by phorbol ester exposure, do not reflect the situation in normal primary macrophages (35). However, such studies are urgently required to understand the multi-faceted role of PPARβ/δ in immune regulation. In the present study, we applied next-generation sequencing technologies to determine the PPARβ/δ-regulated transcriptome and the PPARβ/δ-RXR cistrome in human monocyte-derived macrophages (MDMs) with the goal to establish the PPARβ/δ-controlled regulatory network in these cells.

MATERIALS AND METHODS

Ligands

L165,041 was purchased from Biozol (Eching, Germany) and GW501516 from Axxora (Lörrach, Germany). ST247 was synthesized as described (33,34). The inverse PPARβ/δ agonist PT-S264 is a novel derivative of ST247 with improved plasma stability (Toth, P.M. *et al.*, submitted for publication). Ligands were used at a concentration of 1 μM in all experiments.

Cell culture

MDA-MB-231 cells were purchased from Caliper Life Science (MDA-MB-231-luc2). WPMY-1 cells were obtained from the ATCC. Cells were maintained in Dulbecco's modified Eagle's medium supplemented with 10% fetal bovine serum, 100 U/ml penicillin and 100 μg/ml streptomycin in a humidified incubator at 37°C and 5% CO_2.

Isolation of $CD14^+$ cells

Peripheral blood mononuclear cells were obtained from healthy adult volunteers for MDM stimulation. Mononuclear cells were isolated by Lymphocyte Separation Medium 1077 density gradient centrifugation (PromoCell GmbH, D-69126 Heidelberg, Germany) and further purified by adherent cell positive selection.

Cell culture and cytokine treatment of MDMs

$CD14^+$ monocytes were cultured either in RPMI1640 with 10% fetal calf serum (FCS) (R10 medium) or in serum-free macrophage X-VIVO 10 medium (Biozym Scientific GmbH, Hessisch Oldendorf, Germany; subsequently referred to as XV0 medium). MDMs were differentiated from $CD14^+$ monocytes of healthy volunteers for 5–7 days at 1×10^6 cells/ml. In some experiments MDMs were treated with 20 ng/ml IL-4 (Biozol, Eching, Germany), 100 ng/ml (lipopolysaccharide (LPS); *Escherichia coli* 0111:b4 L4391; Sigma Aldrich, Steinheim, Germany) or 10 ng/ml IFNγ (Biomol, Hamburg, Germany) during differentiation for

5–7 days. Isolation of murine bone marrow cells (BMCs), differentiation to macrophages (BMDMs) by granulocyte-macrophage colony stimulating factor (GM-CSF) and ligand treatment were carried out as described (36).

Propidium iodide uptake under hypoxia

MDMs were treated with ligands as indicated and kept under 1% oxygen starting directly after isolation of monocytes. Propidium iodide (Sigma Aldrich, Steinheim, Germany) was added to a 1 ml cell suspension containing 1–2 × 10^6 MDMs to yield a final concentration of 1 μg/ml. Cells were kept at ambient temperature in the dark for 1 h followed by fluorescence-activated cell sorting (FACS) analysis using an FACS Canto cytometer and BD FACSDiva software (BD Biosciences, Heidelberg, Germany).

Phagocytosis assay

Phagocytosis assay was performed with d6 MDMs using 0.5 mg/ml fluorescein isothiocyanate (FITC) dextran (Sigma Aldrich, Steinheim, Germany). Cells were kept under standard culture conditions for 1 h. Negative control cells were incubated for 1 h at 4°C. Following the incubation, cells were washed three times and analyzed by FACS.

FACS phenotyping

Cells were pretreated and stained for macrophage markers as previously described (37). In addition, FITC-labeled anti-human CD86 (Miltenyi Biotech, Bergisch Gladbach, Germany), FITC-labeled anti-CD32A (Clone IV.3, Stemcell Technologies, Cologne, Germany) and allophycocyanin (APC)-labeled anti-CD274 (BD Biosciences) were used. Intracellular staining of permeabilized cells with anti-CD32B (Clone C2C3, Genetex, Irvine, CA, USA) and FITC-labeled secondary antibody (eBioscience, Frankfurt a.M., Germany) was performed as published (37). Isotype control antibodies were purchased from BD Biosciences, Miltenyi Biotech and eBioscience. Cells were analyzed using an FACS Canto cytometer and BD FACSDiva software (BD Biosciences). Results were calculated as mean fluorescence intensities.

T cell activation

For antigen-specific T cell activation, autologous $CD14^+$ monocytes from buffy coats of healthy donors were differentiated to MDMs in the presence of different stimuli for 5–7 days and used as antigen-presenting cells for antigen-specific T cell activation. Eighty thousand MDMs per 96 well culture plate were loaded with 1 μg/ml cytomegalovirus, Epstein-Barr virus, influenza virus and tetanus toxoid (CEFT) peptide pool of 27 peptides (jpt Peptide Technologies, Berlin, Germany) for 24 h (37°C, 5% CO_2). After washing with phosphate buffered saline, peptide-pulsed MDMs were cocultured with 4 × 10^5 autologous lymphocytes ($CD14^-$ fraction after MACS selection of buffy coats) at a 5:1 ratio of lymphocytes to MDMs in XV0 medium. MDMs pulsed with dimethylsulfoxide (DMSO; 0.2% final concentration) were used as unstimulated controls for antigen-specific T cell activation.

For polyclonal T cell stimulation, 4 × 10^5 lymphocytes were incubated in 96 well culture plates coated with mouse anti-human CD3 mAb (500 ng/well; clone OKT3, Biolegend, San Diego, CA, USA) in the absence of autologous MDMs. Experimental controls included non-stimulated lymphocytes cultured without anti-CD3 mAb. Polyclonal and peptide-specific T cell stimulation were performed at 37°C and 5% CO_2 for a total of 18 h with 5 μg/ml Brefeldin A (Sigma Aldrich, Steinheim, Germany) for the last 16 h. Activated lymphocytes were harvested and stained with surface markers anti-human CD8 APC (Miltenyi Biotec, Bergisch Gladbach, Germany). After permeabilization (BD Cytofix/Cytoperm Kit, BD Bioscience, Heidelberg, Germany) anti-human IFNγ FITC (eBioscience, Frankfurt a.M., Germany) was added according to the manufacturer's instructions. Frequencies of activated T cells were measured by flow cytometry (FACS Canto, BD Bioscience, Heidelberg, Germany) and expressed as IFNγ+/CD8+ cells after subtracting background staining of corresponding non-stimulated controls.

Immunoblotting

Immunoblots were performed according to standard protocols using the following antibodies: α-PPARβ/δ (sc-74517; Santa Cruz, Heidelberg, Germany); α-IDO-1 (MAB10009; Millipore, Darmstadt, Germany), α-LDH (sc-33781; Santa Cruz, Heidelberg, Germany), α-rabbit IgG HRP-linked AB and α-mouse IgG HRP-linked AB (cs7074, cs7076; Cell Signaling, NEB, Frankfurt, Germany). Imaging and quantification was done using the ChemiDoc MP system and Image Lab software version 5 (Bio-Rad, München, Germany).

Kynurenine assay

Kynurenine was measured according to a published procedure (38). Supernatant of MDM cultures (360 μl) was incubated with 180 μl of 30% trichloroacetic acid (TCA) for 30 min at 50°C. After centrifugation at 3000 × g for 10 min, the supernatant was collected, mixed with an equal volume of freshly prepared Ehrlich Reagent (2% p-dimethylaminobenzaldehyde in glacial acetic acid) and incubated for 12–30 min at ambient temperature. The absorbance was measured at 492 nm and compared to a calibration curve obtained with L-kynurenine (Santa Cruz, Heidelberg, Germany).

Reverse transcription quantitative polymerase chain reaction (RT-qPCR)

cDNA isolation and qPCR analyses were performed as described (33). L27 was used for normalization. Primer sequences are listed in Supplementary Table S1.

RNA sequencing

RNA was extracted with TRIfast (Peqlab, Erlangen, Germany) according to the manufacturer's instructions. Genomic DNA was removed by incubation with RNase-free DNase (Macherey-Nagel, Düren, Germany) for 15 min at

room temperature. After column-based purification (Qiagen Minelute, Hilden Germany), 0.1–0.5 μg of DNA-depleted RNA was used for library preparation according to the manufacturer's instructions (ScriptSeq Complete Gold Kit, Human/Mouse/Rat-Low Input, Epicentre, Madison, WI, USA) utilizing Qiagen Minelute columns and Beckman Coulter Agencourt AMpure XP beads. Samples were sequenced on an Illumina HiSeq 1500.

Chromatin immunoprecipitation (ChIP) sequencing

ChIP was performed and evaluated as described (18,19) using the following antibodies: IgG pool, I5006 (Sigma-Aldrich, Steinheim, Germany); α-PPARβ/δ, sc-7197; α-RXR, sc-774 (Santa Cruz, Heidelberg, Germany). For precipitation, a mixture of Dynabeads Protein A (10002D) and Dynabeads Protein G (10004D; both from Life Technologies, Carlsbad, CA, USA) was blocked with 1 g/l bovine serum albumin overnight, and 50 μl was used per immunoprecipitation (IP). DNA was purified using Qiagen Minelute columns. Preceding the PE washing step, the membranes were washed twice with pure methanol in order to remove contaminating DNA-binding lipids that inhibit subsequent low-temperature enzymatic modification steps, which we found to be present in samples from primary macrophages. Libraries were synthesized from 1–2 ng of genomic DNA using the MicroPlex kit (Diagenode, Seraing, Belgium). Samples were sequenced on an Illumina Hi-Seq 1500 (Illumina, San Diego, CA, USA).

Mapping of ChIP sequencing reads and peak calling

ChIP sequencing (ChIP-Seq) mapping and peak calling was performed as described (18,19) except that (i) Subread (version 1.4.3-p1) (39) was used for alignment, (ii) reads were filtered to a maximum of five mismatches and five repetitions of each read start site (deduplication) and (iii) updated versions of Ensembl (v74) and MACS (1.4.0rc2 20110214) were employed. The number of usable reads was 46 299 322 (PPARβ/δ), 39 483 674 (RXR) and 42 750 342 (IgG control). Peaks were filtered for at least 15 deduplicated tags, a fold change (FC) over IgG of ≥2 (normalized total read counts) and at most 60 deduplicated IgG tags. Venn diagrams for peak overlaps were calculated by building the interval union and testing each resulting interval for overlaps with the initial peak sets. Genes were associated with peaks based on the closest transcription start site (TSS) from the peak summit and all TSSs within 50 kb of the summit (internal TSSs were considered). A peak could thus be assigned to multiple genes.

RNA sequencing analysis

RNA sequencing (RNA-Seq) data were aligned to Ensembl v74 using STAR (version STAR_2.3.1z13_r470) (40). Gene read counts were established as read count within merged exons of protein coding transcripts (for genes with a protein gene product) or within merged exons of all transcripts (for non-coding genes). FPKM (fragments per kb per million) were calculated based on the total gene read counts and length of merged exons. Raw read counts were quantile normalized within each comparison and logFC values were calculated (after adding 1/60 to the normalized FPKM values to avoid undefined values). Genes were considered regulated if they had a logFC of at least 0.7 (∼1.62-fold), a minimum FPKM of 0.3 in any condition and at least 50 raw reads.

Comparisons with published ChIP-Seq data

For comparison of the PPAR bound gene sets, signal transducer and activator of transcription 1 (STAT1) data were retrieved from (41) and gene IDs updated to Ensembl v74. STAT3 data were retrieved from Supplementary Table S1 in (42), updated to Ensembl v74 and translated from mouse to human via Ensembl Compara. NFκB bound regions (24) were retrieved from Gene Expression Omnibus (GSM61116, GSM61117, union), lifted from mm9 to mm10 using UCSCs liftOver utility and associated with the mouse gene with the closest transcription start site (internal TSSs were considered). Translation to human genes was again by Ensembl Compara. BCL6 bound sites from the same publication (24) (GSE16723, top level data file) were treated identically. P300 associated genes were extracted from (43) (Supplementary Table S1), assigned to mouse stable IDs using the 'Official Gene Symbol' column and Ensembl v64, updated to Ensembl v74 and translated to human genes via Ensembl Compara.

Comparisons with published stimulus-specific MDM transcriptomes

Raw microarray data (3) (GSE46903, 'GSE46903_non-normalized.txt.gz') quantile normalized using the lumi Bioconductor package annotated using Supplementary Table S1B in (3) were used to calculate logFC values versus basal (M0) condition based on expression values averages within each condition. Only GM-CSF stimulated macrophage samples were analyzed. WGCNA output (49 modules; Supplementary Table S2B in (3)) was translated to Ensembl stable gene IDs using Illumina Human-HT-12_v3 annotation ('HumanHT-12_V3_0_R3_11283641_A'). Translation was preferentially based on Entrez IDs with gene symbols as a fall back. Overlaps between modules and L165,041 regulated genes were assessed by Fisher's exact test. For Figure 8, a directional score for overlapping genes was calculated as follows: the number of genes regulated in the same direction by L165,041 and a given stimulus minus the number of genes regulated in the opposite direction. Only genes showing an at least 1.5-fold induction by the respective stimulus [3] and 1.62-fold by L165,041 (Supplementary Table S2) were included.

Comparison with published genomic PPARβ/δ data for other cell types

For comparisons based on peaks, original sequencing data (18,19) were reanalyzed as described in section 'Mapping of ChIP-Seq reads and peak calling'. Microarray based transcription assay results were retrieved from supplementary tables of the aforementioned publications and their gene stable IDs updated to the Ensembl revision used. In comparisons depicting both RNA-Seq and microarray data,

genes were filtered to those occurring on both microarray chip types used (Agilent-028004 and Agilent-014850).

Databases

All genomic sequence and gene annotation data were retrieved from Ensembl release 74, genome assembly hg19. Our full analysis scripts and computational pipeline are available upon request.

Statistical analysis of experimental data

Data are presented as the average of biological replicates ($n \geq 3$; precise numbers for each experiment indicated in the figure legends) ± standard deviations (error bars). Comparative data were statistically analyzed by Student's *t*-test (two-sided, equal variance) using GraphPad Prism 6.0. Results were expressed as follows: $*P < 0.05$, $**P < 0.01$ and $***P < 0.001$. When appropriate, correction for multiple hypothesis testing was done by Benjamini–Hochberg adjustment, as indicated.

Functional annotations, networks and pathway analyses

RNA-Seq data were analyzed using the Ingenuity Pathway Analysis (IPA) application and knowledge database (Qiagen Redwood City, CA, USA). The functions 'Upstream Regulators, Diseases and Bio Functions and Networks' were applied using the default settings. Results were sorted according to *P*-value of overlap (minimum 10^{-5}) and activation z-scores (≤ -2.0 or $\geq +2.0$ required).

RESULTS

Induction of PPARβ/δ during differentiation of human monocytes to MDMs

First, we sought to identify an experimental system suitable for studying the PPARβ/δ cistrome and ligand-regulated transcriptome. Human monocytes were differentiated to MDMs in RPMI1640 with 10% FCS medium (R10) and characterized with respect to PPARβ/δ expression and activity. RT-qPCR analysis showed increasing PPARD mRNA levels after initiation of cultures reaching a maximum around day 5 (Figure 1A), which was paralleled by a strong increase in PPARβ/δ protein expression (Figure 1B and Supplementary Figure S1) and ligand inducibility of the well-established target gene *PDK4* (Figure 1C), both reaching maximum levels around day 6. Chromatin-bound PPARβ/δ and RXR were detected by ChIP at the PPAR-responsive *PDK4* enhancer already on day 0 (monocytes; Figure 1D), which explains the ligand responsiveness of the *PDK4* gene at early time points (Figure 1C). Re-ChIP analyses showed that PPARβ/δ and RXR formed complexes on the PDK4 enhancer, as expected (Supplementary Figure S2). The induction of PPARβ/δ expression and activity during differentiation was paralleled by an increased surface expression of the macrophage markers CD32, CD63, CD86, CD206 and HLA-DR and an induction of intracellular CD68 (Supplementary Figure S3). MDMs thus appear to be suitable for investigating effects of PPARβ/δ ligands on macrophage activation and/or polarization, in particular since plastic adherence partially activates monocytes and macrophages (44–48), including increased STAT1 and NFκB signaling (49,50), thus allowing for a potential modulation by agonists or inverse agonists in either direction. We therefore chose day-6 MDMs for the subsequent studies.

The transcriptome of PPARβ/δ ligand-regulated genes in human MDMs

We used this experimental system to identify ligand-responsive genes as well as PPARβ/δ and RXR binding sites in macrophages by deep sequencing technologies. RNA-Seq data obtained with MDMs cultured either in R10 or serum-free synthetic X-VIVO 10 medium (XV0) revealed a total of 285 protein-coding genes upregulated by PPARβ/δ agonist L165,041 and 246 genes downregulated by the inverse agonists ST247 or PT-S264; logFC $\geq$ 0.7; FPKM $\geq$ 0.3), 29.6% of the latter ($n = 73$) overlapping with the agonist-induced gene set (Figure 2A; Supplementary Table S2). Our RNA-Seq also identified a large fraction of genes repressed by the agonist L165,041 ($n = 388$) and upregulated by the inverse agonist ST247 ($n = 174$), with 40 genes (10.3%) overlapping (Figure 2B; Supplementary Table S2). Diseases and functions annotation of the L165,041-induced gene set showed a strong association with the inhibition of cell death of immune cells and suppression of immune cell functions, including migration, inflammatory response, activation, homing, adhesion, chemotaxis and phagocytosis (Figure 2C; Supplementary Table S3). The gene set representing inflammation clearly overlapped with cell survival, migration/movement, adhesion and recruitment/infiltration/ chemotaxis (Figure 2D), suggesting that these to a large extent represent genes with functions in immune regulation. Interestingly, 'Inflammation of intestine' and 'Colitis' showed a positive activation z-score (Figure 2C), providing a first hint that the response to L165,041 may not be strictly anti-inflammatory. Likewise, lipid metabolism ('Concentration of acylglycerol') was upregulated, consistent with the known metabolic role of PPARβ/δ. Finally, analysis of the known upstream regulators of these genes (signaling molecules and transcription factors) identified two groups: canonically regulated (L165,041-induced) genes known to be activated by PPAR agonists (pirixinic acid, fibrates, glitazones) were upregulated by L165,041, while genes induced by pro-inflammatory signaling via LPS, TNFα, IFNγ, IL-1β, STAT3 or TLR4 were downregulated (inverse target genes).

To rule out the possibility that inverse regulation may be due to PPARβ/δ-independent off-target mechanisms we analyzed the regulation of target genes in bone marrow-derived macrophages (BMDMs) from wild-type and *Ppard* null mice. As shown in Figure 2F, *Ccl24, Tnfsf15* and *Serpinb2* were repressed upon agonist treatment specifically in wild-type cells. Two other genes found to be repressed by agonists in human MDMs were not regulated *(Ccl8)* or not expressed *(Enpp2)* in murine BMDMs, while the canonical target *genes Pdk4* and *Angptl4* showed the expected PPARβ/δ-dependent induction. These observations confirm the PPARβ/δ dependence of agonist-mediated regulation, but also point to cell type (BMDM versus MDM)

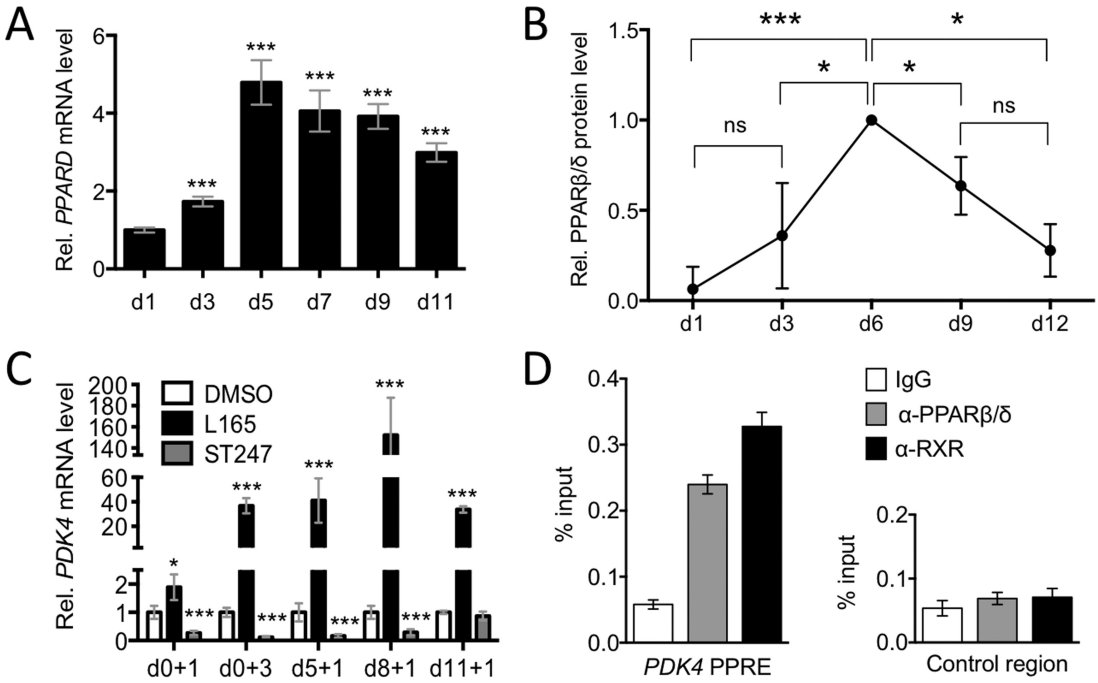

Figure 1. PPARβ/δ expression and activity in differentiating human MDMs. Human monocytes were differentiated in R10 medium for 11 days and analyzed at the indicated times after initiation of differentiation. (**A**) Expression of *PPARD* mRNA measured by RT-qPCR relative d1 (sample size = 3). (**B**) Quantitation of immunoblot analyses of PPARβ/δ protein expression in differentiating MDMs from four different donors relative to LDH (loading control). The individual blots are shown in Supplementary Figure S1. Values were normalized to 1.0 on d6 (maximum expression). (**C**) Ligand-mediated induction relative to DMSO of *PDK4* determined by RT-qPCR. Cells (sample size = 3) were exposed to L165,041 for 1 or 3 days (+1 or +3) at the indicated d (d0, d5, d8, d11). (**D**) PPARβ/δ and RXR enrichment at the *PDK4* enhancer at −12 kb from the transcription start site and an irrelevant control region (Con) in human monocytes (ChIP analysis; sample size = 6). Statistical significance was tested relative to d0 (panel (A)) or DMSO (panel (C)).

and/or species-specific differences in the regulation of inverse PPARβ/δ target genes.

To gain further insight into the diverse functions and regulatory mechanisms suggested by the data in Figure 1 we separately analyzed canonically regulated and inverse target genes as described in the following.

Canonical PPARβ/δ target genes in MDMs

ChIP-Seq analyses identified 1175 enrichment sites for PPARβ/δ associated with 3798 genes located within a distance of 50 kb, and 27 255 RXR enrichment sites associated with 32 720 genes (Figure 3A and B; Supplementary Tables S4 and S5). The majority of overlapping binding sites occurred at transcription start sites (within 1250 bp, 29.1%), within introns (31.6%) or upstream locations (5000 bp, 5.7%) (Figure 3C). A large fraction of the L165,041-induced genes ($n = 132$; 46.3%) showed clear enrichment of PPARβ/δ *in vivo*, and most of these sites ($n = 130$; 98.5%) were co-occupied by RXR (Figure 3A and B). Another fraction of L165,041-induced genes were occupied by RXR, but enrichment for PPARβ/δ at the same genomic region was less clear or not visible ($n = 139$; 48.8%; Figure 3A). These include the strongly regulated (Supplementary Figure S4) and established (51) canonical PPARβ/δ target gene *ANGPTL4*, which shows readily detectable ChIP-Seq peaks in other cell types under identical assay conditions (18,19). This may be due to cell type-specific PPARβ/δ transcription complexes in macrophages that limit accessibility to the antibody. We therefore assume that the presence of RXR on PPREs of L165,041-induced genes indicates canonical PPARβ/δ regulation. This is supported by the results of the upstream regulator analysis of L165,041-induced genes, which identified PPAR ligands and the PPAR coactivator PPARGC1A as the top regulators (nine out of 10; Figure 3D).

Diseases and functions annotation of the canonical target genes showed the strongest positive correlation (by *P*-value) with lipid metabolism (Figure 3E). The identified genes include established PPAR target genes with functions in lipid metabolism, such as *ACADVL, ACAA2, ANGPTL4, CAT, CPT1A, FABP4, ECH1, PDK4, SLC25A20* and *PLIN2*, but also novel target genes, such as *ETFB, ETFDH* and *ISCA1,* the products of which play important roles in electron transfer and iron-sulfur cluster assembly, respectively. Other sets of canonical target genes were either positively associated with cell movement or negatively correlated with systemic autoimmune syndrome (Figure 3E). Consistent with this finding, the canonical target gene set encompasses a number of genes with functions in immune regulation, e.g. *CD1D, CD36, CD52, CD300A, LRP5, NLRC4* and *PHACTR1* (Table 1 and Figure 3B). Several of these examples were validated by RT-qPCR with MDMs from three to seven independent donors (Supplementary Figure S4).

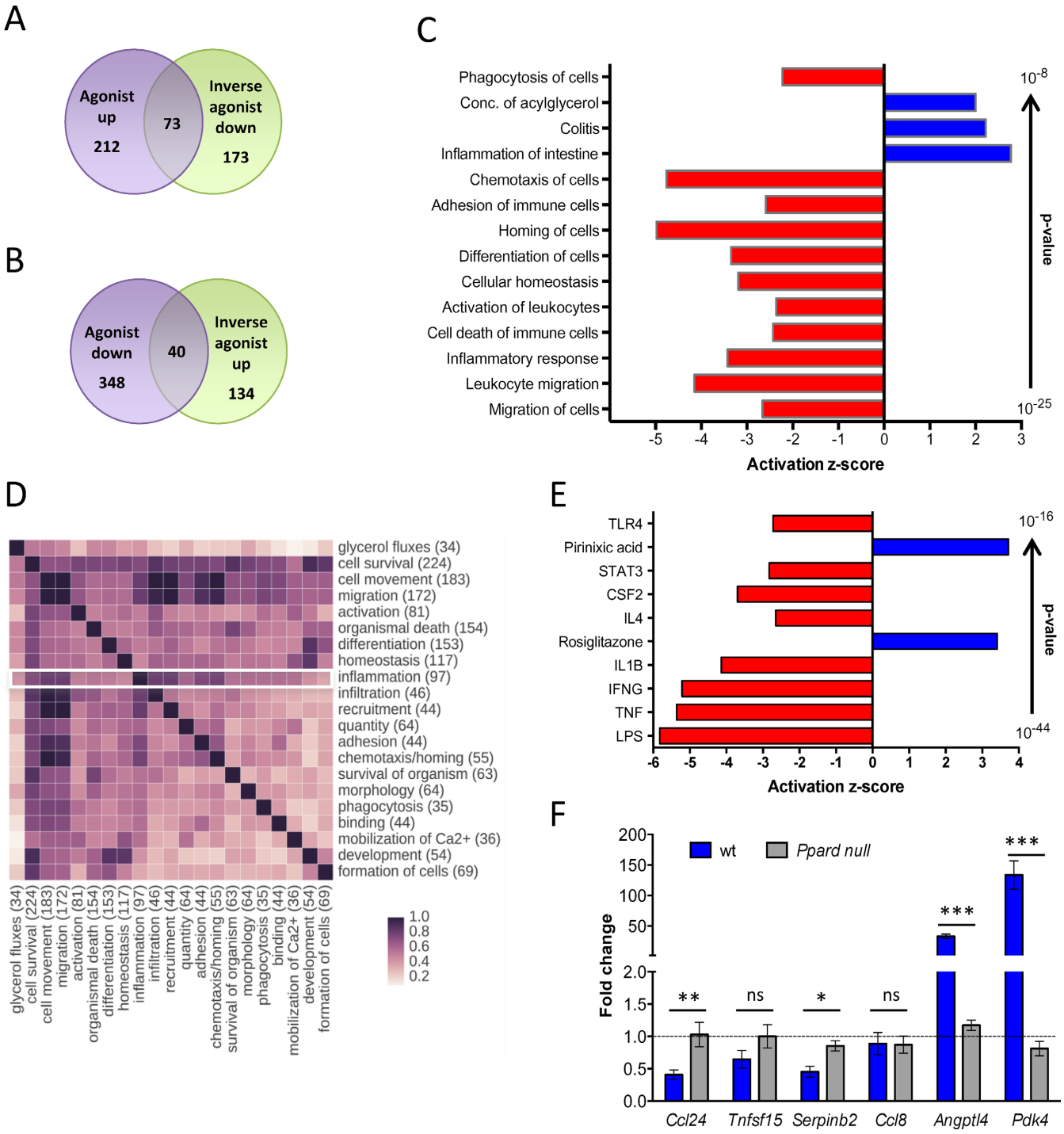

Figure 2. Genome-wide identification of PPARβ/δ target genes in macrophages. (**A**) Overlap of genes induced by L165,041 and repressed by ST247 or PT-S264 in MDMs cultured for 6 days followed by treatment with DMSO or ligands for 24 h. Data are derived from two independent experiments using either R10 (L165,041, ST247) or XV0 (L165,041, PT-S264) medium. Genes with a logFC > 0.7 in one culture condition, a logFC > 0 in both media, an FPKM ≥ 0.3 and a raw tag count of at least 50 were scored as positive. (**B**) Overlap of genes repressed by L165,041 and activated by ST247 in MDMs (conditions as in (A)). (**C**) IPA 'Diseases and Functions Annotation' of L165,041-regulated genes (examples of functionally different clusters with low *P*-values and high z-scores). (**D**) Overlap of L165,041-regulated genes linked to different functions (according to IPA 'Diseases and Functions Annotation'; all clusters with $n > 30$ genes). (**E**) IPA 'Upstream Regulator Analysis' of L165,041-regulated genes (top regulators by *P*-value). (**F**) RT-qPCR analysis of target gene regulation by the PPARβ/δ agonist GW501516 in BMDMs from wild-type and *Ppard* null mice differentiated for 6 days in the presence of GM-CSF (sample size: 3 each). The data show the fold change (mean of triplicates) in response to the ligand relative to solvent treated wild-type and *Ppard* null control cells.

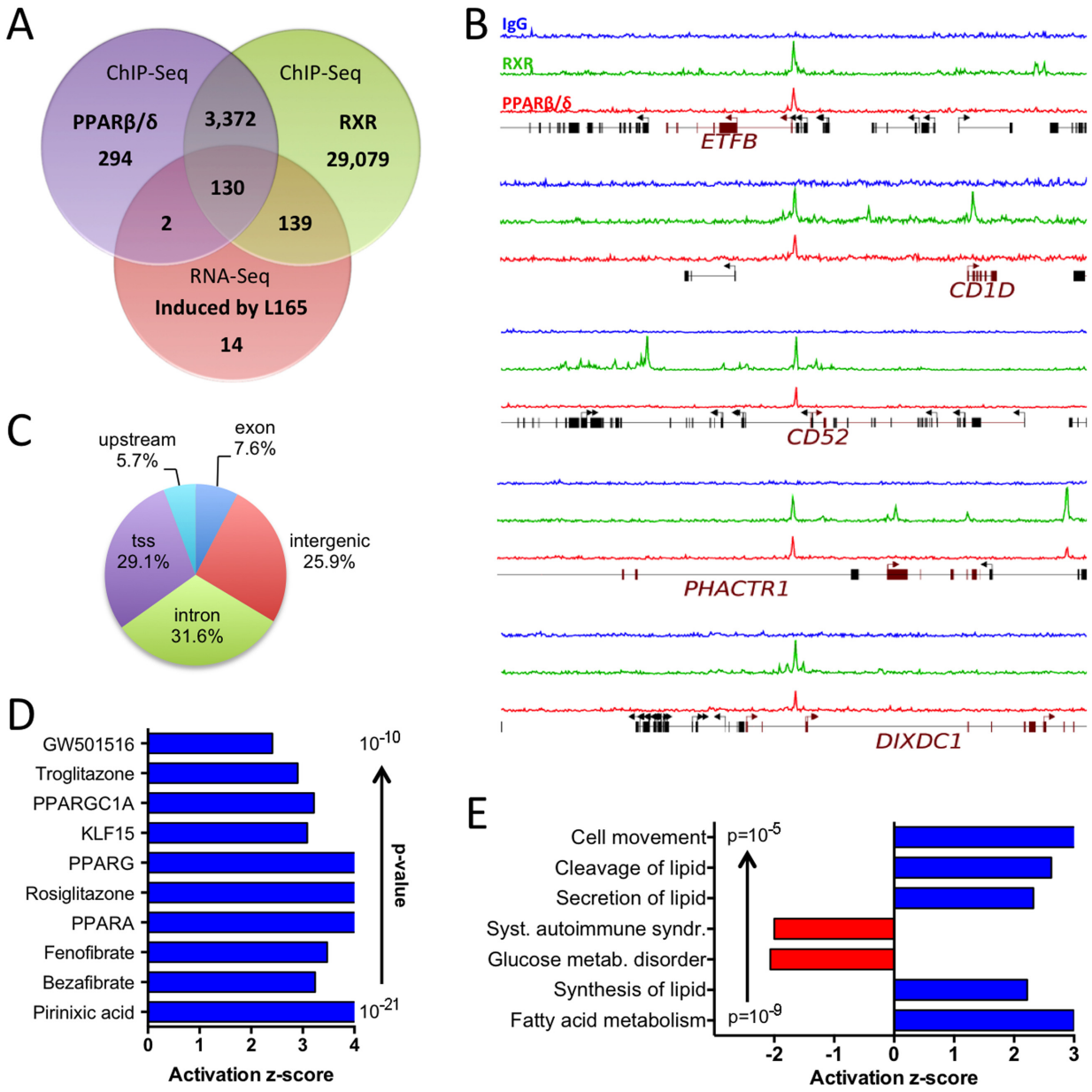

Figure 3. Genome-wide identification of agonist-induced direct PPARβ/δ target genes in MDMs. (**A**) Overlap of genes associated with PPARβ/δ and RXR binding sites in MDMs (ChIP-Seq; peaks filtered and associated with genes as described in the Materials and Methods section) and L165,041-induced genes (RNA-Seq). (**B**) Examples of RXR (green) and PPARβ/δ (red) enrichment peaks at novel canonical target genes (ChIP-Seq data). Blue: control IgG. (**C**) Locations of PPARβ/δ sites identified by ChIP-Seq. tss: within 1250 bp of a transcription start site; upstream: within 5 kb upstream of a transcription start site. (**D**) IPA 'Upstream Regulator Analysis' of L165,041-induced genes (top regulators by *P*-value). (**E**) IPA 'Diseases and Functions Annotation' of L165,041-induced genes in MDMs.

Inverse PPARβ/δ target genes in MDMs

As described above, our RNA-Seq also identified a large fraction of genes repressed by the agonist L165,041, which we subsequently refer to as 'inverse target genes'. As shown in Figure 4A, less than 9% of these genes (34 out of 385) harbored a PPARβ/δ-RXR binding site, which almost uniformly showed low enrichment compared to canonical, agonist-induced PPARβ/δ genes (Figure 4B). This could be due to their regulation by a non-canonical mechanism involving indirect chromatin recruitment, but these genomic regions could also be fortuitous non-functional enrichment sites.

Upstream regulator analysis of the inverse target gene set identified exclusively cytokine signaling pathways (12 out of 12) as top regulators (Figure 4C). In agreement with this finding, published binding sites detected by ChIP-Seq for IFNγ-induced STAT1 (41), LPS-induced NFκB-p65 (24), BCL-6 (24) or LPS-induced P300 (43) were found in a sub-

Table 1. Canonical and inverse PPARβ/δ target genes with immune regulatory functions in MDMs (examples)

Canonical target genes	
CD1D	CD1D molecule
CD36	CD36 molecule (thrombospondin receptor)
CD52	CD52 molecule
CD300A	CD300a molecule
CD300LB	CD300 molecule-like family member b
DIXDC1	DIX domain containing 1
LRP5	Low density lipoprotein receptor-related protein 5
MME	Membrane metallo-endopeptidase
NLRC4	NLR family, CARD domain containing 4
PHACTR1	Phosphatase and actin regulator 1
S100Z	S100 calcium binding protein Z
SCARB2	Scavenger receptor class B, member 2
SLAMF9	SLAM family member 9
ST14	Suppression of tumorigenicity 14
Inverse target genes	
ARG2	Arginase 2
BCL3	B-Cell CLL/Lymphoma 3
CASP5	Caspase 5, apoptosis-related cysteine peptidase
CCL13	Chemokine (C-C motif) ligand 13
CCL24	Chemokine (C-C motif) ligand 24
CCL8	Chemokine (C-C motif) ligand 8
CD1A	CD1a molecule
CD1B	CD1b molecule
CD1E	CD1e molecule
CD300E	CD300e molecule
CXCL1	Chemokine (C-X-C motif) ligand 1
CXCL10	Chemokine (C-X-C motif) ligand 10
CXCL11	Chemokine (C-X-C motif) ligand 11
CXCL6	Chemokine (C-X-C motif) ligand 6
CXCL9	Chemokine (C-X-C motif) ligand 9
FCGR2B	Fc fragment of IgG, low affinity IIb, receptor (CD32B)
IDO1	Indoleamine 2,3-dioxygenase 1
IDO2	Indoleamine 2,3-dioxygenase 2
IL10	Interleukin 10
IL8	Interleukin 8
NLRP12	NLR family, pyrin domain containing 12
TLR3	Toll-like receptor
TNF	Tumor necrosis factor α

stantial fraction of the inverse PPARβ/δ target genes (Figure 4D), with BCL-6 and LPS-induced P300 presumably indicative of NFκB recruitment. These associations suggest that NFκB plays an essential role in the regulation of inverse target genes by PPARβ/δ agonists. RNA-Seq analyses also identified *BCL3* as an inverse target gene (Supplementary Table S2). Since BCL-3 can activate transcription via nuclear NFκB complexes (52), its repression by L165,041 potentially contributes to the inhibition of NFκB target genes.

Proteasome inhibitors block the function of NFκB by different mechanisms, including a blockade of IκB degradation or an inhibition of NFκB precursor processing (53). Consistent with the predicted role of NFκB in the regulation of inverse PPARβ/δ target genes, we found that the 'bona fide' (24) NFκB target genes *APOBEC3A, BCL3, CCL24, FCGR2B, IL10, S100A8* and *S100A9* were strongly downregulated by the proteasome inhibitor MG132. The only exception was *IL8*, which was strongly induced by MG132, indicating a different mechanism of regulation, consistent with published observations (54). A role of NFκB in the agonist-mediated regulation of inverse target genes is supported by our observation that MG132 diminished the magnitude of repression of several of these genes to a statistically not significant level in all cases but *APOBEC3A* and *BCL3*. However, repression by L165,041 was not completely abrogated, pointing to the involvement of other signaling pathways.

In contrast to the canonically regulated genes, the inverse target genes are mostly associated with functions in immune regulation as indicated by the diseases and functions annotation in Figure 4F. Strong negative correlations were found for leukocyte migration/movement/homing, proliferation and cell death, indicating an anti-inflammatory and pro-survival agonist effect via inverse target genes. However, positive associations with pro-inflammatory functions were also observed ('Inflammation of organ' and 'Colitis').

The inverse target genes include cytokines, chemokines and enzymes involved in immune regulation (Table 1). Most of these genes are pro-inflammatory (e.g. *IL8*), but a small number of immunosuppressive genes are also found among the inverse target genes (e.g. *IDO1*), consistent with the results of the diseases and functions annotation analysis above.

Functional networks derived from genomic data

In view of the above findings, several functional networks centered on NFκB (or its upstream regulator TNFα) or biological functions relevant to immune regulation were

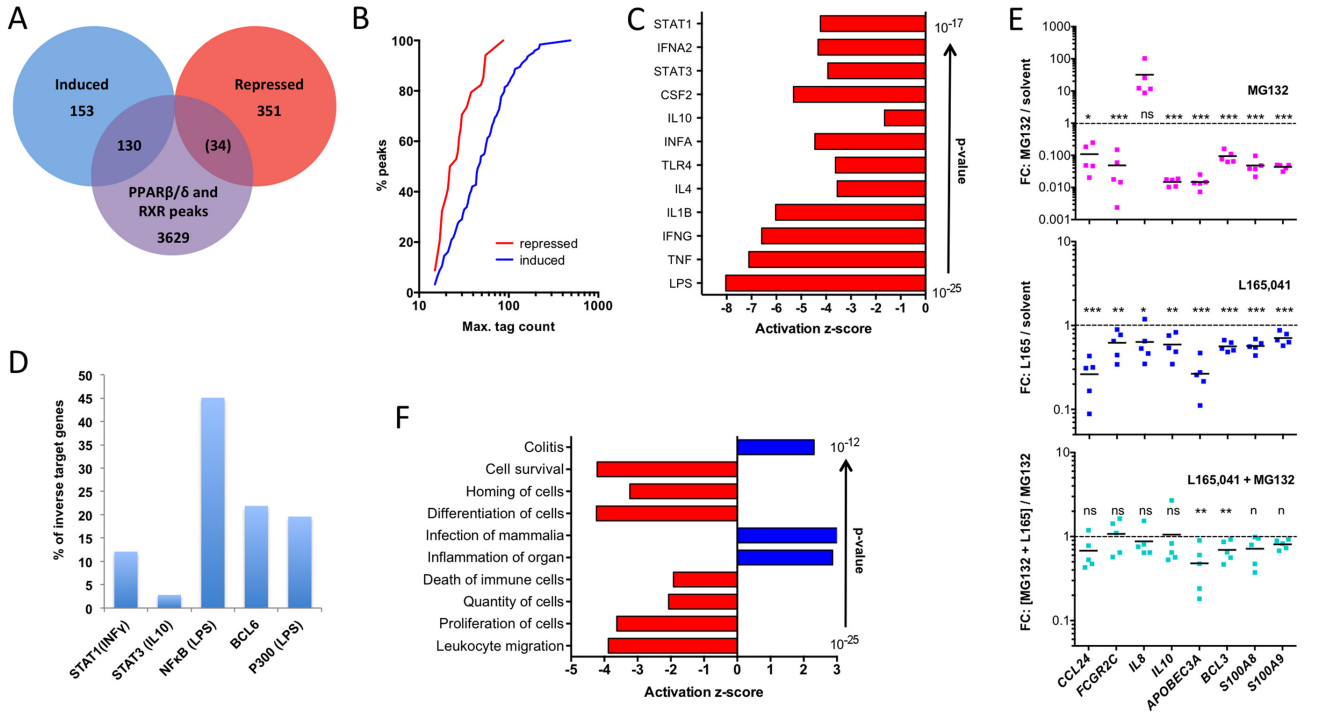

Figure 4. Genome-wide identification of agonist-repressed (inverse) PPARβ/δ target genes. (**A**) Overlap of genes associated with PPARβ/δ and RXR binding sites in MDMs with L165,041-regulated genes. Number in parentheses indicates low enrichment sites. (**B**) Cumulative read distribution for all PPARβ/δ binding sites separated into agonist induced and agonist repressed genes. Plotted is the percentage of reads with *n* or fewer reads in PPARβ/δ ChIP-Seq analyses. (**C**) IPA 'Upstream Regulator Analysis' of L165,041-repressed genes (top regulators by *P*-value). (**D**) Percentage of inverse PPARβ/δ target genes in MDMs (this study) with published binding sites (ChIP-Seq) for STAT1 (INFγ induced) (41), STAT3 (IL-10 induced) (42), NFκB-p65 (24), BCL-6 (24) (43) or P300 (LPS-induced). (**E**) Effect (fold change) of MG132 (10 μM), L165,041 or a combination of both compounds on inverse target genes with 'bona fide' NFκB binding sites (24-h treatment) in MDMs from five donors. *T*-tests of the corresponding groups in the two L165,041 panels against each other showed a statistical significance for *CCL24* ($P < 0.05$). (**F**) IPA 'Diseases and Functions Annotation' of L165,041-repressed genes in MDMs.

studied in further detail. It is obvious from the pathways depicted in Figure 5 that numerous L165,041-regulated genes impact on various aspects of inflammation and/or immune modulation. Anti-inflammatory, agonist-mediated mechanisms include inhibition of the NALP1 inflammasome through modulation of caspase 5 and multiple members of the NOD-like receptor (NLR) family (Figure 5A), reduced TLR signaling (Figure 5B) and diminished NFκB activation (Figure 5A).

In contrast, repression of indoleamine 2,3-dioxygenase 1 (encoded by *IDO1;* Figure 5B), which catabolizes tryptophan to kynurenine, would be predicted to be immune stimulatory, since both tryptophan depletion and kynurenine production have been linked to T cell suppression (55). Moreover, *CD274*, which codes for the transmembrane glycoprotein PD-L1 (PD-1 ligand; B7-H1) and suppresses T cell proliferation (56), is repressed by PPARβ/δ agonists (Figure 5B). L165,041 also impinges on the regulation of macrophage activity by immunoglobulin binding to Fc receptors (Figure 5C). In this context, repression of the inhibitory *FCGR2B* gene encoding CD32B is of particular interest and points to another immune stimulatory action of PPARβ/δ agonists.

In addition, different pathways of antigen presentation are modulated by PPARβ/δ agonists. These include both MHCI and MHCII (HLA-DR, HLA-B27) complexes and MHC-like CD1 proteins involved in the presentation of different lipid antigens (57). These are modulated either directly by PPARβ/δ ligands, by ligand-regulated members of the leukocyte immunoglobulin-like receptor (LIR) family and/or by NFκB (Figure 5A and D). As the genes involved are either canonically or inversely regulated by ligands, and their encoded proteins include both inhibitory and stimulatory molecules, the immune modulatory effect of L165,041 on antigen presentation is likely to be context-dependent.

These predictions clearly point to a specific phenotype triggered by PPARβ/δ agonists that includes both positive and negative effects on immune regulation, consistent with the conclusions drawn from the functional annotation analyses above (Figures 2–4).

Ligand-induced anti-inflammatory alterations in human MDMs

To elucidate the phenotypic alterations induced by PPARβ/δ agonists in MDMs we first analyzed potential morphological alterations triggered by the PPARβ/δ agonists during the 6-day differentiation period of MDMs. For comparison, LPS with or without IFNγ (inducing M1 polarization) or IL-4 (triggering M2 polarization) were added to separate cultures. Figure 6A–E shows a clear

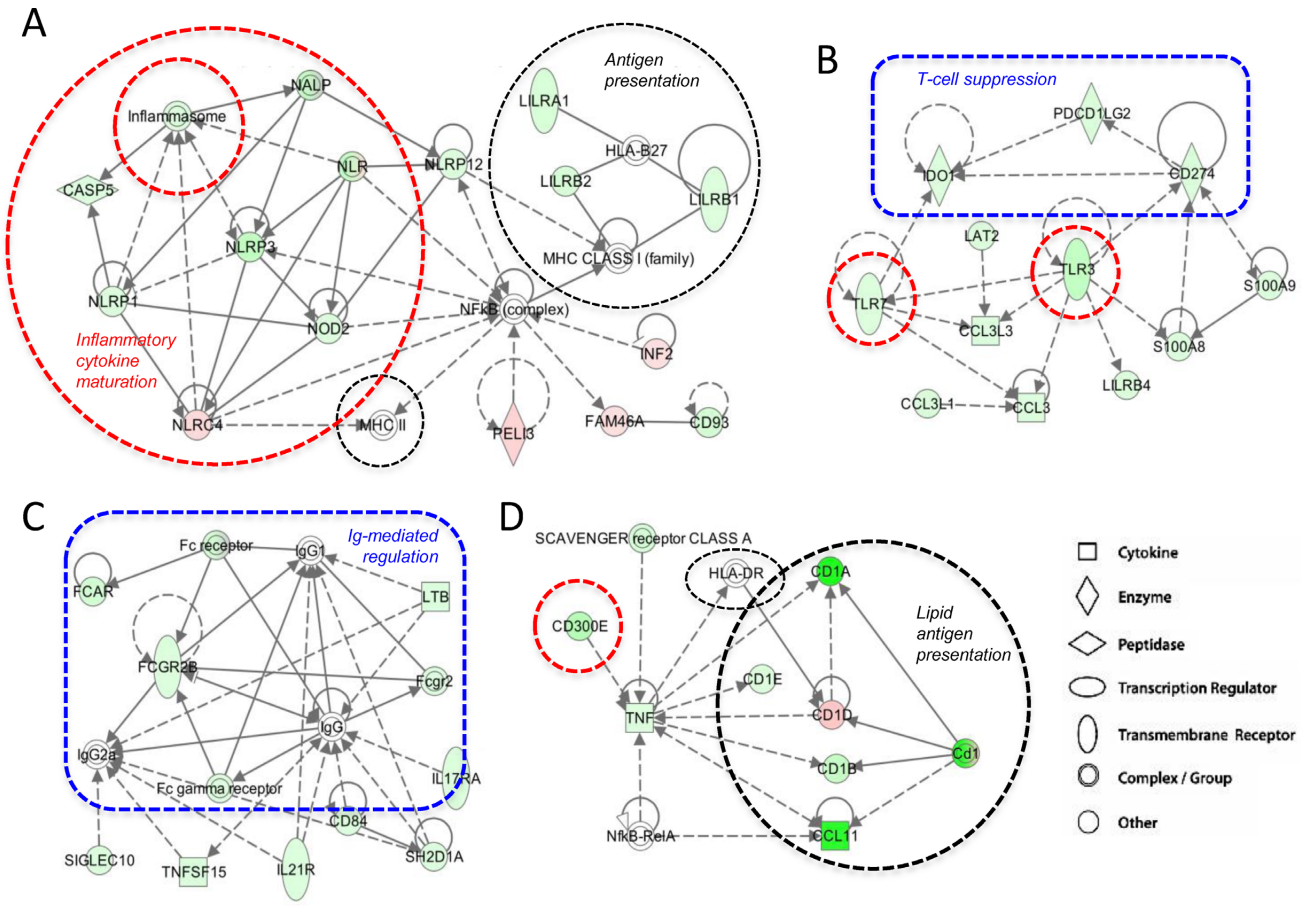

Figure 5. Effects of L165,041 on immune regulatory modules. The scheme displays functional modules derived from the IPA 'Functional Network Analysis' (Supplementary Table S6; modules 2, 3, 4 and 10). Pink symbols: genes upregulated by L165,041; green symbols: genes downregulated by L165,041. Dashed lines: indirect effects or interactions. Encircled areas indicate functional units with pro-inflammatory (red), anti-inflammatory (blue) or context-dependent (black) functions.

morphological resemblance between L165,041 (agonist) and IL-4 treated cultures, while PT-S264 (inverse agonist) induced a morphology reminiscent of M1 cells. Very similar results were obtained irrespective of the culture medium (R10 in Figure 6; XV0 medium in Supplementary Figure S5).

These morphological alterations are in agreement with the observed downregulation of pro-inflammatory genes by L165,041, exemplified by *IL8* and *CCL24* (Figure 4E), which was confirmed for GW501516 (Supplementary Figure S6). Consistent with this conclusion we also found that L165,041 inhibited phagocytosis. As shown in Figure 6F, L165,041 significantly decreased the macropinocytotic/phagocytotic activity for FITC-dextran upon PPARβ/δ activation in six independent experiments, as determined by the diminished uptake of fluorescent FITC-dextran by MDMs.

Ligand-induced immune stimulatory alterations in human MDMs

The functional networks in Figure 5 also predicted an increased T cell activation by agonist-treated MDMs as antigen-presenting cells. We tested this hypothesis by measuring intracellular IFNγ in $CD8^+$ T cells after coculture with MDMs exposed to an antigen peptide mix (CEFT). Figure 7A shows that L165,041 pretreatment of MDMs (during the 6-day differentiation period) led to a clear increase in the fraction of $IFN\gamma^+CD8^+$ cells with samples from five out of six donors.

The product of the inverse PPARβ/δ target gene *IDO1*, which suppresses T cell activation via the production of kynurenine (55), may be involved in this effect. As shown in Figure 7, the agonist-mediated transcriptional repression of *IDO1* (Figure 7B) was paralleled by a decreased protein level (Figure 7C; Supplementary Figure S7) and a clearly diminished release of kynurenine into the supernatant of MDM cultures (Figure 7D). Importantly, the level of kynurenine produced under these conditions was sufficient to significantly inhibit polyclonal (CD3 antibody-mediated) T cell activation (Figure 7E).

Another potentially important player in this scenario is the *CD274* gene. Figure 7F shows that the inverse regulation of *CD274* resulted in a reduced surface expression of its encoded product, the PD-1 ligand, a key regulator of an inhibitory T cell checkpoint (56). The agonist-mediated in-

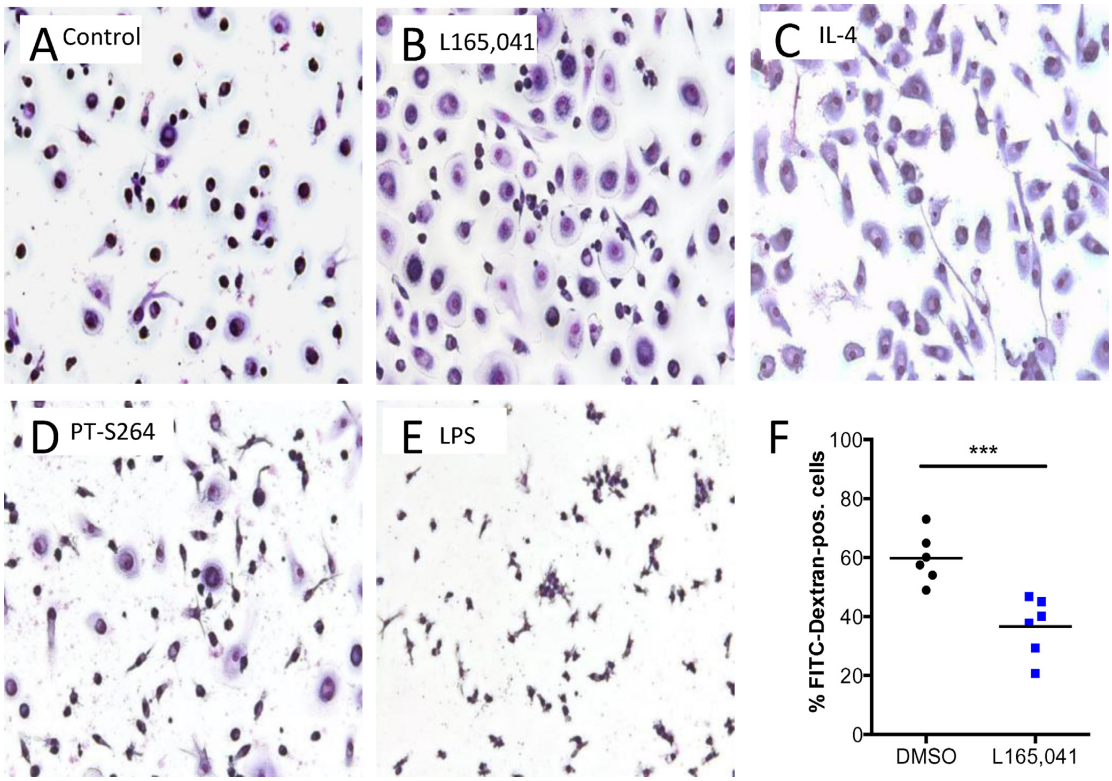

Figure 6. Inhibitory effects of PPARβ/δ ligands on human MDMs. Human monocytes were differentiated in XV0 medium for 6 days in the presence of the indicated additives. Cells were stained with Giemsa dye after treatment with (**A**) DMSO (solvent control), (**B**) L165,041 (agonist), (**C**) IL-4 ('M2' macrophages), (**D**) PT-S264 (inverse agonist) and (**E**) LPS ('M1' macrophages). (**F**) Effect of L165,041 on FITC-dextran uptake (FACS analysis) by MDMs. Data of six biological replicates with cells from four different donors are shown.

hibition of kynurenine production may thus cooperate with downregulation of PD-1 ligand expression to stimulate T cell activation.

Our bioinformatic analyses also pointed to immune stimulatory effects via the agonist-mediated repression of the *FCGR2B* gene. *FCGR2B* codes for CD32B, a low affinity Fcγ receptor that inhibits the phagocytosis of opsonized antigens (58). In contrast to *FCGR2B, FCGR2A* was only weakly repressed by L165,041 and not significantly affected by the inverse agonists ST247 (Figure 7G). *FCGR2B* repression led to downregulation of CD32B protein as determined by flow cytometry (Figure 7H). *FCGR2B* thus represents a PPARβ/δ target gene potentially mediating an agonist-triggered immune stimulatory event.

The functional annotation and networks analysis (Figure 2C; Supplementary Table S3) also predicted an inhibition of cell death of immune cells by L165,041 (Figure 2C), which could be relevant under the stressful conditions of inflammation. We therefore tested this prediction in the context of hypoxia and found a clear pro-survival effect of L165,041, while PT-S264 exacerbated hypoxia-induced cell death, as indicated by the fraction of healthy cells and cell debris in Supplementary Figure S8A. A similar effect was seen in MMT-based viability assays of the adherent cell fraction (Supplementary Figure S8B). Propidium iodide uptake assays showed a time-dependent pro-survival effect of both PPARβ/δ agonists tested (L165,041, GW501516) peaking on day 4 (Figure 7I). As MDMs do not proliferate under the culture conditions used here, a ligand effect on proliferation could not contribute to these observations.

Finally, time-lapse video microscopy revealed a slight, but statistically significant inhibitory effect of L165,041 on the motility of MDMs (Supplementary Figure S9), as predicted by the functional annotation analysis in Figure 2C.

Comparison of the PPARβ/δ agonist-induced transcriptome with defined MDM activation states

A recent study (3) defined a spectrum of macrophage activation/polarization states extending the M1/M2-model based on microarray data derived from MDMs exposed to an array of different stimuli (28 plus baseline). In an attempt to define the PPARβ/δ agonist-induced MDM phenotype more precisely we compared the L165,041-induced transcriptome to the 143 comparable microarray data sets provided by the quoted study (3), as outlined in Figure 8A. Toward this end, we first identified overlaps between the PPARβ/δ target gene set and the 49 modules representing coregulated gene sets as defined by Xue *et al.* (3). Five modules yielding P-value <0.001 by hypergeometric test were identified and further analyzed (modules 8, 15, 16, 21 and 43; Figure 8B). For each gene in the overlap between a module and the L165,041 regulated set, we determined the direction of regulation by L165,041 (as in Supplementary Table S2) and the 28 non-baseline stimuli. The heatmap in

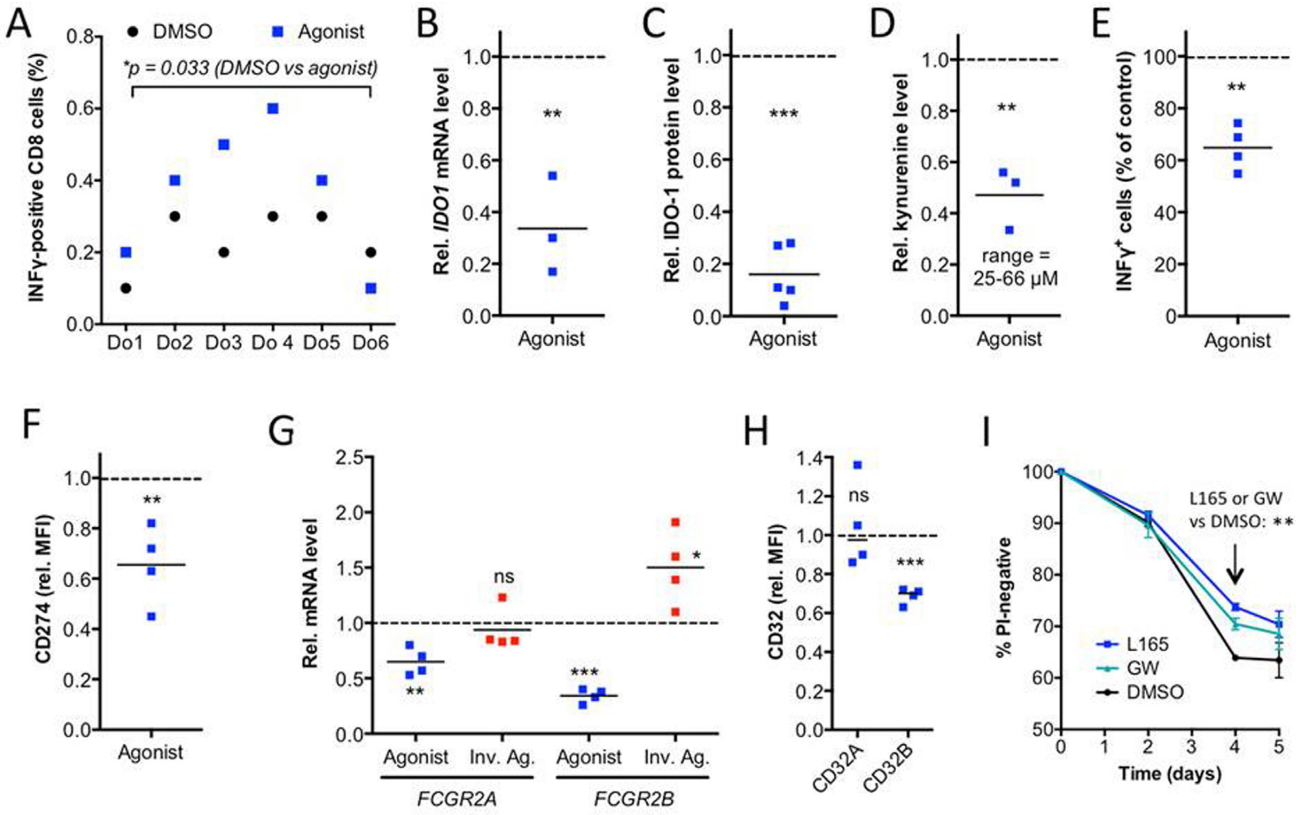

Figure 7. PPARβ/δ ligand-induced immune stimulatory alterations in human MDMs. (**A**) Effects of L165,041 on T cell activation by the recall antigen peptide mix CEFT. MDMs from six different donors differentiated in the presence of agonist or DMSO (solvent control) were analyzed for their ability to stimulate CEFT-peptide induced INFγ production by co-cultured autologous T cells. The fraction of $CD8^+IFN\gamma^+$ cells was determined by FACS. The experiment was performed with six independent donors (Do1–Do6) showing a CEFT-directed response. (**B**) RT-qPCR analysis of *IDO1* by L165,041 (24 h) in MDMs from three donors relative to DMSO control. Each dot represents the average of technical triplicates. (**C**) Quantitation of immunoblot analyses of IDO-1 protein expression in L165,041-treated (24 h) MDMs from five different donors relative to DMSO control. Blots are shown in Supplementary Figure S7. (**D**) Kynurenine production by MDMs from three different donors treated with L165,041 for 24 h relative to DMSO control. (**E**) Effect of L165,041 on polyclonal T cell activation relative to DMSO control (four different donors). (**F**) FACS analysis of CD274 expression on MDMs treated with L165,041 or solvent (DMSO) during differentiation (four different donors). (**G**) RT-qPCR analysis of *FCGR2A* and *FCGR2B* expression on MDMs treated with L165,041 or ST247 during differentiation relative to DMSO control (four donors as in (F)). (**H**) FACS analysis of CD32A and CD32B, conditions as in (F). (**I**) Effect of PPARβ/δ ligands on the time course of hypoxia-induced cell death. MDMs were cultured in XV0 medium at <1% oxygen for up to 5 days in the presence or absence of L165,041 or GW501516 and analyzed for propidium (PI) uptake by flow cytometry. Data represent the mean of three biological replicates with cells from different donors. Horizontal lines in panels (B–H) and error bars in panel (I) indicate the average.

Figure 8B represents gene subsets regulated in the same or opposite direction in red and blue, respectively. It is evident that for most stimulation conditions the five module-specific subsets show divergent directions of regulation. For instance, the classical inducers of alternative macrophage polarization (M2), IL-4 and IL-13, regulate genes in modules 15 and 43 in the same direction as L165,041, but in the opposite direction in module 16. Pro-inflammatory stimuli, like TNFα, IFNγ and LPS (stimulation conditions 10, 19–29), predominantly yield opposite patterns (modules 8 and 16), but also show a weak coordinate regulation within modules 15 and 43, consistent with a predominantly, but not exclusive anti-inflammatory effect exerted by L165,041. On the other hand, lipid-triggered (conditions 14–18) and agonist-induced patterns are similar in modules 15, 21 and 43. These data are in good agreement with our conclusion that PPARβ/δ induces a unique activation phenotype with components of anti-inflammatory, pro-inflammatory and fatty acid-mediated activation states.

Common and cell type-specific PPARβ/δ target genes

Finally, we compared the PPARβ/δ cistrome and the ligand-responsive transcriptome with those obtained with the human myofibroblastic cell line WPMY-1 (18) and the human breast cancer cell line MDA-MB-231 (19). The Venn diagrams in Figure 9A indicate a clear overlap of genes with PPARβ/δ binding sites in all three cell types ($n = 129$; Supplementary Table S7). Diseases and functions annotation revealed a statistically highly significant overlap with energy production and lipid metabolism ($P = 4.3 \times 10^{-9}$). In contrast, there was no inverse target gene common to all three cell types (Figure 9B). Our genomic studies in conjunction with the RT-qPCR analyses thus led to three conclusions: (i) a subgroup of canonical target genes are common target genes, including those with functions in intermediary metabolism (Figure 9A); (ii) another subgroup of canonical target genes are cell type-specific, such as *CD52* and *LRP5*, which are ligand-responsive only in MDMs (Supple-

mentary Figure S4 and Supplementary Table S2) compared to WPMY-1 and MDA-MB-231 cells (Figure 9C); and (iii) inverse target genes, such as *IDO1* and *IL8,* are not regulated in WPMY1 and MDA-MB-231 cells (Figure 9C) as opposed to the clear ligand regulation in MDMs (Figures 4E and 7B; Supplementary Table S2).

DISCUSSION

Our data show that PPARβ/δ target genes in normal macrophages (MDMs) fall into two major classes. The first class represents canonical genes with PPARβ/δ–RXR binding sites (PPREs), induced by agonists and repressed by inverse agonists. The second class is composed of genes lacking direct PPARβ/δ contact sites that are repressed by agonists, which we have termed inverse regulation. Importantly, inverse regulation was also seen in murine BMDMs for several target genes, and was impaired in cells with disrupted *Ppard* alleles, unequivocally demonstrating the dependence of non-canonical, ligand-mediated repression on functional PPARβ/δ. Clear evidence for the high selectivity of one of the ligands (GW501516) used in our study is also provided by published microarray data (36) obtained with differentiating murine BMCs, as depicted in the evaluation in Supplementary Figure S10.

Canonical and inverse target genes

A considerable fraction of canonical PPARβ/δ target genes have roles in lipid metabolism shared with other cell types. These include the known PPAR target genes with functions in fatty acid oxidation (*ACADVL, ACAA2, CAT, CPT1A, ECH1, PDK4, SLC25A20)* or other aspects of lipid metabolism (*ANGPTL4, FABP4, PLIN2*), but also genes not previously described as PPARβ/δ targets, such as *ETFDH* and *ISCA1*. Another large fraction of direct PPARβ/δ target genes are associated with non-metabolic functions, in particular immune regulation, such as *CD300A, CD52, LRP5, NLRC4* and *PHACTR1*, and most of these genes are cell type-selective with respect to agonist-mediated regulation.

In contrast, inverse target genes are almost exclusively regulated by PPARβ/δ ligands in a cell type-specific fashion, at least for the three cell types analyzed, i.e. macrophages, myofibroblastic cells and breast cancer cells. Consistent with this finding, a large fraction of these genes are associated with pro-inflammatory functions exerted by macrophages, including immune cell activation, migration, chemotaxis and cellular survival, exemplified by a number of cytokine and chemokine genes (e.g. *IL8, CCL24*). However, several inverse target genes have immune suppressive rather than pro-inflammatory functions, for example *IDO1*, *CD274* (PD-1L) and *CD32B*, which play essential roles in the inhibition of T cell activation. This data strongly suggested that the response to PPARβ/δ agonists is mainly anti-inflammatory, but also has immune stimulatory components.

Bioinformatic analyses showed that many of the inverse target genes are controlled by NFκB and STAT1 signaling pathways. This finding is consistent with the reported upregulation of inflammatory signaling through these pathways in adherent monocytic cells (49,50), which apparently is attenuated by PPARβ/δ agonists. PPARβ/δ has been reported to impinge on NFκB signaling by physically and/or functionally interacting with p65 in endothelial cells, cardiomyocytes, smooth muscle cells and keratinocytes (14,20,59,60) or though ERK1/2 signaling in adipocytes (22). However, in most cases the precise underlying mechanisms are not entirely clear. In mouse macrophages, a cell type selective mechanism involving the transcriptional repressor BCL-6 has been identified (23). BCL-6 is a repressor of NFκB target genes, which is sequestered by PPARβ/δ in the absence of PPARβ/δ agonists.

Our own data are consistent with the conclusion that PPARβ/δ agonists repress a subset of NFκB-regulated genes in macrophages, based on the observation that MG132 diminished the L165,041 effect on several NFκB target genes previously identified by ChIP-Seq in mouse macrophages (24). This effect of MG132 is presumably due to the inhibition of IκB degradation or a blockade of proteasome-dependent processing of p105 to p50 (53). Both effects would lead to the loss of regulation by NFκB and agonist-mediated regulation, as observed in our experiments, independent of a potential role of BCL-6 and/or other signaling pathways impinging on NFκB regulation. Obviously, proteasome inhibitors also target numerous other signaling pathways and transcription factors that might contribute to the observed effect, as exemplified by *IL8*, which has been suggested to be induced by proteasome inhibitors via reactive oxygen-mediated AP-1 activation (54).

The involvement of PPARβ/δ in modulating STAT activity is even less understood with all published evidence restricted to STAT3 (61–64). The identification of strongly regulated inverse target genes in the present study paves the way for addressing these open questions using individual genes as experimental models and for elucidating the mechanisms underlying the crosstalk between PPARβ/δ and pro-inflammatory signaling cascades.

Effects of PPARβ/δ agonists on inflammatory pathways

'Functional Annotation and Networks Analysis' indicated that inflammatory signaling is targeted by PPARβ/δ agonists at two different levels. First, several genes encoding pro-inflammatory cytokines (e.g. *IL8, IFNG*) and chemokines (e.g. *CCL3/MIP1A, CCL8/MCP2, CCL11/eotaxin, CCL13/MCP4*) are downregulated as inverse target genes with predicted anti-inflammatory effects. In addition, a few anti-inflammatory cytokine genes (e.g. *IL10, IL13*) are similarly affected, suggesting that agonist effects on immune cells are not exclusively inhibitory. Second, our RNA-Seq analyses identified several key components of NALP inflammasomes as novel PPARβ/δ targets (Figure 5C). These include the canonical target gene *NLR4C* and the inverse target genes *NLRP1*, *NLRP3* and *CASP5*. NLR family proteins act as a sensor of pathogenic signals and promotes inflammasome assembly, leading to caspase-1 activation and inflammatory cytokine (IL-1β, IL-18) production (65). *NLR4C* encoded CARD12 is activated by microbial proteinaceous ligands, while

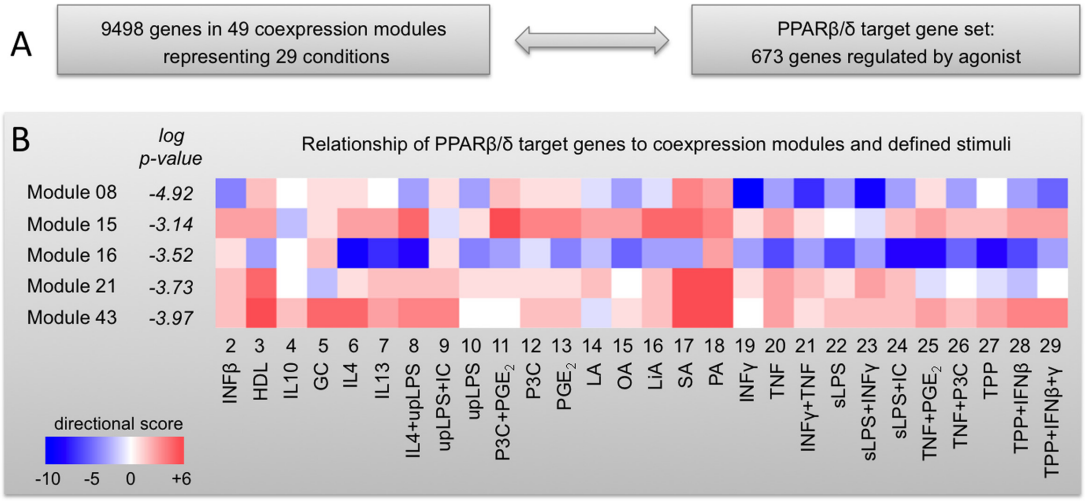

Figure 8. Comparison of the PPARβ/δ transcriptome with a spectrum of defined MDM activation states. (**A**) Scheme outlining the basis for the comparative analyses. (**B**) Relationship of PPARβ/δ target genes to expression data obtained with 29 different stimuli grouped into 49 coexpression modules (3). Overlaps between PPARβ/δ target genes and each module were determined by hypergeometric test. Modules yielding *P*-values <0.001 (modules 8, 15, 16, 21 and 43) were further analyzed by determining for each gene the direction of regulation by L165,041 (Supplementary Table S2) compared to all 29 stimuli (3). Results are displayed for each subset of genes (defined by specific stimulation conditions within individual modules) as a heatmap. The color code is based on a directional score reflecting the number of genes regulated in the same direction (red) or in opposite directions (blue; for details see the Materials and Methods section). GC, glucocorticoid; HDL, high density lipoprotein; IC, immune complexes; LA, lauric acid; LiA, linoleic acid; OA, oleic acid; P3C, Pam3CysSerLys4; PA, palmitic acid; SA, stearic acid; sLPS, standard lipopolysaccharide; TPP, TNFα+PGE_2+P3C; upLPS, ultrapure lipopolysaccharide.

NLRP1 recognizes muramyl dipeptide and diverse stimuli (e.g. crystalline material, peptide aggregates, bacterial toxins) can trigger NLRP3 activation (65). Non-canonical inflammasome activation by Gram-negative bacteria can involve the additional recruitment of caspase 5, encoded by another inverse PPARβ/δ target gene. Taken together, these findings indicate that PPARβ/δ agonists can have pro- and anti-inflammatory effects on specific inflammasome functions and suggest that the precise outcome is stimulus-dependent.

Our data confirm and extend a previous study identifying *CD300A* as a PPARβ/δ target gene in macrophage-like cells derived from the human leukemia cell line THP-1 (35). In mice, disruption of the *Cd300a* gene resulted in pro-inflammatory activation of peritoneal macrophages, identifying CD300a-mediated inhibitory signaling in macrophages as a critical regulator of intestinal immune homeostasis (35). *CD300E*, coding for an activating CD300 subtype, is repressed by L165,041 (Figure 5D) simultaneously with the induction of the inhibitory *CD300A* gene, consistent with an immunosuppressive agonist function via regulation of CD300 family members.

We also identified *PHACTR1* as a novel canonical PPARβ/δ target gene. This gene encodes phosphatase and actin regulator 1, which is involved in the G-actin mediated control of actomyosin assembly (66) and may thus play a role in modulating macrophage migration and phagocytosis. However, the agonist-mediated induction of *PHACTR1* appears to be inconsistent with the observed inhibition of phagocytosis/macropinocytosis of FITC-dextran, suggesting that other genes contribute to this effect. An example is *DIXDC1*, another canonical PPARβ/δ target gene implicated in cell migration by modulating the WNT and PI_3K signaling pathways (67,68).

Immune stimulatory effects of PPARβ/δ agonists

As shown by our functional studies, PPARβ/δ agonists stimulate CD8+ T cell activation. Based on our bioinformatic analyses at least two mechanisms may be involved in this effect, i.e. the IDO-1 mediated catabolism of tryptophan and synthesis of PD-1 ligand (CD274). The inhibitory effect of agonists on *CD274* and *IDO1* transcription resulted in a decreased expression of both proteins and synthesis of the IDO-1 product kynurenine. The latter is a known suppressor of T cell activation (55), which we confirmed for the concentrations achieved in our experimental system. Repression of *CD274* by PPARβ/δ agonist has previously also been described for human myofibroblastic cells (69), emphasizing the potential relevance of this regulatory effect of PPARβ/δ. *CD274*/PD-L1 engagement of the PD-1 receptor on T cells activates a key checkpoint restraining T cell activation (56), which constitutes a key component of immune suppression in the tumor microenvironment. We also found several genes with functions in antigen presentation to be modulated by PPARβ/δ agonists. Whether these changes play a role in the observed stimulation of T cell activation remains to be investigated.

Pro-survival effects of PPARβ/δ agonists

Another clear biological effect of PPARβ/δ agonists is the suppression of macrophage cell death under hypoxia, which is frequently associated with inflammation (70) and imposes environmental stress on the resident inflammatory

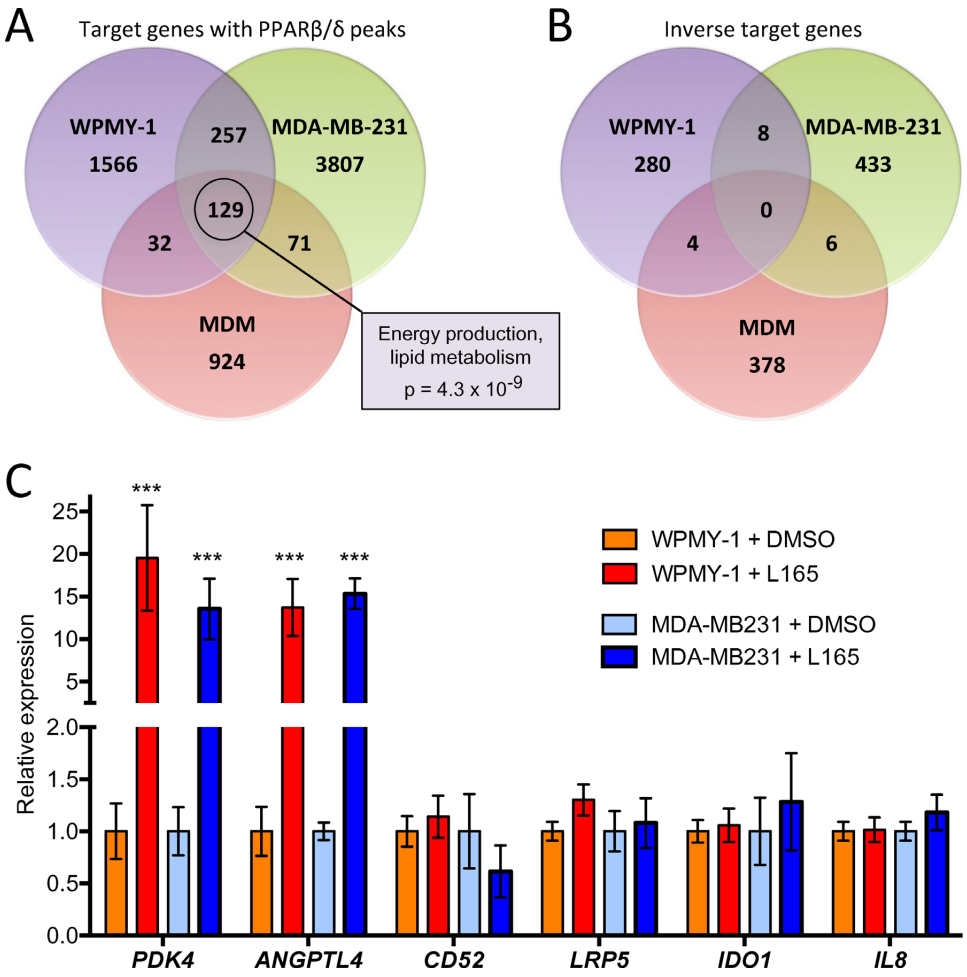

Figure 9. Identification of common and cell type-specific PPARβ/δ target genes. **(A)** Overlap of PPARβ/δ binding sites in WPMY-1 myofibroblast-like cells, MDA-MB-231 breast cancer cells and MDMs. Common target genes (n = 129) were analyzed by IPA *Diseases and Functions Annotation*. The box shows the top term by p-value of overlap. **(B)** Overlap of agonist-repressed genes. **(C)** RT-qPCR validation of common and macrophage-specific PPARβ/δ target genes in WPMY-1 and MDA-MB-231 cells. Values were normalized to 1 for untreated cells (solvent only) individually for each gene and cell line. Statistical significance was tested relative to DMSO-treated cells.

cells. This biological effect of PPARβ/δ agonists is mirrored by the observed changes in gene expression. Thus, several transcription factor genes with death promoting functions (e.g. *ID3* and *MYC*) are downregulated by agonists, while genes with pro-survival effects are upregulated (e.g. *EGR3* and *VDR*). Our functional annotation analyses also showed a strong overlap of PPARβ/δ target genes associated with the inhibition of inflammation and cell survival, suggesting a functional link. This group indeed harbors a number of inverse target genes with both pro-inflammatory and death-promoting functions, for example the cytokines TNFα and IL-1β. In these cases, the downregulation of the same genes by PPARβ/δ agonist may thus contribute to both an attenuation of the inflammatory response and a promotion of cell survival.

A specific macrophage activation state induced by PPARβ/δ agonists

The bioinformatic analyses and biological data described above clearly indicate that PPARβ/δ agonists have a predominantly, but not exclusively, anti-inflammatory effect on MDMs. A recent study (3) reporting the transcriptomes for MDMs exposed to 28 different stimuli provided a resource to characterize the phenotype of agonist-stimulated MDMs in further detail. The authors used these data to define 49 modules of coregulated genes and determined the extent to which each of these modules was associated with the different stimulation conditions, resulting in the development of a spectrum model of macrophage activation. Comparison of these modules with the transcriptomes of L165,041-stimulated cells unraveled highly significant overlaps with activation states triggered by IL-4/IL13, TNFα/INFγ and fatty acids. These observations clearly confirm the hypothesis that PPARβ/δ induces a unique activation phenotype with components of anti-inflammatory, immune stimulatory and lipid-triggered activation states.

CONCLUSIONS

Numerous literature reports have documented an anti-inflammatory effect of PPARβ/δ agonists with few dis-

crepant findings. However, the molecular mechanisms underlying the regulation of immune cells by PPARβ/δ are only partially understood. In the present study, we have determined the PPARβ/δ transcriptome and PPARβ/δ-RXR cistrome in human MDMs to establish the global PPARβ/δ-regulated signaling network in human macrophages. This study showed that genes with immune regulatory functions are regulated by PPARβ/δ agonists in a macrophage-selective fashion by at least two mechanisms: (i) canonical regulation, analogous to ubiquitous PPARβ/δ target genes with metabolic functions, which involves transcriptional induction by agonists and direct DNA contacts of PPARβ/δ-RXR heterodimers, and (ii) repression by agonists (inverse regulation) in the absence of PPARβ/δ DNA binding. The latter mechanism affects to a large extent NFκB and STAT1 target genes, resulting in the inhibition of multiple pro-inflammatory mediators in line with the known anti-inflammatory effect of PPARβ/δ activation. However, consistent with the results of different bioinformatic approaches, we also identified specific immune stimulatory effects exerted by PPARβ/δ agonists. Besides a pro-survival effect on macrophages and inhibition of CD32B surface expression, the most prominent example in this context is the stimulation of T cell activation. The latter is presumably linked to the repression of the *CD274* and *IDO1* genes, resulting in a diminished surface expression of PD-1 ligand and a decreased production of the immune suppressive kynurenine. Consistent with these observations, the PPARβ/δ agonist-regulated transcriptome shows a significant overlap with coexpression modules triggered by either the anti-inflammatory IL-4 and IL-13 cytokines or the pro-inflammatory mediators TNFα and IFNγ. These findings clearly indicate that PPARβ/δ agonists induce a novel and unique macrophage activation state with strong anti-inflammatory but also specific immune stimulatory components. Collectively, these findings suggest that contrary to the prevailing opinion PPARβ/δ exerts context-dependent rather than merely inhibitory functions in immune regulation.

It is obviously of great interest to analyze the effects of PPARβ/δ ligands on macrophages in the context of other immune cells *in vivo*. However, the identification of a mouse model suitable to recapitulate the global role of PPARβ/δ in the human immune system is associated with problems that cannot easily be solved, if at all. Thus, as suggested by our own data obtained with murine BMCs, murine BMDMs and human MDMs, the effect of PPARβ/δ ligands on the transcriptome of myeloid cells appears to be influenced by their differentiation and/or activation state, and perhaps also by species-specific effects. This suggests that data obtained with human MDMs may not be easily transferable to a mouse model. Testing the relevance of our findings in a physiological setting therefore remains a major challenge of future studies.

ACCESSION NUMBERS

RNA-Seq and ChIP-Seq data sets have been deposited at EBI ArrayExpress under accession numbers E-MTAB-3114 and E-MTAB-3113, respectively.

SUPPLEMENTARY DATA

Supplementary Data are available at NAR Online.

ACKNOWLEDGEMENTS

We are grateful to Dr Robert Geffers (Helmholtz-Zentrum für Infektionsforschung, Braunschweig, Germany) for valuable discussions on ChIP-Seq library synthesis. We thank Margitta Alt, Traute Plaum and Achim Allmeroth for expert technical assistance.

FUNDING

The Deutsche Forschungsgemeinschaft [MU601/13 to R.M.]; the Wilhelm-Sander-Stiftung [to S.M.B. and S.R.]; the Universitätsklinikum Giessen-Marburg [to T.A. and S.R.].
Conflict of interest statement. None declared.

REFERENCES

1. Sica,A. and Mantovani,A. (2012) Macrophage plasticity and polarization: in vivo veritas. *J. Clin. Invest.*, **122**, 787–795.
2. Martinez,F.O. and Gordon,S. (2014) The M1 and M2 paradigm of macrophage activation: time for reassessment. *F1000Prime Rep.*, **6**, 13.
3. Xue,J., Schmidt,S.V., Sander,J., Draffehn,A., Krebs,W., Quester,I., De Nardo,D., Gohel,T.D., Emde,M., Schmidleithner,L. *et al.* (2014) Transcriptome-based network analysis reveals a spectrum model of human macrophage activation. *Immunity*, **40**, 274–288.
4. Kostadinova,R., Wahli,W. and Michalik,L. (2005) PPARs in diseases: control mechanisms of inflammation. *Curr. Med. Chem.*, **12**, 2995–3009.
5. Yang,Y., Lovett-Racke,A.E. and Racke,M.K. (2010) Regulation of immune responses and autoimmune encephalomyelitis by PPARs. *PPAR Res.*, **2010**, 104705.
6. Wahli,W. and Michalik,L. (2012) PPARs at the crossroads of lipid signaling and inflammation. *Trends Endocrinol. Metab.*, **23**, 351–363.
7. Michalik,L. and Wahli,W. (2008) PPARs mediate lipid signaling in inflammation and cancer. *PPAR Res.*, **2008**, 134059.
8. Peters,J.M., Lee,S.S., Li,W., Ward,J.M., Gavrilova,O., Everett,C., Reitman,M.L., Hudson,L.D. and Gonzalez,F.J. (2000) Growth, adipose, brain, and skin alterations resulting from targeted disruption of the mouse peroxisome proliferator-activated receptor beta(delta). *Mol. Cell. Biol.*, **20**, 5119–5128.
9. Chong,H.C., Tan,M.J., Philippe,V., Tan,S.H., Tan,C.K., Ku,C.W., Goh,Y.Y., Wahli,W., Michalik,L. and Tan,N.S. (2009) Regulation of epithelial-mesenchymal IL-1 signaling by PPARbeta/delta is essential for skin homeostasis and wound healing. *J. Cell Biol.*, **184**, 817–831.
10. Bassaganya-Riera,J., DiGuardo,M., Climent,M., Vives,C., Carbo,A., Jouni,Z.E., Einerhand,A.W., O'Shea,M. and Hontecillas,R. (2011) Activation of PPARgamma and delta by dietary punicic acid ameliorates intestinal inflammation in mice. *Br. J. Nutr.*, **106**, 878–886.
11. Kanakasabai,S., Chearwae,W., Walline,C.C., Iams,W., Adams,S.M. and Bright,J.J. (2010) Peroxisome proliferator-activated receptor delta agonists inhibit T helper type 1 (Th1) and Th17 responses in experimental allergic encephalomyelitis. *Immunology*, **130**, 572–588.
12. Kang,K., Reilly,S.M., Karabacak,V., Gangl,M.R., Fitzgerald,K., Hatano,B. and Lee,C.H. (2008) Adipocyte-derived Th2 cytokines and myeloid PPARdelta regulate macrophage polarization and insulin sensitivity. *Cell Metab.*, **7**, 485–495.
13. Odegaard,J.I., Ricardo-Gonzalez,R.R., Red Eagle,A., Vats,D., Morel,C.R., Goforth,M.H., Subramanian,V., Mukundan,L., Ferrante,A.W. and Chawla,A. (2008) Alternative M2 activation of Kupffer cells by PPARdelta ameliorates obesity-induced insulin resistance. *Cell Metab.*, **7**, 496–507.
14. Westergaard,M., Henningsen,J., Johansen,C., Rasmussen,S., Svendsen,M.L., Jensen,U.B., Schroder,H.D., Staels,B., Iversen,L., Bolund,L. *et al.* (2003) Expression and localization of peroxisome

proliferator-activated receptors and nuclear factor kappaB in normal and lesional psoriatic skin. *J. Invest. Dermatol.*, **121**, 1104–1117.
15. Romanowska,M., Reilly,L., Palmer,C.N., Gustafsson,M.C. and Foerster,J. (2010) Activation of PPARbeta/delta causes a psoriasis-like skin disease in vivo. *PLoS One*, **5**, e9701.
16. Hack,K., Reilly,L., Palmer,C., Read,K.D., Norval,S., Kime,R., Booth,K. and Foerster,J. (2012) Skin-targeted inhibition of PPAR beta/delta by selective antagonists to treat PPAR beta/delta - mediated psoriasis-like skin sisease in vivo. *PLoS One*, **7**, e37097.
17. Peters,J.M., Shah,Y.M. and Gonzalez,F.J. (2012) The role of peroxisome proliferator-activated receptors in carcinogenesis and chemoprevention. *Nat. Rev. Cancer*, **12**, 181–195.
18. Adhikary,T., Kaddatz,K., Finkernagel,F., Schönbauer,A., Meissner,W., Scharfe,M., Jarek,M., Blöcker,H., Müller-Brüsselbach,S. and Müller,R. (2011) Genomewide analyses define different modes of transcriptional regulation by peroxisome proliferator-activated receptor-beta/delta (PPARbeta/delta). *PLoS One*, **6**, e16344.
19. Adhikary,T., Brandt,D.T., Kaddatz,K., Stockert,J., Naruhn,S., Meissner,W., Finkernagel,F., Obert,J., Lieber,S., Scharfe,M. *et al.* (2013) Inverse PPARbeta/delta agonists suppress oncogenic signaling to the ANGPTL4 gene and inhibit cancer cell invasion. *Oncogene*, **32**, 5241–5252.
20. Planavila,A., Rodriguez-Calvo,R., Jove,M., Michalik,L., Wahli,W., Laguna,J.C. and Vazquez-Carrera,M. (2005) Peroxisome proliferator-activated receptor beta/delta activation inhibits hypertrophy in neonatal rat cardiomyocytes. *Cardiovasc. Res.*, **65**, 832–841.
21. Stockert,J., Wolf,A., Kaddatz,K., Schnitzer,E., Finkernagel,F., Meissner,W., Müller-Brüsselbach,S., Kracht,M. and Müller,R. (2013) Regulation of TAK1/TAB1-mediated IL-1beta signaling by cytoplasmic PPARbeta/delta. *PLoS One*, **8**, e63011.
22. Rodriguez-Calvo,R., Serrano,L., Coll,T., Moullan,N., Sanchez,R.M., Merlos,M., Palomer,X., Laguna,J.C., Michalik,L., Wahli,W. *et al.* (2008) Activation of peroxisome proliferator-activated receptor beta/delta inhibits lipopolysaccharide-induced cytokine production in adipocytes by lowering nuclear factor-kappaB activity via extracellular signal-related kinase 1/2. *Diabetes*, **57**, 2149–2157.
23. Lee,C.H., Chawla,A., Urbiztondo,N., Liao,D., Boisvert,W.A., Evans,R.M. and Curtiss,L.K. (2003) Transcriptional repression of atherogenic inflammation: modulation by PPARdelta. *Science*, **302**, 453–457.
24. Barish,G.D., Yu,R.T., Karunasiri,M., Ocampo,C.B., Dixon,J., Benner,C., Dent,A.L., Tangirala,R.K. and Evans,R.M. (2010) Bcl-6 and NF-kappaB cistromes mediate opposing regulation of the innate immune response. *Genes Dev.*, **24**, 2760–2765.
25. Xu,H.E., Lambert,M.H., Montana,V.G., Parks,D.J., Blanchard,S.G., Brown,P.J., Sternbach,D.D., Lehmann,J.M., Wisely,G.B., Willson,T.M. *et al.* (1999) Molecular recognition of fatty acids by peroxisome proliferator-activated receptors. *Mol. Cell*, **3**, 397–403.
26. Naruhn,S., Meissner,W., Adhikary,T., Kaddatz,K., Klein,T., Watzer,B., Müller-Brüsselbach,S. and Müller,R. (2010) 15-hydroxyeicosatetraenoic acid is a preferential peroxisome proliferator-activated receptor β/δ agonist. *Mol. Pharmacol.*, **77**, 171–184.
27. Lim,H., Gupta,R.A., Ma,W.G., Paria,B.C., Moller,D.E., Morrow,J.D., DuBois,R.N., Trzaskos,J.M. and Dey,S.K. (1999) Cyclo-oxygenase-2-derived prostacyclin mediates embryo implantation in the mouse via PPARdelta. *Genes Dev.*, **13**, 1561–1574.
28. Fauti,T., Müller-Brüsselbach,S., Kreutzer,M., Rieck,M., Meissner,W., Rapp,U., Schweer,H., Kömhoff,M. and Müller,R. (2006) Induction of PPARbeta and prostacyclin (PGI2) synthesis by Raf signaling: failure of PGI2 to activate PPARbeta. *FEBS J.*, **273**, 170–179.
29. Rao,G.H., Reddy,K.R., Hagert,K. and White,J.G. (1980) Influence of pH on the prostacyclin (PGI2) mediated inhibition of platelet function. *Prostaglandins Med.*, **4**, 263–273.
30. Billin,A.N. (2008) PPAR-beta/delta agonists for Type 2 diabetes and dyslipidemia: an adopted orphan still looking for a home. *Expert Opin. Investig. Drugs*, **17**, 1465–1471.
31. Peraza,M.A., Burdick,A.D., Marin,H.E., Gonzalez,F.J. and Peters,J.M. (2006) The toxicology of ligands for peroxisome proliferator-activated receptors (PPAR). *Toxicol. Sci.*, **90**, 269–295.
32. Shearer,B.G., Steger,D.J., Way,J.M., Stanley,T.B., Lobe,D.C., Grillot,D.A., Iannone,M.A., Lazar,M.A., Willson,T.M. and Billin,A.N. (2008) Identification and characterization of a selective peroxisome proliferator-activated receptor beta/delta (NR1C2) antagonist. *Mol. Endocrinol.*, **22**, 523–529.
33. Naruhn,S., Toth,P.M., Adhikary,T., Kaddatz,K., Pape,V., Dörr,S., Klebe,G., Müller-Brüsselbach,S., Diederich,W.E. and Müller,R. (2011) High-affinity peroxisome proliferator-activated receptor beta/delta-specific ligands with pure antagonistic or inverse agonistic properties. *Mol. Pharmacol.*, **80**, 828–838.
34. Toth,P.M., Naruhn,S., Pape,V.F., Dörr,S.M., Klebe,G., Müller,R. and Diederich,W.E. (2012) Development of improved PPARbeta/delta inhibitors. *ChemMedChem*, **7**, 159–170.
35. Tanaka,T., Tahara-Hanaoka,S., Nabekura,T., Ikeda,K., Jiang,S., Tsutsumi,S., Inagaki,T., Magoori,K., Higurashi,T., Takahashi,H. *et al.* (2014) PPARbeta/delta activation of CD300a controls intestinal immunity. *Sci. Rep.*, **4**, 5412.
36. Lieber,S., Scheer,F., Finkernagel,F., Meissner,W., Giehl,G., Brendel,C., Diederich,W.E., Muller-Brusselbach,S. and Muller,R. (2015) The inverse agonist DG172 triggers a PPARbeta/delta-independent myeloid lineage shift and promotes GM-CSF/IL-4-induced dendritic cell differentiation. *Mol. Pharmacol.*, **87**, 162–173.
37. Reinartz,S., Schumann,T., Finkernagel,F., Wortmann,A., Jansen,J.M., Meissner,W., Krause,M., Schworer,A.M., Wagner,U., Muller-Brusselbach,S. *et al.* (2014) Mixed-polarization phenotype of ascites-associated macrophages in human ovarian carcinoma: Correlation of CD163 expression, cytokine levels and early relapse. *Int. J. Cancer*, **134**, 32–42.
38. Braun,D., Longman,R.S. and Albert,M.L. (2005) A two-step induction of indoleamine 2,3 dioxygenase (IDO) activity during dendritic-cell maturation. *Blood*, **106**, 2375–2381.
39. Liao,Y., Smyth,G.K. and Shi,W. (2013) The Subread aligner: fast, accurate and scalable read mapping by seed-and-vote. *Nucleic Acids Res.*, **41**, e108.
40. Dobin,A., Davis,C.A., Schlesinger,F., Drenkow,J., Zaleski,C., Jha,S., Batut,P., Chaisson,M. and Gingeras,T.R. (2013) STAR: ultrafast universal RNA-seq aligner. *Bioinformatics*, **29**, 15–21.
41. Satoh,J. and Tabunoki,H. (2013) A comprehensive profile of ChIP-Seq-based STAT1 target genes suggests the complexity of STAT1-mediated gene regulatory mechanisms. *Gene Regul. Syst. Bio.*, **7**, 41–56.
42. Hutchins,A.P., Poulain,S. and Miranda-Saavedra,D. (2012) Genome-wide analysis of STAT3 binding in vivo predicts effectors of the anti-inflammatory response in macrophages. *Blood*, **119**, e110–e119.
43. Ghisletti,S., Barozzi,I., Mietton,F., Polletti,S., De Santa,F., Venturini,E., Gregory,L., Lonie,L., Chew,A., Wei,C.L. *et al.* (2010) Identification and characterization of enhancers controlling the inflammatory gene expression program in macrophages. *Immunity*, **32**, 317–328.
44. Haskill,S., Johnson,C., Eierman,D., Becker,S. and Warren,K. (1988) Adherence induces selective mRNA expression of monocyte mediators and proto-oncogenes. *J. Immunol.*, **140**, 1690–1694.
45. Sporn,S.A., Eierman,D.F., Johnson,C.E., Morris,J., Martin,G., Ladner,M. and Haskill,S. (1990) Monocyte adherence results in selective induction of novel genes sharing homology with mediators of inflammation and tissue repair. *J. Immunol.*, **144**, 4434–4441.
46. Kelley,J.L., Rozek,M.M., Suenram,C.A. and Schwartz,C.J. (1987) Activation of human blood monocytes by adherence to tissue culture plastic surfaces. *Exp. Mol. Pathol.*, **46**, 266–278.
47. Fuhlbrigge,R.C., Chaplin,D.D., Kiely,J.M. and Unanue,E.R. (1987) Regulation of interleukin 1 gene expression by adherence and lipopolysaccharide. *J. Immunol.*, **138**, 3799–3802.
48. Eierman,D.F., Johnson,C.E. and Haskill,J.S. (1989) Human monocyte inflammatory mediator gene expression is selectively regulated by adherence substrates. *J. Immunol.*, **142**, 1970–1976.
49. Coccia,E.M., Del Russo,N., Stellacci,E., Testa,U., Marziali,G. and Battistini,A. (1999) STAT1 activation during monocyte to macrophage maturation: role of adhesion molecules. *Int. Immunol.*, **11**, 1075–1083.
50. Rosales,C. and Juliano,R. (1996) Integrin signaling to NF-kappa B in monocytic leukemia cells is blocked by activated oncogenes. *Cancer Res.*, **56**, 2302–2305.

51. Mandard,S., Zandbergen,F., Tan,N.S., Escher,P., Patsouris,D., Koenig,W., Kleemann,R., Bakker,A., Veenman,F., Wahli,W. *et al.* (2004) The direct peroxisome proliferator-activated receptor target fasting-induced adipose factor (FIAF/PGAR/ANGPTL4) is present in blood plasma as a truncated protein that is increased by fenofibrate treatment. *J. Biol. Chem.*, **279**, 34411–34420.
52. Bours,V., Franzoso,G., Azarenko,V., Park,S., Kanno,T., Brown,K. and Siebenlist,U. (1993) The oncoprotein Bcl-3 directly transactivates through kappa B motifs via association with DNA-binding p50B homodimers. *Cell*, **72**, 729–739.
53. Palombella,V.J., Rando,O.J., Goldberg,A.L. and Maniatis,T. (1994) The ubiquitin-proteasome pathway is required for processing the NF-kappa B1 precursor protein and the activation of NF-kappa B. *Cell*, **78**, 773–785.
54. Wu,H.M., Wen,H.C. and Lin,W.W. (2002) Proteasome inhibitors stimulate interleukin-8 expression via Ras and apoptosis signal-regulating kinase-dependent extracellular signal-related kinase and c-Jun N-terminal kinase activation. *Am. J. Respir. Cell Mol. Biol.*, **27**, 234–243.
55. Munn,D.H. and Mellor,A.L. (2013) Indoleamine 2,3 dioxygenase and metabolic control of immune responses. *Trends Immunol.*, **34**, 137–143.
56. Francisco,L.M., Sage,P.T. and Sharpe,A.H. (2010) The PD-1 pathway in tolerance and autoimmunity. *Immunol. Rev.*, **236**, 219–242.
57. Silk,J.D., Salio,M., Brown,J., Jones,E.Y. and Cerundolo,V. (2008) Structural and functional aspects of lipid binding by CD1 molecules. *Annu. Rev. Cell Dev. Biol.*, **24**, 369–395.
58. Guilliams,M., Bruhns,P., Saeys,Y., Hammad,H. and Lambrecht,B.N. (2014) The function of Fcgamma receptors in dendritic cells and macrophages. *Nat. Rev. Immunol.*, **14**, 94–108.
59. Rival,Y., Beneteau,N., Taillandier,T., Pezet,M., Dupont-Passelaigue,E., Patoiseau,J.F., Junquero,D., Colpaert,F.C. and Delhon,A. (2002) PPARalpha and PPARdelta activators inhibit cytokine-induced nuclear translocation of NF-kappaB and expression of VCAM-1 in EAhy926 endothelial cells. *Eur. J. Pharmacol.*, **435**, 143–151.
60. Ding,G., Cheng,L., Qin,Q., Frontin,S. and Yang,Q. (2006) PPARdelta modulates lipopolysaccharide-induced TNFalpha inflammation signaling in cultured cardiomyocytes. *J. Mol. Cell. Cardiol.*, **40**, 821–828.
61. Wang,L.H., Yang,X.Y., Zhang,X., Huang,J., Hou,J., Li,J., Xiong,H., Mihalic,K., Zhu,H., Xiao,W. *et al.* (2004) Transcriptional inactivation of STAT3 by PPARgamma suppresses IL-6-responsive multiple myeloma cells. *Immunity*, **20**, 205–218.
62. Kino,T., Rice,K.C. and Chrousos,G.P. (2007) The PPARdelta agonist GW501516 suppresses interleukin-6-mediated hepatocyte acute phase reaction via STAT3 inhibition. *Eur. J. Clin. Invest.*, **37**, 425–433.
63. Serrano-Marco,L., Barroso,E., El Kochairi,I., Palomer,X., Michalik,L., Wahli,W. and Vazquez-Carrera,M. (2011) The peroxisome proliferator-activated receptor (PPAR) beta/delta agonist GW501516 inhibits IL-6-induced signal transducer and activator of transcription 3 (STAT3) activation and insulin resistance in human liver cells. *Diabetologia*, **55**, 743–751.
64. Serrano-Marco,L., Rodriguez-Calvo,R., El Kochairi,I., Palomer,X., Michalik,L., Wahli,W. and Vazquez-Carrera,M. (2011) Activation of peroxisome proliferator-activated receptor-beta/-delta (PPAR-beta/-delta) ameliorates insulin signaling and reduces SOCS3 levels by inhibiting STAT3 in interleukin-6-stimulated adipocytes. *Diabetes*, **60**, 1990–1999.
65. Latz,E., Xiao,T.S. and Stutz,A. (2013) Activation and regulation of the inflammasomes. *Nat. Rev. Immunol.*, **13**, 397–411.
66. Wiezlak,M., Diring,J., Abella,J., Mouilleron,S., Way,M., McDonald,N.Q. and Treisman,R. (2012) G-actin regulates the shuttling and PP1 binding of the RPEL protein Phactr1 to control actomyosin assembly. *J. Cell Sci.*, **125**, 5860–5872.
67. Singh,K.K., Ge,X., Mao,Y., Drane,L., Meletis,K., Samuels,B.A. and Tsai,L.H. (2010) Dixdc1 is a critical regulator of DISC1 and embryonic cortical development. *Neuron*, **67**, 33–48.
68. Xu,Z., Liu,D., Fan,C., Luan,L., Zhang,X. and Wang,E. (2014) DIXDC1 increases the invasion and migration ability of non-small-cell lung cancer cells via the PI3K-AKT/AP-1 pathway. *Mol. Carcinog.*, **53**, 917–925.
69. Stockert,J., Adhikary,T., Kaddatz,K., Finkernagel,F., Meissner,W., Müller-Brüsselbach,S. and Müller,R. (2011) Reverse crosstalk of TGFβ and PPARβ/δ signaling identified by transcriptional profiling. *Nucleic Acids Res.*, **39**, 119–131.
70. Eltzschig,H.K. and Carmeliet,P. (2011) Hypoxia and inflammation. *N. Engl. J. Med.*, **364**, 656–665.

Deregulation of PPARβ/δ target genes in tumor-associated macrophages by fatty acid ligands in the ovarian cancer microenvironment

Tim Schumann[1,*], Till Adhikary[1,*], Annika Wortmann[1,*], Florian Finkernagel[1], Sonja Lieber[1], Evelyn Schnitzer[1], Nathalie Legrand[1], Yvonne Schober[2], W. Andreas Nockher[2], Philipp M. Toth[3], Wibke E. Diederich[3], Andrea Nist[4], Thorsten Stiewe[4], Uwe Wagner[5], Silke Reinartz[5], Sabine Müller-Brüsselbach[1] and Rolf Müller[1]

[1] Institute of Molecular Biology and Tumor Research (IMT), Philipps University, Marburg, Germany

[2] Metabolomics Core Facility and Institute of Laboratory Medicine and Pathobiochemistry, Philipps University, Marburg, Germany

[3] Medicinal Chemistry Core Facility and Institute of Pharmaceutical Chemistry, Philipps University, Marburg, Germany

[4] Genomics Core Facility, Philipps University, Marburg, Germany

[5] Clinic for Gynecology, Gynecological Oncology and Gynecological Endocrinology, Center for Tumor Biology and Immunology (ZTI), Philipps University, Marburg, Germany

[*] These authors have contributed equally to this work

Correspondence to: *Rolf Müller*, ***email***: *rmueller@imt.uni-marburg.de*

Keywords: *PPARβ/δ, ANGPTL4, ovarian carcinoma, tumor-associated macrophages, linoleic acid*

Received: *December 23, 2014* ***Accepted***: *March 29, 2015* ***Published***: *April 15, 2015*

ABSTRACT

The nuclear receptor peroxisome proliferator-activated receptor β/δ (PPARβ/δ) is a lipid ligand-inducible transcription factor associated with macrophage polarization. However, its function in tumor-associated macrophages (TAMs) has not been investigated to date. Here, we report the PPARβ/δ-regulated transcriptome and cistrome for TAMs from ovarian carcinoma patients. Comparison with monocyte-derived macrophages shows that the vast majority of direct PPARβ/δ target genes are upregulated in TAMs and largely refractory to synthetic agonists, but repressible by inverse agonists. Besides genes with metabolic functions, these include cell type-selective genes associated with immune regulation and tumor progression, e.g., *LRP5, CD300A, MAP3K8 and ANGPTL4*. This deregulation is not due to increased expression of PPARβ/δ or its enhanced recruitment to target genes. Instead, lipidomic analysis of malignancy-associated ascites revealed high concentrations of polyunsaturated fatty acids, in particular linoleic acid, acting as potent PPARβ/δ agonists in macrophages. These fatty acid ligands accumulate in lipid droplets in TAMs, thereby providing a reservoir of PPARβ/δ ligands. These observations suggest that the deregulation of PPARβ/δ target genes by ligands of the tumor microenvironment contributes to the pro-tumorigenic polarization of ovarian carcinoma TAMs. This conclusion is supported by the association of high *ANGPTL4* expression with a shorter relapse-free survival in serous ovarian carcinoma.

INTRODUCTION

Macrophages of the tumor microenvironment play a pivotal role in promoting the growth, invasion, metastazation and therapy resistance of malignant tumors, as suggested by the correlation of disease progression with macrophage density in different types of human cancer and shown in mouse tumor models [1, 2]. Under the influence of chemokines, cytokines and growth factors secreted by tumor cells and other host-derived cells, monocytes are recruited from the circulation and differentiate into tumor-associated macrophages (TAMs) that are programmed

to promote tumor progression [3-5]. Macrophages react to their microenvironment with an extreme plasticity [6], resulting in highly diverse phenotypes, with pro-inflammatory "M1" and anti-inflammatory "M2" macrophages [4] as the extremes. Macrophages can also adopt mixed-polarization phenotypes with properties of both M1 and M2 cells [6], TAMs being a prominent example [4, 5, 7, 8].

Macrophage polarization is regulated by a plethora of signaling molecules and transcriptional regulators. These include the nuclear receptor proliferator-activated receptor β/δ (PPARβ/δ), a ligand-inducible transcription factor with established functions in intermediary metabolism and immune regulation [9, 10]. The latter has been documented in several reports addressing the role of PPARβ/δ in inflammatory responses of the skin [11, 12] and the M2-like polarization of macrophages in adipose tissue and liver [13, 14]. PPARβ/δ has also been implicated in tumorigenesis in a number of studies with conflicting results [15], which may be due to divergent functions of the receptor in tumor cells and tumor-associated host cells as well as differences in the experimental models used (mouse strains, synthetic ligands).

PPARβ/δ binds to PPAR response elements (PPREs) at its target genes as a heterodimer with a retinoid X receptor (RXR), which is activated only upon interaction with an agonistic ligand (canonical regulation) [15]. These include unsaturated fatty acids [16], prostaglandin I_2 (prostacyclin) [17], 15-hydroxyeicosatetraenoic acid (15-HETE) [18] and a range of synthetic ligands, originally developed in light of the association of PPARβ/δ with metabolic diseases [15]. Genome-wide analyses have identified PPRE-mediated repression as a major mechanism of transcriptional regulation by unliganded PPARβ/δ, and showed that an agonist-mediated switch induces a subset of these genes [19]. PPRE-mediated repression is enhanced by inverse agonists, such as ST247 [20], which establish a repressor complex that apparently is different from the unliganded receptor complex [21].

PPARβ/δ can also regulate genes by interacting with specific transcription factors both in a PPRE-dependent [22] and independent fashion [23]. For example, unliganded PPARβ/δ in murine macrophages sequesters BCL6, a transcriptional repressor of inflammatory NFκB-regulated genes [23]. PPARβ/δ also modulates NFκB signaling by other mechanisms, including its interaction with the p65 subunit of NFκB [24-27].

We have recently addressed the function of PPARβ/δ in normal human macrophages by determining the global PPARβ/δ-regulated signaling network in primary monocyte-derived macrophages [28]. Besides canonically regulated genes with metabolic functions, we also identified a number of target genes with immune regulatory functions. These are type-selective and subject to either canonical regulation, such as *CD1D, CD52, CD300A, LRP5, NLRC,* or indirect repression by agonists, mainly affecting NFκB and STAT target genes. Consistent with these findings, PPARβ/δ agonists triggered hallmarks of an anti-inflammatory phenotype. However, we also identified positive regulatory effects on specific immune modulatory modules, in particular a stimulation of T-cell activation. PPARβ/δ agonists thus induce a unique macrophage activation state with strong anti-inflammatory but also specific stimulatory components, suggesting a context-dependent function of PPARβ/δ in immune regulation.

To date, transcriptome data for human TAMs has not been reported. Furthermore, the gene regulatory function of PPARβ/δ in TAMs has not been analyzed. Ovarian cancer is an excellent model to study TAMs, since these cells can be isolated in large quantities from the malignancy-associated peritoneal ascites. These ascites-derived macrophages display a mixed-polarization phenotype expressing both M1 and M2 markers [8]. Consistent with this finding, interpatient polarization differences unrelated to the M1/M2 classification scheme showed a clear association with the clinical outcome [8]. To elucidate the mechanisms underlying the pro-tumorigenic polarization of TAMs in ovarian cancer and the role of PPARβ/δ in this context we determined the PPARβ/δ-regulated transcriptome and PPARβ/δ cistrome in ovarian carcinoma TAMs in comparison to normal human monocyte-derived macrophages (MDMs).

RESULTS

Ligand-induced cellular alterations in human MDMs

$CD14^+$ cells from human serous ovarian carcinoma ascites (TAMs) rapidly adhere to cell culture dishes and assume a macrophage-like morphology. We used this experimental system to investigate the affects of the synthetic PPARβ/δ agonist L165,041 on freshly isolated TAMs in short-term culture in comparison to normal monocyte-derived macrophages (MDMs). This comparison is conceptually relevant, since TAMs, including ascites-associated macrophages, are derived from blood monocytes [29-32]. Under the experimental conditions used TAMs showed a clearly enhanced expression of *CD163* and a very low level of *MMP9* mRNA relative to MDMs (Figure 1A), which is consistent with the polarization phenotype of TAMs *in vivo* [8]. We therefore conclude that our experimental system is suitable to investigate ligand-induced changes in TAMs compared to MDMs.

We have previously described that the synthetic PPARβ/δ agonist L165,041 induces a morphology in MDMs that resembles that of IL-4 treated macrophages [28] (Figure 1B and 1C). TAMs, on the other hand,

displayed an unchanged morphology upon L165,041 treatment (Figure 1D and 1E). This observation suggests that TAMs are largely unresponsive to exogenous PPARβ/δ ligands. In order to address the mechanistic basis of this observation we performed comprehensive genome-wide studies as described below.

Impaired ligand response and upregulation of PPARβ/δ target genes in cultured ovarian carcinoma TAMs

Ascites-derived adherent macrophages showed a clear accumulation of PPARβ/δ and RXR at the upstream enhancer of the established PPARβ/δ target gene *PDK4* [19, 33] *in vivo* (Figure 2A) with a strong enrichment of both factors (30-fold relative to IgG control for PPARβ/δ; 40-fold for RXR). This is similar to the enrichment in MDMs (30- and 43-fold, respectively), but much higher compared to monocytes (4- to 5-fold, respectively). These data are therefore consistent with the definition of ascites-derived $CD14^+$ cells as TAMs rather than ascites-associated monocytes and confirm their suitability for PPARβ/δ centered genome-wide studies.

Toward this end, MDMs in normal growth medium and freshly isolated TAMs in ascites were exposed to a synthetic PPARβ/δ agonist, inverse PPARβ agonists or solvent (DMSO) for 1 day and analyzed by RNA-Seq (Table S2). The specificity of these ligands for PPARβ/δ is illustrated in Figure S1. Only a small number of genes (n = 30) were found to be induced by the agonist L165,041 in TAMs (logFC≥1; FPKM≥0.3) compared to MDMs (n = 102) with a small intersection (n = 7; Figure 2B, top; Figure 2C; Table S3). On the other hand, the number of genes downregulated by the inverse agonists ST247 or PT-S264 was considerably greater in TAMs (n = 50) relative to MDMs (n = 18) with a minor overlap (n = 8; Figure 2B, bottom; Table S3). These findings would be consistent with the presence of high concentrations of PPARβ/δ agonists in TAMs relative to MDMs.

The observation that the majority of PPARβ/δ target genes were refractory to synthetic agonists was confirmed by RT-qPCR for *PDK4 and ANGPTL4* (Figure 2D). Both genes were induced by L165,041 in MDMs >50-fold (average; blue symbols), whereas induction in TAMs cultured in ascites (orange symbols) was <10-fold (*PDK4*) or undetectable (*ANGPTL4*). When TAMs were cultured in R10 for 24 h instead of ascites, *PDK4* induction was only slightly higher (grey symbols). These findings indicate that the loss of ligand regulation in TAMs is not dependent on the continuous presence of ascites, pointing to a relatively stable alteration affecting the regulation of PPARβ/δ target genes.

We have previously identified canonical PPARβ/δ

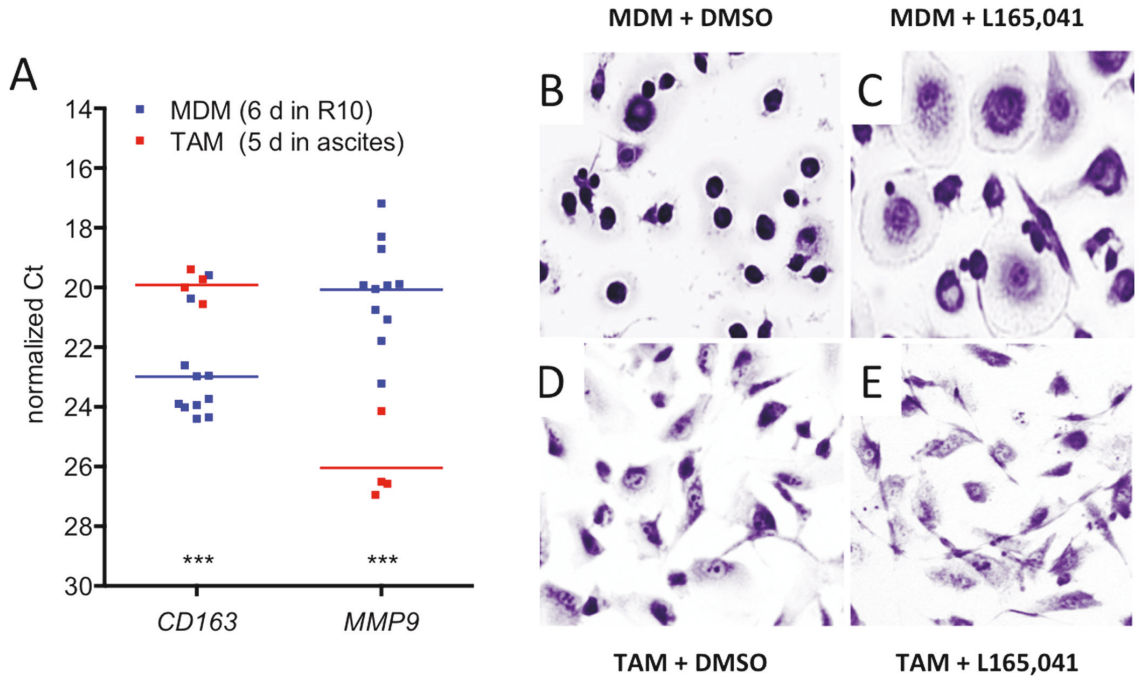

Figure 1: Effects of PPARβ/δ ligands on the morphology of human MDMs and ovarian carcinoma TAMs. A. Expression of the macrophage polarization marker genes *CD163* and *MMP9* in cultured TAMs and MDMs. The data were obtained by RT-qPCR analysis of TAMs (red data points; n = 4) and MDMs (blue: n = 11) from different donors. Horizontal lines show the medians; asterisks indicate statistical significance. **B, C.** Giemsa staining of human MDMs differentiated in XV0 medium for 8 days in the presence of the PPARβ/δ agonist L165,041 or solvent (DMSO). **D, E.** TAMs treated with agonist or DMSO as in panel B and C.

target genes in human MDMs that are agonist-induced and occupied by PPARβ/δ-RXR complexes [28]. In combination with the additional RNA-Seq data of the present study, a total of 195 ligand-regulated target genes were identified, defined as "upregulated by agonist versus inverse agonist", 95 of which were associated with PPARβ/δ enrichment sites (Figure 2E; Table S3, columns "L" and "K"). Delineation of the PPARβ/δ cistrome for 3 different patient samples in the present study (Suppl. Table S4) showed that at least 45 of these genomic loci were also occupied by PPARβ/δ in TAMs (Figure 2E; Table S3, column "J"), including those genes showing an altered ligand regulation in TAMs, exemplified by *PDK4, CPT1A, SLC25A20, CD52* and *PHACTR1* (Figure 2F).

Deregulation of PPARβ/δ target genes in ovarian carcinoma TAMs *in vivo*

We next compared the expression and ligand regulation of PPARβ/δ target genes in ascites-associated macrophages from ten different patients (Table S5) with the set of 195 ligand-regulated target genes in MDMs identified by RNA-Seq analysis of cells from 5 healthy donors (see above; Table S3). Intriguingly, a large fraction of these PPARβ/δ target genes (dark blue dots; n = 54)

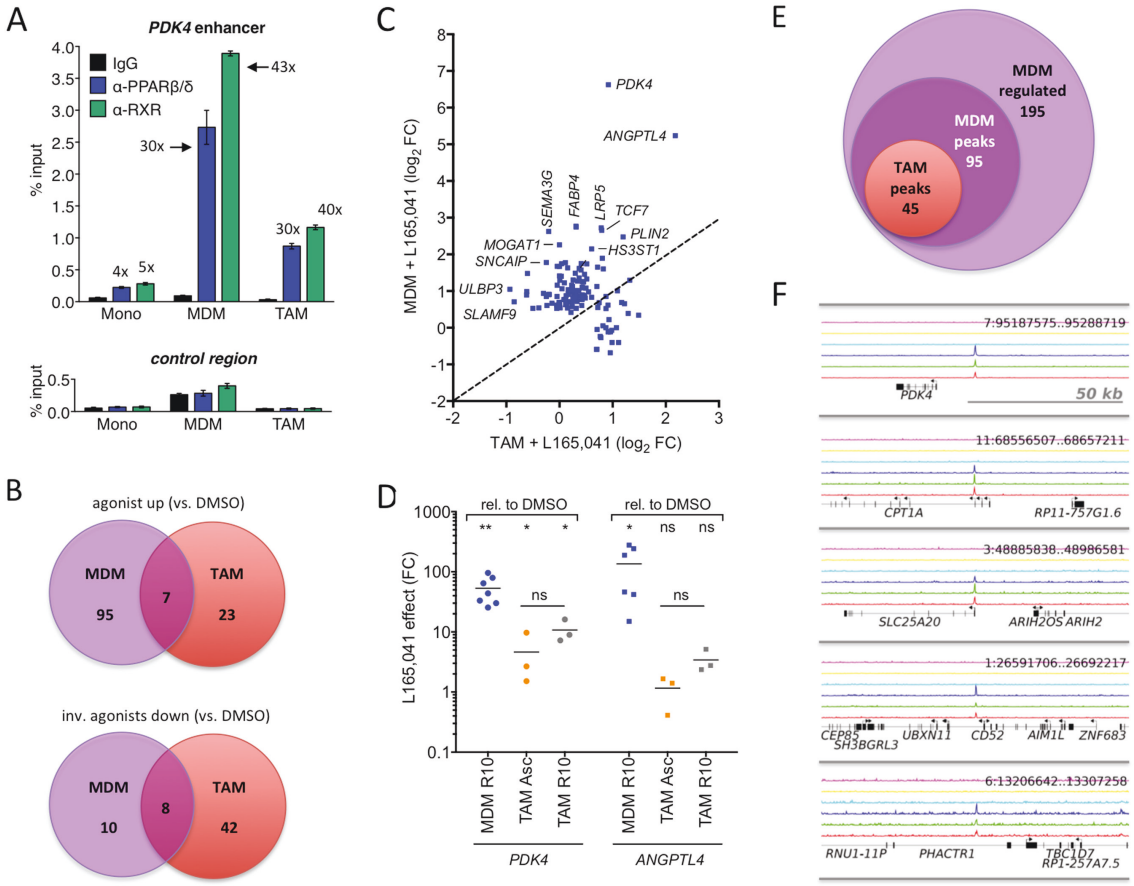

Figure 2: Deregulation of PPARβ/δ target genes in cultured ovarian carcinoma TAMs. A. PPARβ/δ and RXR enrichment at the *PDK4* enhancer and an irrelevant control region in human monocytes, MDMs and TAMs (ChIP-qPCR; sample size: 4). **B.** Venn diagrams of RNA-Seq data showing overlaps of ligand-regulated high-confidence direct target genes in MDMs grown in R10 medium or purified TAMs cultured in ascites for 1 day in the presence of agonist (L165,041), inverse agonist (ST247or PT-S264) or solvent (DMSO). **C.** Ligand response of PPARβ/δ target genes in TAMs versus MDMs. Data represents the $\log_2$ fold change (L165,041 relative to DMS0) calculated from RNA-Seq data. The diagonal line indicates equal regulation in both cell types. **D.** Expression and ligand response of *PDK4* and *ANGPTL4* by L165,041 in MDMs in R10 (n = 7) and TAMs (n = 3) cultured in either ascites or R10 medium. Cells were cultured in the presence of ligand or DMSO for 24 h and analyzed by RT-qPCR. Data are expressed as fold regulation (FC) relative to DMSO-treated cells. **E.** Overlap of genes regulated in MDMs (agonist versus inverse agonist), genomic regions with PPARβ/δ binding sites in MDMs and PPARβ/δ enrichment sites in TAMs (ChIP-Seq). **F.** PPARβ/δ enrichment (ChIP-Seq) at the *PDK4, CPT1A, SLC25A20, CD52* and *PHACTR1* loci for 3 different TAM samples (bottom 3 lines: dark blue, green, red). The top 3 lanes (magenta, yellow, light blue) represent the corresponding control IgG runs.

Table 1: PPARβ/δ target genes upregulated[1] in ovarian cancer TAMs.

Gene	Description	agonist MDM (FC)[2]	PPARβ/δ peak[3]	refractory in TAM[4]
ACADVL	acyl-CoA dehydrogenase, very long chain	3.3	+	+
ACSS3	acyl-CoA synthetase short-chain family member 3	2.3	-	+
AMOTL1	angiomotin like 1	1.9	-	+
ANGPTL4	angiopoietin-like 4	37.8	+	+
ANKRD1	ankyrin repeat domain 1 (cardiac muscle)	1.8	-	-
C19orf59	chromosome 19 open reading frame 59	6.7	+	+
C1orf162	chromosome 1 open reading frame 162	2.2	+	+
C1QC	complement component 1, q subcomponent, C chain	1.5	-	-
CABLES1	Cdk5 and Abl enzyme substrate 1	3.2	-	+
CACNB1	calcium channel, voltage-dependent, beta 1 subunit	2.4	+	+
CD300A	CD300a molecule	1.5	+	-
CLDND2	claudin domain containing 2	2.2	+	+
CPT1A	carnitine palmitoyltransferase 1A (liver)	3.4	+	+
CXorf21	chromosome X open reading frame 21	1.8	+	+
DLG4	discs, large homolog 4 (Drosophila)	1.6	+	+
FAM3B	family with sequence similarity 3, member B	2.7	-	+
FCGR3A	Fc fragment of IgG, low affinity IIIa, receptor (CD16a)	1.5	+	-
FCGRT	Fc fragment of IgG, receptor, transporter, alpha	1.5	+	-
FOS	FBJ murine osteosarcoma viral oncogene homolog	1.1	+	-
GPA33	glycoprotein A33 (transmembrane)	1.8	-	+
HMOX1	heme oxygenase (decycling) 1	1.3	+	-
HP	haptoglobin	2.2	-	-
HPR	haptoglobin-related protein	2.6	-	-
HS3ST1	heparan sulfate (glucosamine) 3-O-sulfotransferase 1	4.4	-	+
IL27	interleukin 27	1.2	-	-
IMPA2	inositol(myo)-1(or 4)-monophosphatase 2	2.6	+	+
INF2	inverted formin, FH2 and WH2 domain containing	1.5	-	+
KBTBD11	kelch repeat and BTB (POZ) domain containing 11	1.3	-	-
KLF11	Kruppel-like factor 11	1.4	-	-
KRT4	keratin 4	1.9	-	+
LRP5	low density lipoprotein receptor-related protein 5	6.6	+	+
MACC1	metastasis associated in colon cancer 1	1.8	+	-
MAP3K8	mitogen-activated protein kinase kinase kinase 8	1.5	-	+
MEGF9	multiple EGF-like-domains 9	1.5	+	-
MS4A14	membrane-spanning 4-domains, subfam. A, member 14	1.6	-	+
MS4A7	membrane-spanning 4-domains, subfamily A, member 7	1.6	-	-

PCOLCE2	procollagen C-endopeptidase enhancer 2	1.9	-	-
PDE1B	phosphodiesterase 1B, calmodulin-dependent	2.2	-	-
PDK4	pyruvate dehydrogenase kinase 4	99.0	+	+
PHACTR1	phosphatase and actin regulator 1	3.1	+	+
PLIN2	perilipin 2	5.5	+	+
PPP1R15B	protein phosphatase 1, regulatory subunit 15B	1.6	+	-
RBP7	retinol binding protein 7, cellular	1.8	-	+
RCN3	reticulocalbin 3, EF-hand calcium binding domain	2.6	+	+
RETN	resistin	1.3	+	+
S100Z	S100 calcium binding protein Z	3.1	+	-
SIPA1L2	signal-induced proliferation-associated 1 like 2	2.1	+	+
ST14	suppression of tumorigenicity 14 (colon carcinoma)	2.4	+	+
TCF7	transcription factor 7 (T-cell specific, HMG-box)	6.3	+	+
TMEM150B	transmembrane protein 150B	1.2	+	-
TMEM37	transmembrane protein 37	1.7	+	+
TRIM14	tripartite motif containing 14	1.6	-	+
TSKS	testis-specific serine kinase substrate	0.8	+	-
VSIG10L	V-set and immunoglobulin domain containing 10 like	1.4	+	-

[1] LogFC TAMs in vivo vs MDMs > 0.7 (Figures 4A and 4B; Tables S3, S5)
[2] Ratio FPKM L165,041 / FPKM DMSO in MDMs (Figure 2B; Table S2)
[3] Peak in MDMs or TAMs: ChIP-Seq data (Figures 2E ad 2F; Table S4; Adhikary et al., 2015)
[4] Refractory to synthetic agonist in TAMs (Figure 3C; Table S3); <2.0-fold (Fig. 2D, 4A, 4C; Table S2)

were upregulated ($log_2FC \geq 0.7$) in freshly isolated TAMs relative to MDMs (Figure 3A). Approximately half of the genes upregulated in cultured TAMs (21/40) overlapped with the genes upregulated *in vivo* (Figure 3B; Table S3), thus validating the results obtained *in vitro*. Most of the genes upregulated in TAMs were also refractory to regulation by a synthetic agonist ($n = 32$; Figure 3C; Table S3), suggesting a link between upregulation and loss of ligand regulation. A summary of these data is shown in Table 1.

Comparison of the expression levels of three PPARβ/δ target genes, *PDK4, ANGPTL4* and *CPT1A* in TAMs from 12 patients and MDMs from 12 healthy donors confirmed this result (Figure 3D). As shown for *PDK4*, deregulation of gene expression in TAMs correlated with increased protein levels, which, in contrast to MDMs, were largely insensitive to ligand stimulation (Figure 3E).

Interestingly, we also found a number of PPARβ/δ target genes downregulated in TAMs relative to MDMs, for example *FABP4* and *ABCG2* (Figure 3A; cyan data points). Ovarian cancer is known to consist of a plethora of signaling mediators, including cytokines [8] and lipids (see data below). It is therefore likely that a subset of target genes is downregulated by repressive signaling pathways triggered by specific components of the ovarian cancer microenvironment, thereby preventing their potential stimulation analogous to the PPARβ/δ target genes discussed in the preceding paragraph.

The deregulation of *ANGPTL4* is of particular interest, since its secreted product has been associated with cancer cell invasion and metastasis and is present in substantial amounts in the malignancy-associated ascites of most serous ovarian carcinoma patients (Figure 3F). We therefore tested the Cancer Genome Atlas (TCGA) cohort of 506 high grade serous ovarian cancer patients [34] for a potential link of *ANGPTL4* expression to the clinical outcome of the disease. As depicted by the Kaplan-Meier plot in Figure 3G, *ANGPTL4* levels showed a significant inverse association with relapse-free survival (RFS) [p = 0.0154; hazard ratio = 1.38 (1.06-1.79); median RFS: 15.63 versus 19.8 months].

Annotation of all PPARβ/δ target genes constitutively upregulated in TAMs by Ingenuity Pathway Analysis (IPA) identified metabolism (glucose, lipid), inflammation, cell migration and survival as top functions (Figure 4A). As expected, the PPAR ligands (benzafibrate, EPA, rosiglitazone, pirinixic acid) were found among the top upstream regulators (Figure 4B). The presence of the pro-inflammatory mediator LPS in this list is consistent with the results obtained by the functional annotation analysis (inflammation).

Deregulation of PPARβ/δ target genes by soluble mediators in malignancy-associated ascites

The data in Figure 2 suggests that the unaltered occupancy of direct target genes by PPARβ/δ-RXR in conjunction with a TAM-specific mechanism activating these chromatin-bound complexes is responsible for their deregulation in TAMs. One explanation for this deregulation could be the presence of ascites-associated activators of PPARβ/δ. We addressed this question by testing the effect of cell-free ascites samples on the regulation of PPARβ/δ target genes in MDMs. Figure 5A shows a clear upregulation of the target genes *PDK4, CPT1A, ANGPTL4, LRP5 and CD300A* by two different ascites samples, which in several cases reached the level of L165,041 induction (Figure 5B; blue dots). Furthermore, induction of all 5 genes by L165,041 was severely diminished in the presence of ascites (Figure 5B; orange dots).

Therefore, we sought to investigate whether deregulation of target genes by ascites might be attributable to the activation of PPARβ/δ, and thus dependent on PPARβ/δ binding sites (PPREs) in these genes. It has previously been shown that an upstream enhancer with three contiguous PPREs mediates induction of *PDK4* by PPARβ/δ ligands [19]. A luciferase construct with a genomic 1.5 kb fragment encompassing this enhancer showed a dramatic upregulation by three

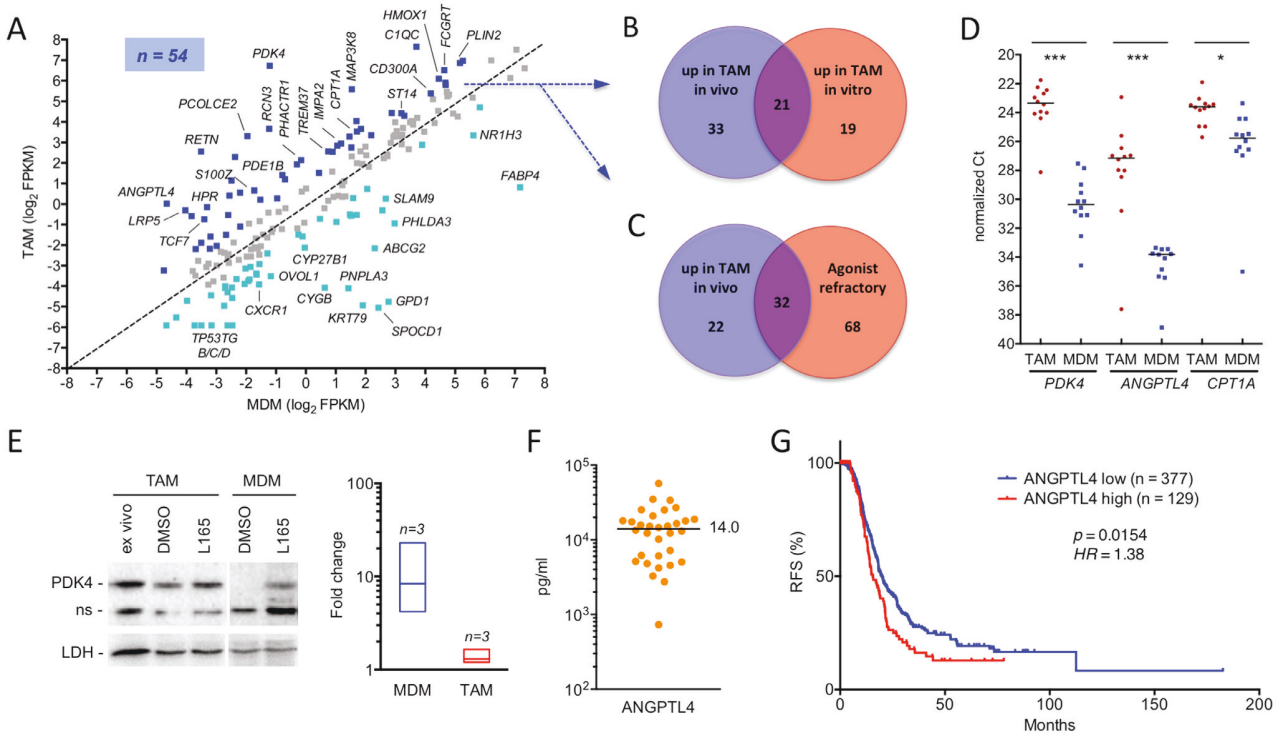

Figure 3: Deregulation of PPARβ/δ target genes in ovarian carcinoma TAMs *in vivo*. A. Expression of PPARβ/δ target genes (median FPKM values) in freshly isolated TAMs (median of 10 samples) versus MDMs (5 samples). The diagonal line indicates equal levels in both cell types. Blue dots: upregulation in TAMs ≥2-fold; cyan dots: downregulation ≥2-fold in TAMs; grey dots: no change. **B.** Overlap of PPARβ/δ target genes upregulated in freshly isolated TAMs versus MDMs (blue dots in A) and in cultured TAMs (experimental setup as in Figure 2). **C.** Overlap of PPARβ/δ target genes upregulated in TAMs versus MDMs (blue dots in A) and target genes refractory to synthetic agonists in TAMs (data from Figure 2B). **D.** RT-qPCR analysis of *PDK4, ANGPTL4* and *CPT1A* mRNA expression levels in freshly isolated TAMs and MDMs from ovarian cancer patients ($n = 12$) and healthy donors ($n = 12$), respectively. Horizontal bars indicate the median. Statistical significance was tested between the respective TAM and MDM groups. **E.** Immunoblot analysis of PDK4 protein induction by PPARβ/δ agonist in MDMs and TAMs. The figure shows representative immunoblots (including PPARβ/δ and LDH as the loading control) for both cell types and a quantitative evaluation of biological replicates with TAMs from 3 different patients and MDMs from 3 donors. Cells were exposed to ligands for 1 d in R10 medium; TAMs were also analyzed directly after isolation ("*ex vivo*"). Signal intensities were quantified and standardized to LDH. The diagram on the right depicts the induction by L165,041 (fold change) in TAMs and MDMs *in vitro*; boxes show the ranges of inducibility and the median for each group of samples. Induction values for MDMs represent estimations due to the extremely low basal level of PDK4 in MDMs. The α-PDK4 antibody was validated as shown in Figure S2. n.s., non-specific band. **F.** Concentrations of ANGPTL4 protein in the ascites of serous ovarian carcinoma patients ($n = 32$) determined by ELISA. The horizontal line indicated the median. **G.** Meier-Kaplan plot showing a correlation of high *ANGPTL4* expression with the relapse-free survival of high grade serous ovarian carcinoma patients of the TCGA cohort ($n = 377$ in *ANGPTL4* high group; $n = 129$ *ANGPTL4* low) [62].

different ascites samples (Figure 5C). These effects were clearly PPRE-dependent, since the mutation of 1, 2 or 3 sites gradually abrogated the induction of luciferase activity by ascites (Figure 5C).

We found that PPARβ/δ target genes are inducible by ascites in murine bone marrow-derived macrophages (BMDMs), similar to human MDMs. We were therefore able to show that the observed target gene deregulation was dependent on functional PPARβ/δ. Ascites upregulated the *Pdk4* and *Angptl4* genes and abrogated their induction by L165,041 in wild-type BMDMs, whereas no significant ascites effect was detected on *PDK4* in cells with disrupted *Ppard* alleles (Figure 5D). Likewise, the ascites-mediated induction of *ANGPTL4* was either absent (Asc69) or strongly reduced (Asc78) in *Ppard* null cells. These observations indicate that PPARβ/δ is responsible for the deregulation of PPARβ/δ target genes by ascites, even though a minor contribution by other PPAR subtypes cannot be unequivocally ruled out. *ANGPTL4* is induced by a plethora of signaling pathways [35], which presumably explains the residual induction by Asc78 in Ppard null cells.

Endogenous agonists present in ovarian carcinoma ascites deregulate PPARβ/δ target genes in MDMs

The results described above suggest that ovarian cancer associated ascites might contain high levels of endogenous PPARβ/δ agonists. Since all known PPARβ/δ agonists are fatty acids or fatty acid derivatives, we performed a systematic lipidomic analysis of 97 molecules in 38 different ascites samples by LC-MS/MS (Suppl. Table S6). This analysis revealed consistently very high concentrations of several polyunsaturated fatty acids (PUFAs) known as PPARβ/δ agonists [16], with the highest levels observed with linoleic acid (LA) (Figure 6A). The median concentration for LA was ~50 µg/ml (~180 µM), which is far above the described IC_{50} of 0.75 µM for PPARβ/δ binding [16]. This also applies to arachidonic acid (AA) and docosahexaenoic acid (DHA) with median ascites concentrations around 10 µg/ml (Figure 6A).

Addition of AA, LA or DHA to MDM cultures at a concentration of 20 µM for 24 h resulted in a strong induction of the *PDK4* gene, while eicosapentaenoic acid (EPA) and α-linolenic acid (ALA) had only very modest effects (Figure 6B). *PDK4* induction by LA was dose-dependent and rapid with a nearly 10-fold induction

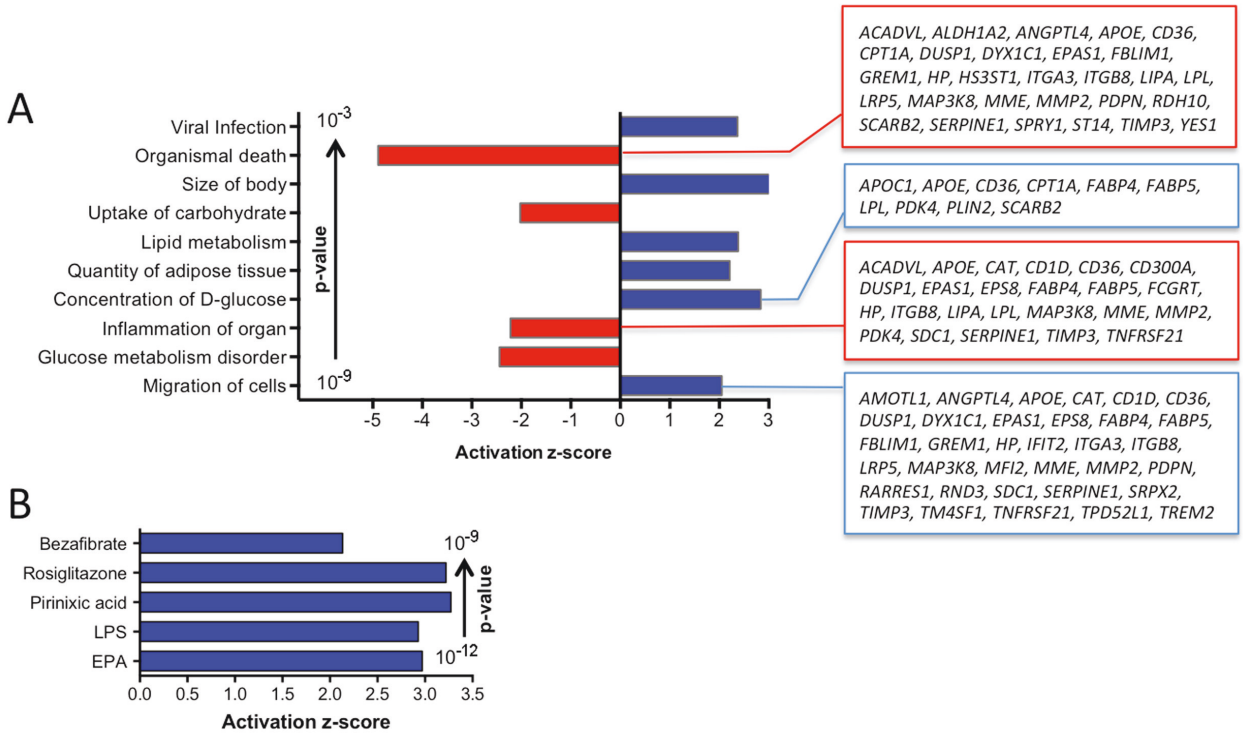

Figure 4: Pathway analyses of PPARβ/δ target genes constitutively upregulated in TAMs. A. IPA *Diseases and Functions Annotation* (functionally different clusters with lowest p-values and highest z-scores). Gene names are shown for the clusters with the largest number of genes. **B.** IPA *Upstream Regulator Analysis* (5 top regulators by p-value; z-score >2).

already after 3 h (Figure 6C). Similar results were obtained with the conjugated LAs 9(Z),11(E)LA and 10(Z),12(E) LA (Figure 6C). LA also potently induced other direct PPARβ/δ target genes, and this induction was close, or even equal, to activation by L165,041, as shown for *PDK4, CPT1A, PLIN2, SLC25A20, ANGPTL4, LRP5 and CD300A* in Figure 6D.

A number of PPARβ/δ target genes deregulated by ovarian cancer ascites have functions in oncogenesis and immune regulation. It was therefore of great interest to investigate whether their overexpression could be reverted by inverse PPARβ/δ agonists in spite of the high concentrations of agonists in ascites. As shown in Figure 6E, treatment of MDMs cultured in ascites with increasing concentrations of PT-S264 for 24 h led to progressively lower levels of *PDK4* mRNA expression. At the highest tested concentration (20 μM), expression was reduced to less than 5%. Likewise, *CPT1A, SLC25A20, LRP5* and *ANGPTL4* mRNA expression was reduced to basal levels by PT-S264, with *LRP5* and *ANGPTL4* being strongly repressed already at concentrations of 1 μM. These results clearly indicate that inverse agonists are suitable to counteract the deregulation of PPARβ/δ target genes in ovarian carcinoma TAMs.

We also found two other endogenous PPARβ/δ agonists, 15-HETE [18] and 6-keto-prostglandin $F_{1\alpha}$ (6-kPGF$_{1\alpha}$), the stable degradation product of prostacyclin [17, 36] in all ascites samples (Figure 6F). Both, 6-kPGF$_{1\alpha}$ and 15-HETE were found at median levels of ~10 ng/ml (~30 nM), which corresponds to approximately 3% of the IC_{50} concentrations required for PPARβ/δ activation [18, 36]. Both metabolites are therefore unlikely to play a role in the deregulation of PPARβ/δ target genes in TAMs.

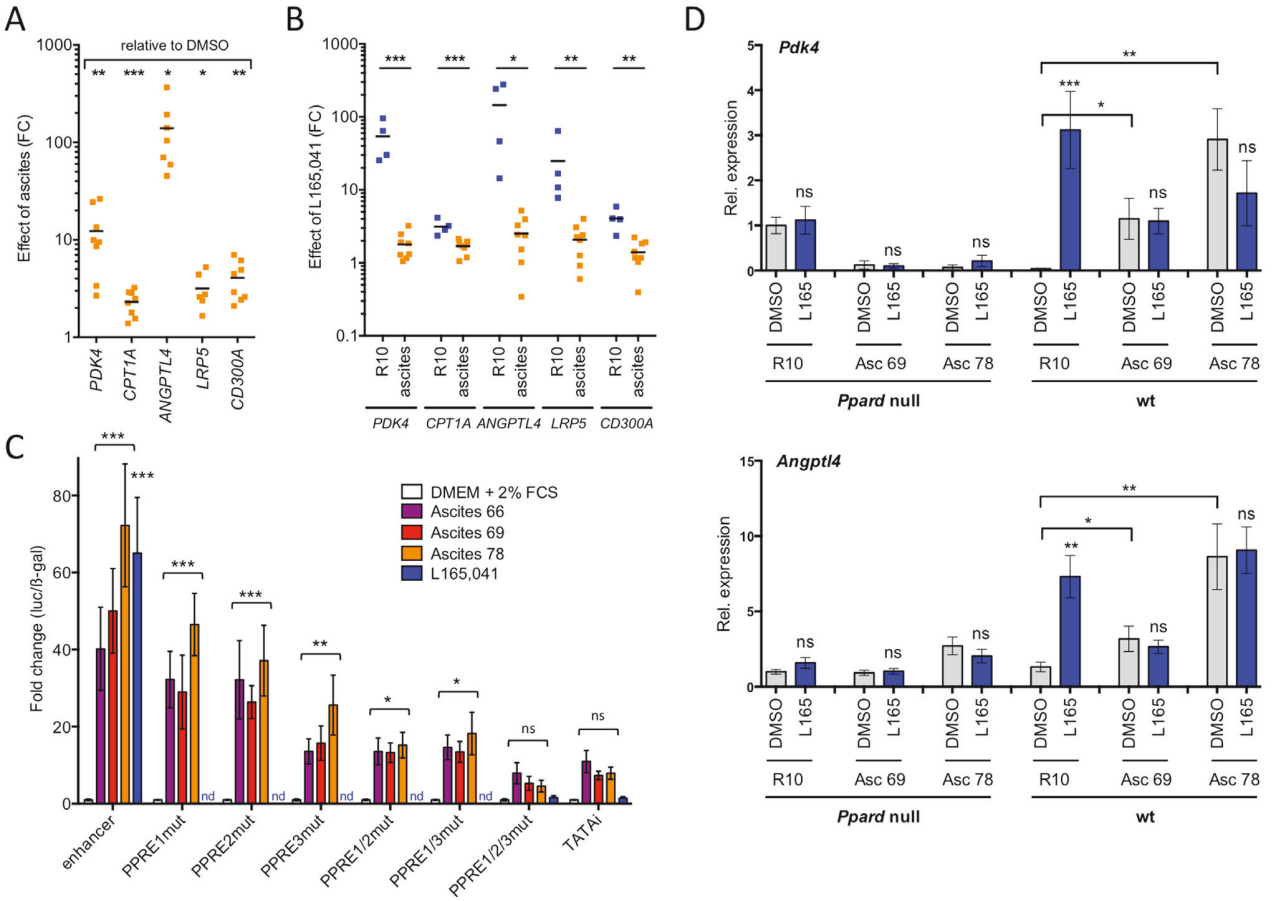

Figure 5: Ascites deregulates PPARβ/δ target genes in normal macrophages and in a PPARβ/δ-dependent fashion. **A.** Upregulation of PPARβ/δ target genes by ascites in MDMs (n = 8; 4 different MDM samples; 2 different ascites samples). RT-qPCR data are expressed as fold change (FC) relative to MDMs R10 medium. **B.** Regulation of target genes by L165,041 in MDMs (n = 4) in R10 or ascites (2 different samples). Data indicate FC relative to DMSO-treated cells. **C.** PPRE-dependent induction of a *PDK4* enhancer-luciferase construct in transiently transfected HEY cells (n = 3). Constructs were mutated in either 1, 2 or all 3 PPREs, as indicated. Data were normalized to β-galactosidase activity from a co-transfected CMV-β-gal expression vector. **D.** Response of the direct PPARβ/δ target genes *Pdk4* and *Angptl4* to two different ascites samples and L165,041 in bone marrow-derived macrophages from wild-type and *Ppard* null mice (sample size: 3 each). Statistical significance was tested for induction by ascites relative to DMSO-treated cells in C and D (asterisks/ns above square brackets) and for induction by L165,041 or in D (asterisks/ns above blue bars).

Fatty acid accumulation in lipid droplets correlates with transcriptional deregulation

The data in Figure 2D showed that ligand regulation in TAMs can only be partially restored by culturing the cells in normal cell culture medium. Since macrophages have a propensity to accumulate intracellular lipids, which is enhanced by PPARβ/δ [37], we tested this for ovarian carcinoma TAMs. As shown by staining with the fluorescent dye Nile Red, ascites-derived TAMs harbor a huge amount of lipid droplets, which remains basically unchanged upon culturing these cells in normal growth medium for 4 days (Figure 7A, 7B). The stability of lipid droplets correlated with a compromised ligand regulation of the PPARβ/δ target gene *PDK4* (Figure 7C). Consistent with this finding, MDMs rapidly accumulate lipid droplets when exposed to LA at a high level found in ascites, which persisted upon withdrawal of the fatty acids (Figure 7D, 7E), concomitantly with an impaired inducibility by synthetic ligands (Figure 7F). It is therefore likely that internalization of PUFAs from the tumor microenvironment generates a reservoir of agonists contributing to a stable upregulation of PPARβ/δ target genes.

DISCUSSION

PPARβ/δ regulates a large group of genes with functions in intermediary metabolism, inflammation and tumor progression, which are coordinately upregulated in TAMs by PUFA ligands present at high concentrations in the ascites of ovarian cancer patients (Table 1). Functional annotation analyses showed that these genes are not only associated with cell type-independent roles in energy production, fatty acid oxidation and lipid storage, but also figure in inflammation, cell migration and cell survival. Upregulation of several of these genes in TAMs is compatible with the pro-tumorigenic role of TAMs and may serve not only to skew TAM polarization but may

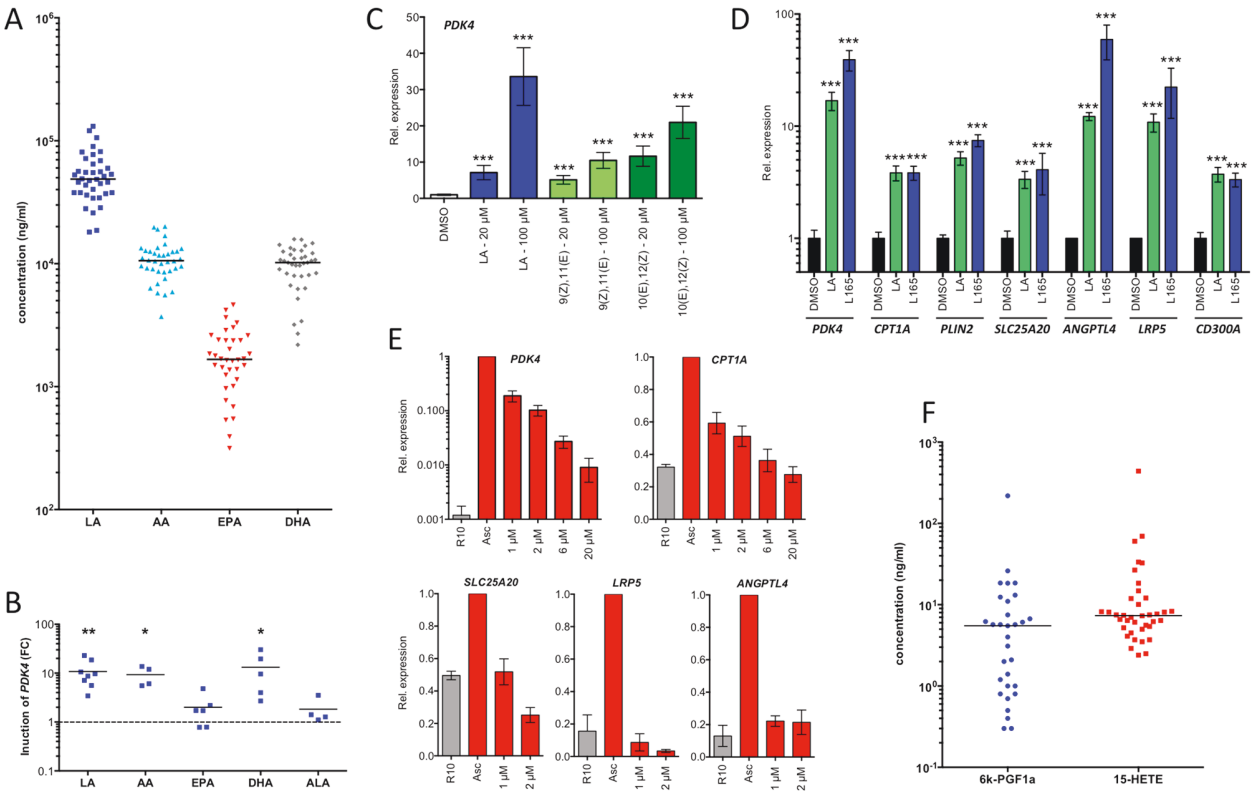

Figure 6: PPARβ/δ ligands are present in ascites at high concentrations and induce PPARβ/δ target genes. A. LC-MS/MS analysis of polyunsaturated fatty acids (PUFAs) in ascites from ovarian carcinoma patients (n = 38). **B.** Induction of *PDK4* in MDMs after 24 h exposure to different PUFAs in different donors (n = 4-8). Each data point represents a biological replicate. **C.** Rapid induction (3 h stimulus) of *PDK4* by LA and conjugated 9(Z),11(E)-LA and 10(Z),12(E)-LA in MDMs (triplicates). **D.** Induction of PPARβ/δ target genes in MDMs after 24 h exposure to linoleic acid (LA) in comparison to L165,041 (triplicates). **E.** Repression of PPARβ/δ target genes in MDMs (n = 3) cultured in ascites for 48 h by different concentrations of PT-S264 added during for the last 24 h of the experiment. Values were normalized to 1 for cells in ascites. **F.** LC-MS analysis of 15-HETE and the stable prostacyclin derivative 6k-PGF1α in the same samples as in A. Horizontal bars show the medians in panels A and B. Values represent averages of triplicate measurements ± standard deviation in all panels. Significance was tested relative to control cells.

also directly promote tumor progression, for instance via the secretion of soluble mediators, such as ANGPTL4. We therefore propose that the deregulation of PPARβ/δ target genes by mediators of the tumor environment acts in conjunction with other signaling mechanisms to effect the pro-tumorigenic conversion of host-derived monocytic cells.

Fatty acid PPARβ/δ ligands in ascites

Several PUFAs known to act as PPARβ/δ agonists were found in all ascites samples tested at levels exceeding the concentrations required for maximal PPARβ/δ activation, in particular LA, but also arachidonic acid and docosahexaenoic acid [16]. High levels of lipoprotein complexes in ovarian cancer ascites have been described in a previous study, but their fatty acid composition was not determined [38]. Another report suggests the mobilization of LA from omentum in ovarian cancer patients [39], consistent with the very high levels of this fatty acid in the malignancy-associated ascites found in the present study. Several studies also indicate that fatty acids are relevant to the biology and clinical outcome of ovarian cancer. Thus, the increased expression of the fatty acid synthase gene (*FAS*) predicts shorter survival [40], dietary fat intake and altered lipid metabolism are linked to ovarian cancer risk [41] and in a mouse model tumor growth and invasion are fueled by direct transfer of lipids from omental adipocytes to ovarian cancer with a key role for fatty acid-binding protein 4 [42].

Blood plasma also contains high concentrations of PUFAs [43], yet PPARβ/δ target genes are expressed at low levels in blood monocytes, which is presumably

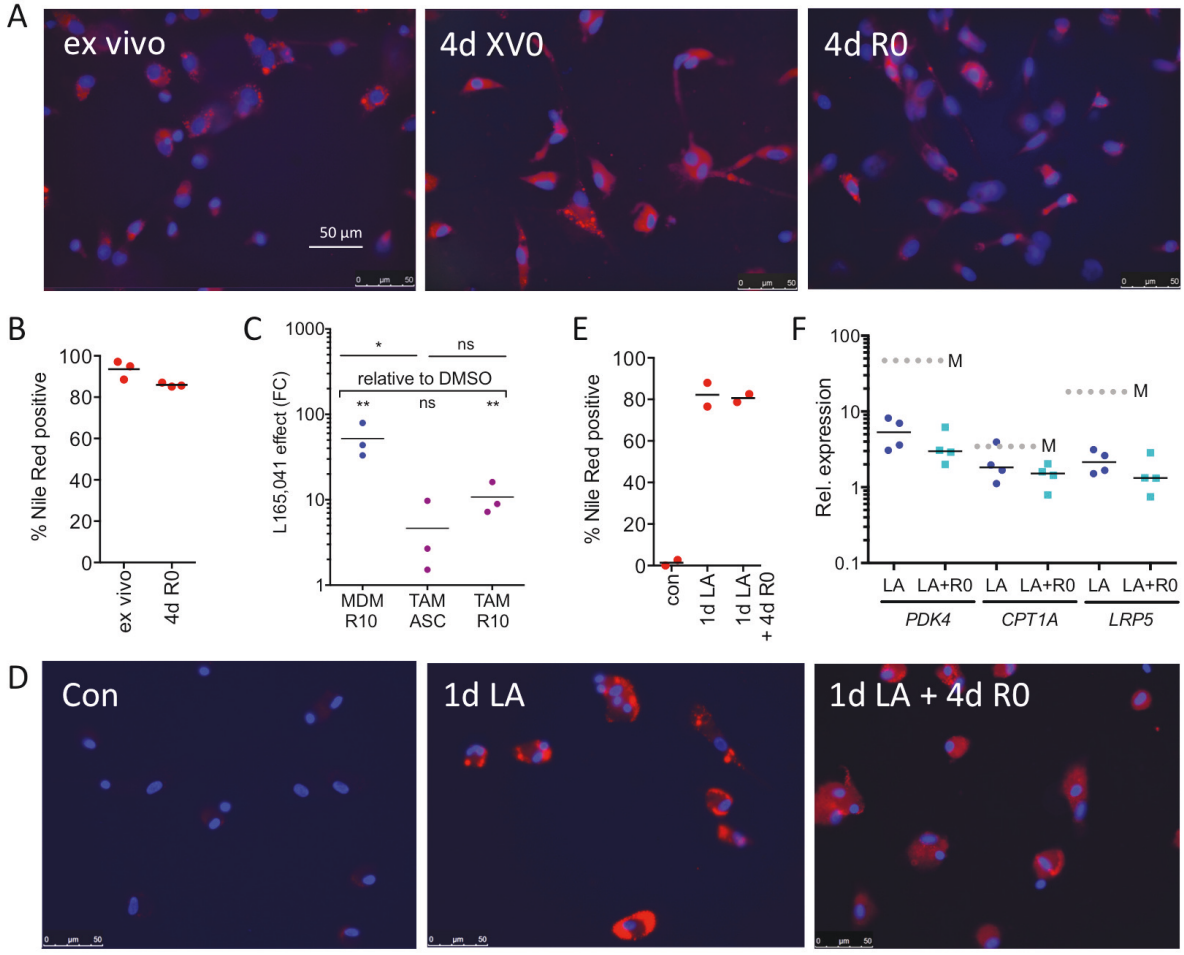

Figure 7: Association of the stable accumulation of lipid droplets in TAMs with the deregulation of the PPARβ/δ target gene *PDK4*. **A.** Staining of primary TAMs with Nile Red 0 h (*ex vivo*) and 4 d after plating in serum-free XV0 or R0 medium. **B.** Quantification of Nile Red stained TAMs ($n = 3$) treated as in A. **C.** L165,041 induction of *PDK4* in MDMs ($n = 3$) and in TAMs ($n = 3$) cultured for 4d in ascites or R10 medium. **D.** Staining of MDMs with Nile Red before (d0) and after a 24-hour exposure to LA (d1), followed by a 4d fatty acid withdrawal in serum-free R0 medium (d1+4). **E.** Quantification of Nile Red stained MDMs ($n = 2$) before and after LA exposure as in **D**. **F.** L165,041 induction of PPARβ/δ target genes in MDMs ($n = 4$) pretreated with LA for 1 d, followed by a 4d serum-free R0 medium lacking fatty acids.

due to the low level of PPARβ/δ expression in monocytes (Figure 2A and [28]), at least in part. TAMs represent a special situation in that these cells express PPARβ/δ at readily detectable levels and at the same time are exposed to high levels of ligands in the tumor microenvironment. Our findings also suggest that PPARβ/δ may serve as a marker to distinguish monocytes from macrophages, and also support the conclusion that ascites-associated $CD14^+$ cells are macrophages rather than monocytes.

Deregulated PPARβ/δ target genes in TAMs

The target gene *ANGPTL4* [44, 45] is of particular interest in the context of the present study, since it not only figures in lipid metabolism as a regulator of lipoprotein lipase, but also plays an apparently essential role in tumor progression [46]. Thus, ANGPTL4 secreted by tumor cells in response to TGF-β and released into the circulation increases the permeability of lung capillaries and facilitates the extravasation of disseminated breast cancer cells in a mouse model [35]. Furthermore, *ANGPTL4* increases cancer cell invasion [21] and is part of gene expression signatures associated with distant metastasis in human cancer patients [35, 47]. ANGPTL4 also inhibits anoikis, which is essential for the survival of circulating tumor cells [48]. Consistent with these observations, several oncogenic signaling pathways converge on the *ANGPTL4* gene, including TGFβ [21, 35, 45] and AP1 [45].

Deregulated PPARβ/δ target genes with potential roles in macrophage regulation are *CD300A* and *FOS*. CD300A is a membrane glycoprotein with anti-inflammatory functions. For example, deletion of the *Cd300a* gene in mice has been shown to result in pro-inflammatory activation of peritoneal macrophages [49], suggesting that its upregulation in TAMs has an immune suppressive effect. On the other hand, FOS has been strongly associated with the pro-inflammatory activation of macrophages [50]. These observations are compatible with a role of deregulated PPARβ/δ target genes in mediating the mixed-polarization phenotype of TAMs [4, 5, 7, 8].

Several other novel PPARβ/δ target genes upregulated in TAMs potentially play a role in promoting macrophage migration. i.e., *PHACTR1* (phosphatase and actin regulator 1), *MACC1* and *ST14*. PHACTR1 plays a role in the G-actin mediated control of actomyosin assembly [51], MACC1 is a transcriptional activator of *MET* (HGF receptor) and acts as a key regulator of cell motility [52], and ST14/epithin is a protease transcriptionally induced in macrophages by pro-inflammatory pathways to mediate transendothelial migration [53].

Another PPARβ/δ target gene upregulated in TAMs is *LRP5*. Its product LRP5 acts as a Frizzled co-receptor and activator of Wnt signaling [54]. In macrophages, LRP5 is involved in the innate inflammatory reaction to lipid infiltration by activating the Wnt pathway and promoting lipid uptake, leading to the formation of foam cells [55]. It is possible that the deregulation of LRP5 in TAMs contributes to the intracellular accumulation of fatty acids in lipid droplets observed in the present study.

Finally, the dramatic upregulation of *PDK4* probably affect energy metabolism in TAMs such that glucose catabolism is shifted towards glycolysis and lactate production (Warburg effect) [56]. This would render TAMs largely independent from the availability of oxygen, thus endowing the cells with the ability to cope with the hypoxic conditions frequently encountered in the tumor microenvironment.

Our data also show that a large number of target genes that are deregulated by ovarian cancer ascites are repressed by inverse PPARβ/δ agonists, with PT-S264 being able to suppress these genes below the basal level observed in the absence of ascites. Since several of these genes have functions in disease-associated processes as discussed above, inverse PPARβ/δ agonists may represent invaluable experimental tools to interfere with the tumor-promoting effects of the ovarian cancer microenvironment.

Expression of indirect PPARβ/δ target genes in TAMs

A large group of PPARβ/δ target genes in macrophages is repressed by PPARβ/δ agonists independent of direct DNA contacts (see Introduction). These genes are mostly associated with pro-inflammatory functions exerted by macrophages. In TAMs these inverse target genes are also frequently deregulated and refractory to synthetic ligands. However, the underlying mechanisms are complex, as indicated by the extreme variability of expression levels, ligand inducibility and ascites effects observed for different genes as well as individual patients (see Suppl. Figures S3 and S4 for examples). It is likely that the inverse target genes are highly prone to such variations, since they are regulated by multiple signaling pathways that are triggered by numerous cytokines whose concentrations are highly divergent among patients. It is obvious that these variabilities contribute to the observed heterogeneity, in many cases presumably without a significant contribution of PPARβ/δ itself. To understand the mechanistic basis of the altered transcriptome of inverse PPARβ/δ target genes in TAMs it will be necessary to perform in-depth analyses of transcription factor occupancy and epigenetic modifications at individual genes and relate this data to specific pathways and mediators.

MATERIALS AND METHODS

Ligands

L165,041 was purchased from Biozol. ST247 was synthesized as described [20, 57]. The inverse PPARβ/δ agonist PT-S264 is an optimized derivative of ST247 with improved plasma stability (Toth et al., manuscript submitted). Synthetic ligands were used at a concentration of 1 μM in all experiments unless indicated otherwise. Cells were treated for 24 h unless indicated otherwise. PUFAs were obtained from Biomol.

Mice

Ppard null and wt mice were generated by crossing floxed *Ppard* mice [58] and Sox2-Cre mice [59] as described [60]. Sox2-Cre mice were obtained from Jackson Laboratory (Bar Harbor, Maine), the floxed *Ppard* mouse strain was kindly provided by Dr. R. Evans (Salk Institute, La Jolla, CA). For genotyping the following primers were used: *Ppard* intron 3 (forward: GGC TGG GTC ACA AGA GCT ATT GTC TC), *Ppard* exon 4 (forward: GGC GTG GGG ATT TGC CTG CTT CA); *Ppard* intron 4 (reverse: GAG CCG CCT CTC GCC ATC CTT TCA G; fragment sizes: *Ppard* wt: 360 bp; *Ppard* floxed: 400 bp; *Ppard* ko: 240 bp; *Cre* (forward: CCT GGA AAA TGC TTC TGT CCG; reverse: CAG GGT GTT ATA AGC AAT CCC); fragment size: 390 bp.

Patient samples

Peripheral blood mononuclear cells (PBMCs) were obtained from healthy adult volunteers. Ascites was collected from untreated high-grade serous ovarian carcinoma patients undergoing surgery at the University Hospital Marburg. Informed consent was obtained from all patients according to the protocols approved by the institutional ethics committee.

Isolation of $CD14^+$ cells

Mononuclear cells were isolated from ascites and peripheral blood by Lymphocyte Separation Medium 1077 (PromoCell) density gradient centrifugation and purified by magnetic cell sorting (MACS) using CD14 microbeads (Miltenyi Biotech) or adherence selection on cell culture dishes for 30 min. For ChIP experiments, TAMs were purified by adherence selection. The purity of $CD14^+$ cells was > 90%. Purified TAMs and MDMs were analyzed by FACS, lysed in PeqGold (Peqlab) for RNA preparation or cultured as described below.

Cell culture and cytokine treatment of TAMs and MDMs

$CD14^+$ monocytes and TAMs were cultured either in RPMI1640 with 10% fetal bovine serum (FCS; R10 medium), serum-free RPMI1640 (R0 medium) or in serum-free macrophage X-VIVO 10 medium (XV0 medium) (Biozym Scientific). Monocyte-derived macrophages (MDMs) were differentiated from $CD14^+$ monocytes of healthy volunteers for 5-7 d at $1x10^6$ cells/ml. HEY ovarian cancer cells (ATCC) were maintained in DMEM plus 10% FCS.

Lipidomic analysis

Ascites samples (1 ml) were spiked with 100 μl deuterated internal standard and extracted using solid reverse phase extraction columns (Strata-X 33, Phenomenex). Fatty acids derivatives were eluted into 1.0 ml of methanol, lyophilized and resuspended in 100 ml of water/acetonitrile/formic acid (70:30:0.02, v/v/v; solvent A) and analyzed by LC-MS/MS on an Agilent 1290 separation system. Samples were separated on a Synergi reverse-phase C18 column (2.1×250 mm; Phenomenex) using a gradient as follows: flow rate =0.3 μl/min, 1 min (acetonitrile/isopropyl alcohol, 50:50, v/v; solvent B), 3 min (25% solvent B), 11 min (45% solvent B), 13 min (60% solvent B), 18 min (75% solvent B), 18.5 min (90% solvent B), 20 min (90% solvent B), 21 min (0% solvent). The separation system was coupled to an electrospray interface of a QTrap 5500 mass spectrometer (AB Sciex). Compounds were detected in scheduled multiple reaction monitoring mode. For quantification a 12-point calibration curve for each analyte was used. Data analysis was performed using Analyst (v1.6.1) and MultiQuant (v2.1.1) (AB Sciex).

Immunoblotting

Immunoblots were performed following standard protocols using the following antibodies: α-PPARβ/δ (sc-74517; Santa Cruz, Heidelberg, Germany), α-PDK4 (ab110336; Abcam, Cambridge, United Kingdom), α-LDH (sc-33781; Santa Cruz, Heidelberg, Germany), α-rabbit IgG HRP-linked AB and α-mouse IgG HRP-linked AB (cs7074, cs7076; Cell Signaling, NEB, Frankfurt, Germany). ChemiDoc MP system and Image Lab software version 5 (Bio-Rad, München, Germany) were used for detection and quantification.

Quantification of secreted ANGPTL4 protein

ANGPTL4 levels in ascites from ovarian cancer patients were determined by ELISA (Aviscera Bioscience,

Santa Clara, CA), according to the instructions of the manufacturer. The antibody used in this kit recognizes the bioactive C-terminal processing product (cANGPTL4).

Nile Red staining

Cells were stained for 10 minutes at 37 °C with 500 nM Nile Red (Biomol, Hamburg, Germany) in PBS and visualized using a Leica DM5000 B microscope. Nuclei were stained using Vecta Shield with DAPI (Biozol, Eching, Germany). For quantification the percentage of Nile Red positive cells was determined by counting 20 faces per donor or patient per treatment.

Luciferase reporter assay

The *PDK4* upstream enhancer region was cloned into pGL3-TATAi [61] via *Kpn*I sites using the following primers:

5'-AAAGGTACCAAATGCTGAGTTTGGGCAAC and 5'-AAAGGTACCAGCCTTGTGAGCAACCAAAG. PPREs were mutated with the following primers 5' -CAGGCTAAGTTGGTGTATGGTCAGTCCCACACC, 5'-GAAGTTTAGTAGGTGTACGGTCACTGCTGCCGA and5'-AGAGCTCACTAGGGGTATGGTCGGGGAGAC CAAG, and their respective reverse complement primers. HEY1 cells were transfected with the indicated reporter vector and pEF6/V5-His-TOPO/*lacZ* (Life Technologies) as described [18] and incubated overnight in DMEM with 2% FCS. On the next day, cells were washed with PBS and received either fresh medium with or without 1 μM L165,041 or ascites for 24 h. Lysates were prepared and measured according to the manufacturer's instructions (Beetle Juice Big and β-Gal Juice PLUS Kit for normalization; pjk GmbH) with an Orion L luminometer (Berthold).

RT-qPCR and RNA-Seq

cDNA isolation and qPCR analyses were performed as described [20]. L27 was used for normalization. Primer sequences are listed in Suppl. Table S1. RNA-Seq was carried out as described elsewhere [28]. Sequencing data were deposited at EBI ArrayExpress (accession number TAM data: E-MTAB-3167; MDM data: E-MTAB-3114 and E-MTAB-3398). Data were quantile normalized using all RNA-Seq datasets. Gene model data were retrieved from Ensembl revision 74.

Bioinformatic analysis of RNA-Seq data

We sequenced 10 TAMs samples from 10 patients directly after harvesting ("*in vivo*"), one additional TAM sample was used for ligand response experiments in autologous ascites ("*in vitro*"; L165,041, ST247 and DMSO). In addition to previously described MDM ligand response experiments from two donors [28] in R10 and X0 medium (L165,041, ST247, PT-S264, DMSO), we performed three additional sets from three donors in R10 (L165,041, PT-S264 and DMSO control). ST247 was used at a concentrations of 300 nM, all others at 1 μM.

Genes were considered for differential expression analyses only if they had an FPKM of at least 0.3 and a minimum of 50 tags in at least one sample. LogFC values for ligand experiments were calculated pairwise for individual donors. For ligand regulation in MDMs (Figure 2B) a logFC of at least 0.7 in 4 out of 5 replicates was required. Figure 2C shows median pairwise logFC data. Regulated target genes in MDMs (n = 195; Figures 2E and 3A) were defined as genes showing regulation in at least one of the following comparisons: agonist *vs* DMSO control (up regulated), inverse agonist *vs* DMSO control (down regulated) or agonist *vs* inverse agonist (up regulated). Figure 3A shows median FPKM values of 10 TAM samples and 5 MDM DMSO control samples. In Figure 3B and 3C, "up in TAM *in vivo*" is a subset of the canonical target genes that showed a 2-fold (1 logFC unit) difference between TAMs and MDMs. Table S5 was filtered based on t-tests between 10 TAM *in vitro* samples and 5 MDM DMSO samples (FDR/Benjamini-Hochberg ≤0.05). The set "up in TAM *in vitro*" is similarly defined as canonical target genes that (i) were upregulated (0.7 logFC) in TAM/DMSO compared to the two previously reported MDM/DMSO samples, and (ii) showed an at least 0.5 units higher FPKM value in the TAM sample compared to both MDM samples. Agonist refractory genes (Figure 3C) are agonist inducible genes in MDMs that showed no such regulation (same logFC threshold) or less than 50% induction (fold change) by L165,041 in TAMs relative to MDMs.

ChIP-PCR and ChIP-Seq

ChIP was performed and evaluated as described using the following antibodies: IgG pool, I5006 (Sigma Aldrich); α-PPARβ/δ, sc-7197; α-RXR, sc-774 (Santa Cruz, Heidelberg, Germany). ChIP-Seq, mapping of ChIP-Seq reads and peak calling were carried out as described [28].

Bioinformatic analysis of ChIP-Seq data

ChIP-Seq peaks were filtered for at least 30 deduplicated tags and a fold change (FC) over IgG of ≥2 (normalized total read counts). Regions were considered bound by PPARβ/δ in TAMs if they enrichment sites were observed in at least two out of three TAM samples sequenced. PPARβ/δ binding in MDMs has been described elsewhere [28]. For Figure 2E, PPARβ/δ-occupied genes

were identified as genes with a transcription start site close to, or within 50 kb of, an enrichment site. All genomic sequence and gene annotation data was retrieved from Ensembl revision 74.

Functional annotations and pathway analyses

Functional annotations and pathway analyses were performed using the Ingenuity Pathway Analysis (IPA) application and knowledge database (Qiagen Redwood City, CA, USA). Results were sorted according to p-value of overlap (minimum 0.001) and activation z-scores (≤-2.0 or ≥+2.0) Sequencing data were deposited at EBI ArrayExpress (accession number E-MTAB-3166).

Statistical analysis of experimental data

Data are presented as the average of replicates (n = 3 unless indicated otherwise) with error bars indicating standard deviations and horizontal lines in dot plots representing averages. Comparative data were statistically analyzed by Student's t-test (two-sided, equal variance) and results expressed as follows: ns, not significant ($p \geq 0.05$); *$p < 0.05$, **$p < 0.01$ or ***$p < 0.001$.

Survival-associated gene expression analysis

Associations between gene expression and relapse-free survival of ovarian cancer patients were analyzed using the web based tool "KM Plotter" (http://kmplot.com/analysis/index.php?p=service&cancer=ovar) [62] with the following settings: 'auto select best cutoff', stage: 2+3+4, histology: serous, dataset: TCGA; other settings: default). Logrank Mantel-Cox test (p-values), logrank Hazard Ratio (HR) and median survival times were calculated using the GraphPad Prism software.

ACKNOWLEDGMENTS

We are grateful to Dr. Robert Geffers (Helmholtz-Zentrum für Infektionsforschung, Braunschweig, Germany) for valuable discussions on ChIP-seq library synthesis and to Margitta Alt, Traute Plaum and Achim Allmeroth for expert technical assistance.

GRANT SUPPORT

This research was supported by research grants from the Deutsche Forschungsgemeinschaft to RM (MU601/13), the Wilhelm-Sander-Stiftung to SMB, SR and UW, the Stiftung P.E. Kempkes and the Universitätsklinikum Giessen-Marburg (UKGM Forschungsförderung) to TA, SR and UW.

CONFLICTS OF INTEREST

All authors have nothing to disclose.

Abbreviations

AA, arachidonic acid; ALA; α-linolenic acid; ANGPTL4: angiopoietin-like 4; ChIP, chromatin immune precipitation; BMDM: marrow-derived macrophage; ChIP-Seq, ChIP sequencing; D10, DMEM with 10% FCS; DHA, docosahexaenoic acid; EPA, eicosapentaenoic acid; FCS, fetal calf serum; 15-HETE, 15-hydroxyeicosatetraenoic acid; IPA: Ingenuity Pathway Analysis; 6-kPGF$_{1\alpha}$: 6-keto-prostglandin F$_{1\alpha}$; LA: linoleic acid; MDM, monocyte-derived macrophage; NFκB: nuclear factor κB; PDK4, pyruvate dehydrogenase 4; PPAR, peroxisome proliferator-activated receptor; PPARβ/δ, proliferator-activated receptor β/δ ; PPRE, PPAR response element; PUFA, polyunsaturated fatty acid; RNA-Seq, RNA sequencing; RT-qPCR, reverse transcriptase quantitative PCR; RXR, retinoid X receptor; TAM: tumor-associated macrophage; XV0: X-VIVO 10 medium without serum.

REFERENCES

1. Condeelis J and Pollard JW. Macrophages: obligate partners for tumor cell migration, invasion, and metastasis. Cell. 2006; 124:263-266.
2. Hagemann T, Biswas SK, Lawrence T, Sica A and Lewis CE. Regulation of macrophage function in tumors: the multifaceted role of NF-kappaB. Blood. 2009; 113:3139-3146.
3. Pollard JW. Tumour-educated macrophages promote tumour progression and metastasis. Nat Rev Cancer. 2004; 4:71-78.
4. Sica A and Mantovani A. Macrophage plasticity and polarization: *in vivo* veritas. J Clin Invest. 2012; 122:787-795.
5. Gabrilovich DI, Ostrand-Rosenberg S and Bronte V. Coordinated regulation of myeloid cells by tumours. Nat Rev Immunol. 2012; 12:253-268.
6. Xue J, Schmidt SV, Sander J, Draffehn A, Krebs W, Quester I, De Nardo D, Gohel TD, Emde M, Schmidleithner L, Ganesan H, Nino-Castro A, Mallmann MR, Labzin L, Theis H, Kraut M, et al. Transcriptome-based network analysis reveals a spectrum model of human macrophage activation. Immunity. 2014; 40:274-288.
7. Qian BZ and Pollard JW. Macrophage diversity enhances tumor progression and metastasis. Cell. 2010; 141:39-51.
8. Reinartz S, Schumann T, Finkernagel F, Wortmann A, Jansen JM, Meissner W, Krause M, Schworer AM, Wagner U, Muller-Brusselbach S and Muller R. Mixed-polarization phenotype of ascites-associated macrophages in human

ovarian carcinoma: Correlation of CD163 expression, cytokine levels and early relapse. Int J Cancer. 2014; 134:32-42.

9. Kostadinova R, Wahli W and Michalik L. PPARs in diseases: control mechanisms of inflammation. Curr Med Chem. 2005; 12:2995-3009.
10. Wahli W and Michalik L. PPARs at the crossroads of lipid signaling and inflammation. Trends Endocrinol Metab. 2012; 23:351-363.
11. Peters JM, Lee SS, Li W, Ward JM, Gavrilova O, Everett C, Reitman ML, Hudson LD and Gonzalez FJ. Growth, adipose, brain, and skin alterations resulting from targeted disruption of the mouse peroxisome proliferator-activated receptor beta(delta). Mol Cell Biol. 2000; 20:5119-5128.
12. Chong HC, Tan MJ, Philippe V, Tan SH, Tan CK, Ku CW, Goh YY, Wahli W, Michalik L and Tan NS. Regulation of epithelial-mesenchymal IL-1 signaling by PPARbeta/delta is essential for skin homeostasis and wound healing. J Cell Biol. 2009; 184:817-831.
13. Kang K, Reilly SM, Karabacak V, Gangl MR, Fitzgerald K, Hatano B and Lee CH. Adipocyte-derived Th2 cytokines and myeloid PPARdelta regulate macrophage polarization and insulin sensitivity. Cell Metab. 2008; 7:485-495.
14. Odegaard JI, Ricardo-Gonzalez RR, Red Eagle A, Vats D, Morel CR, Goforth MH, Subramanian V, Mukundan L, Ferrante AW and Chawla A. Alternative M2 activation of Kupffer cells by PPARdelta ameliorates obesity-induced insulin resistance. Cell Metab. 2008; 7:496-507.
15. Peters JM, Shah YM and Gonzalez FJ. The role of peroxisome proliferator-activated receptors in carcinogenesis and chemoprevention. Nat Rev Cancer. 2012; 12:181-195.
16. Xu HE, Lambert MH, Montana VG, Parks DJ, Blanchard SG, Brown PJ, Sternbach DD, Lehmann JM, Wisely GB, Willson TM, Kliewer SA and Milburn MV. Molecular recognition of fatty acids by peroxisome proliferator-activated receptors. Mol Cell. 1999; 3:397-403.
17. Lim H, Gupta RA, Ma WG, Paria BC, Moller DE, Morrow JD, DuBois RN, Trzaskos JM and Dey SK. Cyclo-oxygenase-2-derived prostacyclin mediates embryo implantation in the mouse via PPARdelta. Genes Dev. 1999; 13:1561-1574.
18. Naruhn S, Meissner W, Adhikary T, Kaddatz K, Klein T, Watzer B, Müller-Brüsselbach S and Müller R. 15-hydroxyeicosatetraenoic acid is a preferential peroxisome proliferator-activated receptor β/δ agonist. Mol Pharmacol. 2010; 77:171-184.
19. Adhikary T, Kaddatz K, Finkernagel F, Schönbauer A, Meissner W, Scharfe M, Jarek M, Blöcker H, Müller-Brüsselbach S and Müller R. Genomewide analyses define different modes of transcriptional regulation by peroxisome proliferator-activated receptor-beta/delta (PPARbeta/delta). PLoS One. 2011; 6:e16344.
20. Naruhn S, Toth PM, Adhikary T, Kaddatz K, Pape V, Dörr S, Klebe G, Müller-Brüsselbach S, Diederich WE and Müller R. High-affinity peroxisome proliferator-activated receptor beta/delta-specific ligands with pure antagonistic or inverse agonistic properties. Mol Pharmacol. 2011; 80:828-838.
21. Adhikary T, Brandt DT, Kaddatz K, Stockert J, Naruhn S, Meissner W, Finkernagel F, Obert J, Lieber S, Scharfe M, Jarek M, Toth PM, Scheer F, Diederich WE, Reinartz S, Grosse R, et al. Inverse PPARbeta/delta agonists suppress oncogenic signaling to the ANGPTL4 gene and inhibit cancer cell invasion. Oncogene. 2013; 32:5241-5252.
22. Oishi Y, Manabe I, Tobe K, Ohsugi M, Kubota T, Fujiu K, Maemura K, Kubota N, Kadowaki T and Nagai R. SUMOylation of Kruppel-like transcription factor 5 acts as a molecular switch in transcriptional programs of lipid metabolism involving PPAR-delta. Nat Med. 2008; 14:656-666.
23. Lee CH, Chawla A, Urbiztondo N, Liao D, Boisvert WA, Evans RM and Curtiss LK. Transcriptional repression of atherogenic inflammation: modulation by PPARdelta. Science. 2003; 302:453-457.
24. Planavila A, Rodriguez-Calvo R, Jove M, Michalik L, Wahli W, Laguna JC and Vazquez-Carrera M. Peroxisome proliferator-activated receptor beta/delta activation inhibits hypertrophy in neonatal rat cardiomyocytes. Cardiovasc Res. 2005; 65:832-841.
25. Westergaard M, Henningsen J, Johansen C, Rasmussen S, Svendsen ML, Jensen UB, Schroder HD, Staels B, Iversen L, Bolund L, Kragballe K and Kristiansen K. Expression and localization of peroxisome proliferator-activated receptors and nuclear factor kappaB in normal and lesional psoriatic skin. J Invest Dermatol. 2003; 121:1104-1117.
26. Ding G, Cheng L, Qin Q, Frontin S and Yang Q. PPARdelta modulates lipopolysaccharide-induced TNFalpha inflammation signaling in cultured cardiomyocytes. J Mol Cell Cardiol. 2006; 40:821-828.
27. Stockert J, Wolf A, Kaddatz K, Schnitzer E, Finkernagel F, Meissner W, Müller-Brüsselbach S, Kracht M and Müller R. Regulation of TAK1/TAB1-Mediated IL-1beta Signaling by Cytoplasmic PPARbeta/delta. PLoS One. 2013; 8:e63011.
28. Adhikary T, Wortmann A, Schumann T, Finkernagel F, Lieber S, Roth K, Toth PM, Diederich WE, Nist A, Stiewe T, Kleinesudeik L, Reinartz S, Müller-Brüsselbach S and Müller R. The transcriptional PPARβ/δ network in human macrophages defines a unique agonist-induced activation state. Nucl Acids Res. 2015:in press.
29. Yamashiro S, Takeya M, Nishi T, Kuratsu J, Yoshimura T, Ushio Y and Takahashi K. Tumor-derived monocyte chemoattractant protein-1 induces intratumoral infiltration of monocyte-derived macrophage subpopulation in transplanted rat tumors. Am J Pathol. 1994; 145:856-867.
30. Silzle T, Kreutz M, Dobler MA, Brockhoff G, Knuechel R and Kunz-Schughart LA. Tumor-associated fibroblasts recruit blood monocytes into tumor tissue. Eur J Immunol.

2003; 33:1311-1320.

31. Murdoch C, Giannoudis A and Lewis CE. Mechanisms regulating the recruitment of macrophages into hypoxic areas of tumors and other ischemic tissues. Blood. 2004; 104:2224-2234.
32. Ahmed N and Stenvers KL. Getting to Know Ovarian Cancer Ascites: Opportunities for Targeted Therapy-Based Translational Research. Front Oncol. 2013; 3:256.
33. Degenhardt T, Saramaki A, Malinen M, Rieck M, Vaisanen S, Huotari A, Herzig KH, Müller R and Carlberg C. Three Members of the Human Pyruvate Dehydrogenase Kinase Gene Family Are Direct Targets of the Peroxisome Proliferator-activated Receptor β/δ. J Mol Biol. 2007.
34. Network TCGAR. Integrated genomic analyses of ovarian carcinoma. Nature. 2011; 474:609-615.
35. Padua D, Zhang XH, Wang Q, Nadal C, Gerald WL, Gomis RR and Massague J. TGFbeta primes breast tumors for lung metastasis seeding through angiopoietin-like 4. Cell. 2008; 133:66-77.
36. Gupta RA, Tan J, Krause WF, Geraci MW, Willson TM, Dey SK and DuBois RN. Prostacyclin-mediated activation of peroxisome proliferator-activated receptor delta in colorectal cancer. Proc Natl Acad Sci U S A. 2000; 97:13275-13280.
37. Vosper H, Patel L, Graham TL, Khoudoli GA, Hill A, Macphee CH, Pinto I, Smith SA, Suckling KE, Wolf CR and Palmer CN. The peroxisome proliferator-activated receptor delta promotes lipid accumulation in human macrophages. J Biol Chem. 2001; 276:44258-44265.
38. Caselmann WH and Jungst D. Isolation and characterization of a cellular protein-lipid complex from ascites fluid caused by various neoplasms. Cancer Res. 1986; 46:1547-1552.
39. Yam D, Ben-Hur H, Dgani R, Fink A, Shani A and Berry EM. Subcutaneous, omentum and tumor fatty acid composition, and serum insulin status in patients with benign or cancerous ovarian or endometrial tumors. Do tumors preferentially utilize polyunsaturated fatty acids? Cancer Lett. 1997; 111:179-185.
40. Gansler TS, Hardman W, 3rd, Hunt DA, Schaffel S and Hennigar RA. Increased expression of fatty acid synthase (OA-519) in ovarian neoplasms predicts shorter survival. Hum Pathol. 1997; 28:686-692.
41. Tania M, Khan MA and Song Y. Association of lipid metabolism with ovarian cancer. Curr Oncol. 2010; 17:6-11.
42. Nieman KM, Kenny HA, Penicka CV, Ladanyi A, Buell-Gutbrod R, Zillhardt MR, Romero IL, Carey MS, Mills GB, Hotamisligil GS, Yamada SD, Peter ME, Gwin K and Lengyel E. Adipocytes promote ovarian cancer metastasis and provide energy for rapid tumor growth. Nat Med. 2011; 17:1498-1503.
43. Fraser DA, Thoen J, Rustan AC, Forre O and Kjeldsen-Kragh J. Changes in plasma free fatty acid concentrations in rheumatoid arthritis patients during fasting and their effects upon T-lymphocyte proliferation. Rheumatology (Oxford). 1999; 38:948-952.
44. Mandard S, Zandbergen F, van Straten E, Wahli W, Kuipers F, Muller M and Kersten S. The fasting-induced adipose factor/angiopoietin-like protein 4 is physically associated with lipoproteins and governs plasma lipid levels and adiposity. J Biol Chem. 2006; 281:934-944.
45. Kaddatz K, Adhikary T, Finkernagel F, Meissner W, Müller-Brüsselbach S and Müller R. Transcriptional profiling identifies functional interactions of TGFβ and PPARβ/δ signaling: synergistic induction of ANGPTL4 transcription. J Biol Chem. 2010; 285:29469-29479.
46. Zhu P, Goh YY, Chin HF, Kersten S and Tan NS. Angiopoietin-like 4: a decade of research. Biosci Rep. 2012; 32:211-219.
47. Hu Z, Fan C, Livasy C, He X, Oh DS, Ewend MG, Carey LA, Subramanian S, West R, Ikpatt F, Olopade OI, van de Rijn M and Perou CM. A compact VEGF signature associated with distant metastases and poor outcomes. BMC Med. 2009; 7:9.
48. Zhu P, Tan MJ, Huang RL, Tan CK, Chong HC, Pal M, Lam CR, Boukamp P, Pan JY, Tan SH, Kersten S, Li HY, Ding JL and Tan NS. Angiopoietin-like 4 Protein Elevates the Prosurvival Intracellular O(2)(-):H(2)O(2) Ratio and Confers Anoikis Resistance to Tumors. Cancer Cell. 2011; 19:401-415.
49. Tanaka T, Tahara-Hanaoka S, Nabekura T, Ikeda K, Jiang S, Tsutsumi S, Inagaki T, Magoori K, Higurashi T, Takahashi H, Tachibana K, Tsurutani Y, Raza S, Anai M, Minami T, Wada Y, et al. PPARbeta/delta activation of CD300a controls intestinal immunity. Sci Rep. 2014; 4:5412.
50. Higuchi Y, Setoguchi M, Yoshida S, Akizuki S and Yamamoto S. Enhancement of c-fos expression is associated with activated macrophages. Oncogene. 1988; 2:515-521.
51. Wiezlak M, Diring J, Abella J, Mouilleron S, Way M, McDonald NQ and Treisman R. G-actin regulates the shuttling and PP1 binding of the RPEL protein Phactr1 to control actomyosin assembly. J Cell Sci. 2012; 125:5860-5872.
52. Zhang Y, Wang Z, Chen M, Peng L, Wang X, Ma Q, Ma F and Jiang B. MicroRNA-143 targets MACC1 to inhibit cell invasion and migration in colorectal cancer. Mol Cancer. 2012; 11:23.
53. Lee D, Lee HS, Yang SJ, Jeong H, Kim DY, Lee SD, Oh JW, Park D and Kim MG. PRSS14/Epithin is induced in macrophages by the IFN-gamma/JAK/STAT pathway and mediates transendothelial migration. Biochem Biophys Res Commun. 2011; 405:644-650.
54. Tamai K, Semenov M, Kato Y, Spokony R, Liu C, Katsuyama Y, Hess F, Saint-Jeannet JP and He X. LDL-receptor-related proteins in Wnt signal transduction. Nature. 2000; 407:530-535.

55. Borrell-Pages M, Romero JC, Juan-Babot O and Badimon L. Wnt pathway activation, cell migration, and lipid uptake is regulated by low-density lipoprotein receptor-related protein 5 in human macrophages. Eur Heart J. 2011; 32:2841-2850.

56. Grassian AR, Metallo CM, Coloff JL, Stephanopoulos G and Brugge JS. Erk regulation of pyruvate dehydrogenase flux through PDK4 modulates cell proliferation. Genes Dev. 2011; 25:1716-1733.

57. Toth PM, Naruhn S, Pape VF, Dörr SM, Klebe G, Müller R and Diederich WE. Development of Improved PPARbeta/delta Inhibitors. ChemMedChem. 2012; 7:159-170.

58. Barak Y, Liao D, He W, Ong ES, Nelson MC, Olefsky JM, Boland R and Evans RM. Effects of peroxisome proliferator-activated receptor delta on placentation, adiposity, and colorectal cancer. Proc Natl Acad Sci U S A. 2002; 99:303-308.

59. Hayashi S, Lewis P, Pevny L and McMahon AP. Efficient gene modulation in mouse epiblast using a Sox2Cre transgenic mouse strain. Mech Dev. 2002; 119 Suppl 1:S97-S101.

60. Scholtysek C, Katzenbeisser J, Fu H, Uderhardt S, Ipseiz N, Stoll C, Zaiss MM, Stock M, Donhauser L, Bohm C, Kleyer A, Hess A, Engelke K, David JP, Djouad F, Tuckermann JP, et al. PPARbeta/delta governs Wnt signaling and bone turnover. Nat Med. 2013:19.

61. Jérôme V and Müller R. Tissue-specific, cell cycle-regulated chimeric transcription factors for the targeting of gene expression to tumor cells. Hum Gene Ther. 1998; 9:2653-2659.

62. Gyorffy B, Lanczky A and Szallasi Z. Implementing an online tool for genome-wide validation of survival-associated biomarkers in ovarian-cancer using microarray data from 1287 patients. Endocr Relat Cancer. 2012; 19:197-208.

The transcriptional signature of human ovarian carcinoma macrophages is associated with extracellular matrix reorganization

Florian Finkernagel[1,*], Silke Reinartz[2,*], Sonja Lieber[1,*], Till Adhikary[1], Annika Wortmann[1], Nathalie Hoffmann[1], Tim Bieringer[1], Andrea Nist[3], Thorsten Stiewe[3], Julia M. Jansen[2], Uwe Wagner[2], Sabine Müller-Brüsselbach[1], Rolf Müller[1]

[1]Institute of Molecular Biology and Tumor Research (IMT), Center for Tumor Biology and Immunology (ZTI), Philipps University, Marburg, Germany

[2]Clinic for Gynecology, Gynecological Oncology and Gynecological Endocrinology, Center for Tumor Biology and Immunology (ZTI), Philipps University, Marburg, Germany

[3]Genomics Core Facility, Center for Tumor Biology and Immunology (ZTI), Philipps University, Marburg, Germany

[*]These authors have contributed equally to this work

Correspondence to: *Rolf Müller,* ***email:*** *rmueller@imt.uni-marburg.de*

Keywords: *tumor-associated macrophages, resident peritoneal macrophages, macrophage polarization, transcriptional signature, extracellular matrix*

Received: *July 25, 2016* ***Accepted:*** *September 09, 2016* ***Published:*** *September 21, 2016*

ABSTRACT

Macrophages occur as resident cells of fetal origin or as infiltrating blood monocyte-derived cells. Despite the critical role of tumor-associated macrophages (TAMs) in tumor progression, the contribution of these developmentally and functionally distinct macrophage subsets and their alteration by the tumor microenvironment are poorly understood. We have addressed this question by comparing TAMs from human ovarian carcinoma ascites, resident peritoneal macrophages (pMPHs) and monocyte-derived macrophages (MDMs). Our study revealed striking a similarity between TAMs and pMPHs, which was considerably greater that the resemblance of TAMs and MDMs, including their transcriptomes, their inflammation-related activation state, the presence of receptors mediating immune functions and the expression of tumor-promoting mediators. Consistent with these results, TAMs phagocytized bacteria, presented peptide antigens and activated cytotoxic T cells within their pathophysiological environment. These observations support the notion that tumor-promoting properties of TAMs may reflect, at least to some extent, normal features of resident macrophages rather than functions induced by the tumor microenvironment. In spite of these surprising similarities between TAMs and pMPHs, bioinformatic analyses identified a TAM-selective signature of 30 genes that are upregulated relative to both pMPHs and MDMs. The majority of these genes is linked to extracellular matrix (ECM) remodeling, supporting a role for TAMs in cancer cell invasion and ovarian cancer progression.

INTRODUCTION

High-grade serous ovarian carcinoma (HGSC) is the most common ovarian malignancy with a dire prognosis with an overall 5-year survival rate of <40% [1]. The features that contribute to the fatal nature of ovarian HGSC and distinguish this cancer from other human malignancies include the peritoneal environment, which is frequently formed by the effusion building up in the peritoneal cavity. This malignancy associated ascites is rich in tumor-promoting soluble factors [2] and immune cells, in particular tumor-associated T cells (TATs) [3] and tumor-associated macrophages [4, 5] (TAMs).

TAMs play a crucial role in promoting tumor cell proliferation, dissemination, chemoresistance and immune evasion, as suggested by the correlation of disease progression with macrophage density in different types of human cancer and mouse models, including ovarian

HGSC [6–8]. Although TAMs can be derived from recruited blood monocytes [9–11], more recent evidence clearly points to a substantial contribution by tissue-resident macrophages [12–18].

A hallmark of macrophages is their plasticity in response to their microenvironment [19], with "M1" and "M2" macrophages as operationally defined extremes [20]. Classical M1 activation confers immune stimulatory, pro-inflammatory properties, while alternatively activated M2 macrophages comprise a wide spectrum of subtypes with functions in tissue repair, angiogenesis and immune regulation. TAMs have been proposed to resemble "M2" macrophages, in agreement with their role in tumor promotion and immune suppression. Consistent with this conclusion, expression of the classical M2 marker CD163 on TAMs showed a strong correlation with early relapse of serous ovarian carcinoma after first-line therapy [4]. Furthermore, data derived from mouse models showed that pro-inflammatory signaling pathways are defective in TAMs [7, 20–23]. However, macrophages can also adopt properties of both M1 and M2 cells [19], and several studies suggest that TAMs represent such a mixed-polarization phenotype [4, 11, 20, 24].

Macrophages in the adult mouse can have two developmentally different origins. While infiltrating macrophages are derived from blood monocytes produced by the bone marrow, tissue macrophages, including alveolar, peritoneal, splenic, hepatic (Kupfer cells) and dermal (Langerhans cells) macrophages, are of fetal (yolk sac) origin [17, 25–30]. The transcription factor MYB is essential for the development of murine bone-marrow macrophages [25], whereas GATA6 is indispensable for the fetal lineage and distinguishes resident from infiltrating macrophage [26, 31]. Whether ovarian cancer ascites-associated macrophages are derived from infiltrating monocytes, resident peritoneal macrophages or both is unclear.

Our current view of the tumor-mediated activation state of macrophages is largely based on studies comparing TAMs to monocyte-derived macrophages (MDMs) [9, 32]. Systematic analyses comparing TAMs to normal, uncultured macrophages are currently not available. The present study reveals for the first time a surprising similarity between TAMs and resident peritoneal macrophages (pMPHs) with respect to both their differentiation and polarization state, but also delineates a TAM-selective signature associated that is associated with extracellular matrix remodeling.

RESULTS

Similar expression of differentiation and activation markers by TAMs and pMPHs

We first compared pMPHs from patients undergoing hysterectomy for non-malignant diseases and TAMs from ovarian cancer ascites (Supplementary Table S1) for expression of inflammation and activation markers by flow cytometry. The data in Figure 1A and 1B show that surface expression of the Fcγ receptors CD16 (FCGR3), CD32 (FCGR2) and CD64 (FCGR1) was similar for both cell types, with respect to both the fraction of positive cells (Figure 1A) and the mean fluorescence intensity (MFI; Figure 1B). HLA-DR was expressed on >95% of all cells analyzed, but the measured MFI was clearly higher on MPHs (Figure 1B). The "M2" markers CD163, CD206 and intracellular IL-10 were similarly expressed by both TAMs and pMPHs, except for a tendency towards a higher fraction of $CD163^+$ and $CD206^+$ in MPH samples (Figure 1B). Our data also indicate that neither CD163 nor CD206 distinguishes TAMs from pMPHs, regardless of the underlying non-malignant condition of the patients (Figure 1C). Consistent with our observation, human pMPHs have previously been shown to express high levels of CD163 and display characteristics of anti-inflammatory macrophages [33]. Thus, while there are detectable differences between TAMs and pMPHs, both cell types do not differ in terms of a directional inflammation-related polarization switch.

To identify differences between TAMs and pMPHs by a systematic approach we compared the transcriptome of 17 TAM, 4 pMPH and 3 of non-polarized (M0) MDM samples by RNA sequencing (all RNA-Seq data in Supplementary Dataset S1; TAM and pMPH samples were uncultured primary cells). Pearson correlation of median gene expression values showed a high similarity of all TAM and pMPH transcriptomes (r = 0.93), while MDM were considerably more divergent (r = 0.79; Supplementary Figure S1). Pearson correlation analysis for individual samples yielded a similar result (median r = 0.84 for TAMs versus pMPHs; r = 0.74 for TAMs versus MDMs; Figure 2A, 2B). These results were confirmed by PCA which split our samples in two groups: TAM/pMPH and MDM (Figure 2C). As expected the correlation between TAMs and TATs or tumor cells was very low (r = 0.34; Figure 2B).

Consistent with the global resemblance of TAMs and pMPHs, at least 3 markers selectively expressed in resident macrophages in the mouse [26–29, 31, 34–36], i.e., *ADGRE1* (F4/80), *GATA6* and *TIMD4,* were expressed at similar levels in both TAMs and pMPHs, but much lower, if at all, in MDMs (Figure 3A). The opposite scenario was observed for *CD52*, reported to be preferentially expressed in monocyte-derived cells [37]. In agreement with these data, TIMD4 surface expression was stronger on TAMs compared to MDMs (Figure 1D), whereas CD52 was higher on MDMs (Figure 1E).

The RNA-Seq data also revealed similar expression levels in TAMs and MPHs for all markers of macrophage functions tested, including phagocytosis-associated receptor genes *(CD36, MSR1, SCAR* family genes, *TIMD4, CD163), FCGR* genes, complement receptor genes (*CD93/C1Q-R1, C3AR, CR1, C5AR1*) and all polarization marker genes tested, including *CD163* and *IL10* (Figure 3A).

These observations are in perfect agreement with the flow cytometry analysis described above (Figure 1A–1C). Similar observations were made for genes encoding pro-tumorigenic cytokines or growth factor (Figure 3B), previously found to be mainly expressed by TAMs within the ovarian cancer microenvironment [38]. These results indicate that ovarian carcinoma ascites-associated TAMs closely resemble pMPHs not only with respect to their activation state but also with regard to some of their pro-tumorigenic functions.

Immune functions of TAMs

The similarity with pMPHs described above suggested that macrophage-mediated immune functions might be preserved in ovarian carcinoma TAMs, at least to some extent. While TAMs can be maintained ex vivo for functional assays under conditions resembling their pathophysiological microenvironment (ascites), it is not possible to culture pMPHs under physiological conditions (e.g, peritoneal fluid). We therefore focused our analyses on short-term cultures of TAMs in ascites, and used MDMs as positive controls.

An essential function of tissue resident macrophages is the phagocytosis of pathogens and apoptotic cells [27, 33, 39–41]. Consistent with the expression pattern of phagocytosis-associated receptors (Figure 3A) the TAMs were able to efficiently phagocytize labelled *E. coli* particles (Figure 4A, 4B).

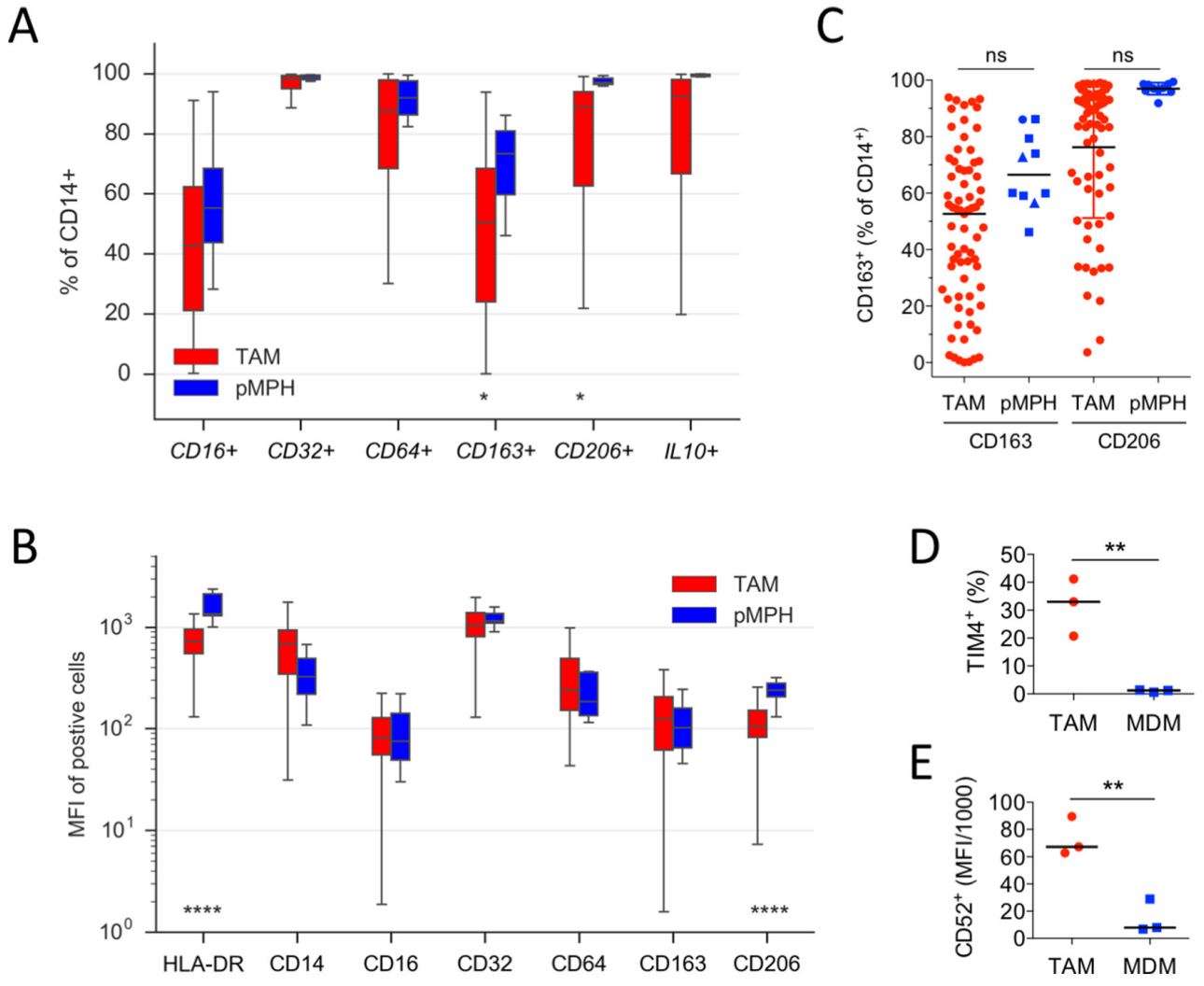

Figure 1: Similarities of TAMs and pMPHs. A, B. Flow cytometry analysis of freshly isolated TAMs and MPHs for cell surface receptor and intracellular IL-10 expression. The data show the fraction of $CD14^+$ cells (A) or the median fluorescence intensity (MFI) of positive cells (B). Sample sizes were n=71 (TAM) and n=10 (pMPH), respectively. **C.** Quantification of $CD163^+$ and $CD206^+$ cells in TAM (n=71) and pMPH (n=10) samples isolated from patients undergoing surgery for myomatosis (squares), ovarian cysts (triangles) or endometriosis (circle). **D, E.** Flow cytometry analysis of TIMD4 (% positive) and CD52 (MFI) on TAMs (n=3) and MDMs (n=3). *p<0.05; **p<0.01; ****p<0.0001 by *t*-test; ns: not significant; horizontal lines: median.

Another function reported for human pMPHs is the presentation of peptide antigens [42–46]. In view of the high expression of *HLA* genes in TAMs (Figure 1) we therefore investigated the capacity of TAMs to trigger antigen-specific cytotoxic T cell activation. For this purpose, we exposed TAMs to a mixture of antigens (CEFT) derived from pathogens most individuals have previously been sensitized to and have developed antigen-specific memory T cells. Restimulation with these recall antigens results in the activation of this subset of antigen-specific T cells (1% of all T cells). Using intracellular IFNγ production as an activation marker, we found a clear stimulation of $CD8^+$ T cells by TAMs within a range similar to the positive control (Figure 4C; non-stimulated cells served as negative controls for background substraction). Collectively, these data show that known immune functions of pMPHs are retained by TAMs in their pathophysiological environment.

Previous studies in mouse models have shown that pro-inflammatory signaling pathways are non-functional in TAMs in different tumor types [7, 20–23], and that ovarian cancer TAMs are refractory to pro-inflammatory stimuli [47]. In agreement with these observations we found that both expression of the pro-inflammatory mediator gene *IL12B* and secretion of its product p40 are not inducible by lipopolysaccharide (LPS) and interferon-γ (INFγ) in TAMs, whereas a strong induction was observed with the positive control (Figure 4D, 4E).

Genome-wide expression profiles of TAMs and pMPHs and delineation of a TAM-specific signature

We next sought to gain further insight into the specific phenotype of ovarian cancer TAMs by in-depth analysis of the transcriptomic data. Toward this end, we started out by analyzing the RNA-Seq data sets with edgeR, a Bioconductor package specifically developed for reliable gene-specific dispersion estimation in small samples by ranking genes that behave consistently across replicates more highly than genes that do not [48, 49]. The edgeR tool identified a group of 21 genes expressed at significantly different levels in TAMs versus pMPHs (Supplementary Table S1). We then searched for genes showing highly correlated expression pattern across all TAM samples ($r > 0.9$) and a higher median expression in TAMs versus pMPH or vice versa (FC >3-fold). This resulted in the definition of an extended datasets of 30 genes upregulated in TAMs (Supplementary Dataset S2; Supplementary Figure S2; Figure 5A). PCA of TAM, pMPH and MDM samples for the upregulated gene set yielded clearly separable clusters for TAMs versus pMPHs or MDMs (Figure 5A), showing that the chosen strategy was successful.

We performed similar analyses with TAMs and MDMs (Supplementary Table S2) leading to an extended datasets of 497 upregulated genes (Figure 5B). The majority of genes upregulated in TAMs versus pMPHs (20/30) were also upregulated relative to

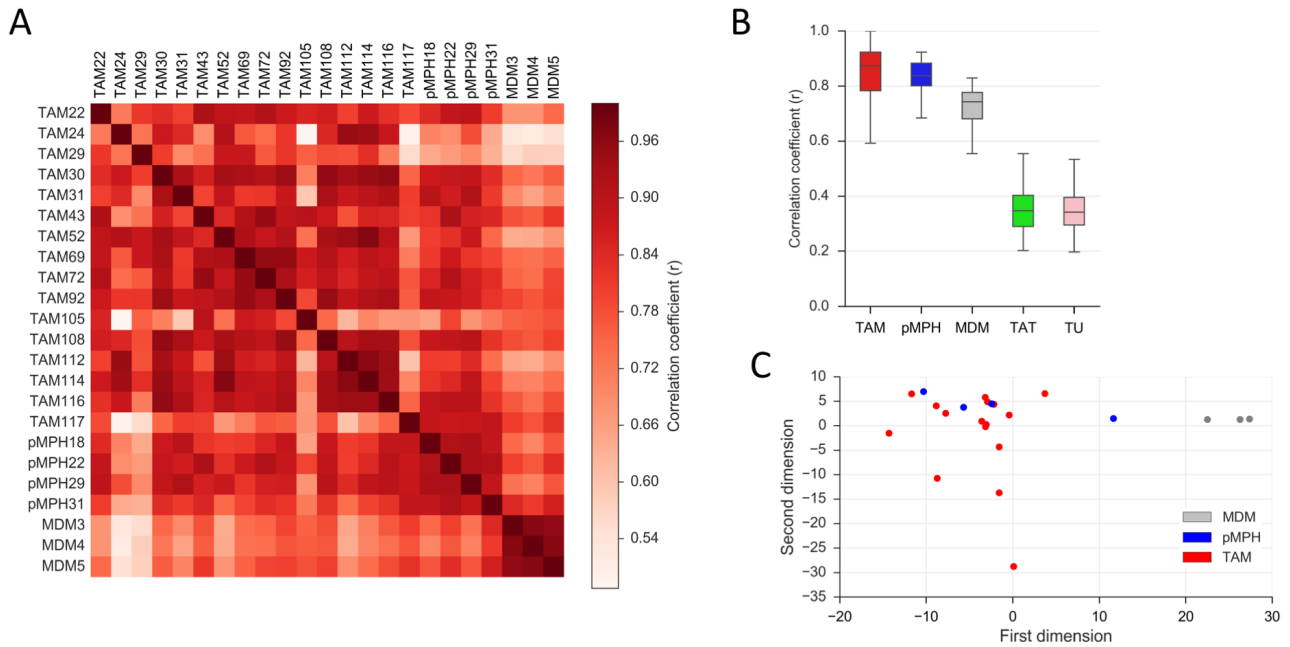

Figure 2: Similarity of TAMs and pMPH transcriptomes. A. Correlation heatmap (Pearson r) of the transcriptomes of TAM, pMPH and MDM samples. **B.** Pearson correlation (r) of the TAM transcriptome to that of pMPHs, MDMs, TATs and tumor cells (TU) for all individual samples. Bars: 95% CI; horizontal lines: median. **C.** Principle component analysis (PCA) of TAM, pMPH and MDM samples. Sample sizes were n=16 (TAM), n=4 (pMPH), n=3 (MDM), n=5 (TAT) and n=19 (TU), respectively, in all panels.

MDMs (Figure 5B), thus providing a further validation of the upregulated gene set. Since only few genes were downregulated in TAMs versus pMPHs (n = 4; Supplementary Dataset S3; Supplementary Figure S3 and Supplementary Figure S4), we focused all further analyses on the upregulated gene set.

A TAM-specific ECM gene cluster

Gene Ontology (GO) term analysis showed a very strong association of the upregulated genes with extracellular matrix (ECM) and collagen fibril organization (Figure 5C; Supplementary Table S3). IPA Upstream Regulator Analysis identified these genes as targets mainly of TGFB and pro-inflammatory (LPS, TNF, INFG) signaling pathways (Figure 5D). This is intriguing in light of previous studies reporting the presence of TNFα and TGFβ1 in the ascites of the vast majority of ovarian cancer patients and their association with disease progression [2, 4, 50–53]. Hierarchial clustering using correlation as distance metric identified a group of 19 co-regulated genes, which make up 63% of all upregulated genes identified (Figures 5E and Supplementary Figure S2). Intriguingly, this cluster harbors virtually all regulated genes associated with ECM remodeling. We subsequently refer to these genes as the "ECM cluster".

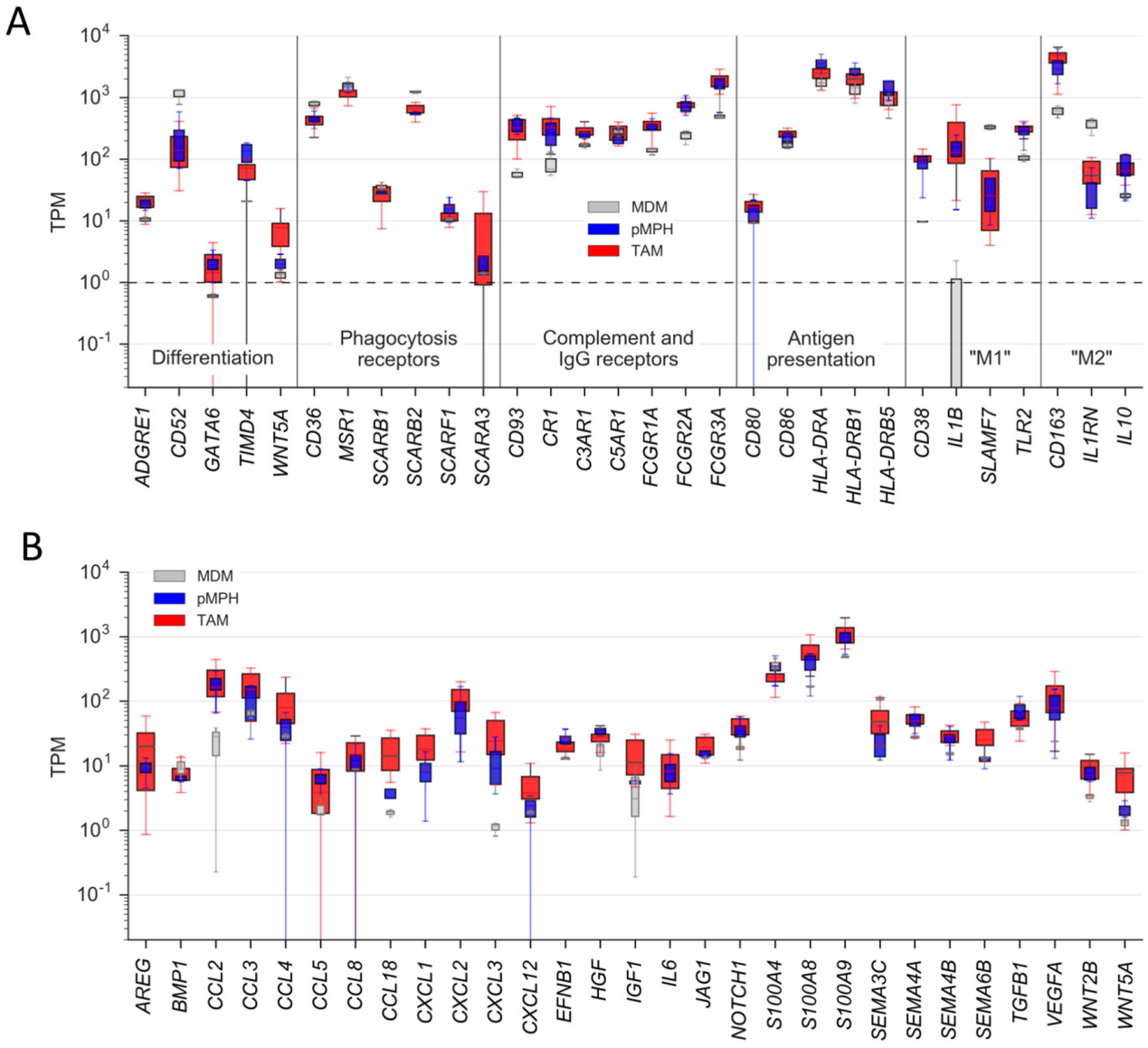

Figure 3: Expression of genes coding for proteins with immune or pro-tumorigenic functions by TAMs and normal macrophages. A. Expression of genes coding for differentiation markers (resident/infiltrating macrophages), immune functions or "M1/M2" polarization markers (RNA-Seq data). **B.** Expression of genes associated with pro-tumorigenic functions. Boxes show the upper and lower quartiles, whiskers the 95% confidence intervals amd horizontal lines the median. Sample sizes were n=16 (TAM), n=4 (pMPH), n=4 (MDM), respectively. *p<0.05; **p<0.01; ****p<0.0001 by *t*-test; ns: not significant.

The expression patterns of the ECM signature genes in TAMs and pMPHs shown in Figure 6A (red versus blue bars) clearly document their selective upregulation in TAMs. Similar results were obtained when expression in TAMs was compared to MDMs (red versus grey bars in Figure 6A) with only few exceptions, providing further evidence tor the robustness of the ECM signature and its association with tumor-triggered events. Comparison with tumor cells and TATs showed that most of these genes are mainly expressed by TAMs and tumor cells (Figure 6B). We also analyzed several genes of the ECM signature by RT-qPCR and could fully verify the RNA-Seq data in all for cases (Figure 6C). Finally, we also found readily detectable levels of PCOLCE2 protein by ELSIA in ovarian cancer ascites (Figure 6D), supporting a potential functional relevance of the upregulated ECM signature genes.

Contamination of TAM samples with tumor cells was very low in most samples, in several cases even undetectable (Supplementary Table S4). Furthermore, none of the ECM cluster genes were expressed at substantially higher levels by tumor cells relative to TAMs (Figure 6B), thus ruling out the possibility that the expression observed in TAM samples results from residual tumor cells. Another cell type present in ascites, albeit at low numbers, are carcinoma-associated fibroblasts (CAFs) [54]. Importantly, all CAF marker genes analyzed were either expressed at similar levels in both TAMs and pMPHs (Supplementary Figure S5) and/or did not show any appreciable correlation with expression of ECM cluster genes, as exemplified for

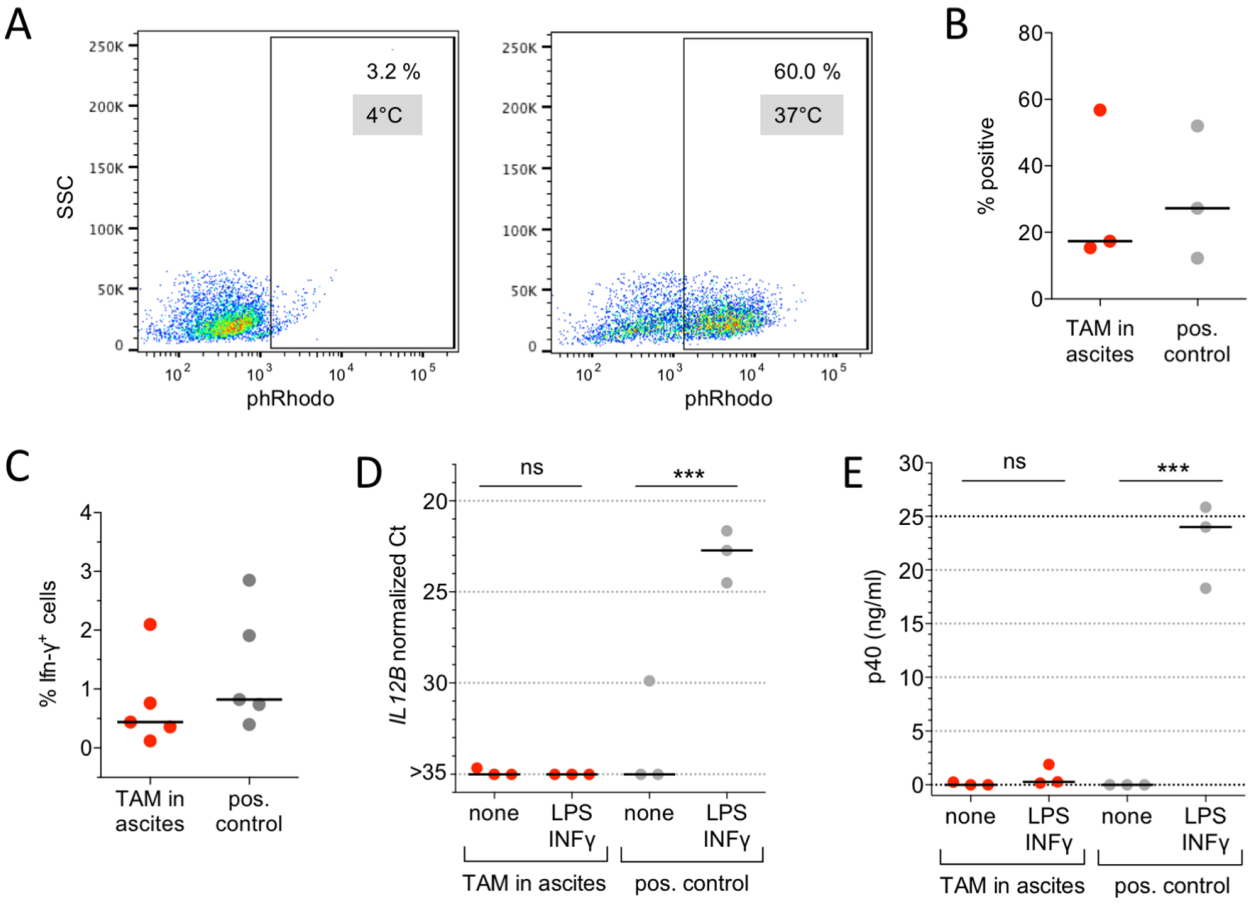

Figure 4: Immune functions of ovarian carcinoma TAMs. A. Phagocytosis of E. coli particles conjugated to a pH-sensitive fluorochrome (pHrodo) by ovarian cancer TAMs in ascites. The plots show flow cytometry analysis of cells incubated at 37°C (active phagocytosis) and 4°C (background control). **B.** Quantification of 3 independent experiments as in panel A with TAMs in ascites. MDMs in RPMI medium were included as positive control. **C.** Antigen-specific $CD8^+$ T cell stimulation. TAMs from the ascites of 5 ovarian cancer patients cultured in ascites were loaded with the recall antigen peptide mix CEFT and analyzed for their ability to stimulate INFγ production by co-cultured T cells. The fraction of $CD8^+IFN\gamma^+$ cells was determined by flow cytometry. MDMs established from 5 different donors were used as positive control. **D.** *IL12B* expression in TAMs (n=3) cultured in autologous ascites for 2 d. Cultures were stimulated with LPS (100 ng/ml) and INFγ (20 ng/ml) or solvent only (none) for 24 h and RNA was analyzed by RT-qPCR. MDMs (n=3) in RPMI were included as positive control. **E.** p40 (IL-12B/IL-23) protein concentrations in the culture medium of the experiments in panel D. Each dot represents an independent sample in B-E. Horizontal lines: median; vertical bars: range. ***p<0.001 by *t*-test between unstimulated and INFγ/LPS-stimulated cells in panels D and E; ns: not significant.

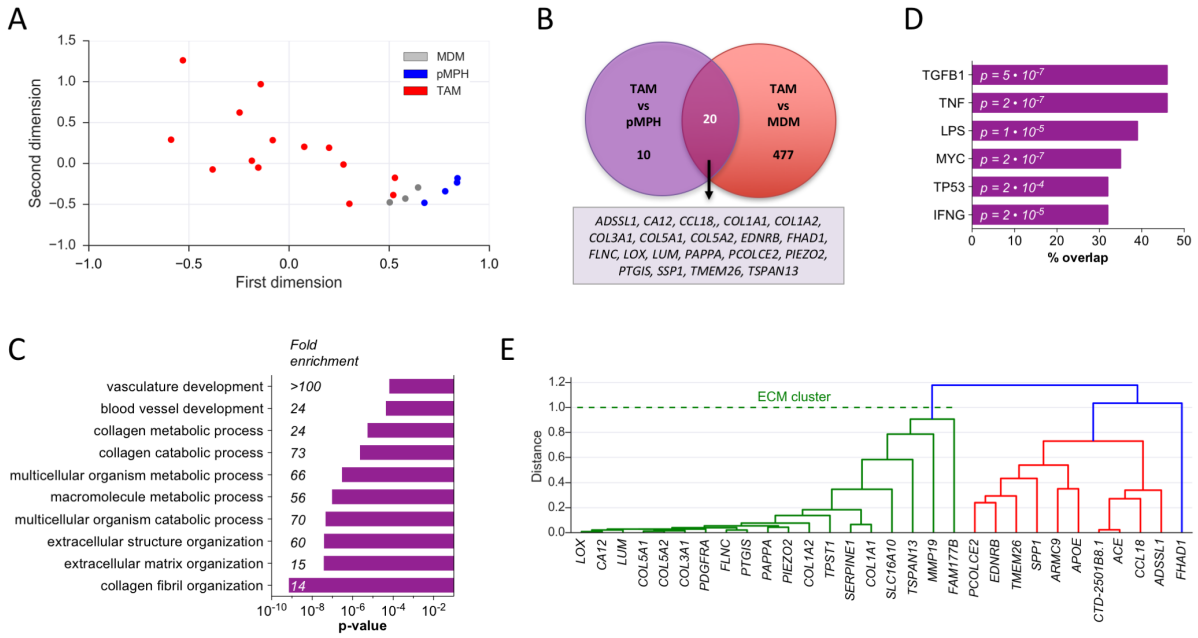

Figure 5: Identification of a transcriptional ECM signature of genes upregulated in TAMs versus normal macrophages. **A.** PCA of TAM, pMPH and MDM samples for the upregulated gene set. TAM52 (x=3.4) is outside the range displayed. **B.** Venn diagram of genes upregulated in TAMs versus pMPHs or MDMs (FC >3; TPM>1.5). **C.** Functional annotation of upregulated genes by GO term analysis (Supplementary Table S3). The bar plot shows the top 5 terms ($p < 0.001$). **D.** Upstream regulator analysis (Ingenuity pathway database) of upregulated genes with a minimum overlap of gene sets of 30% (query gene set and genes targeted by indicated pathways). **E.** Correlation-based hierarchial clustering of upregulated genes. See Materials and Methods for details.

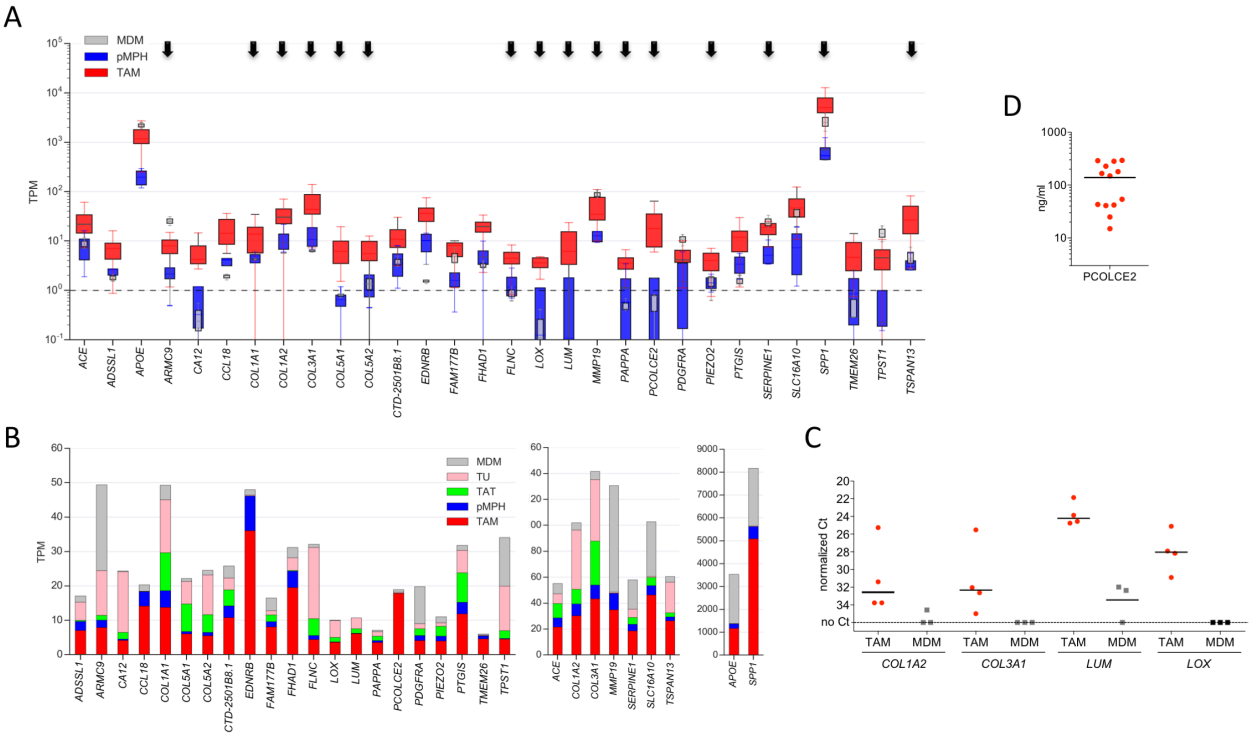

Figure 6: Expression of ECM signature genes. **A.** Expression of upregulated genes across TAM, pMPH and MDM samples. Data are represented as in Figure 2. Arrows point to genes with functions in ECM remodeling. **B.** Expression of upregulated genes (panel B) in different ovarian carcinoma-associated cell types, pMPHs and MDMs. The stacked boxes show the respective median expression values (TPM). **C.** Validation of RNA-Seq data by RT-qPCR. Each symbol represents a biological replicate (TAM: n=4; MDM: n=3). Horizontal lines: median. **D.** Concentrations of PCOLCE 2 in ascites from ovarian HGSC patients determined by ELISA (n=10).

COL3A1 in Supplementary Figure S6. Similar results were obtained for markers of mesenchymal stem cells (MSCs) and mesothelial cells (Supplementary Figure S5 and Supplementary Figure S7), known to be present ovarian cancer ascites in ascites [54]. We therefore conclude that potential contaminations of TAM samples do are unlikely to make a significant contribution to the observed TAM-specific signature.

Importantly, proteins encoded by upregulated genes are also found in the ascites fluid from ovarian cancer patients, supporting potentially relevant functions. This is exemplified in Figure 5C for PCOLCE 2 (upregulated in TAMs ~20-fold). Furthermore, previous proteomic profiling of ovarian cancer ascites identified several proteins relevant in this context, including multiple collagens and lumican [55]. In addition, collagen type I, III and IV fragments have been found at elevated levels in serum samples from ovarian cancer patients [56].

Taken together, these observations suggest that the upregulation of ECM remodeling genes is a hallmark of ovarian cancer TAMs. The coordinate regulation of the genes within this cluster is presumably caused by a tumor-triggered signaling pathway rather than merely a consequence of a genomic co-localization. The 5 *COL* genes of the ECM cluster, for instance, are localized on 4 different human chromosomes (2, 7, 9 and 17), *LUM* on chromosome 12 and *PCOLCE2* on chromosome 3 (Ensembl).

DISCUSSION

Activation state and immune functions of TAMs

Our flow cytometry and transcriptome data clearly show that markers are expressed in ovarian cancer TAMs in a way inconsistent with a directional inflammation-related polarization. On the other hand, these analyses revealed a surprisingly high similarity of TAMs and pMPHs, including their activation state and the expression of molecules with essential roles in immune functions. Thus, tissue resident macrophages, like TAMs, are characterized by a high expression of the alternative activation markers CD163 and CD206 [33]. and both TAMs and pMPHs express genes with essential functions in phagocytosis or antigen presentation at similarly high levels (Figures 1A–1C, Figure 3A).

Consistent with the high expression of scavenger receptors and other molecules involved in phagocytosis (Figure 3A), TAMs efficiently phagocytosed bacteria within their pathophysiological environment, i.e., ovarian cancer ascites (Figure 4A, 4B). TAMs share this function with pMPHs, known as major players in the clearance of pathogens and damaged cells [33]. Furthermore, in agreement with the strong expression of multiple HLA genes (Figure 3A), TAMs were able to trigger an antigen-specific cytotoxic T cell response (Figure 4C), which is also known as a function of pMPHs [42–45].

Previous work has shown that peritoneal macrophages in the mouse consist of two functionally and developmentally distinct subsets, with cells of fetal origin representing the vast majority [30]. In the mouse, these resident cells differ from infiltrating monocyte-derived macrophages by the specific expression of several markers, including *ADGRE1* (F4/80), *GATA6* and *TIMD4* [26–29, 31, 34–36]. Our data show that human pMPHs also express much higher levels of these marker genes than MDMs (Figure 1D, 1E), suggesting that these markers may also be applicable to human cells. TAMs and pMPHs showed very similar expression patterns of these markers, consistent with the hypothesis that pMPHs are a major origin of TAMs. However, it cannot be ruled out that infiltrating monocytes are converted to TAMs resembling pMPHs by tumor-borne mediators.

Previous work has identified TAMs as the major source of a number of pro-tumorigenic or immune suppressive protein mediators within the ovarian cancer microenvironment [38], The data presented here show that the corresponding genes are expressed at similar levels in TAMs and pMPHs, while their expression is lower in MDMs in most cases (Figure 2D). It is therefore likely that some pro-tumorigenic effects mediated by TAMs reflect functions of pMPHs rather than tumor-induced alterations.

Our data also confirm the previously described refractoriness of TAMs to inflammatory stimuli [7, 20–23, 47], exemplified by the unresponsiveness of the *IL12B* gene to LPS and INFγ in ovarian cancer TAMs (Figure 4D, 4E). Since pMPHs are principally inducible by pro-inflammatory stimuli (Figure 4D, E) and the induction of proinflammatory genes in MDMs is repressed by ascites (as shown for *IL12B* in Supplementary Figure S8), it is likely that the observed lack of TAMs to LPS and INFγ is caused by the tumor microenvironment. This suggests that ovarian cancer ascites affects macrophage functions to varying degrees, with phagocytosis and antigen presentation remaining intact and inflammatory responses being suppressed. The molecular mechanisms underlying this repression remain obscure, as the comparative RNA-Seq data did not provide insights into the transcriptional signaling pathways affected.

Upregulation of ECM remodeling genes in TAMs

Our study identified an ECM gene cluster as a specific feature of ovarian cancer TAMs (Figures 5 and Figure 6), suggesting that TAMs figure in collagen deposition, fibrillogenesis and ECM remodeling. In this context it is noteworthy that fibrillar collagen has been shown to enhance the invasive properties of tumor cells by accelerating their movement along these fibers and macrophages clearly enhance cancer cell invasion [6, 24].

Macrophages are also indispensable for mouse mammary gland development owing to their critical function in promoting collagen fibrillogenesis [57].

A number of published observations have linked the products of several of the ECM cluster genes to macrophage-mediated matrix remodeling and cancer cell invasion [24]. Apart from the collagens, other proteins encoded by the ECM cluster with instrumental functions in matrix deposition and remodeling include (i) lumican (LUM), which regulates collagen fibril organization and growth [58, 59], (ii) lysyl oxidase (LOX) with crucial functions in the cross-linking of ECM proteins [60] and (iii) procollagen C-endopeptidase enhancer 2 (PCOLCE2), which promotes the enzymatic cleavage of type I procollagen to yield mature structured fibrils [61, 62]. Importantly, PCOLCE2 protein was detectable at appreciable levels in the ascites of ovarian cancer patients (Figure 6D).

Clinical relevance of ECM remodelling

On the basis of our observations it is tempting to speculate that TAMs support tumor cell adherence and invasion by secreting ECM remodeling proteins. Such a scenario is indeed strongly supported by a mouse model of transcoelomic ovarian cancer dissemination, which showed a clear dependence of peritoneal colonization on macrophage-mediated effects on the ECM through metalloproteinase 9 [63]. Furthermore, other researchers showed that macrophage depletion in mice resulted in decreased ascites formation and peritoneal colonization [64–66].

Tumor cell spheroids from ovarian cancer ascites can adhere to, disintegrate and spread on ECM components [67, 68], suggesting that the macrophage-triggered reorganization of collagen deposition may promote ovarian cancer cell invasion. This result is consistent with previous observations associating ECM remodeling genes with a poor clinical course of ovarian cancer [51, 69–73]. For example, Cheon et al [69]. described a relapse-associated signature that consists of genes coding for collagen/ECM remodeling proteins. Intriguingly, this signature is regulated by TGFβ1 signaling as predicted for the ECM cluster identified in the present work (Figure 4D).

Busuttil and colleagues [71] identified a "stromal-response" signature in ovarian cancer that is associated with poor survival and enriched for genes encoding inflammatory and extracellular matrix proteins expressed by the tumor-associated stroma. Furthermore, the mesenchymal subtype of ovarian HGSC, characterized by the upregulation of ECM remodeling genes, has the worst clinical outcome of all subtypes [72, 73]. Our observations extend these findings by providing compelling evidence that genes associated with ECM restructuring are coordinately upregulated in ovarian cancer TAMs. This may explain, at least in part, the critical role of macrophages in ovarian cancer progression [4, 74].

MATERIALS AND METHODS

Patient samples

Clinical samples (Supplementary Table S5) were obtained from untreated patients undergoing surgery for ovarian carcinoma (mostly HGSC) or hysterectomy for non-malignant diseases lacking peritoneal effusions. Informed consent was obtained from all patients according to the protocols approved by the local ethics committee. All experiments were conducted in agreement with the Helsinki declaration.

Isolation and culture of primary immune cells

Macrophages were isolated from ascites (TAMs) or peritoneal lavage fluids (pMPHs) by density gradient centrifugation (Lymphocyte Separation Medium 1077; PromoCell) and subsequent enrichment on magnetic CD14 microbeads (Miltenyi Biotech). Tumor cells and $CD3^+$ T cells were isolated as described [38]. MDMs were generated from monocytes (6-day differentiation for RNA experiments, 10-day cultures for flow cytometry) from healthy donors as described [75] and in RPMI with human AB serum.

Flow cytometry analysis of macrophages

TAMs from malignant ascites or pMPHs from peritoneal lavage fluid were stained with FITC-labeled anti-CD14 (Miltenyi Biotech), APC-labeled anti-CD206 (BioLegend), APC-labeled anti-HLA-DR or APC-labeled anti-CD206 (Biozol), PE-labeled anti-CD163, PE-labeled anti-CD64, PE-Cy7-labeled anti-CD16 and APC-labeled anti-CD32 (eBioscience) as described previously [4]. Intracellular staining was performed with PE-labeled anti-IL-10 (BD Biosciences) after permeabilization for 20 min at 4 C using BD Cytofix Cytoperm Plus Fixation Permeabilization Kit (BD Biosciences). Additionally, APC-labeled anti-CD52 or APC-labeled anti-TIMD4 (Biolegend) was used for surface staining of TAMs and MDMs from healthy donors. Isotype control antibodies were from BD Biosciences, Miltenyi Biotech and eBioscience. Cells were analyzed by flow cytometry and results were calculated as percentage of positive cells and mean fluorescence intensities (MFI).

ELISA of ascites

Concentrations of PCOLCE 2 in ascites from ovarian cancer patients were determined using an ELISA Kit from Biozol according to the instructions of the manufacturer.

T cell activation

Antigen-specific T cell activation by macrophages was determined essentially as described [75]. In brief, MDMs or TAMs were loaded with 1µg/ml CEFT peptide pool (jpt Peptide Technologies, Berlin, Germany) as recall antigens and incubated with a 5-fold excess of lymphocytes for 18 h in the presence of Brefeldin A (Sigma Aldrich, Steinheim, Germany). Lymphocytes were harvested and stained with anti-CD8-APC (Miltenyi Biotec, Bergisch Gladbach, Germany) and after permeabilization with anti-IFNγ-FITC (eBioscience, Frankfurt, Germany). Flow cytometry (FACS Canto, BD Bioscience, Heidelberg, Germany) data were expressed as IFNγ+/CD8+ cells after subtracting background staining of non-stimulated controls.

Analysis of phagocytosis

Phagocytotic capacity was determined by incubating macrophages with pHrodo® Red E. coli BioParticles conjugate (Thermo Fisher) for 15 min in R10AB medium and subsequent quantification by flow cytometry.

RT-qPCR

Isolation of total RNA and RT-qPCR were carried out as described [76], using the following primers:

RPL27_fw: 5′ AAAGCTGTCATCGTGAAGAAC
RPL27_rv: 5′ GCTGTCACTTTGCGGGGGTAG
IL12B_fw: 5′ GCGAGGTTCTAAGCCATTCG
IL12B_rev: 5′ ACTCCTTGTTGTCCCCTCTG
COL1A2_fw: 5′ AGCTCCAAGGACAAGAAAC ACGTCTGG
COL1A2_rev: 5′ AGGCGCATGAAGGCAAG TTGGGTAG
COL3A1_fw: 5′ CTGGACCCCAGGGTCTTC
COL3A1_rev: 5′ CATCTGATCCAGGGTTTCCA
LOX_fw: 5′ TGGCACAGTTGTCATCAACA
LOX_rev: 5′ TCTTCAAGACAGAAACTT GCTTT
LUM_fw: 5′ TGGAGGTCAATCAACTTGAGAA
LUM_rev: 5′ CCAAACGCAAATGCTTGAT.

RNA Sequencing (RNA-Seq)

RNA-Seq was performed as described [75]. Sequencing data were deposited at EBI ArrayExpress (E-MTAB-3167, E-MTAB-3398, E-MTAB-4162, E-MTAB-4764). Genome assembly and gene model data were retrieved from Ensembl release 81, hg38. RNA-Seq data were aligned using STAR (version STAR_2.3.1z13_r470) [77]. Gene read counts were established and TPM (transcripts per million) values were calculated as published [75]. Adjustment of RNA-Seq data for contaminating tumor and T cells was performed as describe [38]. Batch effects were removed using Bioconductor tool ComBat [78, 79] after filtering all genes with a variance <1.

Identification of regulated genes

RNA-Seq data (Supplementary Dataset S1) were filtered for genes with minimum TPM values of 3 and median TPM ratios TAM/TAT >0.1 and TAM/tumor cells >0.1. For the delineation of genes selectively up- or down-regulated in TAMs we applied the Bioconductor package edgeR [48, 49] and identified a group of 21 genes expressed at significantly different levels in TAMs versus pMPHs (FDR = 0.2; Supplementary Table S1). We then used this gene set to identify additional genes showing highly correlated expression patterns across all TAM samples (r >0.9) and no overlaps of TAM and pMPH samples using the upper and lower quartiles, respectively, as thresholds. Upregulated genes were defined by 2-fold higher median TPM values in TAMs versus pMPH, or *vice versa* for down-regulated genes. This resulted in the definition of extended datasets of 30 genes upregulated and 4 genes downregulated in TAMs (Supplementary Dataset S2 and Supplementary Dataset S3). Similar analyses performed for with TAMs and MDMs (Supplementary Table S2) lead to extended datasets of 497 upregulated genes.

Statistical and bioinformatic analyses

Flow cytometry, ELISA and RT-qPCR data were statistically analyzed by Student's *t*-test (two-sided, equal variance). Results are shown as follows: *p<0.05; **p<0.01; ***p<0.001; ****p<0.0001. Quantiles, confidence intervals and correlation coefficients were calculated using the Python functions *pandas.DataFrame.boxplot ()* and *scipy.stats.pearsonr ()*, respectively. Hierarchical cluster analysis was performed using the scipy.cluster.hierarchy functions *linkage (method="weighted", metric="correlation")* and *dendrogram ()*. Gene sets were analyzed for *Upstream Regulators* using the Ingenuity Pathway Analysis (IPA) database (Qiagen Redwood City, CA, USA) as described [75]. Functional annotations were performed by gene ontology (GO) enrichment analysis (http://geneontology.org).

Abbreviations

CI, confidence interval; ELISA, enzyme-linked immunosorbent assay; HGSC, high-grade serous ovarian carcinoma; RNA-Seq, RNA sequencing; TAM, tumor-associated macrophage; TAT, tumor-associated lymphocyte; TPM: transcripts per million.

ACKNOWLEDGMENTS

We are grateful to T. Plaum, A. Allmeroth and M. Alt for expert technical assistance.

CONFLICTS OF INTEREST

All authors have nothing to disclose.

GRANT SUPPORT

This work was supported by grants from the Deutsche Forschungsgemeinschaft to S.R and R.M., the Wilhelm-Sander-Stiftung to S.M.-B., S.R. and U.W. and from UKGM to S.L. and T.A.

REFERENCES

1. Colombo N, Peiretti M, Parma G, Lapresa M, Mancari R, Carinelli S, Sessa C, Castiglione M, Group EGW. Newly diagnosed and relapsed epithelial ovarian carcinoma: ESMO Clinical Practice Guidelines for diagnosis, treatment and follow-up. Ann Oncol. 2010; 21:v23-30.
2. Kulbe H, Chakravarty P, Leinster DA, Charles KA, Kwong J, Thompson RG, Coward JI, Schioppa T, Robinson SC, Gallagher WM, Galletta L, Salako MA, Smyth JF, Hagemann T, Brennan DJ, Bowtell DD, et al. A dynamic inflammatory cytokine network in the human ovarian cancer microenvironment. Cancer Res. 2012; 72:66-75.
3. Preston CC, Goode EL, Hartmann LC, Kalli KR, Knutson KL. Immunity and immune suppression in human ovarian cancer. Immunotherapy. 2011; 3:539-556.
4. Reinartz S, Schumann T, Finkernagel F, Wortmann A, Jansen JM, Meissner W, Krause M, Schwörer AM, Wagner U, Müller-Brüsselbach S, Müller R. Mixed-polarization phenotype of ascites-associated macrophages in human ovarian carcinoma: Correlation of CD163 expression, cytokine levels and early relapse. Int J Cancer. 2014; 134:32-42.
5. Takaishi K, Komohara Y, Tashiro H, Ohtake H, Nakagawa T, Katabuchi H, Takeya M. Involvement of M2-polarized macrophages in the ascites from advanced epithelial ovarian carcinoma in tumor progression via Stat3 activation. Cancer Sci. 2010; 101:2128-2136.
6. Condeelis J, Pollard JW. Macrophages: obligate partners for tumor cell migration, invasion, and metastasis. Cell. 2006; 124:263-266.
7. Hagemann T, Biswas SK, Lawrence T, Sica A, Lewis CE. Regulation of macrophage function in tumors: the multifaceted role of NF-kappaB. Blood. 2009; 113:3139-3146.
8. Lengyel E. Ovarian cancer development and metastasis. Am J Pathol. 2010; 177:1053-1064.
9. Mantovani A, Sozzani S, Locati M, Allavena P, Sica A. Macrophage polarization: tumor-associated macrophages as a paradigm for polarized M2 mononuclear phagocytes. Trends Immunol. 2002; 23:549-555.
10. Pollard JW. Tumour-educated macrophages promote tumour progression and metastasis. Nat Rev Cancer. 2004; 4:71-78.
11. Gabrilovich DI, Ostrand-Rosenberg S, Bronte V. Coordinated regulation of myeloid cells by tumours. Nat Rev Immunol. 2012; 12:253-268.
12. Williams CB, Yeh ES, Soloff AC. Tumor-associated macrophages: unwitting accomplices in breast cancer malignancy. NPJ Breast Cancer. 2016; 2.
13. Campbell MJ, Tonlaar NY, Garwood ER, Huo D, Moore DH, Khramtsov AI, Au A, Baehner F, Chen Y, Malaka DO, Lin A, Adeyanju OO, Li S, Gong C, McGrath M, Olopade OI, et al. Proliferating macrophages associated with high grade, hormone receptor negative breast cancer and poor clinical outcome. Breast Cancer Res Treat. 2011; 128:703-711.
14. Tymoszuk P, Evens H, Marzola V, Wachowicz K, Wasmer MH, Datta S, Muller-Holzner E, Fiegl H, Bock G, van Rooijen N, Theurl I, Doppler W. In situ proliferation contributes to accumulation of tumor-associated macrophages in spontaneous mammary tumors. Eur J Immunol. 2014; 44:2247-2262.
15. Liu Y, Cao X. The origin and function of tumor-associated macrophages. Cell Mol Immunol. 2015; 12:1-4.
16. Pucci F, Venneri MA, Biziato D, Nonis A, Moi D, Sica A, Di Serio C, Naldini L, De Palma M. A distinguishing gene signature shared by tumor-infiltrating Tie2-expressing monocytes, blood "resident" monocytes, and embryonic macrophages suggests common functions and developmental relationships. Blood. 2009; 114:901-914.
17. Wynn TA, Chawla A, Pollard JW. Macrophage biology in development, homeostasis and disease. Nature. 2013; 496:445-455.
18. Franklin RA, Liao W, Sarkar A, Kim MV, Bivona MR, Liu K, Pamer EG, Li MO. The cellular and molecular origin of tumor-associated macrophages. Science. 2014; 344:921-925.
19. Xue J, Schmidt SV, Sander J, Draffehn A, Krebs W, Quester I, De Nardo D, Gohel TD, Emde M, Schmidleithner L, Ganesan H, Nino-Castro A, Mallmann MR, Labzin L, Theis H, Kraut M, et al. Transcriptome-based network analysis reveals a spectrum model of human macrophage activation. Immunity. 2014; 40:274-288.
20. Sica A, Mantovani A. Macrophage plasticity and polarization: in vivo veritas. J Clin Invest. 2012; 122:787-795.
21. Biswas SK, Gangi L, Paul S, Schioppa T, Saccani A, Sironi M, Bottazzi B, Doni A, Vincenzo B, Pasqualini F, Vago L, Nebuloni M, Mantovani A, Sica A. A distinct and unique transcriptional program expressed by tumor-associated macrophages (defective NF-kappaB and enhanced IRF-3/STAT1 activation). Blood. 2006; 107:2112-2122.
22. Saccani A, Schioppa T, Porta C, Biswas SK, Nebuloni M, Vago L, Bottazzi B, Colombo MP, Mantovani A, Sica A. p50 nuclear factor-kappaB overexpression in tumor-associated macrophages inhibits M1 inflammatory responses and antitumor resistance. Cancer Res. 2006; 66:11432-11440.

23. Hagemann T, Lawrence T, McNeish I, Charles KA, Kulbe H, Thompson RG, Robinson SC, Balkwill FR. "Re-educating" tumor-associated macrophages by targeting NF-kappaB. J Exp Med. 2008; 205:1261-1268.
24. Qian BZ, Pollard JW. Macrophage diversity enhances tumor progression and metastasis. Cell. 2010; 141:39-51.
25. Schulz C, Gomez Perdiguero E, Chorro L, Szabo-Rogers H, Cagnard N, Kierdorf K, Prinz M, Wu B, Jacobsen SE, Pollard JW, Frampton J, Liu KJ, Geissmann F. A lineage of myeloid cells independent of Myb and hematopoietic stem cells. Science. 2012; 336:86-90.
26. Rosas M, Davies LC, Giles PJ, Liao CT, Kharfan B, Stone TC, O'Donnell VB, Fraser DJ, Jones SA, Taylor PR. The transcription factor Gata6 links tissue macrophage phenotype and proliferative renewal. Science. 2014; 344:645-648.
27. Davies LC, Jenkins SJ, Allen JE, Taylor PR. Tissue-resident macrophages. Nat Immunol. 2013; 14:986-995.
28. Davies LC, Taylor PR. Tissue-resident macrophages: then and now. Immunology. 2015; 144:541-548.
29. Cassado Ados A, D'Imperio Lima MR, Bortoluci KR. Revisiting mouse peritoneal macrophages: heterogeneity, development, and function. Front Immunol. 2015; 6:225.
30. Ghosn EE, Cassado AA, Govoni GR, Fukuhara T, Yang Y, Monack DM, Bortoluci KR, Almeida SR, Herzenberg LA, Herzenberg LA. Two physically, functionally, and developmentally distinct peritoneal macrophage subsets. Proc Natl Acad Sci U S A. 2010; 107:2568-2573.
31. Yona S, Kim KW, Wolf Y, Mildner A, Varol D, Breker M, Strauss-Ayali D, Viukov S, Guilliams M, Misharin A, Hume DA, Perlman H, Malissen B, Zelzer E, Jung S. Fate mapping reveals origins and dynamics of monocytes and tissue macrophages under homeostasis. Immunity. 2013; 38:79-91.
32. Sica A, Porta C, Morlacchi S, Banfi S, Strauss L, Rimoldi M, Totaro MG, Riboldi E. Origin and Functions of Tumor-Associated Myeloid Cells (TAMCs). Cancer Microenviron. 2012; 5:133-149.
33. Xu W, Schlagwein N, Roos A, van den Berg TK, Daha MR, van Kooten C. Human peritoneal macrophages show functional characteristics of M-CSF-driven anti-inflammatory type 2 macrophages. Eur J Immunol. 2007; 37:1594-1599.
34. Miyanishi M, Tada K, Koike M, Uchiyama Y, Kitamura T, Nagata S. Identification of Tim4 as a phosphatidylserine receptor. Nature. 2007; 450:435-439.
35. Thornley TB, Fang Z, Balasubramanian S, Larocca RA, Gong W, Gupta S, Csizmadia E, Degauque N, Kim BS, Koulmanda M, Kuchroo VK, Strom TB. Fragile TIM-4-expressing tissue resident macrophages are migratory and immunoregulatory. J Clin Invest. 2014; 124:3443-3454.
36. Gautier EL, Shay T, Miller J, Greter M, Jakubzick C, Ivanov S, Helft J, Chow A, Elpek KG, Gordonov S, Mazloom AR, Ma'ayan A, Chua WJ, Hansen TH, Turley SJ, Merad M, et al. Gene-expression profiles and transcriptional regulatory pathways that underlie the identity and diversity of mouse tissue macrophages. Nat Immunol. 2012; 13:1118-1128.
37. Buggins AG, Mufti GJ, Salisbury J, Codd J, Westwood N, Arno M, Fishlock K, Pagliuca A, Devereux S. Peripheral blood but not tissue dendritic cells express CD52 and are depleted by treatment with alemtuzumab. Blood. 2002; 100:1715-1720.
38. Reinartz S, Finkernagel F, Adhikary T, Rohnalter V, Schumann T, Schober Y, Nockher WA, Nist A, Stiewe T, Jansen JM, Wagner U, Muller-Brusselbach S, Muller R. A transcriptome-based global map of signaling pathways in the ovarian cancer microenvironment associated with clinical outcome. Genome Biol. 2016; 17:108.
39. Henson PM, Hume DA. Apoptotic cell removal in development and tissue homeostasis. Trends Immunol. 2006; 27:244-250.
40. Lech M, Grobmayr R, Weidenbusch M, Anders HJ. Tissues use resident dendritic cells and macrophages to maintain homeostasis and to regain homeostasis upon tissue injury: the immunoregulatory role of changing tissue environments. Mediators Inflamm. 2012; 2012:951390.
41. Wong K, Valdez PA, Tan C, Yeh S, Hongo JA, Ouyang W. Phosphatidylserine receptor Tim-4 is essential for the maintenance of the homeostatic state of resident peritoneal macrophages. Proc Natl Acad Sci U S A. 2010; 107:8712-8717.
42. Perkins EH, Massucci JM, Glover PL. Antigen presentation by peritoneal macrophages from young adult and old mice. Cell Immunol. 1982; 70:1-10.
43. Betjes MG, Tuk CW, Struijk DG, Krediet RT, Arisz L, Beelen RH. Antigen-presenting capacity of macrophages and dendritic cells in the peritoneal cavity of patients treated with peritoneal dialysis. Clin Exp Immunol. 1993; 94:377-384.
44. Singh RA, Sodhi A. Antigen presentation by cisplatin-activated macrophages: role of soluble factor(s) and second messengers. Immunol Cell Biol. 1998; 76:513-519.
45. Yeh K, Silberman D, Gonzalez D, Riggs J. Complementary suppression of T cell activation by peritoneal macrophages and CTLA-4-Ig. Immunobiology. 2007; 212:1-10.
46. Becker S, Johnson C, Halme J, Haskill S. Interleukin-1 production and antigen presentation by normal human peritoneal macrophages. Cell Immunol. 1986; 98:467-476.
47. Gordon IO, Freedman RS. Defective antitumor function of monocyte-derived macrophages from epithelial ovarian cancer patients. Clin Cancer Res. 2006; 12:1515-1524.
48. Robinson MD, Smyth GK. Moderated statistical tests for assessing differences in tag abundance. Bioinformatics. 2007; 23:2881-2887.
49. Robinson MD, McCarthy DJ, Smyth GK. edgeR: a Bioconductor package for differential expression analysis of digital gene expression data. Bioinformatics. 2010; 26:139-140.

50. Charles KA, Kulbe H, Soper R, Escorcio-Correia M, Lawrence T, Schultheis A, Chakravarty P, Thompson RG, Kollias G, Smyth JF, Balkwill FR, Hagemann T. The tumor-promoting actions of TNF-alpha involve TNFR1 and IL-17 in ovarian cancer in mice and humans. J Clin Invest. 2009; 119:3011-3023.

51. Riester M, Wei W, Waldron L, Culhane AC, Trippa L, Oliva E, Kim SH, Michor F, Huttenhower C, Parmigiani G, Birrer MJ. Risk prediction for late-stage ovarian cancer by meta-analysis of 1525 patient samples. J Natl Cancer Inst. 2014; 106.

52. Eng KH, Ruggeri C. Connecting prognostic ligand receptor signaling loops in advanced ovarian cancer. PLoS One. 2014; 9:e107193.

53. Kulbe H, Thompson R, Wilson JL, Robinson S, Hagemann T, Fatah R, Gould D, Ayhan A, Balkwill F. The inflammatory cytokine tumor necrosis factor-alpha generates an autocrine tumor-promoting network in epithelial ovarian cancer cells. Cancer Res. 2007; 67:585-592.

54. Ahmed N, Stenvers KL. Getting to Know Ovarian Cancer Ascites: Opportunities for Targeted Therapy-Based Translational Research. Front Oncol. 2013; 3:256.

55. Kuk C, Kulasingam V, Gunawardana CG, Smith CR, Batruch I, Diamandis EP. Mining the ovarian cancer ascites proteome for potential ovarian cancer biomarkers. Mol Cell Proteomics. 2009; 8:661-669.

56. Bager CL, Willumsen N, Leeming DJ, Smith V, Karsdal MA, Dornan D, Bay-Jensen AC. Collagen degradation products measured in serum can separate ovarian and breast cancer patients from healthy controls: A preliminary study. Cancer Biomark. 2015; 15:783-788.

57. Ingman WV, Wyckoff J, Gouon-Evans V, Condeelis J, Pollard JW. Macrophages promote collagen fibrillogenesis around terminal end buds of the developing mammary gland. Dev Dyn. 2006; 235:3222-3229.

58. Chen S, Birk DE. The regulatory roles of small leucine-rich proteoglycans in extracellular matrix assembly. FEBS J. 2013; 280:2120-2137.

59. Nikitovic D, Papoutsidakis A, Karamanos NK, Tzanakakis GN. Lumican affects tumor cell functions, tumor-ECM interactions, angiogenesis and inflammatory response. Matrix Biol. 2014; 35:206-214.

60. Herchenhan A, Uhlenbrock F, Eliasson P, Weis M, Eyre D, Kadler KE, Magnusson SP, Kjaer M. Lysyl Oxidase Activity Is Required for Ordered Collagen Fibrillogenesis by Tendon Cells. J Biol Chem. 2015; 290:16440-16450.

61. Vadon-Le Goff S, Kronenberg D, Bourhis JM, Bijakowski C, Raynal N, Ruggiero F, Farndale RW, Stocker W, Hulmes DJ, Moali C. Procollagen C-proteinase enhancer stimulates procollagen processing by binding to the C-propeptide region only. J Biol Chem. 2011; 286:38932-38938.

62. Bourhis JM, Vadon-Le Goff S, Afrache H, Mariano N, Kronenberg D, Thielens N, Moali C, Hulmes DJ. Procollagen C-proteinase enhancer grasps the stalk of the C-propeptide trimer to boost collagen precursor maturation. Proc Natl Acad Sci U S A. 2013; 110:6394-6399.

63. Huang S, Van Arsdall M, Tedjarati S, McCarty M, Wu W, Langley R, Fidler IJ. Contributions of stromal metalloproteinase-9 to angiogenesis and growth of human ovarian carcinoma in mice. J Natl Cancer Inst. 2002; 94:1134-1142.

64. Robinson-Smith TM, Isaacsohn I, Mercer CA, Zhou M, Van Rooijen N, Husseinzadeh N, McFarland-Mancini MM, Drew AF. Macrophages mediate inflammation-enhanced metastasis of ovarian tumors in mice. Cancer Res. 2007; 67:5708-5716.

65. Germano G, Frapolli R, Belgiovine C, Anselmo A, Pesce S, Liguori M, Erba E, Uboldi S, Zucchetti M, Pasqualini F, Nebuloni M, van Rooijen N, Mortarini R, Beltrame L, Marchini S, Fuso Nerini I, et al. Role of macrophage targeting in the antitumor activity of trabectedin. Cancer Cell. 2013; 23:249-262.

66. Reusser NM, Dalton HJ, Pradeep S, Gonzalez-Villasana V, Jennings NB, Vasquez HG, Wen Y, Rupaimoole R, Nagaraja AS, Gharpure K, Miyake T, Huang J, Hu W, Lopez-Berestein G, Sood AK. Clodronate inhibits tumor angiogenesis in mouse models of ovarian cancer. Cancer Biol Ther. 2014; 15:1061-1067.

67. Burleson KM, Casey RC, Skubitz KM, Pambuccian SE, Oegema TR, Jr., Skubitz AP. Ovarian carcinoma ascites spheroids adhere to extracellular matrix components and mesothelial cell monolayers. Gynecol Oncol. 2004; 93:170-181.

68. Burleson KM, Hansen LK, Skubitz AP. Ovarian carcinoma spheroids disaggregate on type I collagen and invade live human mesothelial cell monolayers. Clin Exp Metastasis. 2004; 21:685-697.

69. Cheon DJ, Tong Y, Sim MS, Dering J, Berel D, Cui X, Lester J, Beach JA, Tighiouart M, Walts AE, Karlan BY, Orsulic S. A collagen-remodeling gene signature regulated by TGF-beta signaling is associated with metastasis and poor survival in serous ovarian cancer. Clin Cancer Res. 2014; 20:711-723.

70. Tang Z, Ow GS, Thiery JP, Ivshina AV, Kuznetsov VA. Meta-analysis of transcriptome reveals let-7b as an unfavorable prognostic biomarker and predicts molecular and clinical subclasses in high-grade serous ovarian carcinoma. Int J Cancer. 2014; 134:306-318.

71. Busuttil RA, George J, Tothill RW, Ioculano K, Kowalczyk A, Mitchell C, Lade S, Tan P, Haviv I, Boussioutas A. A signature predicting poor prognosis in gastric and ovarian cancer represents a coordinated macrophage and stromal response. Clin Cancer Res. 2014; 20:2761-2772.

72. Tothill RW, Tinker AV, George J, Brown R, Fox SB, Lade S, Johnson DS, Trivett MK, Etemadmoghadam D, Locandro B, Traficante N, Fereday S, Hung JA, Chiew YE, Haviv I, Australian Ovarian Cancer Study G, et al. Novel molecular

subtypes of serous and endometrioid ovarian cancer linked to clinical outcome. Clin Cancer Res. 2008; 14:5198-5208.

73. Cancer Genome Atlas Research N. Integrated genomic analyses of ovarian carcinoma. Nature. 2011; 474:609-615.

74. Colvin EK. Tumor-associated macrophages contribute to tumor progression in ovarian cancer. Front Oncol. 2014; 4:137.

75. Adhikary T, Wortmann A, Schumann T, Finkernagel F, Lieber S, Roth K, Toth PM, Diederich WE, Nist A, Stiewe T, Kleinesudeik L, Reinartz S, Müller-Brüsselbach S, Müller R. The transcriptional PPARβ/δ network in human macrophages defines a unique agonist-induced activation state. Nucleic Acids Res. 2015; 43:5033-5051.

76. Rohnalter V, Roth K, Finkernagel F, Adhikary T, Obert J, Dorzweiler K, Bensberg M, Müller-Brüsselbach S, Müller R. A multi-stage process including transient polyploidization and EMT precedes the emergence of chemoresistent ovarian carcinoma cells with a dedifferentiated and pro-inflammatory secretory phenotype. Oncotarget. 2015; 6:40005-40025.

77. Dobin A, Davis CA, Schlesinger F, Drenkow J, Zaleski C, Jha S, Batut P, Chaisson M, Gingeras TR. STAR: ultrafast universal RNA-seq aligner. Bioinformatics. 2013; 29:15-21.

78. Johnson WE, Li C, Rabinovic A. Adjusting batch effects in microarray expression data using empirical Bayes methods. Biostatistics. 2007; 8:118-127.

79. Chen C, Grennan K, Badner J, Zhang D, Gershon E, Jin L, Liu C. Removing batch effects in analysis of expression microarray data: an evaluation of six batch adjustment methods. PLoS One. 2011; 6:e17238.

CHAPTER 7

APPENDICIES

7.1 All publications of the author

In chronlogical order

[FF1] K. Heimel, M. Scherer, M. Vranes, R. Wahl, C. Pothiratana, D. Schuler, V. Vincon, **Finkernagel, Florian**, I. Flor-Parra, and J. Kämper. "The transcription factor rbf1 is the master regulator for b-mating type controlled pathogenic development in Ustilago maydis". In: *PLoS Pathogens* (2010). DOI: 10.1371/journal.ppat.1001035.

[FF2] B. Herkert, A. Dwertmann, S. Herold, M. Abed, J.-F. Naud, **Finkernagel, Florian**, G. S. Harms, A. Orian, M. Wanzel, and M. Eilers. "The Arf tumor suppressor protein inhibits Miz1 to suppress cell adhesion and induce apoptosis". In: *The Journal of Cell Biology* (2010). DOI: 10.1083/jcb.200908103.

[FF3] K. Kaddatz, T. Adhikary, **Finkernagel, Florian**, W. Meissner, S. Müller-Brüsselbach, and R. Müller. "Transcriptional profiling identifies functional interactions of TGFβ and PPARβ/δ signaling: synergistic induction of ANGPTL4 transcription." In: *The Journal of biological chemistry* (2010). DOI: 10.1074/jbc.M110.142018.

[FF4] B. Stielow, I. Krüger, R. Diezko, **Finkernagel, Florian**, N. Gillemans, J. Kong-a-San, S. Philipsen, and G. Suske. "Epigenetic silencing of spermatocyte-specific and neuronal genes by SUMO modification of the transcription factor Sp3." In: *PLoS genetics* (2010). DOI: 10.1371/journal.pgen.1001203.

[FF5] T. Adhikary, K. Kaddatz, **Finkernagel, Florian**, A. Schönbauer, W. Meissner, M. Scharfe, M. Jarek, H. Blöcker, S. Müller-Brüsselbach, and R. Müller. "Genomewide analyses define different modes of transcriptional regulation by peroxisome proliferator-activated receptor-β/δ (PPARβ/δ)". In: *PLoS ONE* (2011). DOI: 10.1371/journal.pone.0016344.

[FF6] J. Stockert, T. Adhikary, K. Kaddatz, **Finkernagel, Florian**, W. Meissner, S. Müller-Brüsselbach, and R. Müller. "Reverse crosstalk of TGFβ and PPARβ/δ signaling identified by transcriptional profiling." In: *Nucleic acids research* (2011). DOI: 10.1093/nar/gkq773.

[FF7] E. L. Mathieu, **Finkernagel, Florian**, M. Murawska, M. Scharfe, M. Jarek, and A. Brehm. "Recruitment of the ATP-dependent chromatin remodeler dMi-2 to the transcribed region of active heat shock genes". In: *Nucleic Acids Research* (2012). DOI: 10.1093/nar/gks178.

[FF8] K. Meier, E. L. Mathieu, **Finkernagel, Florian**, L. M. Reuter, M. Scharfe, G. Doehlemann, M. Jarek, and A. Brehm. "LINT, a novel dL(3)mbt-containing complex, represses malignant brain tumour signature genes". In: *PLoS Genetics* (2012). DOI: 10.1371/journal.pgen.1002676.

[FF9] G. Terrados, **Finkernagel, Florian**, B. Stielow, D. Sadic, J. Neubert, O. Herdt, M. Krause, M. Scharfe, M. Jarek, and G. Suske. "Genome-wide localization and expression profiling establish Sp2 as a sequence-specific transcription factor regulating vitally important genes". In: *Nucleic Acids Research* (2012). DOI: 10.1093/nar/gks544.

[FF10] T. Adhikary, D. T. Brandt, K. Kaddatz, J. Stockert, S. Naruhn, W. Meissner, **Finkernagel, Florian**, J. Obert, S. Lieber, M. Scharfe, M. Jarek, P. M. Toth, F. Scheer, W. E. Diederich, S. Reinartz, R. Grosse, S. Müller-Brüsselbach, and R. Müller. "Inverse PPARβ/δ agonists suppress oncogenic signaling to the ANGPTL4 gene and inhibit cancer cell invasion". In: *Oncogene* (2013). DOI: 10.1038/onc.2012.549.

[FF11] J. Esterlechner, N. Reichert, F. Iltzsche, M. Krause, **Finkernagel, Florian**, and S. Gaubatz. "LIN9, a Subunit of the DREAM Complex, Regulates Mitotic Gene Expression and Proliferation of Embryonic Stem Cells". In: *PLoS ONE* (2013). DOI: 10.1371/journal.pone.0062882.

[FF12] K. Schlereth, C. Heyl, A. M. Krampitz, M. Mernberger, **Finkernagel, Florian**, M. Scharfe, M. Jarek, E. Leich, A. Rosenwald, and T. Stiewe. "Characterization of the p53 Cistrome - DNA Binding Cooperativity Dissects p53's Tumor Suppressor Functions". In: *PLoS Genetics* (2013). DOI: 10.1371/journal.pgen.1003726.

[FF13] J. Stockert, A. Wolf, K. Kaddatz, E. Schnitzer, **Finkernagel, Florian**, W. Meissner, S. Müller-Brüsselbach, M. Kracht, and R. Müller. "Regulation of TAK1/TAB1-Mediated IL-1β Signaling by Cytoplasmic PPARβ/δ". In: *PLoS ONE* (2013). DOI: 10.1371/journal.pone.0063011.

[FF14] J. M. Jansen, S. Reinartz, R. Müller, S. Müller-Brüsselbach, T. Schumann, **Finkernagel, Florian**, A. Wortmann, W. Meissner, M. Krause, and U. Wagner. "Der Zusammenhang zwischem dem Polarisationsphänotyp von Tumor-assoziierten Makrophagen (TAM), Zytokinspiegeln und dem progressionsfreien Überleben bei Ovarialkarzinompatientinnen". In: *Geburtshilfe und Frauenheilkunde* (2014). DOI: 10.1055/s-0034-1388410.

[FF15] N. Kellner, K. Heimel, T. Obhof, **Finkernagel, Florian**, and J. Kämper. "The SPF27 Homologue Num1 Connects Splicing and Kinesin 1-Dependent Cytoplasmic Trafficking in Ustilago maydis". In: *PLoS Genetics* (2014). DOI: 10.1371/journal.pgen.1004046.

[FF16] G. Kumari, T. Ulrich, M. Krause, **Finkernagel, Florian**, and S. Gaubatz. "Induction of p21CIP1 protein and cell cycle arrest after inhibition of Aurora B kinase is attributed to aneuploidy and reactive oxygen species". In: *Journal of Biological Chemistry* (2014). DOI: 10.1074/jbc.M114.555060.

[FF17] S. Lieber, F. Scheer, **Finkernagel, Florian**, W. Meissner, G. Giehl, C. Brendel, W. E. Diederich, S. Muller-Brusselbach, and R. Muller. "The Inverse Agonist DG172 Triggers a PPARβ/δ-Independent Myeloid Lin-

eage Shift and Promotes GM-CSF/IL-4-Induced Dendritic Cell Differentiation". In: *Molecular Pharmacology* (2014). DOI: 10.1124/mol.114.094672.

[FF18] M. Preußner, I. Wilhelmi, A.-S. Schultz, **Finkernagel, Florian**, M. Michel, T. Möröy, and F. Heyd. "Rhythmic U2af26 alternative splicing controls PERIOD1 stability and the circadian clock in mice." In: *Molecular cell* (2014). DOI: 10.1016/j.molcel.2014.04.015.

[FF19] S. Reinartz, T. Schumann, **Finkernagel, Florian**, A. Wortmann, J. M. Jansen, W. Meissner, M. Krause, A.-M. M. Schwörer, U. Wagner, S. Müller-Brüsselbach, and R. Müller. "Mixed-polarization phenotype of ascites-associated macrophages in human ovarian carcinoma: Correlation of CD163 expression, cytokine levels and early relapse". In: *International Journal of Cancer* (2014). DOI: 10.1002/ijc.28335.

[FF20] C. Stielow, B. Stielow, **Finkernagel, Florian**, M. Scharfe, M. Jarek, and G. Suske. "SUMOylation of the polycomb group protein L3MBTL2 facilitates repression of its target genes." In: *Nucleic acids research* (2014). DOI: 10.1093/nar/gkt1317.

[FF21] T. Adhikary, A. Wortmann, T. Schumann, **Finkernagel, Florian**, S. Lieber, K. Roth, P. M. Toth, W. E. Diederich, A. Nist, T. Stiewe, L. Kleinesudeik, S. Reinartz, S. Müller-Brüsselbach, and R. Müller. "The transcriptional PPARβ/δ network in human macrophages defines a unique agonist-induced activation state." In: *Nucleic acids research* (2015). DOI: 10.1093/nar/gkv331.

[FF22] P. K. Dhanyamraju, P. S. Holz, **Finkernagel, Florian**, V. Fendrich, and M. Lauth. "Histone deacetylase 6 represents a novel drug target in the oncogenic Hedgehog signaling pathway." In: *Molecular cancer therapeutics* (2015). DOI: 10.1158/1535-7163.MCT-14-0481.

[FF23] M. Kemmerer, **Finkernagel, Florian**, M. F. Cavalcante, D. S. P. Abdalla, R. Müller, B. Brüne, and D. Namgaladze. "AMP-activated protein kinase interacts with the peroxisome proliferator-activated receptor delta to induce genes affecting fatty acid oxidation in human macrophages". In: *PLoS ONE* (2015). DOI: 10.1371/journal.pone.0130893.

[FF24] V. Rohnalter, K. Roth, **Finkernagel, Florian**, T. Adhikary, J. Obert, K. Dorzweiler, M. Bensberg, S. Müller-Brüsselbach, and R. Müller. "A multi-stage process including transient polyploidization and EMT precedes the emergence of chemoresistent ovarian carcinoma cells with a dedifferentiated and pro-inflammatory secretory phenotype." In: *Oncotarget* (2015). DOI: 10.18632/oncotarget.5552.

[FF25] T. Schumann, T. Adhikary, A. Wortmann, **Finkernagel, Florian**, S. Lieber, E. Schnitzer, N. Legrand, Y. Schober, W. A. Nockher, P. M. Toth, W. E. Diederich, A. Nist, T. Stiewe, U. Wagner, S. Reinartz, S. Müller-Brüsselbach, and R. Müller. "Deregulation of PPARβ/δ target genes in tumor-associated macrophages by fatty acid ligands in the ovarian cancer microenvironment". In: *Oncotarget* (2015). DOI: 10.18632/oncotarget.3826.

[FF26] S. Voelkel, B. Stielow, **Finkernagel, Florian**, T. Stiewe, A. Nist, and G. Suske. "Zinc Finger Independent Genome-Wide Binding of Sp2 Potentiates Recruitment of Histone-Fold Protein Nf-y Distinguishing It from Sp1 and Sp3". In: *PLoS Genetics* (2015). DOI: 10.1371/journal.pgen.1005102.

[FF27] **Finkernagel, Florian**, S. Reinartz, S. Lieber, T. Adhikary, A. Wortmann, N. Hoffmann, T. Bieringer, A. Nist, T. Stiewe, J. M. Jansen, U. Wagner, S. Müller-Brüsselbach, and R. Müller. "The transcriptional signature of human ovarian carcinoma macrophages is associated with extracellular matrix reorganization." In: *Oncotarget* (2016). DOI: 10.18632/oncotarget.12180.

[FF28] J. Gossmann, M. Stolte, M. Lohoff, P. Yu, R. Moll, **Finkernagel, Florian**, H. Garn, C. Brendel, A. Bittner, A. Neubauer, and M. Q. Huynh. "A Gain-Of-Function Mutation in the Plcg2 Gene Protects Mice from Helicobacter felis-Induced Gastric MALT Lymphoma." In: *PloS one* (2016). DOI: 10.1371/journal.pone.0150411.

[FF29] M. Hampel, M. Jakobi, L. Schmitz, U. Meyer, **Finkernagel, Florian**, G. Doehlemann, and K. Heimel. "Unfolded Protein Response (UPR) Regulator Cib1 Controls Expression of Genes Encoding Secreted Virulence Factors in Ustilago maydis". In: *PLOS ONE* (2016). DOI: 10.1371/journal.pone.0153861.

[FF30] S. Reinartz, **Finkernagel, Florian**, T. Adhikary, V. Rohnalter, T. Schumann, Y. Schober, W. A. Nockher, A. Nist, T. Stiewe, J. M. Jansen, U. Wagner, S. Müller-Brüsselbach, and R. Müller. "A transcriptome-based global map of signaling pathways in the ovarian cancer microenvironment associated with clinical outcome." In: *Genome biology* (2016). DOI: 10.1186/s13059-016-0956-6.

[FF31] T. Adhikary, A. Wortmann, **Finkernagel, Florian**, S. Lieber, A. Nist, T. Stiewe, U. Wagner, S. Müller-Brüsselbach, S. Reinartz, and R. Müller. "Interferon signaling in ascites-associated macrophages is linked to a favorable clinical outcome in a subgroup of ovarian carcinoma patients". In: *BMC Genomics* (2017). DOI: 10.1186/s12864-017-3630-9.

[FF32] J. Kreher, K. Kovač, K. Bouazoune, I. Mačinković, A. L. Ernst, E. Engelen, R. Pahl, **Finkernagel, Florian**, M. Murawska, I. Ullah, and A. Brehm. "EcR recruits dMi-2 and increases efficiency of dMi-2-mediated remodelling to constrain transcription of hormone-regulated genes". In: *Nature Communications* (2017). DOI: 10.1038/ncomms14806.

[FF33] C. Schütz, S. Inselmann, S. Sausslele, C. T. Dietz, M. C. Müller, E. Eigendorff, C. A. Brendel, S. K. Metzelder, T. H. Brümmendorf, C. Waller, J. Dengler, M. E. Goebeler, R. Herbst, G. Freunek, S. Hanzel, T. Illmer, Y. Wang, T. Lange, F. Finkernagel, R. Hehlmann, M. Huber, A. Neubauer, A. Hochhaus, J. Guilhot, F. Xavier Mahon, M. Pfirrmann, and A. Burchert. "Expression of the CTLA-4 ligand CD86 on plasmacytoid dendritic cells (pDC) predicts risk of disease recurrence after treatment discontinuation in CML". In: *Leukemia* (2017). DOI: 10.1038/leu.2017.9.

7.2 Curriculum vitae/Lebenslauf

Birth/Geburt: 09. April 1983
Scolarship / Schulische und Akademische Laufbahn:

- Grundschule Oberes Ohmtal 1988-1993
- Gesamtschule Nieder Ohmen 1993-1999
- Alan C. Pope Highschool 1999-2000
- Laubach Kolleg der evangelischen Kirche Hessen-Nassau 2000-2002, Abschluss: Abitur
- Philipps Universität Marburg, 2002-2007, Abschluss: Diplom der Biologie

7.3 Directory of academic teachers

My academic teachers in Marburg were:

Batschauer, Beck, Bölker, Bremer, Buckel, Galland, Heldmeier, Homberg, Kahmann, Kämper, Kirchner, Klein, Kost, Mösch, Renkawitz-Pohl, Succhard, and Weber.

7.4 Acknowlegments

Foremost, I would like to express my immense gratitude to my advisor Prof. Rolf Müller for his continous support during my Ph.D studies and the opportunity to work on ovarian carcinoma. I appreciate you pushing me around.

My sincere thanks goes to all my collaborators and coworkers, especially (and in no particular order) Till, Tim, Kerstin, Simone, Jörg, Guntram, Sonja, Marco, Boris, Annika, Basti, Gloria, Josephine, Silke, Verena, Eve-Lyne, Kai - without your expertise, skill and input this work would not have been possible.

I also appreciate the work of the poor fellows I press-ganged into proof reading my thesis - your hours were most certainly not in waste.

Last but certainly not least I thank both my families for their never ending support during this endeavor.